DOE/NE-0134

2007 Annual Report

Nuclear Energy Research Initiative

GEN IV Nuclear Energy Systems

Global Nuclear Energy Partnership

NHI
Nuclear Hydrogen Initiative

Disclaimer

Available to DOE, DOE contractors, and the public from the
U.S. Department of Energy
Office of Nuclear Energy
1000 Independence Avenue, S.W.
Washington, D.C. 20585

Printed with soy ink on recycled paper.

Foreword

The Nuclear Energy Research Initiative (NERI) is at the core of a Federal effort to develop advanced nuclear energy concepts and technologies. This program supports the National Energy Policy by conducting research that addresses the long-term barriers to both maintaining and expanding nuclear generation of electricity in this country. Currently funded NERI projects are closely linked to the principal research programs sponsored by the Department of Energy Office of Nuclear Energy (DOE-NE): the Generation IV Nuclear Energy Systems Initiative, the Global Nuclear Energy Partnership/Advanced Fuel Cycle Initiative, and the Nuclear Hydrogen Initiative. With its focus on applied nuclear energy research, NERI has been realizing its goal of both developing advanced nuclear energy systems and providing state-of-the-art research concerning nuclear science and technology.

Since its inception in 1999, NERI has helped to maintain and improve the nuclear research infrastructure in this country by encouraging, preserving, and advancing nuclear science and technology R&D. To further this mission, NE decided to refocus NERI in 2004 to exclusively fund research led solely by the Nation's universities, with national laboratories and industry partners providing valuable contributions as collaborators. Strong university involvement is particularly important to promote and maintain a robust nuclear science and engineering infrastructure to meet future technical challenges. This revised focus enables educational institutions across the country to remain at the forefront of nuclear science research. In addition, it renews student interest in pursuing degrees in nuclear engineering and related sciences and further integrates the Nation's universities with research efforts and initiatives at DOE.

The *Nuclear Energy Research Initiative 2007 Annual Report* summarizes the progress of the 35 research projects initiated in fiscal year (FY) 2005, the 25 projects initiated in FY 2006, the 22 projects initiated in 2007, and the objectives and work scope of the 11 newly awarded FY 2007 NERI-consortia research projects. The final summaries of projects initiated in FY 1999 through FY 2002 can be found in previous NERI Annual Reports. This report disseminates the results of NERI-sponsored research to the R&D community to spur yet more innovation, assuring a bright future for nuclear energy in the United States and the world.

R. Shane Johnson
Principal Deputy Assistant Secretary for Nuclear Energy
U.S. Department of Energy

Table of Contents

Nuclear Energy Research Initiative

1. Overview

The Nuclear Energy Research Initiative

The United States DOE created NERI in FY 1999 in response to recommendations provided by the President's Committee of Advisors on Science and Technology (PCAST). The importance of nuclear power to the Nation's future energy supply requires that DOE apply its unique resources, specialized expertise, and national leadership to address all of the potential barriers to maintaining and expanding its use.

NERI is a national, research-oriented initiative managed and funded by DOE-NE. The purpose is to sponsor R&D that addresses the principal barriers related to the growth of nuclear energy in the United States. The initiative has helped DOE foster innovative ideas in NE's primary research programs: advanced nuclear energy systems, hydrogen production from nuclear power, and advanced nuclear fuels and fuel cycles. In addition to responding to the Nation's need for current nuclear energy research to advance the development of nuclear energy technology, NERI is helping to preserve the Nation's nuclear science and engineering infrastructure—enabling the United States to maintain a competitive position in the nuclear energy arena at home and abroad.

To achieve the Nation's long-range goal of establishing nuclear energy as a viable and expandable energy option, NERI has the following objectives:

- To address and help overcome the potential technical and scientific obstacles to the long-term, future use of nuclear energy in the United States, including non-proliferation, economics, and nuclear waste disposition
- To advance the state of U.S. nuclear technology so that it can maintain a competitive position in overseas and domestic markets
- To promote and maintain a nuclear science and engineering infrastructure to meet present and future technical challenges

NERI 2007 Annual Report

This *Nuclear Energy Research Initiative 2007 Annual Report* serves to inform interested parties of progress made in NERI on a programmatic level as well as research progress made on individual NERI projects. Following is an overview of each section:

- Section 2 provides background on the creation and implementation of NERI, its corresponding international I-NERI component, and the evolving research focus.
- Section 3 presents the scope of the three NE R&D programs supported by NERI.
- Section 4 highlights the major accomplishments of the NERI program in 2007.
- Section 5 discusses the impact NERI has had on U.S. university nuclear programs.
- Section 6 presents progress reports for each of the 82 FY 2005—2007 projects and provides abstracts for the 11 newly awarded FY 2007 NERI-C projects.

Projects are organized by their primary research area: Generation IV, AFCI, and NHI. Numbering is designated by the fiscal year in which the award was made. At the end of the document, there is an index of NERI projects grouped by fiscal year and sequentially ordered by project number.

NUCLEAR ENERGY RESEARCH INITIATIVE

2. Program History

NERI Development

In January 1997, the President tasked PCAST to review the current national energy R&D portfolio and to provide a strategy to ensure that the United States has a program to address the Nation's energy and environmental needs for the next century. In a report responding to this request, the PCAST panel on Energy Research and Development determined that ensuring a viable nuclear energy option was essential to help meet U.S. future energy needs. Specifically, the panel recommended that DOE implement an R&D effort to address the principal obstacles to achieving a viable nuclear energy option, targeting such areas as nuclear waste, proliferation, safety, and economics. DOE was to fund research through this new initiative based on a competitive selection of proposals from the national laboratories, universities, and industry.

In response to these recommendations, DOE established NERI in 1999 and the program received Congressional appropriations to begin sponsoring innovative scientific and engineering R&D that address the key issues affecting the future use of nuclear energy and preserve the Nation's nuclear science and technology leadership. Currently, NERI employs the following process for selecting new projects. First, DOE-NE issues one or more annual solicitations requesting applications from eligible participants on a noted scope of work. Principal investigators (PIs) select research topics of interest and define the scope and extent of the R&D in their application responses. Then, an independent peer review panel evaluates the scientific and technical merit of the R&D proposals and a relevance review is conducted by the program's Campaign Directors, Systems Integration Managers, and Technical Directors. Finally, DOE program managers review the proposals that are judged to have the highest merit and relevance to ensure their conformance with policy and programmatic requirements and recommend project awards to DOE's Source Selection Official.

Additional information on the NERI program, including previous annual reports, is available at the NERI website: *http://nuclear.energy.gov/neri/neNERIresearch.html*.

International Cooperation (I-NERI)

Recognizing the need for an international component, PCAST issued a report in 1999 entitled *Powerful Partnerships: The Federal Role in International Cooperation on Energy Innovation* to promote "bilateral and multilateral research focused on advanced technologies for improving the cost, safety, waste management, and proliferation-resistance of nuclear fission energy systems." In response, DOE launched the new International Nuclear Energy Research Initiative (I-NERI) for bilateral and multilateral nuclear energy research. Since FY 2001, I-NERI funding has supported 75 bilateral, cost-shared research projects with the Republic of Korea, France, the European Union, Brazil, Canada, Japan, and the Organisation for Economic Co-operation and Development (OECD).

I-NERI allows DOE to leverage Federal investment and international resources by cost-sharing research with participating countries on a wide range of nuclear technology topics. This initiative enhances the influence of the United States and DOE in international policy discussions on the future direction of nuclear energy. Further information can be found on the program website at *http://www.nuclear.gov*, including separate annual reports for research conducted under the I-NERI program.

NERI Focus

In order to determine the initial focus of the NERI research areas, DOE convened a workshop of nuclear community stakeholders in April 1998, representing national laboratories, universities, and industry. As a result of this NERI workshop, DOE focused its initial scientific and engineering R&D on five specific research areas:

1) Proliferation-resistant reactors and fuel technology
2) New reactor designs to achieve improved performance, higher efficiency, and reduced cost (including low-output power reactors for use where large reactors are not attractive)
3) Advanced nuclear fuels
4) New technologies for managing nuclear waste
5) Fundamental nuclear science

Since its initiation, the focus of NERI's research activities has been influenced by several Federal directives. A synopsis of each of these directives is provided.

Federal Directives

The Long-Term Nuclear Technology Research and Development Plan. In 1998, DOE established the independent Nuclear Energy Research Advisory Committee (NERAC). This committee provides advice to the Secretary and to the Assistant Secretary for Nuclear Energy on DOE's civilian nuclear technology program. In June 2000, NERAC issued the *Long-Term Nuclear Technology Research and Development Plan*. This plan identifies the research and technology development that is necessary over the next 10–20 years to help ensure the long-term viability of nuclear energy as an electricity generation option in the United States. NERAC also established a task force to identify R&D needs related to non-proliferation issues associated with nuclear power production. Their recommendations for appropriate research in this area were provided to DOE in a January 2001 report titled *Technical Opportunities to Increase the Proliferation Resistance of Global Civilian Nuclear Power Systems (TOPS)*.

The National Energy Policy. Issued in May 2001 by the Vice President's National Energy Policy Development Group, the *National Energy Policy* supports the expansion of nuclear energy as one of its major initiatives for meeting the growing energy requirements of the United States. The *National Energy Policy* provides the core element in the planning for DOE's nuclear energy research programs, addressing, among other areas, the research and development of advanced reactor and fuel cycle concepts, hydrogen production from nuclear energy, and the associated enabling sciences and technologies.

The Technology Roadmap for Generation IV Nuclear Energy Systems. In September 2002, NERAC issued the *Draft Technology Roadmap for Generation IV Nuclear Energy Systems*. In coordination with the eleven-country-member Generation IV International Forum, six reactor system concepts were selected for further development: 1) the very high-temperature reactor (VHTR), 2) the gas-cooled fast reactor (GFR), 3) the supercritical water-cooled reactor (SCWR), 4) the lead-cooled fast reactor (LFR), 5) the sodium-cooled fast reactor (SFR), and 6) the molten salt reactor (MSR).

Energy Policy Act of 2005 (EPAct 2005). On signing EPAct 2005 into law August 8, 2005, President George W. Bush reiterated the importance of nuclear energy as a clean, safe component of our Nation's energy supply: "With the practical steps in this bill, America is moving closer to a vital national goal. We will start building nuclear power plants again by the end of this decade." The law directly addresses DOE-NE's core R&D programs, including NERI and its constituent parts: Generation IV, AFCI, and NHI. EPAct 2005 allows the Secretary of Energy to conduct a set of nuclear energy programs that increase the efficiency of nuclear-energy-intensive sectors via improved technologies, promote diversity of the energy supply, decrease the United States' dependence on foreign energy sources, improve energy security, and decrease the environmental impact of energy-related activities. It also authorizes $1.25 billion for FYs 2006 through 2015 to fund a prototype Next Generation Nuclear Plant (NGNP) to produce both electricity and hydrogen.

Advanced Energy Initiative. In February 2006, the President rolled out his *Advanced Energy Initiative*, which aims to improve the country's economic and national security by reducing dependence on foreign sources of energy. This initiative provides a 22 percent increase in funding for clean-energy technology research at DOE to change how Americans fuel their vehicles and power their homes and businesses, generating electricity and hydrogen fuel from safe, advanced nuclear power. The initiative also calls for the development of the Global Nuclear Energy Partnership (GNEP) to address spent nuclear fuel; eliminate proliferation risks; and expand the promise of clean, reliable, and affordable nuclear energy on an international scale. Under GNEP, nations with advanced civilian nuclear energy programs will develop technology to recycle nuclear fuel and supply small, secure reactors and fuel services to other countries in exchange for non-proliferation guarantees. *The National Security Strategy of the United States of America*, which the President issued in March 2006, further reinforces the importance of GNEP in meeting global energy demand while keeping nuclear weapons materials out of the hands of rogue states and terrorists.

NERI's New Focus

Initially, NERI projects were focused on providing a supportive role to government nuclear energy-related R&D programs, such as the Generation IV, AFCI, and NHI. In 2004, the focus of NERI research changed to exclusively fund applied R&D that specifically supports these three initiatives. In addition, only U.S. universities were now allowed to serve as the principal investigators for new projects; however, national laboratories and private companies would still participate as collaborating organizations. This new focus directly supports NERI's goal to preserve, improve, and advance the United States' nuclear science and engineering infrastructure and will further assist these nuclear energy initiatives in accomplishing their goals and objectives.

The scope of the FY 2006 NERI solicitation, for awards announced in early 2007, focused on current federal R&D priorities, as outlined in the *EPAct 2005* and the *Advanced Energy Initiative*. For example, the United States is limiting its reactor development work under the Generation IV initiative to the VHTR for use as the NGNP and the SFR as the GNEP advanced burner design.

Nuclear Energy Research Initiative

3. NERI Research Areas

Projects undertaken since 2004 are aligned with NERI's new focus to conduct applied nuclear energy research related to the three primary Office of Nuclear Energy R&D programs: 1) Generation IV, 2) AFCI, and 3) NHI. These three initiatives are contributing to the revitalization of nuclear technology by developing efficient technologies for future electrical power production, hydrogen production, and other energy conversion systems. All three clearly support R&D efforts necessary to position nuclear energy as a viable fuel source that will help the United States sustain its growing energy needs. The selection of new NERI research projects is based on their relevance to these specific initiatives, and their achievements will play an integral role in the success of the overall NE mission. Following are descriptions of these programs.

Generation IV Nuclear Energy Systems Initiative

Generation IV nuclear energy systems are being developed to achieve high burnup using transmutation and recycled fuel, allowing for efficient use of domestic uranium resources and minimizing radioactive waste. Advances in safety and physical protection will guard against possible acts of terror or the diversion of nuclear materials, helping to ensure public confidence in nuclear technology. The program is focused on developing six new reactor systems to be deployed during the next 20 years:

1) Very High-Temperature Reactor (VHTR)
2) Sodium-Cooled Fast Reactor (SFR)
3) Supercritical Water-Cooled Reactor (SCWR)
4) Lead-Cooled Fast Reactor (LFR)
5) Gas-Cooled Fast Reactor (GFR)
6) Molten Salt Reactor (MSR)

The United States is not actively pursuing all of these reactor designs at the present time. Current U.S. efforts are focused on developing the SFR and VHTR technologies, while foreign collaborators are leading research on the other reactor systems under the Generation IV International Forum (GIF).

In addition to the development of these six types of reactor systems, Generation IV includes three cross-cutting programmatic areas of research. These activities are germane to two or more reactor concepts:

1) Design and evaluation methods
2) Crosscutting materials for advanced reactors
3) Energy conversion

The Very High-Temperature Reactor concept is being pursued in the United States under the NGNP program. The major aim of the NGNP program is to build and demonstrate advanced high-temperature reactor technology that is able to economically produce both hydrogen and electricity. The VHTR is believed to be the most suitable candidate and is the subject of U.S. research efforts. The first phase of project development will lead to the design, construction, and operation of a demonstration facility consisting of an advanced nuclear reactor coupled with a hydrogen production plant. New research projects focus on validating reactor physics and core design analyses tools, developing and validating reactor thermal-hydraulic and mechanical design analyses tools, performing materials research and power-conversion unit assessments, and conducting safety and risk analysis. The scope of these projects includes reactor design; system design, analysis, and optimization methodologies; and fuel development and qualification. The longer term NGNP research objectives are to 1) demonstrate a full-scale prototype unit in the 2021 timeframe, 2) demonstrate the Brayton Cycle for the full-scale unit, 3) test the safety capabilities of an advanced VHTR, 4) obtain a construction and operations license from the Nuclear Regulatory Commission (NRC), and 5) support the development of other technologies involving hydrogen applications.

Sodium-Cooled Fast Reactor. The SFR is the leading candidate design for the advanced burner reactor (ABR) being developed under GNEP. As such, research being conducted on this reactor concept is described in the AFCI program area below.

Supercritical Water-Cooled Reactor. This research area is demonstrating the technical feasibility of a light water reactor (LWR) design operating with a supercritical water coolant, i.e., water above the thermodynamic critical pressure and temperature point. The focus of this research includes three main areas: 1) the evaluation of dynamic power/flow instabilities, 2) corrosion and stress-corrosion cracking testing of materials for the core and vessel internals, and 3) the investigation of basic thermal and heat transfer phenomena for the reactor. The United States is not currently pursuing this technology. In FY 2007, domestic SCWR activities focused on monitoring

international R&D efforts and participating in related international forums.

Lead-Cooled Fast Reactor. The objective of this research is to produce a small, proliferation-resistant nuclear energy system for deployment in remote locations and in developing countries. The LFR system has a closed fuel cycle and uses a fast-spectrum lead or lead-bismuth liquid metal coolant. This design allows for efficient conversion of uranium and management of actinides. R&D efforts will define and select the reference system, prepare a defensible safety case, and license a demonstration reactor system; however, the United States is not currently pursuing this technology. In FY 2007, U.S. LFR activities focused on monitoring international R&D efforts and participating in related international forums.

Gas-Cooled Fast Reactor. The objective of this program is to develop a safe and sustainable helium-cooled fast reactor that has a closed fuel cycle, is highly efficient, and is capable of producing both electrical power and hydrogen. Preliminary design concepts use a direct-cycle Brayton Cycle secondary power conversion system. The fast spectrum and full recycle of actinides minimize the production of radioactive waste. Research for this reactor concept includes defining design features (fuel, coolant, and unit power); designing safety systems for decay heat removal; identifying/testing fuel and core materials capable of high-temperature operation, including developing fuels with high fission product confinement and reasonable burnup and fluence; and developing fabrication techniques. NERI project researchers previously identified possible passive/semi-passive safety systems, conducted materials testing of CO_2, and identified candidate high-temperature fuels. The United States is not currently pursuing this technology. In FY 2007, GFR activities focused on monitoring international R&D efforts and participating in related international forums.

Molten Salt Reactor. MSRs can be used for producing electricity, hydrogen, or fissile fuels, as well as actinide burning. In this design, the nuclear fuel is dissolved directly in a molten fluoride salt coolant which circulates throughout the primary system. Energy is transferred to a clean molten salt intermediate heat transport loop, then a high-temperature Brayton power conversion cycle. As the NGNP uses similar liquid salt technology in the hydrogen production loop, many areas of research are shared, such as Brayton power cycles, compact heat exchangers (HXs), and carbon composite materials. Therefore, the United States is not pursuing this technology as a separate area of research.

Design and Evaluation Methods. Analytical methods, modeling techniques, computer codes, and databases must be developed for Generation IV plants. In addition, research needs to be performed to evaluate the economic feasibility of these new plants and to ensure the proliferation resistance and physical protection to the public. Major activities under this research area include 1) improving the NGNP analytical capabilities and then validating these capabilities, 2) defining fast reactor modeling requirements for the GFR and LFR designs, and 3) improving the Generation IV evaluation methodologies and selecting preferred options. Other activities include 1) identifying phenomena and parameters to be included in thermal/hydraulic and safety analysis codes and 2) improving Monte Carlo and deterministic methods for neutronic, fuel depletion, and material damage analyses.

Materials. Projects in this area include selecting, developing, and qualifying structural materials and other components necessary to design and construct advanced reactors, such as the NGNP, GFR, SCWR, and LFR reactor systems and their energy conversion systems. Specific cross-cutting activities applicable to all designs will be performed, including 1) designing a test facility, then initiating low-flux and high-flux, high-temperature irradiations; 2) establishing a database of candidate materials for high temperature and radiation service, then performing studies to identify mechanical properties; 3) preparing documents for alloys 316FR and 617 to initiate American Society of Mechanical Engineers (ASME) codification; 4) performing microstructural analysis and modeling for materials of interest; and 5) developing a high-temperature design methodology for materials/applications of interest.

Energy Conversion. Projects in this area will focus on research for both the supercritical carbon dioxide Brayton cycle and the high-temperature helium Brayton cycle. Objectives associated with the supercritical carbon dioxide Brayton cycle include 1) completing system design and economic assessment; 2) performing an experiment to validate key features; and 3) conducting research on engineering seals, materials, HXs, and piping and duct work. A demonstration experiment and simulation model are also planned to determine plant characteristics, performance, and the supercritical cycle dynamic response. For the high-temperature helium Brayton cycle, project goals include engineering analyses, designing HXs and turbo-machinery, and constructing a small-scale demonstration experiment.

Advanced Fuel Cycle R&D

The AFCI program focuses on developing advanced fuels, spent fuel treatment techniques, and transmutation technologies to facilitate the transition towards a sustainable advanced nuclear fuel cycle. In FY 2007, AFCI focused on near-term activities to support the most promising technologies developed to date. The chief goals of AFCI are to reduce the amount of high-level radioactive waste requiring geologic disposal, to reduce accumulated plutonium from the PUREX processing of commercial spent fuel, and to extract more useful energy from material that normally would be disposed of as waste. The program will develop fuel systems and create enabling fuel technologies such as fuel, cladding, waste forms, separations, and disposal technology to decrease spent fuel volume; separate long-lived, highly radiotoxic elements; and recover valuable energy from spent fuel. The technologies will support both existing and forthcoming nuclear energy systems.

Spent fuel treatment and recycling are critical to support the expansion of proliferation-resistant nuclear power. This multifaceted program involves recycling spent fuel, fabricating fuel assemblies containing the removed long-lived actinides and transuranics (TRUs), burning the assemblies in a fast reactor, and developing more benign waste disposal technologies for the remaining radioisotopes and process wastes. Resulting technologies from this work will satisfy requirements for a controlled, proliferation-resistant nuclear materials management system. Planned NERI research efforts related to this program will focus on the following technologies and research areas:

- SFR
- Separations
- Fuels
- Transmutation science and engineering
- Systems analysis
- Demonstration facilities

Sodium-Cooled Fast Reactor. The SFR system features a liquid metal fast-spectrum reactor that can operate on recycled spent fuel to help manage high-level radioactive wastes, particularly plutonium and other actinides. With innovations to reduce capital cost, the mission can extend to economic electricity production. The SFR can also lead to sustainable energy production, given the proven capability of sodium reactors to utilize almost all of the energy in natural uranium. Activities under this research area focus on comparative technical and economic studies of various SFR designs, fuel development activities, and advanced modeling and simulations techniques. Other topics include selection and testing of alloy materials and conceptual design studies of supercritical carbon dioxide secondary plant systems.

Separations. Research in this area includes the development of aqueous and pyrochemical separations technologies, advancement of spent fuel treatment processes, improvement of waste storage forms, treatment of spent fuel from the experimental breeder reactor (EBR-II) in preparation for disposal, and conceptual planning of future spent fuel treatment plants and advanced processing technologies. The current focus is on improving separations processes for LWR spent fuel reprocessing, fabricating waste/storage forms suitable for storage in a repository; demonstrating TRU extraction processes; accelerating the EBR-II blanket treatment with advanced processing technology; demonstrating advanced LWR spent fuel processing techniques; demonstrating americium/curium separations processes; and developing storage/disposal forms for uranium, plutonium-neptunium, americium-curium, and cesium-strontium.

Fuels. This research area is developing advanced fuel for LWRs, Generation IV reactors, and dedicated transmuter facilities. Researchers will model, fabricate, characterize, and test the fuel of various compositions. Associated safety analyses, development of remote fuel fabrication techniques, and advanced clad materials are included in the scope. Current NERI research projects focus on irradiation and post-irradiation examination (PIE) of fuels for the ABR.

Transmutation Science and Engineering. This research area is studying the use of the transmutation process to convert long-lived radioactive isotopes into short-lived isotopes via neutron capture or fission. This research supports accelerator-driven systems, transmuter materials and coolants, and transmutation physics. The primary purpose is to develop an engineering basis for the transmutation of plutonium and minor actinides. Current research focuses on 1) continued measurements and evaluations of higher actinides to reduce transmutation uncertainty, 2) new irradiations at the PHENIX reactor in France, 3) examination of irradiated materials from the Fast Flux Test Facility (FFTF) and the European Paul Scherrer Institute (PSI) facility, 4) development of an intense fast neutron source for materials testing, and 5) development of alloys and surface treatment to increase the corrosion resistance of lead-bismuth eutectic (LBE).

Systems Analysis. This area includes broad-based systems studies and analyses such as 1) transmutation systems and integrated model development; 2) fuel cycle proliferation resistance; 3) economic analyses; and 4) material transportation, storage, and disposal analyses. The objectives of this research are to analyze fuel cycle infrastructure needs, to supply recommendations on fuel types and reactor systems from the perspective of the overall fuel cycle, and to perform analyses to assist DOE in determining the need for a second spent fuel repository.

Demonstration Facilities. An Advanced Fuel Cycle Facility will be designed and constructed to provide enhanced separations and fuels research under the GNEP program. Powerful new simulation and modeling tools will predict reactor and fuel behavior in order to reduce the need for lengthy irradiation experiments. The initial focus of these tests is on the treatment of spent nuclear fuel from existing LWRs. Later, both aqueous and electrochemical processing of fast reactor spent fuel will be studied. Lastly, a sodium-cooled ABR will serve as the focal point for transmutation development. SFR technology will demonstrate the transmutation of both spent LWR fuel and fast reactor recycle fuel. R&D will also continue in the areas of advanced aqueous and electrochemical processing technologies, waste and storage forms, and metal and oxide transmutation fuels.

Nuclear Hydrogen Initiative

The mission of the ***Nuclear Hydrogen Initiative*** is to develop hydrogen production technologies that are fueled by nuclear energy. The goal is to demonstrate hydrogen production that is compatible with nuclear energy systems through scaled experiments, then to couple an engineering-scale demonstration plant with a Generation IV demonstration facility by 2019. NERI research that is planned under this initiative includes projects that are associated with thermochemical cycles, high-temperature electrolysis, and reactor-hydrogen production process support systems.

Thermochemical Cycles. The focus of this research area is to develop thermochemical cycles for hydrogen production that are suitable for nuclear application, such as sulfur-based cycles and alternative cycles. Researchers provide flowsheet methodology for analyzing and comparing the thermochemical cycles as well as high-temperature interface requirements for the HXs and materials. These processes offer the potential for high-efficiency hydrogen production in commercial quantities once technical issues are resolved. Cycles have been selected for development based on a comparison of thermochemical cycles using a consistent analysis methodology. Research planned for the upcoming years will consist of laboratory-scale demonstrations of candidate processes for Sulfur-Iodine and Hybrid Sulfur, alternative thermochemical process assessment, and enhancement of membranes to increase process efficiency. Projects will include materials testing, control system design, and cost evaluations.

High-Temperature Electrolysis (HTE). HTE uses electricity to produce hydrogen from steam. This technology has the potential for higher efficiencies than commercial processes currently available. This research area seeks to reduce the cost of manufacturing electrolytic cells and components and to increase the useful lifetime of these components, thereby producing hydrogen at the lowest possible cost. Research activities include cell and stack experiments, modeling of plant and cell dynamics, and design of plants beginning with a laboratory unit and later scaling up to include a pilot-scale experiment followed by the demonstration and construction of commercial units. Materials analysis for cells, HXs, and separations will also be performed under this research area. Accomplishments to date include completing HTE cell and stack/module testing, completing the design, and then assembling components for the integrated laboratory test unit in 2007. The design and fabrication of a pilot-scale experiment will be completed by 2013 in parallel with conducting tests for high-temperature HXs and separations.

Reactor-Hydrogen Production Process Support Systems. The purpose of this research is to develop and optimize high-temperature HX designs (optimizing HX type, operating conditions, efficiency, and material qualification) and designs of support systems. Program efforts over the next two years will explore laboratory-scale HX development for a variety of high-temperature hydrogen production processes, including design; short- and long-term materials testing; fabrication; and system support, including assessment of the process, infrastructure, and facilities requirements for the pilot plant and the balance-of-plant (BOP) design.

Following is a graphic that summarizes key features of the NERI program. Section 6 explains the work scope associated with these NERI research areas in more detail and presents progress reports for the FY 2005, FY 2006, and FY 2007 projects, along with brief abstracts of the FY 2007 NERI-C projects that were recently awarded.

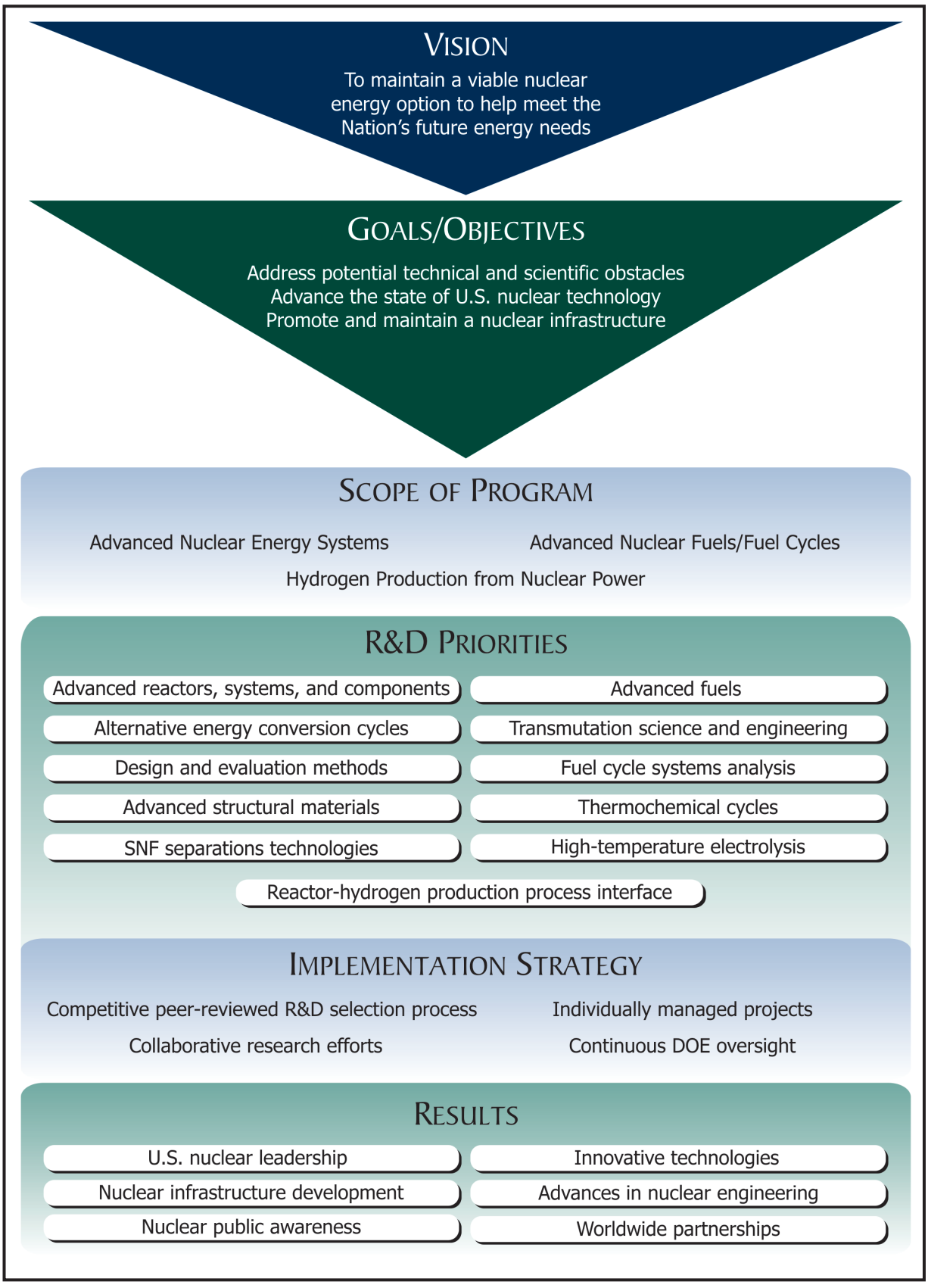
VISION
To maintain a viable nuclear energy option to help meet the Nation's future energy needs
GOALS/OBJECTIVES
Address potential technical and scientific obstacles
Advance the state of U.S. nuclear technology
Promote and maintain a nuclear infrastructure
SCOPE OF PROGRAM
Advanced Nuclear Energy Systems
Advanced Nuclear Fuels/Fuel Cycles
Hydrogen Production from Nuclear Power
R&D PRIORITIES
Advanced reactors, systems, and components
Advanced fuels
Alternative energy conversion cycles
Transmutation science and engineering
Design and evaluation methods
Fuel cycle systems analysis
Advanced structural materials
Thermochemical cycles
SNF separations technologies
High-temperature electrolysis
Reactor-hydrogen production process interface
IMPLEMENTATION STRATEGY
Competitive peer-reviewed R&D selection process
Individually managed projects
Collaborative research efforts
Continuous DOE oversight
RESULTS
U.S. nuclear leadership
Innovative technologies
Nuclear infrastructure development
Advances in nuclear engineering
Nuclear public awareness
Worldwide partnerships

4. NERI Accomplishments

This section discusses the program's progress in attracting research proposals, awarding annual R&D funding, and successfully completing NERI-funded research projects.

Project Awards

In FY 1999, DOE's NERI program received 308 R&D proposals from U.S. universities, national laboratories, and industry in response to its first solicitation. The initial FY 1999 procurement was completed with the award and issue of grants and laboratory work authorizations for 46 R&D projects. The research represented participants from 45 organizations, including 11 foreign R&D organizations. The total cost of these 46 research projects for the three-year period was approximately $52 million.

Similar progress was made in FY 2000–2002, with an additional 47 NERI projects awarded. The total cost of these 47 research projects for the three-year period was approximately $58 million, shared among 20 U.S. universities, 10 national laboratories, 18 private businesses, and 7 foreign R&D organizations. No new NERI projects were awarded in FY 2003 or 2004.

In FY 2005, 35 projects were initiated under the newly revised program focus, as well as an additional 25 projects in FY 2006. The total investment in these projects over their three-year term is $32.1 million, distributed among 37 U.S. universities, 7 national laboratories, and 4 corporations. In addition, 1 university, 1 laboratory, and 3 corporations are participating on strictly a cost-share basis. Two foreign educational institutions participate, but are ineligible for U.S. funding.

DOE awarded 22 projects in FY 2007, involving 20 U.S. universities, 5 national laboratories, 2 U.S. businesses, and 1 international laboratory collaborator. This represents an $11.4 million federal government commitment to nuclear R&D during the three-year lifetime of these projects. With each university contributing an additional 20 percent cost-share, the total funds directed towards nuclear R&D increases to $14.4 million.

There are 11 newly awarded NERI projects involving consortia (NERI-C) for FY 2007, distributed among 38 U.S. universities, 7 national laboratories, and 1 U.S. business. These 11 projects comprise a total of $30.7 million for the three-year period.

Funding History

Congress appropriated annual funding for NERI in FY 1999 through 2004 as a separate budget line item in the Energy and Water Development Appropriations Act. The U.S. government invested over $118 million to fund NERI research projects during the first six years of the NERI program. Figure 1 illustrates the cumulative number of research projects awarded through FY 2004 in each of the four original R&D areas, while Figure 2 shows the distribution of this funding among the national laboratories, U.S. universities, and industry.

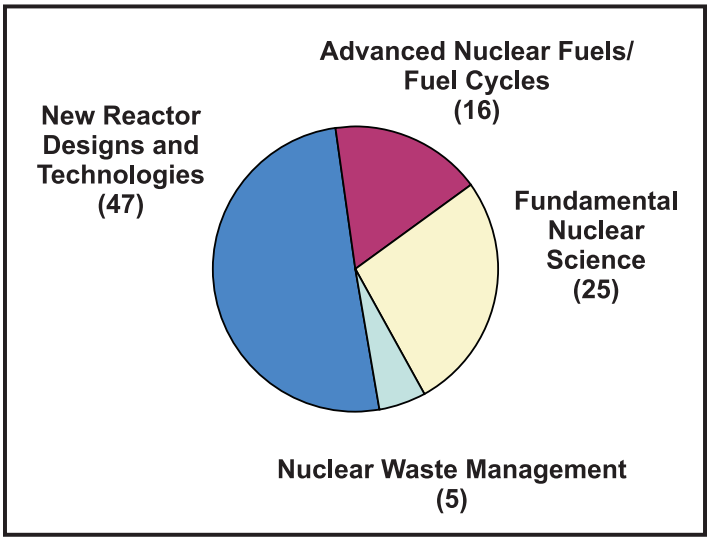

Figure 1. Distribution of FY 1999–2004 NERI Projects by R&D area.

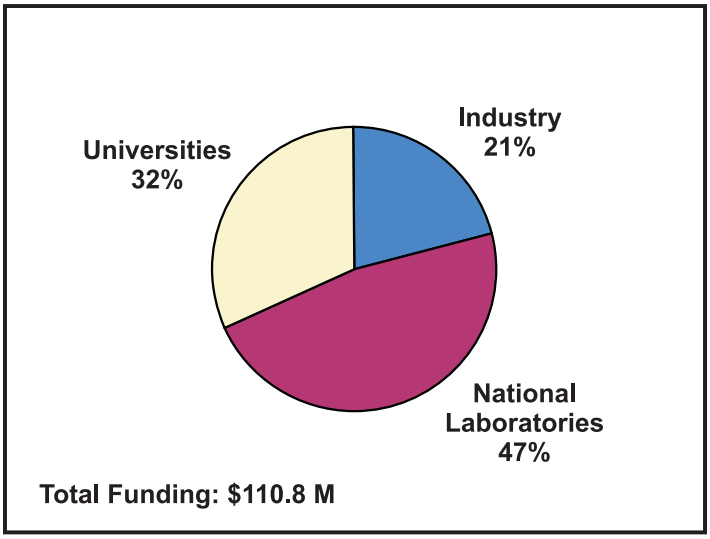

Figure 2. Recipients of NERI research funds from 1999–2004.

DOE does not fund foreign participants as part of the NERI program. Their participation has been supported by the foreign organizations interested in the research being conducted. Although the PIs are responsible for soliciting such support, foreign participation in NERI projects is contingent upon DOE approval.

NERI was refocused in FY 2005 to directly support the goals and objectives of the Generation IV, AFCI, and NHI programs as well as to emphasize the leadership of university research programs.

Figure 3 illustrates the effect of this new program emphasis, showing a significant redistribution in NERI research funds benefiting universities. Figure 4 shows the distribution of NERI research funds in FY 2005–2007 by R&D program area. Figure 5 notes the division of projects awarded in FY 2005 through 2007 by program area.

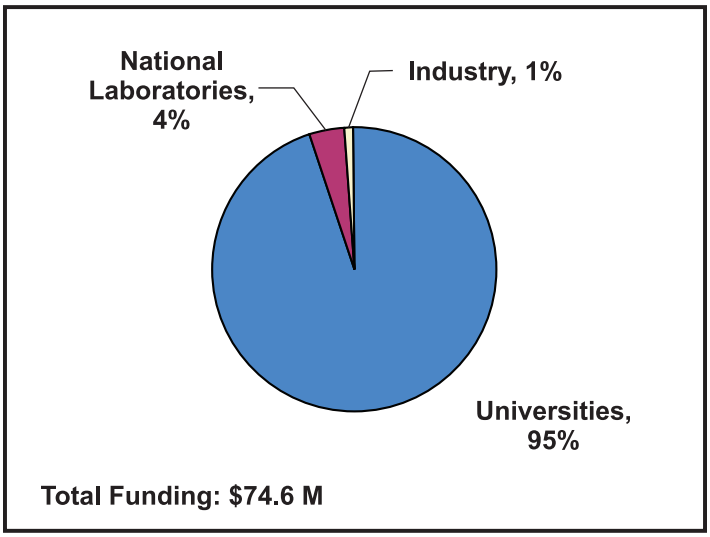

Figure 3. Distribution of NERI research funds by recipient from FY 2005–2007.

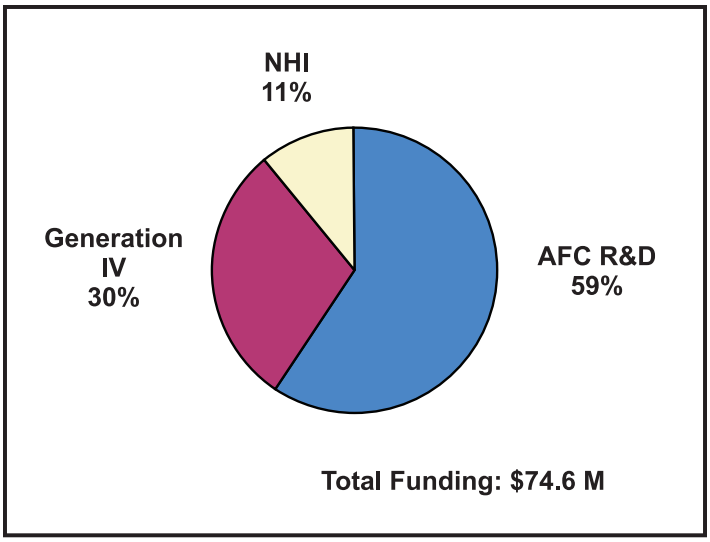

Figure 4. Distribution of NERI research funds by R&D program area.

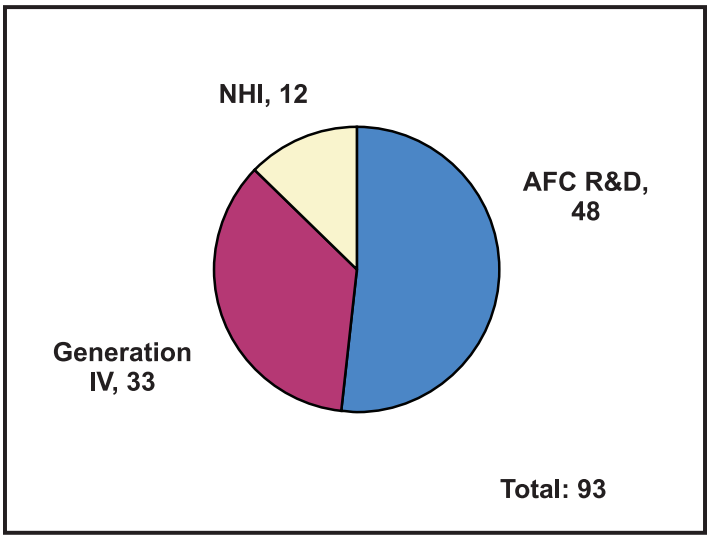

Figure 5. Distribution of FY 2005–2007 NERI projects by R&D program area.

NERI Participants

NERI research participants in 2007 included 64 U.S. universities, 8 national laboratories, 39 private businesses, and 31 foreign organizations. The participating organizations are provided in the following table.

U.S. Universities

Abilene Christian University
Alabama A&M University
Arizona State University
Boise State University
Brigham Young University
California Institute of Technology
California Polytechnic State University
California State University, Northridge
Clemson University
Colorado School of Mines
Columbia University
Cornell University
Georgia Institute of Technology
Hunter College (CUNY)
Idaho State University
Illinois Institute of Technology
Iowa State University
Johns Hopkins University
Kansas State University
Massachusetts Institute of Technology
New Mexico State University
North Carolina State University
Northwestern University
Ohio State University
Ohio University
Oregon State University
Pennsylvania State University
Purdue University
Rensselaer Polytechnic Institute
South Carolina State University
State University of New York, Stony Brook
Tennessee Technological University
Texas A&M University
Tulane University
University of Akron
University of Arizona
University of California, Berkeley
University of California, Davis
University of California, Los Angeles
University of California, Santa Barbara
University of Chicago
University of Cincinnati
University of Florida
University of Idaho
University of Illinois, Chicago
University of Illinois, Urbana-Champaign
University of Kentucky
University of Maryland, College Park
University of Michigan
University of Missouri, Columbia
University of Missouri, Rolla
University of Nevada, Las Vegas
University of New Mexico
University of North Carolina, Wilmington
University of Notre Dame
University of South Carolina
University of Tennessee
University of Texas, Austin
University of Virginia
University of Wisconsin, Madison
Utah State University
Virginia Polytechnic Institute and State University
Washington State University
Washington University, St. Louis

U.S. DOE National Laboratories

Argonne National Laboratory
Brookhaven National Laboratory
Idaho National Laboratory
Los Alamos National Laboratory
Oak Ridge National Laboratory
Pacific Northwest National Laboratory
Sandia National Laboratories
Savannah River National Laboratory

Industrial Organizations

ABB-Combustion Engineering
Aspen Technology, Inc.
Bechtel
Burns & Roe Enterprises
CEGA Corporation
Dominion Generation
Duke Engineering
Egan & Associates
Electric Power Research Institute
Entergy Nuclear, Inc.
Florida Power and Light
Fluent, Inc.
Framatome ANP, Inc.
Gamma Engineering
General Atomics
General Electric
General Electric Global Research Center
Global Nuclear Fuel
Hitachi
Materials Engineering Associates
McDermott Technologies
Newport News Shipbuilding

Northern Engineering and Research
Pacific Sierra
Pacific Southern Electric and Gas
Panlyon Technologies
Rockwell Science Center
Siemens Power Corporation
Special Metals, Inc.
SRI International
Stress Engineering Services, Inc
Studsvik of America
Swales Aerospace
Tennessee Valley Authority
TransWare Enterprises, Inc.
United Technologies Center
(n,p)Energy, Inc.
Veridian
Westinghouse Electric Company LLC

International Collaborators

Atomic Energy of Canada (Canada
Ben Gurion University (Israel)
British Nuclear Fuel (United Kingdom)
Chosun University (Korea)
Commissariat a l'énergie atomique (France)
Framatome (France)
Forschungszentrum (Germany)
Hitachi (Japan)
Imperial College of London (United Kingdom)
Imperial College of Science, Technology, and Medicine (United Kingdom)
Institute of Physics and Power Engineering (Russia)
Italian National Agency for New Technologies, Energy, and Environment (ENEA)
Japan Nuclear Cycle Development Institute (Japan)
Japan Atomic Power Company (Japan)
Korea Atomic Energy Institute (Korea)
Kurchatov Institute (Russia)
Mitsubishi Heavy Industries (Japan)
National Atomic Energy Commission and University of Cuyo (Argentina)
Organisation for Economic Co-operation and Development Nuclear Energy Agency (OECD/NEA) (France)
PBMR, Ltd. (South Africa)
Polytechnic Institute of Milan (Italy)
Studsvik Scanpower Inc. (Sweden)
The Royal Institute of Technology (Sweden)
Tokai University (Japan)
Tokyo Institute of Technology (Japan)
Toshiba (Japan)
Toyama University (Japan)
University of Manchester (United Kingdom)
University of Rome (Italy)
University of Tokyo (Japan)
VTT Manufacturing Technology (Finland)

5. NERI and U.S. Universities: Advancing the Goals of Nuclear R&D Programs

Focus on Universities

One of NERI's long-term goals is to maintain the country's leading position in nuclear energy research by improving the nuclear science and engineering infrastructure. In order to achieve this long-range goal, NERI is focused on cultivating research partnerships with universities across the United States. This helps educational institutions remain at the forefront of science education and research, advances the important work of existing nuclear R&D programs, and serves as training for the next generation of nuclear scientists who will carry on the groundbreaking work being performed at national laboratories, universities, and private corporations. Funding creative research ideas at the Nation's universities and colleges serves another purpose as well—it helps solve important issues that the private sector is unable to fund alone due to the high-risk nature of the research and/or the extended period before a return on investment is realized.

Participants in NERI's initial planning workshop recommended that NERI be viewed as a "seed program" where new nuclear-related technological and scientific concepts could be investigated. Based on this philosophy, NERI has provided universities and colleges with a competitive, peer-reviewed research program that allows faculty and students an opportunity to conduct innovative research in nuclear engineering and related areas. Of the 186 projects awarded through FY 2007, 88 percent involved U.S. colleges and universities as lead investigators or collaborators. To date, a total of 64 national universities and colleges have participated in NERI projects.

NERI has provided U.S. universities and colleges with the opportunity to work closely with industry and DOE national laboratories and has introduced these researchers to other nuclear energy-related government programs. In addition to research related to the AFCI, Generation IV, and NHI programs, NERI's activities are coordinated with other relevant DOE energy research programs in the Office of Science, the Office of Energy Efficiency and Renewable Energy, and the Nuclear Regulatory Commission. Furthermore, the Department leverages NERI program resources by encouraging a no-cost collaboration with international research organizations and nuclear technology agencies. In this way, universities are also given the opportunity to gain experience with international research interests and capabilities.

Student Participation

One great success of NERI and other DOE programs is that nuclear-related educational opportunities at the universities have significantly increased. Universities have benefited from increased research dollars which have served as incentives for new student recruitment. As a result of this involvement, student interest in nuclear engineering has been revitalized. In 1998, only 500 students were enrolled in U.S. universities seeking degrees in nuclear engineering. According to a survey performed for DOE in March 2006 by the Oak Ridge Institute for Science and Education (ORISE), approximately 2,000 students—1,000 undergraduates and another 1,000 graduate/doctoral students—are currently enrolled in nuclear engineering programs.

Approximately 685 undergraduate, graduate, and doctorate students have participated in NERI projects since the program's inception. Figure 6 shows how student participation has changed with time. In addition, numerous post-doctoral fellows at universities have been involved in NERI research projects. In FY 2007 alone, 94 undergraduate, 143 graduate, and 106 doctoral students participated in NERI R&D.

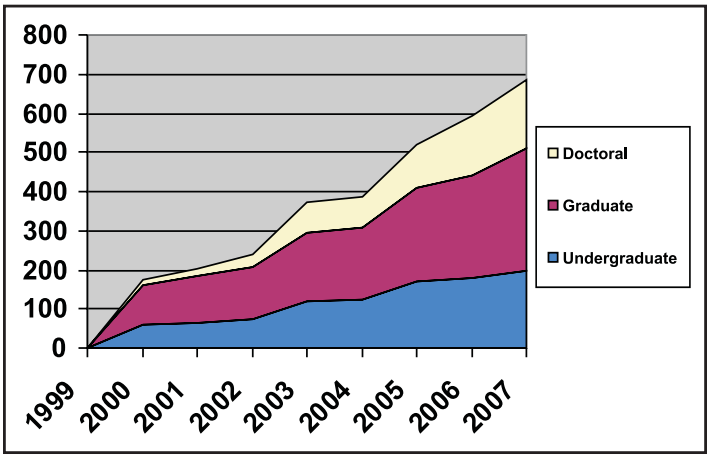

Figure 6. Cumulative NERI Student Participation Profile—FY 1999 through FY 2007 NERI Projects.

Over the past few years, graduates of these programs have had higher than normal grade point averages, showing that these programs are training highly qualified individuals who sustain the future growth of the nuclear power industry. Figure 7 provides a map and complete listing of the 64 universities and colleges that have participated in NERI since the program's inception.

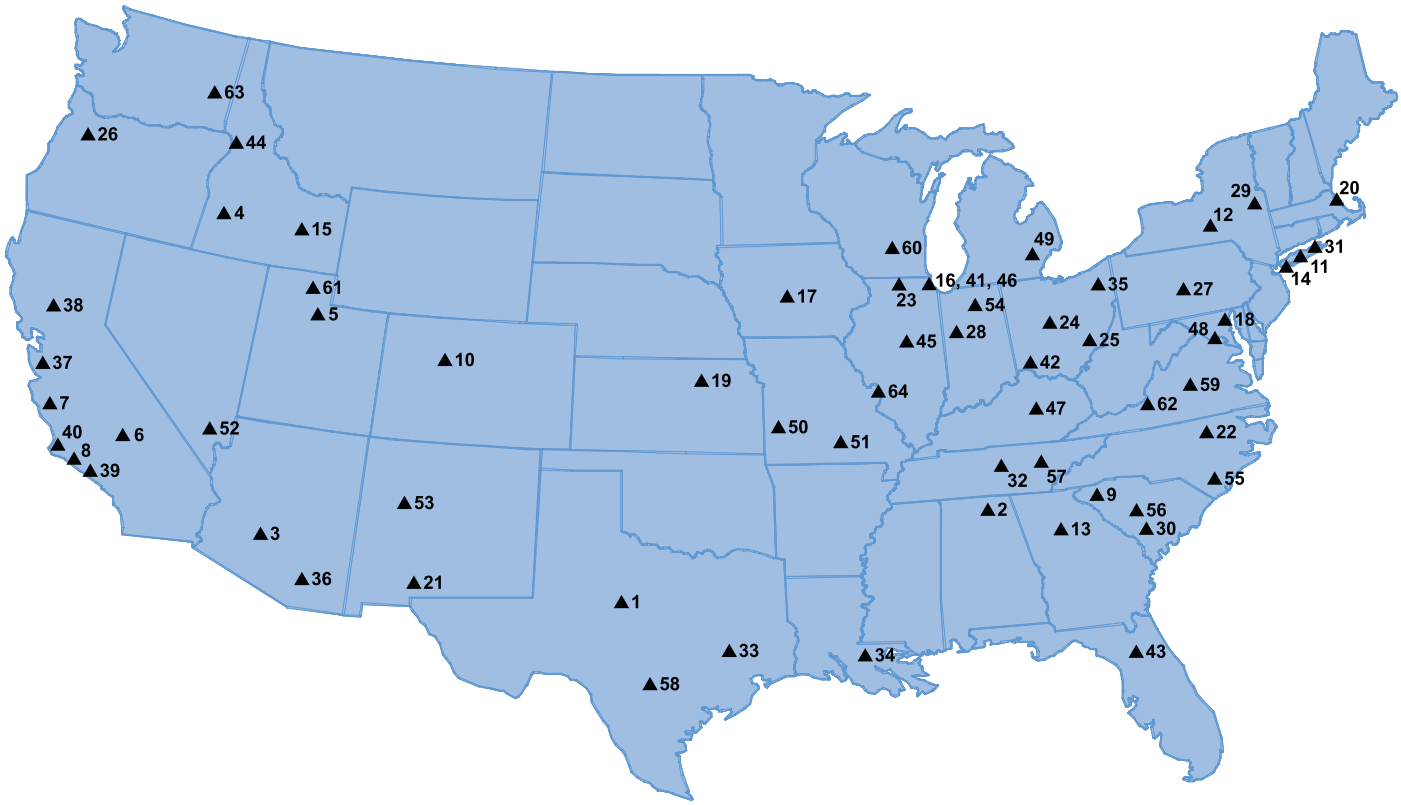

UNIVERSITY KEY

1 Abilene Christian University
2 Alabama A&M University
3 Arizona State University
4 Boise State University
5 Brigham Young University
6 California Institute of Technology
7 California Polytechnic State University
8 California State University, Northridge
9 Clemson University
10 Colorado School of Mines
11 Columbia University
12 Cornell University
13 Georgia Institute of Technology
14 Hunter College (CUNY)
15 Idaho State University
16 Illinois Institute of Technology
17 Iowa State University
18 Johns Hopkins University
19 Kansas State University
20 Massachusetts Institute of Technology
21 New Mexico State University
22 North Carolina State University
23 Northwestern University
24 Ohio State University
25 Ohio University
26 Oregon State University
27 Pennsylvania State University
28 Purdue University
29 Rensselaer Polytechnic University
30 South Carolina State University
31 State University of New York, Stony Brook
32 Tennessee Technological University
33 Texas A&M University
34 Tulane University
35 University of Akron
36 University of Arizona
37 University of California, Berkeley
38 University of California, Davis
39 University of California, Los Angeles
40 University of California, Santa Barbara
41 University of Chicago
42 University of Cincinnati
43 University of Florida
44 University of Idaho
45 University of Illinois, Urbana-Champaign
46 University of Illinois, Chicago
47 University of Kentucky
48 University of Maryland, College Park
49 University of Michigan
50 University of Missouri, Columbia
51 University of Missouri, Rolla
52 University of Nevada, Las Vegas
53 University of New Mexico
54 University of Notre Dame
55 University of North Carolina, Wilmington
56 University of South Carolina
57 University of Tennessee
58 University of Texas, Austin
59 University of Virginia
60 University of Wisconsin
61 Utah State University
62 Virginia Polytechnic Institute and State University
63 Washington State University
64 Washington University

Figure 7. Locations of universities and colleges participating in NERI projects.

6.0 Project Summaries and Abstracts

6.1 Generation IV Nuclear Energy Systems Initiative

There are 31 NERI projects currently being performed under the Generation IV Nuclear Energy Systems Initiative. Fifteen of these projects were awarded in FY 2005, 6 in FY 2006, 8 in FY 2007, and 2 new NERI-C projects in FY 2007.

Work under Generation IV focuses on developing new reactor systems to be deployed during the next 20 years. As discussed in Chapter 3, these systems will achieve high burnup using transmutation and recycled fuel, allowing for efficient use of domestic uranium resources and minimizing radioactive waste. Advances in safety and physical protection will guard against possible acts of terror or the ability to divert nuclear materials, helping to ensure public confidence in nuclear technology.

During FY 2007, researchers worked on projects spanning most of the Generation IV program elements. In the area of Advanced Gas Reactor (AGR) fuel development, they are developing on-line failure monitoring and improving analytical techniques. Design and evaluation projects focus on improving modeling capabilities, neutronic analysis, thermal-hydraulic/heat transfer analysis, model uncertainty evaluations, and risk assessment techniques. Energy conversion projects target nuclear heat transport and supercritical CO_2 systems. Materials evaluations continue to occupy a large percentage of the Generation IV program, with studies on radiation behavior, improvement of corrosion resistance, development of advanced ceramics and metal alloys, and improvement of analytical modeling capabilities. Research is being conducted specific to four reactor technologies: the LFR, the SCWR, the VHTR, and the SFR. These projects involve lead and lead-bismuth corrosion for the LFR, thermal-hydraulic modeling and materials evaluation for the SCWR, and design analysis methods and materials development for the VHTR. Projects related to the SFR can be found in Section 6.2, as they are currently funded under AFCI.

Planned NERI research efforts under the two newly awarded FY 2007 consortia projects related to the Generation IV initiative will focus on NGNP and cross-cutting materials-related activities. These projects will involve the VHTR and structural materials.

A summary of each project being performed under this initiative follows.

NUCLEAR ENERGY RESEARCH INITIATIVE

Project Summaries and Abstracts

FY 2005 Project Summaries

FY 2006 Project Summaries

Nuclear Energy Research Initiative

FY 2007 Project Summaries

FY 2007 NERI-C Project Abstracts

Nuclear Energy Research Initiative

In-Situ X-ray Spectroscopic Studies of the Fundamental Chemistry of Pb and Pb-Bi Corrosion Processes at High Temperatures: Development and Assessment of Composite Corrosion-Resistant Materials

PI: Carlo U. Segre, Illinois Institute of Technology

Collaborators: None

Project Number: 05-028

Project Start Date: January 2005

Project End Date: September 2009

Research Objectives

This project will characterize the corrosion tolerance of various materials for use in advanced liquid metal reactors. Researchers will probe surface interactions with lead (Pb) and lead-bismuth eutectic (LBE) liquid metal coolant at temperatures up to 1,000°C. A thin film of coolant, i.e., a few atomic layers, will be deposited on the surface before heating. This will enable researchers to study the solid–liquid interface between the candidate composite materials and the liquid metal coolants.

Researchers will probe the coolant with X-ray absorption spectroscopy (XAS) as a function of temperature and time to determine how it reacts with the solid underneath and will utilize a unique resource, the undulator beamline, available at the Materials Research Collaborative Access Team. These real-time *in-situ* methods for corrosion characterization methods will enable researchers to directly observe the fundamental chemical mechanisms that lead to corrosion.

In addition, the team will study various promising candidate materials as well as materials whose surfaces have been modified by applying the novel process of ionized plasma deposition (IPD). The IPD process has recently been developed and promises to revolutionize the development of composite coatings and to create surface treatments not possible by simple deposition techniques. IPD can impregnate a substrate material with a coating designed to have a specific composition, thickness, penetration, and nanostructure.

The following tasks will be conducted as part of this research effort:

- Develop techniques for the deposition of thin coolant layers onto a substrate, heat treatment procedures, and XAS measurement methodology
- Study coolant reaction with steel substrates and candidate materials such as molybdenum (Mo), tantalum (Ta), zirconium (Zr), silicon-carbide (SiC), and correlate data with conventional dip tests
- Apply IPD to prepare surface-modified steel samples and perform further in-situ and long-term static tests using the best candidate materials

Research Progress

In the 2006-3 run at the Advanced Photon Source, researchers used four days of beamtime to measure the 316 L stainless steel coated with Mo deposited by a commercial vendor. Figure 1 shows the data at the iron (Fe) edge for various temperatures and indicates that 1) the Mo film is not protecting the stainless steel and 2) the Mo foil is not adhering to the stainless steel at high temperatures. Using the sputtering system on loan from Argonne National Laboratory (ANL), the team will deposit the Mo films

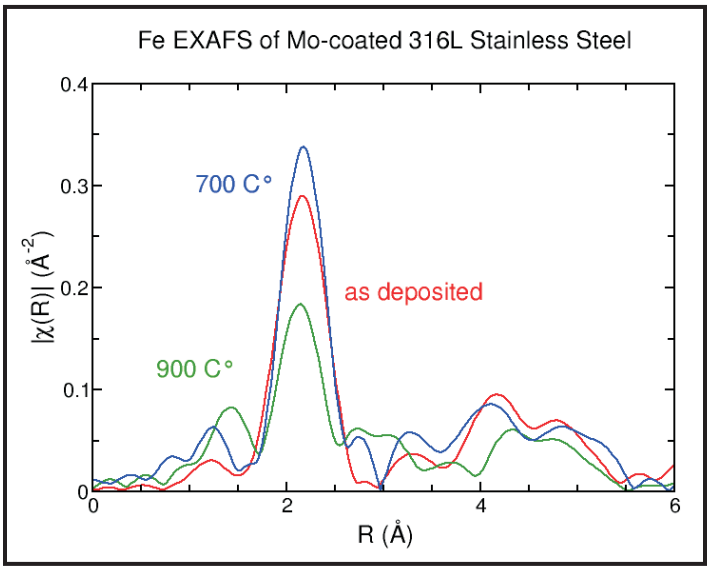

Figure 1. R-space EXAFS of Fe in Mo-coated 316 L stainless steel as deposited and after high temperature processing.

themselves from now on, taking care to properly clean and heat the substrate to ensure optimal adhesion.

The design of the new high-temperature measurement station is completed and parts are being procured. Figure 2 shows a schematic of this system. It includes a liquid nitrogen dewar for rapid cooling of the sample and a load lock for rapid exchange of samples without breaking containment. (The team expected this system to be in use for the 2007-3 experimental run, but the manufacturer has not yet delivered the final component: the sample heating stage.)

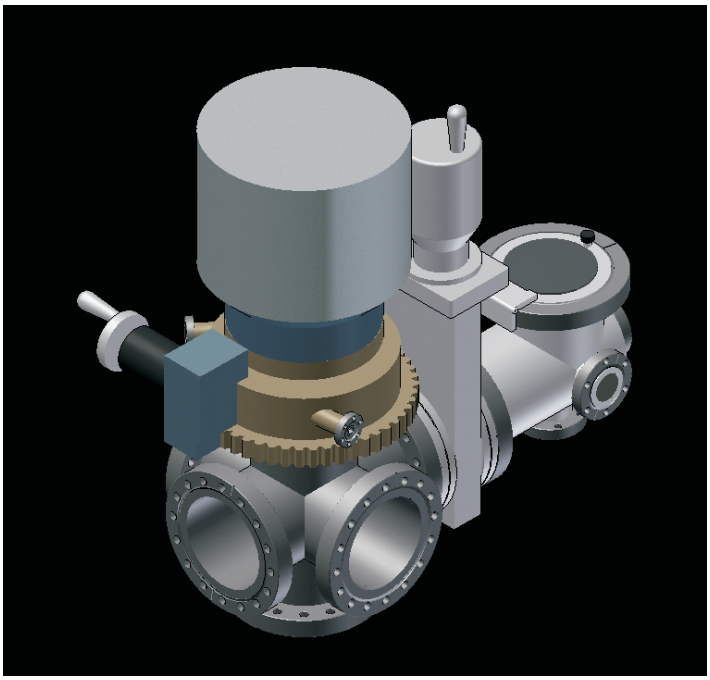

Figure 2. Design for new high temperature furnace.

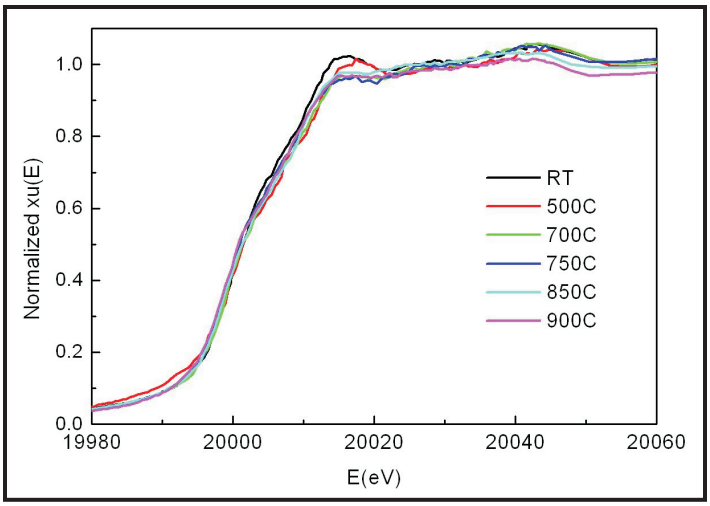

Figure 3. Comparison of Mo edge data from Mo/Pb samples at various temperatures.

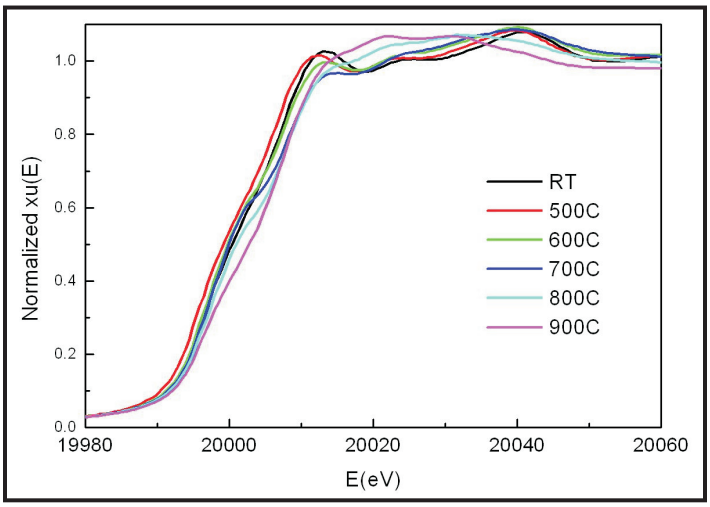

Figure 4. Comparison of Mo edge data from 316 L/Mo/Pb samples at various temperatures.

The major effort of this project has dealt with the data analysis of the X-ray Absorption Near Edge Structure (XANES) spectra. The near-edge structure is characteristic of an environment and valence state. The fits on the measured spectra with linear combinations of XANES spectra of known species, including MoO_2 and MoO_3, determine the proportion of each site/compound in the sample.

The comparison of Mo edge data at different temperatures taken from the Mo/Pb sample (see Figure 3) shows that the white line decreases as the temperature rises. Figure 4 shows a comparison of Mo edge data at different temperatures taken from a sample of SS316L/Mo/Pb. The edge shifts toward higher energy as the temperature rises.

The results of the least squares fitting to standards on both systems indicate that MoO_3 is present predominantly at intermediate temperatures below 750°C while MoO_2 dominates at the highest temperatures. Figure 5 shows the result of the XANES analysis for Mo metal coated by Pb. The dominant oxide species is MoO_2 at low temperatures. At intermediate temperatures, MoO_3 grows in and then disappears to be replaced by MoO_2 once again.

Figure 6 shows the results of the XANES analysis for the 316 L stainless steel with a 1 micron Mo sputtered film coated by Pb. The trend for MoO_3 is identical with a growth at intermediate temperatures followed by a conversion to MoO_2. The difference in this sample is that the Mo film is spalling from the 316 L surface and is therefore becoming more oxidized than was the Mo metal surface shown in Figure 5. The decline of the MoO_3 is well-correlated with the melting point of this compound. It is reasonable to suppose that, as it melts, MoO_3 becomes more susceptible to dissolution in the Pb overlay or conversion to MoO_2. With

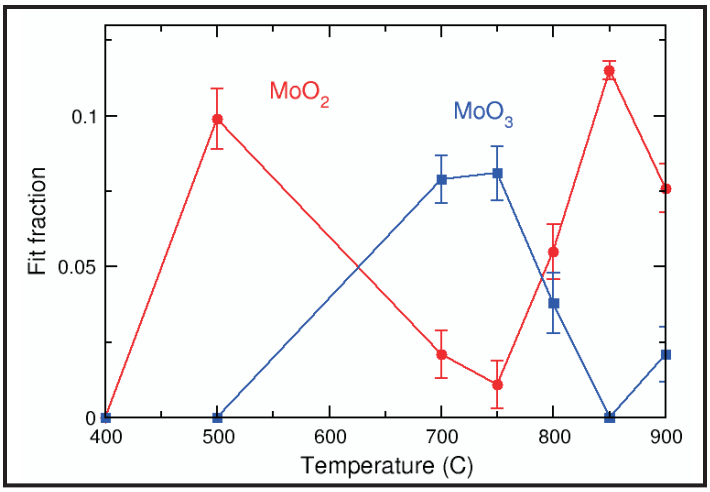

Figure 5. XANES fractions of MoO_2 and MoO_3 as a function of temperature for Mo metal coated by Pb.

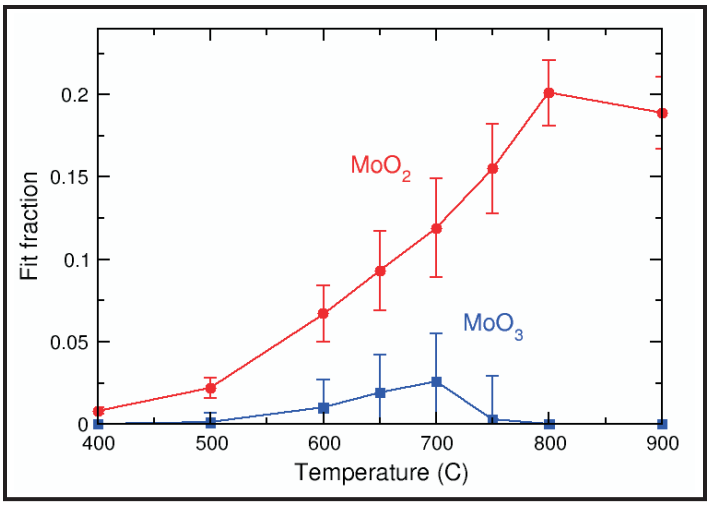

Figure 6. XANES fractions of MoO_2 and MoO_3 as a function of temperature for 316 L stainless steel with a sputtered Mo metal film coated by Pb.

the new chamber, researchers expect to be able to obtain more complete results, including the ability to determine whether the Mo is being dissolved in the Pb overlay.

Analysis of the data has been completed and a new general user proposal to study the titanium edge of ODS steels has been submitted. Analysis of the yttrium edge has shown that the commercial ODS steels have specific signatures in the XANES and EXAFS which differ from steels prepared by Oak Ridge National Laboratory (ORNL) and the University of California-Santa Barbara. The research team expects to take data on the titanium edge in the 2007-3 run at the Advanced Photon Source.

Planned Activities

Over the remaining time period, researchers will use the new furnace system, once it is delivered, to study Pb on Mo surfaces as well as on 316 L stainless steel.

Nuclear Energy Research Initiative

Detailed Reaction Kinetics for CFD Modeling of Nuclear Fuel Pellet Coating for High-Temperature Gas-Cooled Reactors

PI: Francine Battaglia, Rodney O. Fox, and Mark S. Gordon, Iowa State University

Collaborators: None

Project Number: 05-030

Project Start Date: April 2005

Project End Date: April 2008

Research Objectives

The objective of this research is to validate and improve computational models for coating uranium fuel pellets with carbon and silicon carbide (SiC) using the chemical vapor deposition (CVD) process in a spouting bed. Researchers will conduct a state-of-the-art computational study of the CVD process in order to further develop models of the reaction kinetics. This project will take a complementary approach using computational fluid dynamics (CFD) to model the CVD process and apply it as a tool for reactor design, scale-up, and optimization. The work will validate the computations with experimental data for the multiphase fluid mechanics and species chemistry predictions required to describe the CVD process. The specific tasks to achieve the objectives include the following:

1) Develop detailed reaction kinetics models of the gas-phase and surface molecule interaction using computational chemistry to predict surface coating rates
2) Implement the reaction kinetics using in-situ adaptive tabulation for complex chemistry and couple to the Multiphase Flow with Interphase eXchanges (MFIX) computer code
3) Implement a polydispersity model in MFIX to account for effects of particle size distribution

Research Progress

The researchers have improved the accuracy of rate constant calculations for the gas phase reactions in the SiC CVD process. Association reactions between radicals were found to have nontrivial free energy barriers due to the significant entropic effect at high CVD temperatures. The energy profiles of the association/dissociation gas-phase reactions were obtained using the left eigenstate completely renormalized coupled-cluster singles, doubles,

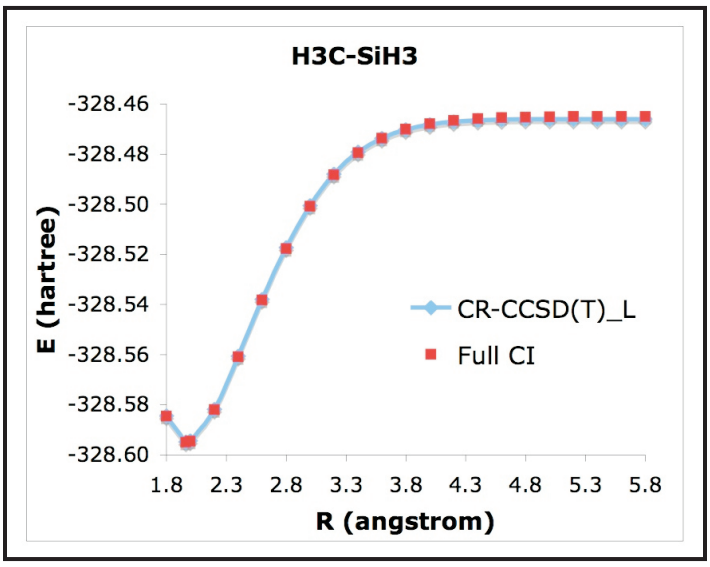

Figure 1. CR-CCSD(T)_L energies compared with the FCI (measured in hartree) at various H_3C-SiH_3 bond distances.

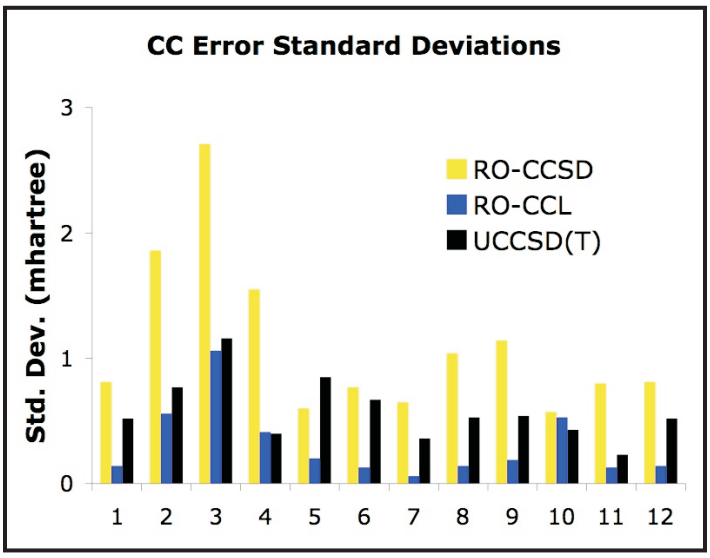

Figure 2. Standard deviations (in mhartree) of the RO-CCSD, RO-CCL, and UCCSD(T) errors for the 12 studied bond-breaking reactions of open-shell species.

and non-iterative triples [CR-CCSD(T)_L] methods. Researchers compared the efficacy of the CR-CCSD(T)_L method with the full configuration interaction (FCI) method for a modest basis set of ten single and one double-bond breaking reactions. Figure 1 illustrates an example of CR-CCSD(T)_L agreeing with FCI for a C-Si bond breaking reaction: $CH_3SiH_3 \rightarrow CH_3 + SiH_3$. They found that the CR-CCSD(T)_L method recovers FCI energies within 1 kcal/mol error for single bond reactions.

The team also made comparisons between the restricted open-shell left eigenstate completely renormalized coupled-cluster (RO-CCL) potential energy surfaces and the FCI method for the bond breaking reactions of several open shell species. The results show that the RO-CCL potential energy surfaces agree with the FCI method within an error of 2 mhartree (1 mhartree = 0.627 kcal/mol) for most of the studied bond breaking reactions. Figure 2 shows that the RO-CCL method predicts more accurate relative energies than the conventional unrestricted (U) coupled-cluster singles, doubles, and noniterative triples [CCSD(T)] method. It was determined that the characteristic coupled-cluster energy error humps appear at longer bond distances on the RO-CCL potential energy surfaces than with the UCCSD(T).

A mechanism consisting of approximately 60 surface reactions involved in the SiC CVD process was proposed, with the surface reactions grouped into four categories: 1) desired reactions that account for SiC growth, 2) side reactions that account for silicon growth, 3) side reactions that account for carbon growth, and 4) diffusion reactions that take place on the SiC surface. Although the diffusion reactions play a less important role in the composition of the SiC coating than the other three types of reactions, diffusion may alter the surface structure and reduce the overall deposition rate by competing with other heterogeneous reactions. The hybrid surface integrated molecular orbital/molecular mechanics (SIMOMM) method was used to study the properties of the surface species and the reaction paths of the surface reactions with a transition state.

Since the final goal is to conduct a CFD simulation of the CVD process in a spouting bed using the MFIX software, the challenge is to efficiently implement the detailed chemistry into MFIX. The reactions are formulated as a source term in the governing equations, solved through a set of ordinary differential equations. Researchers used the in-situ adaptive tabulation (ISAT) methodology coupled with MFIX to efficiently compute the chemistry to obtain the species concentration and source terms at each time step. They developed a procedure to couple the solution of the reaction source term differential equations with the ADIFOR algorithm, which they used to calculate the mapping gradient in ISAT. The implementation was successful and it was determined that 1) as the simulation runs longer, higher speeds are obtained; 2) ISAT speed-up increased dramatically as the error tolerance increased; and 3) switching to ISAT from direct integration after the initial transit state increased speed-up, thus reducing the size of the ISAT table.

An optimization methodology was explored to reduce the computational time needed to simulate the complex CVD process by reducing the number of reactions and species. The optimization first identifies and removes species with extremely low concentrations ($< 10^{-24}$), then the remaining species are used to develop the objective function and numerous simulations are performed to determine the effects of removing species. The same process is then used to eliminate reactions. Of the original 45 species, 9 had low concentrations and were removed. The remaining species and corresponding reactions were used as the chemistry set, with multiple simulations performed for a wide range of initial conditions. Performing the species reduction produced a new mechanism set comprised of 28 species with 83 reactions. By constructing the objective function based on these species in order to perform the reaction reduction, the researchers determined that nearly two-thirds of the reactions could be removed using the optimization methodology, leaving 28 species with 29 reactions in the final reduced mechanism set.

Researchers performed a series of pairwise-mixing stirred reactor (PMSR) simulations to test the speed and efficiency of the reduced mechanism set. These simulations required approximately one-third of the CPU resources when compared with full mechanism simulations. To demonstrate the minimal difference in solutions between the full and reduced mechanism calculations, Figure 3 compares the simulations for the mole fraction of C_2H_3.

Planned Activities

In the final phase, the research team will complete SIMOMM calculations to study the thermodynamics and kinetics of the heterogeneous reactions between the gas phase species and the pyrolytic carbon and SiC solid surfaces. Additional work will include calculations for the surface effects on the predicted rate constants.

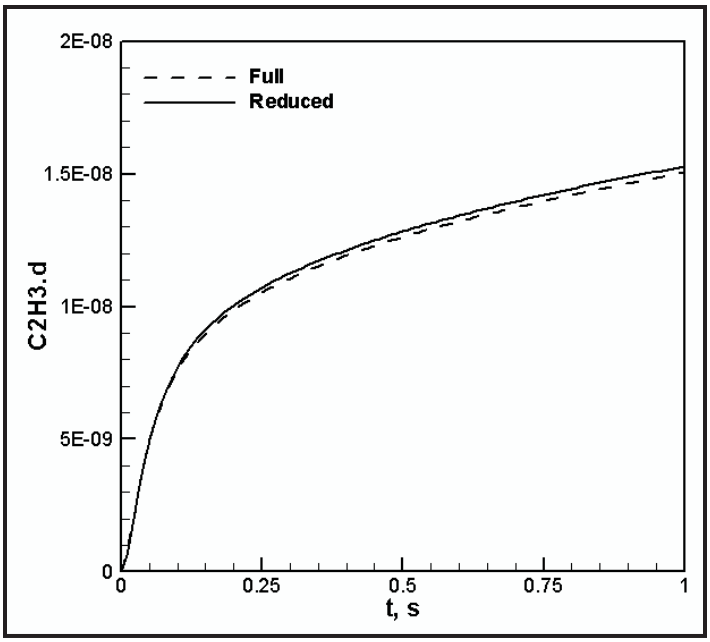

Figure 3. Mole fraction profile of C_2H_3 for an initial temperature of 2,000 K. The initial composition of H_2 is 0.8 and MTS is 0.2.

The team will also complete the study to identify an appropriate reduced chemistry mechanism and will test the results in MFIX with ISAT. Simulations will be conducted to validate the multiphase fluid mechanics and chemistry predictions of major species and temperatures for the spouted-bed CVD reactor. The MFIX code will be used to address scale-up issues for the process-size coater and to study the hydrodynamics and particle mixing patterns.

Nuclear Energy Research Initiative

Optimized, Competitive Supercritical-CO_2 Cycle for Generation IV Service

PI: Michael J. Driscoll, Massachusetts Institute of Technology (MIT)

Collaborators: None

Project Number: 05-044

Project Start Date: April 2005

Project End Date: April 2008

Research Objectives

This project is developing an integrated overall plant design for a gas-cooled fast reactor (GFR) based on the compact and highly efficient, direct supercritical carbon dioxide (S-CO_2) Brayton cycle, which is under development for Generation IV service. This plant will be capable of economical electric power generation, high uranium utilization, burning of transuranics (TRU) and/or minor actinides (MAs), and hydrogen production through the high-temperature electrolysis of steam. Researchers are evaluating prospective plant designs using both the existing deterministic regulations and proposed risk-informed licensing framework. They are applying probabilistic techniques to optimize the tradeoffs between economics and safety assurance.

Most worldwide research on this type of gas reactor is presently based on a helium cycle that operates at temperatures approaching 900°C, which poses severe challenges to the core and component materials. Because the S-CO_2 cycle can achieve high thermodynamic efficiency (approximately 44 to 51 percent) at more modest temperatures of 550 to 650°C, researchers can utilize already-proven technologies in their design.

Major tasks of this project focus on designing the reactor core and decay heat removal systems. In designing the core, researchers have optimized features of the vented fuel concept using tube-in-duct (TID) assemblies (see Figure 1). In addition, they are evaluating a pin-type core design as an alternative and are confirming the capability of burning TRU and MAs. Design of the safety system is guided by probabilistic methods and involves developing a decay heat removal system for accidents, shutdown, and refueling; improving emergency power capabilities, such as microturbines or fuel cells; and integrating both active and passive means of shutdown assurance to preclude an anticipated transient without scram (ATWS). Researchers will also develop a reactor version for integration with a high-temperature steam electrolysis (HTSE) process

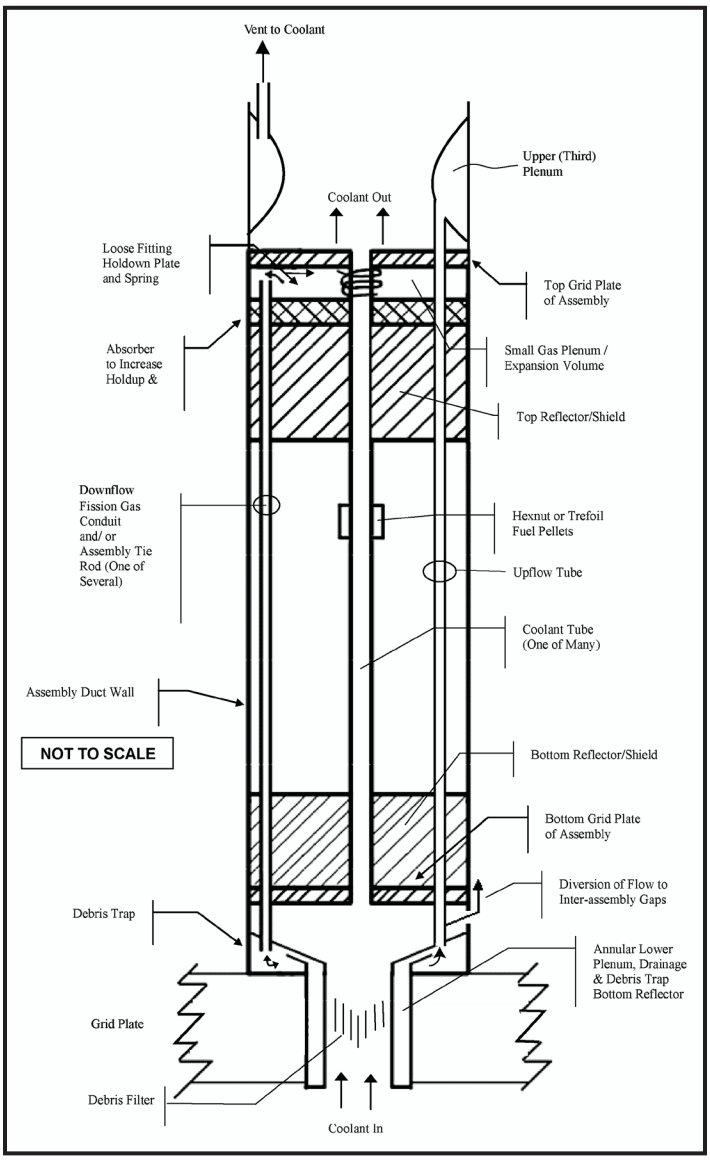

Figure 1. Vertical cross-section view of TID fuel assembly features.

Subsystem	Features	Comments
Core		
Fuel	UO_2 + BeO	LWR TRU fissile ± MA
Clad	ODS-MA956, or HT-9	SiC a long-range possibility
Configuration	Tube-in-duct fuel assemblies, trefoil or "hexnut" pellets, vented, orificed	Pin-type core as fallback is not up to task
Thermal-Hydraulics	Axial peaking factor ≤1.3 Radial peaking factor ≤1.2 Power density ~ 85 W/cc	Vary BeO fraction to flatten power lower than GA GCFR of 1970s @ 235 W/cc
Burnup	≥120 MWd/kg (avg)	In single batch no-reshuffle core, 17-yr lifetime
Safety Systems		
Auxiliary Loops	Combined shutdown & emergency, 4 x 50% capable, active forced convection; Passive natural convection supplemented; Water boiler heat sink	Based on RELAP parallel loop calculations. For P≥0.7 MPa, natural convection alone may suffice
Emergency Power	Fuel cells to supplement diesels	Projected to be more reliable than diesels alone in long run
Plant		
Power Conversion System (PCS)	Supercritical CO_2 Brayton direct 2 x 600 MWe loops = 1200 MWe; 650°C core exit/turbine inlet, 20 MPa pressure	AGRs in UK use CO_2 coolant at 4 MPa and have T~650°C
Reactor Vessel	PCIV (prestressed cast iron reactor vessel)	Vessel houses loop isolation and check valves plus shutdown cooling heat exchangers
Containment	PWR type, steel liner reinforced concrete 0.7 MPa design capability 70,000 m^3 free volume filtered/vented	Internally insulated and CO_2 can be added to keep pressure up to natural convection needs
H_2 production by steam electrolysis (optional)	4 separate water boiler loops at 10% of reactor power; Recuperation of H_2 & O_2 heat allows cell operation at 850°C	Water boiler loops can also serve for self-powered decay heat removal

Table 1. Current status of GFR plant features.

for hydrogen production and will conduct an economic assessment to estimate costs. Overall, this project will provide a sufficient basis for assessing this type of GFR among the other candidate Generation IV designs being evaluated for final selection.

Research Progress

Following is a summary of major tasks that were completed during the past year. Table 1 summarizes the current status of the plant design, incorporating all evolutionary changes since project initiation.

Most core physics, thermal-hydraulics, and fuel cycle activities are now complete. The reference design is based on the use of TID assemblies, which invert the usual pin configuration to put the uranium dioxide (UO_2) fuel outside coolant tubes. This permits high fuel volume fractions, which enable attaining a self-sustainable conversion ratio of unity with UO_2 fuel. Adding beryllium oxide (BeO) diluents

to the fuel and using radial reflector assemblies having a CO_2-only zone result in a negative coolant void reactivity—a rarity in fast reactors. The core has also been shown to have a favorable combination of reactivity feedback mechanisms (in the analytic integral fast reactor [IFR] quasi-static sense), which was confirmed using RELAP numerical simulation, providing self-protection during most severe transients including ATWS. Pin-type designs with UO_2 fuel were also developed and evaluated and were found to have significantly inferior performance; therefore, they are not recommended for implementation. MA burning in fertile-free fuel was found to be possible and not inferior to other fast reactors, but again is not an attractive option.

The researchers have devised a GFR-supercritical CO_2 Brayton cycle combination that is tailored to produce hydrogen by high temperature steam electrolysis. The system layout recuperates enough energy from the hydrogen and oxygen products to heat steam to the required electrolysis cell operating temperature of 850°C, making it possible to keep the reactor core outlet temperature at or below 650°C. The approach is, in principle, applicable to most other reactors. The GFR has four water boiler loops in parallel with the CO_2 power conversion systems to produce the steam feed for the electrolysis cells. These loops also play the role of a highly effective decay heat removal system.

A combination of probabilistic risk assessment (PRA)-guided design and RELAP5-3D loss of coolant accident (LOCA) simulation of parallel loop layouts has led to reliance on active, blower-driven decay heat removal loops which can also function, if necessary, in a backup passive natural circulation mode. This decision was driven by the finding that unaided natural convection loops can experience startup phase flow reversal, which can lead to core coolant bypass. Check valve leakage beforehand as well as the failure to open under the small pressure differentials in a gas circuit are the dominant causative factors. The conditional failure probability of the decay heat removal system (given a LOCA) was unacceptably high even after some design modifications. This task has also served as the MIT contribution to an I-NERI collaboration with the French Commissariat à l'énergie atomique (CEA) that has followed a similar evolutionary path in designing post-accident decay heat removal systems for a helium-cooled GFR.

The major new activity has been to start on a more detailed design and performance analysis of the fuel venting system needed to equalize gas pressure across the coolant tubes and fuel assembly duct walls with that of the primary coolant. By making the escape path for fission product noble gases long enough (and with several plena interspersed), releases are sufficiently suppressed to allow venting into the primary coolant system rather than into a collection plenum built into the core grid structure, as originally conceptualized. A stage-by-stage analysis of fission product transport is in progress: from the fuel to vent system, to the coolant, to the containment atmosphere, and finally to the environs. Initial results are encouraging with respect to protection of both plant personnel and the general public.

Planned Activities

Work is concentrated on four major remaining subtasks in the upcoming year:

- Complete evaluation of the advanced version of the vented fuel assembly design to confirm that primary system, in-containment, and off-site fission product inventories, deposition, and releases are tolerable
- Complete PRA and decay heat removal system studies, focusing on achieving a negligible likelihood of suffering an ATWS event by incorporating a diverse, redundant suite of active and passive reactivity insertion means
- Complete plant and fuel cycle cost estimates to provide busbar cost of electricity values relative to the Gen III and Gen IV reactor competition
- Draft a final summary report

Nuclear Energy Research Initiative

On-Line Fuel Failure Monitor for Fuel Testing and Monitoring of Gas-Cooled Very High-Temperature Reactors

PIs: Ayman I. Hawari and Mohamed Bourham, North Carolina State University (NCSU)

Collaborators: None

Project Number: 05-054

Project Start Date: March 2005

Project End Date: March 2008

Research Objectives

The primary objective of this project is to devise an accurate approach for detecting failures of tristructural isotropic (TRISO) fuel based on measurements of fission gas activity released into the effluent stream. In the gas-cooled very high-temperature reactor (VHTR), the fuel is made up of TRISO microspheres composed of a uranium-carbide (UCO) kernel surrounded by a porous pyrolytic graphite buffer, an inner pyrolytic graphite layer, a silicon carbide (SiC) coating, and an outer pyrolytic graphite layer. The layer/coating system that surrounds the kernel acts as the containment and main barrier against the environmental release of radioactivity. However, due to hostile in-core conditions (e.g., high temperature, fast neutron flux, etc.), it is anticipated that a certain number of TRISO microspheres will fail during reactor operation. To ensure compliance with radiological and safety requirements, it is essential to detect any fuel failure at the earliest stage possible.

The aim of this project is to develop techniques for detecting a single failed TRISO particle per testing capsule. Researchers believe that fuel failure rates on the order of 10^{-5} are detectable and that the detection method will provide insight into the failure mode. Researchers will study various detection methods to differentiate the minute fission product signal from the background. As part of the VHTR fuel development program, they will conduct fuel failure experiments at the Advanced Test Reactor (ATR) at the Idaho National Laboratory (INL). Methods and instrumentation developed by this project are expected to be applicable to on-line fuel failure monitoring of VHTRs.

Research Progress

During the third year, work focused on formulating a more accurate approach for the implementation of gamma-ray spectrometry as a technique for understanding fission gas (mainly krypton [Kr] and xenon [Xe]) release from TRISO fuel. At this stage, the analysis focuses on the Advanced Gas-cooled Reactor (AGR)-1 experiment, which is being performed at the ATR of INL. The uncertainties present in the analysis of the AGR-1 experiment are expected to be improved by eliminating uncertainty sources through the formulation and use of relative release-to-birth (R/B) indicators. The measured indicators are calculated from the combination of the two R/B ratios and given by

$$I_{i,j}^{measured} = \left(\frac{R_i}{R_j}\right)\left(\frac{B_j}{B_i}\right),$$

where i and j represent two different isotopes, and $I_{i,j}$ is the indicator value. The uncertainty in this value is dominated by the release activity ratios. The predicted indicator values are found by taking the ratio of R/B model predictions for two different isotopes.

$$I_{i,j}^{predicted} = \frac{\left(R/B\right)_i}{\left(R/B\right)_j}.$$

In this case, the uncertainty in this value is diminished when diffusion dominates the fission gas release and the reduced diffusion coefficient correlation for isotopes i and j are the same.

Specific trends in the behavior of theoretical gas release models were identified in the relative R/B ratios. The trends were studied using simulated gamma-ray release spectra of Kr and Xe to verify that such trends can be observed in the spectra. Table 1 illustrates some of these trends for the release (due to failure) as predicted by the German, Japanese (Japan Atomic Energy Research Institute [JAERI]), and General Atomics (GA) models. As can be

Failure only Values		Ratio of R/B relative to Kr-85m			% difference from German Model	
Isotope	Half Life	German	JAERI	GA	JAERI	GA
Kr-85m	4.48 h	1	1	1	0.00%	0.00%
Kr-87	1.27 h	0.5368	0.4445	0.5204	-17.19%	-3.05%
Kr-88	2.84 h	0.7988	0.65	0.7793	-18.63%	-2.44%
Kr-89	3.15 m	0.1098	0.0734	0.1257	-33.15%	14.50%
Kr-90	32.3 s	0.0455	0.0294	0.0669	-35.30%	47.11%
XE135	9.10 h	1.4155	1.4542	0.8424	2.73%	-40.49%
XE135M	15.3 m	0.2415	0.2097	0.1123	-13.18%	-53.51%
XE137	3.82 m	0.1209	0.0774	0.0687	-35.96%	-43.21%
XE138	14.1 m	0.2319	0.1534	0.1088	-33.83%	-53.09%
XE139	39.7 s	0.0504	0.0315	0.0433	-37.56%	-13.94%

Table 1. Predicted trends in the relative release due to failure using Kr-85m as the reference R/B value.

seen in the table, the trends show that, according to the German model, the relative R/B values will be decreasing with half-life. This behavior is independent of the type of species (Kr or Xe). This is mainly due to the fact that in failure release, the German model assumes similar diffusion behavior for both Kr and Xe. Alternatively, the GA model shows a difference between Kr and Xe, which is a clear indication of the fact that the GA model assumes different diffusion behavior for Kr and Xe. The JAERI model would be expected to follow similar trends to the German model. However, it can be seen that the trend is broken in certain cases, namely for Xe-135m ($T_{1/2}$ = 15.3 min) and Xe-138 ($T_{1/2}$ = 14.1 min). This is attributed to the fact that the JAERI model considers the half-life of the precursor for a given isotope. Consequently, the long-lived precursor of Xe-135m increases its R/B when compared to a nuclide with a similar half-life, such as Xe-138.

To support the experimental observation of the above trends, researchers continued to develop and test the gas extraction and ionization system during the past year. The main objective of this system is to allow extraction of samples of the effluent gas, ionize it, and then deflect selected fission gas species towards the gamma-ray spectrometer. In this system, the use of radio frequency (RF) power to ionize the gas is an efficient way to produce high fractional ionization; however, RF power at high frequencies (in the MHz range) imposes difficulty on surrounding instrumentation, including any magnet power supply because the magnet coils pick up the RF and introduces a reactive element at the utilized frequency (ωL_{coil}).

For efficient use of RF power, the RF power supply must be totally shielded inside a Faraday shield and situated at least 6 feet from the test cell. The constant current power supply (to power the magnets) must also be situated at least 6 feet from the test cell to eliminate the RF effect on the magnet supply unless the power supply is totally shielded. The use of low frequency (kHz range) can generate plasmas even at higher pressures (up to atmospheric pressure) due to the effect of the dielectric barrier discharge. At such low frequency, there will be no frequency effects on the magnets or on the magnet power supply due to the low value of the reactive component. Two designs have been investigated to implement this approach. The first design generates plasma at a breakdown voltage of 12.5kV; however, few streamers were observed and the total power into the plasma provides lower fractional ionization. The second design, which was found to be more favorable, was tested using a similar system on a neighboring experiment. A well-collimated plasma column was generated at the center of the discharge chamber with better ionization fraction. Consequently, the second design was chosen.

Planned Activities

Plans are currently underway to test the relative release-to-birth approach using data from the AGR experiments. Comparisons will be made between the relative indicators as predicted by various proposed models and the measured data at the ATR. In addition, testing of the gas extraction and detection system will continue to verify its practical utility in the AGR experiments. Coordination will continue with INL staff to transfer this system to the ATR and to apply it in the gamma spectrometry measurements using various types of detectors, including ones with low-resolution room temperature.

NUCLEAR ENERGY RESEARCH INITIATIVE

Development of High-Temperature Ferritic Alloys and Performance Prediction Methods for Advanced Fission Energy Systems

PI: G. R. Odette, University of California-Santa Barbara (UCSB)

Collaborators: Oak Ridge National Laboratory (ORNL), University of California-Berkeley, Illinois Institute of Technology

Project Number: 05-074

Project Start Date: March 2005

Project End Date: March 2009

Research Objectives

The objective of this research project is to develop an advanced high-temperature alloy class, called "nano-structured ferritic alloys" (NFAs), for use in advanced nuclear reactor systems. These alloys manifest remarkable creep strength, have excellent ductility, show good fracture toughness potential, and are highly resistant to radiation damage. These characteristics are due to the presence of a large concentration of nm-scale yttrium-titanium-oxygen (Y-Ti-O)-enriched features.

Researchers are addressing the combined effects of high temperatures (≥ 900°C) and high radiation doses on commercial alloys, especially MA957. They are also carrying out model alloy experiments to better understand NFA thermo-kinetics and structure-property relations in order to optimize processing paths and the balance of properties. Researchers continue to collect data and to conduct thermal aging experiments on NFA MA957 and 9Cr tempered martensitic steels (TMS) to assess softening, non-hardening embrittlement, and high-temperature stability-aging limits.

Following are the five major tasks of this project:

1) Develop a comprehensive mechanical property and microstructural database on MA957, other NFAs, and TMS, emphasizing the effects of irradiation on deformation and fracture; semi-empirical constitutive models, including high-temperature creep; and the master fracture toughness-temperature curve method for application to NFAs
2) Conduct experiments on nano-microstructural evolutions and mechanical properties for both commercial and model NFAs, and optimize processing paths, properties, and service lifetimes; thermal aging of NFAs and TMS; and post-irradiation examination and data analysis of ongoing and future irradiation experiments
3) Investigate advanced joining methods (e.g., diffusion bonding) for MA957 and other NFAs that maintain beneficial NFA micro-nanostructures
4) Develop models of the character, precipitation thermo-kinetics, and high-temperature thermal and irradiation stability of nm-scale precipitates in NFAs; transport fate and consequences of helium; and compare the predictions to the results of thermal aging and irradiation experiments
5) Conduct other activities, including collaboration in new irradiation studies and the design of an advanced reactor surveillance-component monitoring program

Research Progress

Database and Physically Based Constitutive and Fracture Toughness Models. Tensile and creep tests were carried out on MA957 in an as-extruded bar condition (AEB) from ambient temperatures to 1,000°C over a wide range of strain rates. The temperature (T) dependence of the yield stress (σ_y) at a strain rate of 1.3×10^{-3}/s for the MA957 AEB is shown in Figure 1 (filled circles). The σ_y for Eurofer 97 (filled triangles) and other NFA data from the literature are also shown for comparison. The σ_y for AE MA957 thick walled tubing (unfilled diamonds) is higher than for the AEB. In contrast, σ_y for thin walled tubing (unfilled triangles) and recrystallized MA957 (unfilled circles) are lower than the AEB. The MA957 variants and J12YWT (unfilled squares and crosses) that received various post-extrusion thermo-mechanical treatments (TMT) are also significantly stronger than AEB.

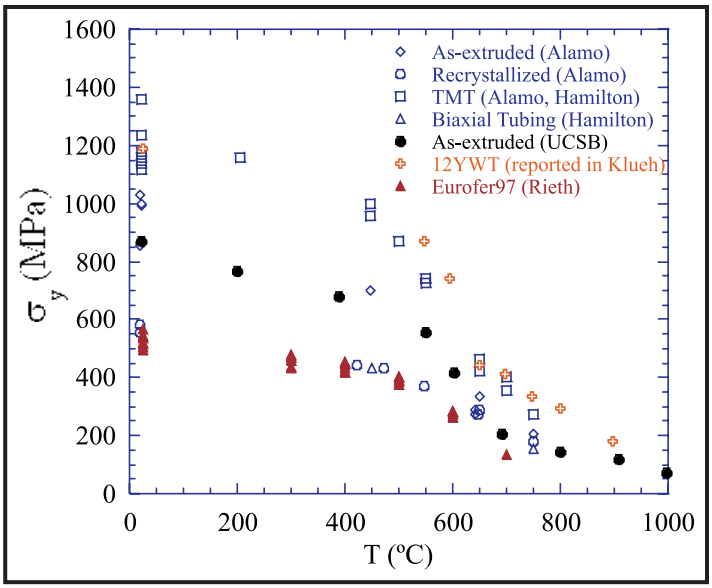

Figure 1. The σ_y of various MA957 alloys as a function of temperature. Data for 12YWT and Eurofer 97 are included for comparison. The data are for a strain rate of around 10^{-3}/s. The σ_y for various TMT conditions of MA957 varies by about a factor of ≈ 2.

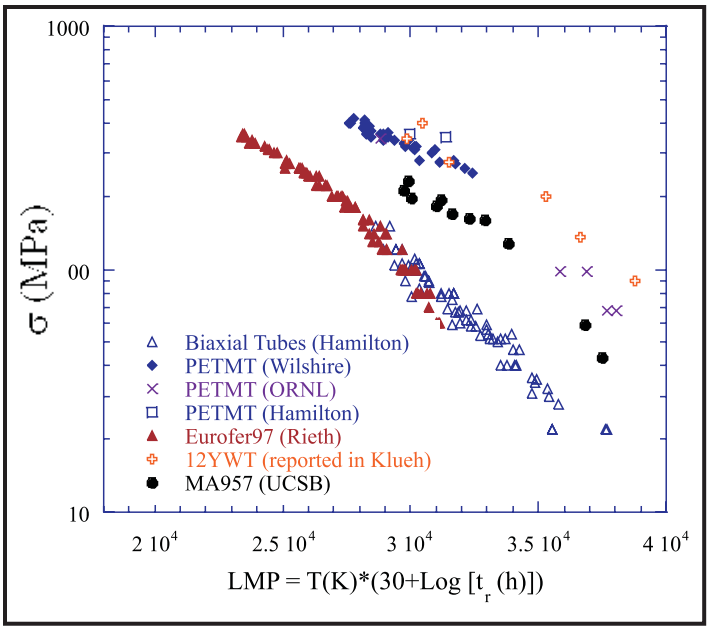

Figure 2. LMP plots for various TMT conditions of MA957 showing strength levels that vary by up to a factor of ≈ 3. Data for 12YWT and Eurofer 97 are included for comparison.

Figure 2 shows some viscoplastic-creep data on the various conditions of MA957 as well as Eurofer 97 and J12YWT. The differences in strength are even more apparent in this Larson Miller Parameter (LMP) creep rupture time (t_r) (LMP= T[30+ log(t_r)]) plot. The thin-walled tubing is much weaker in the hoop direction than the AEB and, especially, the TMT MA957 and J12YWT (including the filled crosses), tested in the axial orientation. The weakness of the tubing in the hoop stress direction is partly due to the crystallographic-microstructural-mechanical property anisotropy of extruded MA957. However, since the nano-features (NFs) are similar in the various alloys, these results show that the creep strength also depends on the balance of microstructures and TMT. Indeed, the effects of the NF may be partly due to stabilizing the dislocation and grain structures. Figures 1 and 2 represent a small subset of data being developed in this program. These data are being used to construct physically based constitutive models of the effect of the overall micro-nanostructure on the tensile deformation and fracture behavior of NFA.

Developing an Alloy Stability Database for NFA and TMS. Long-term thermal aging experiments on NFA and TMS have continued. The status of the aging matrix for both TMS and MA957 as of September 30, 2007, is summarized in Table 1.

Figure 3a shows Vickers microhardness changes in MA957 as a function of aging time at temperatures from 800 to 1,000°C. MA957 aged at 1,000°C shows a continuous decrease in hardness up to approximately 8,000 hours and a slight decrease in the corresponding hardness at 900°C. Significant softening begins at 950°C beyond 4,000 hours. Hardness is unchanged up to about 5,000 hours at 800 and 850°C. Transmission electron microscopy (TEM) and small angle neutron scattering (SANS) characterization studies are broadly consistent with the observed hardness trends. For example, TEM shows that ferrite

Alloy	550°C	600°C	650°C	700°C	800°C	850°C	900°C	950°C	1,000°C
	Aged time as of end of September 2007 (hours)								
MA957	N.A.	N.A.	N.A.	N.A.	4700	5300	8400	6900	8700
Eurofer97	6300	6300	6300	6300	NA	NA	NA	NA	NA
T91	6300	6300	6300	6300	NA	NA	NA	NA	NA
HT9	6600	6600	6600	5600	NA	NA	NA	NA	NA
F82H IEA	6600	6600	6600	6600	NA	NA	NA	NA	NA
Mod 3	6600	6600	6600	6600	NA	NA	NA	NA	NA

Table 1. Current status of the aging matrix for both TMS and MA957 alloys.

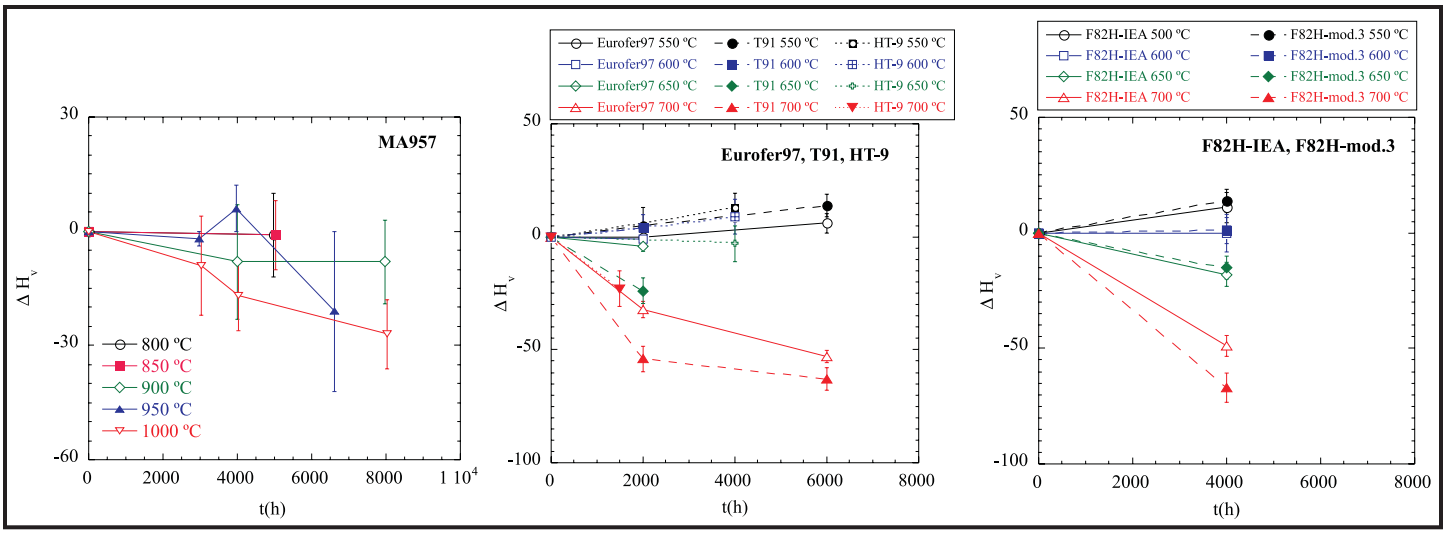

Figure 3. Vicker's micro-hardness change, ΔH_v, versus aging time for (a) MA957 at 800 to 1,000°C. (b) and (c) two different TMS materials at 550 to 700°C.

grains and high dislocation densities are stable up to 4,000 hours at 950°C, but that the dislocation density decreases and the NF slightly coarsen at 1,000°C and 4,000 hours. Analysis of TEM and SANS results is continuing. Figures 3b and 3c show Vickers micro-hardness changes in the TMS as a function of aging time at temperatures from 550 to 700°C. All the TMS showed essentially no change in hardness at 600°C, significant softening at 700°C, and possible hardening at 550°C. At 650°C, two F82H variants and T91 showed a slight softening, while Eurofer 97 and HT-9 showed no change in hardness. These trends are consistent with microstructural observations in companion TEM studies.

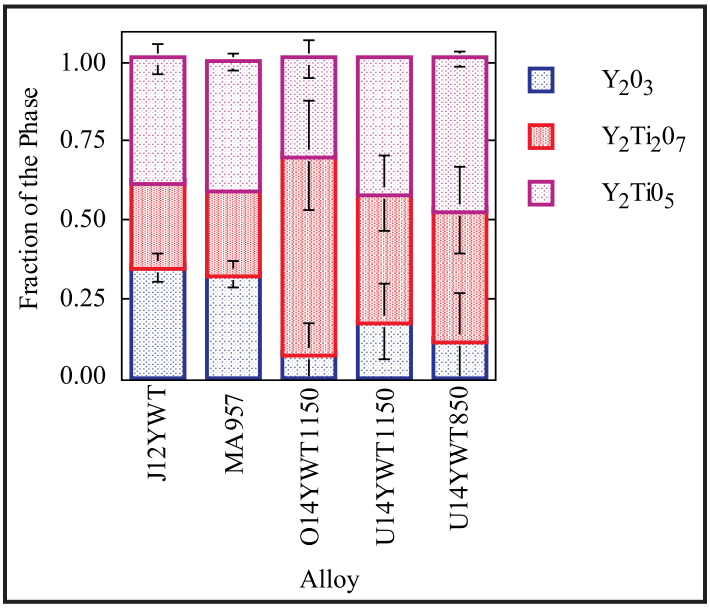

Figure 4. The relative fractions of various oxide phases in a set of NFAs derived from EXAFS and XANES measurements.

Other Activities. Synchrotron X-ray measurements were carried out to identify the nm-scale Y-Ti-O enriched NF in NFA at the Advanced Photon Source (APS). The materials included MA957, J12YWT, and UCSB (U) and ORNL (O) mechanically alloyed 14YWT powders hot isostatic pressing (HIP) at 850 and 1,150°C. X-ray absorption near edge spectroscopy (XANES) and extended x-ray absorption fine structure (EXAFS) spectroscopy data for three oxide standards—Y_2O_3, $Y_2Ti_2O_7$, and Y_2TiO_5—were used to fit the data using the Athena code. The fits were a consistent mixed set of oxide NF, primarily composed of $Y_2Ti_2O_7$ and Y_2TiO_5 plus varying amounts of Y_2O_3. Figure 4 shows the average of fractions of the oxides.

The program also engaged in a number of other activities during the last year, including 1) the development of new means of characterizing static and creep constitutive properties based on hardness measurements, 2) preparation of specimens for irradiation experiments in the BR2 (Belgium) and Pheonix (France) reactors, 3) post irradiation examination of specimens irradiated in the High Flux Isotope Reactor (HFIR) (United States), 4) ab-initio modeling of NF, and 5) additional XANES and EXAFS studies.

Planned Activities

High-temperature mechanical testing of MA957 and collecting related data from literature to develop constitutive models will continue. These studies will include stronger TMT variants of MA957. The long-term aging studies will reach about 12,000 hours by March 2008 and will continue into 2009. All of the other activities listed above will also continue, with some of the tasks transferred to ongoing NERI projects.

Nuclear Energy Research Initiative

Development and Analysis of Advanced High-Temperature Technology for Nuclear Heat Transport and Power Conversion

PI: Per F. Peterson, University of California-Berkeley (UCB)

Collaborators: Oak Ridge National Laboratory (ORNL), Sandia National Laboratories

Project Number: 05-079

Project Start Date: April 2005

Project End Date: April 2009

Research Objectives

This project is studying advanced high-temperature heat transport and power conversion technology in support of the Nuclear Hydrogen Initiative (NHI) and Generation IV. The research focuses on the fundamental and applied problems associated with high-temperature heat transport using different gases (e.g., helium) and liquids (e.g., clean liquid salts [LS]).

The project makes contributions in four areas:

1) Provides design options for the 50 MW(t) Next Generation Nuclear Plant (NGNP) intermediate heat exchanger (IHX) system, exploring the major tradeoffs among high-pressure helium, intermediate-pressure helium, and LS as heat transport fluids for hydrogen production
2) Performs scaled integral experiments to study high-temperature heat transport, heat exchange, and fluid mechanics with simulant fluids for LS
3) Performs multiple-reheat helium Brayton power conversion studies to evaluate its suitability for liquid-cooled, high-temperature systems such as the modular lead-cooled fast reactor (LFR), the liquid-salt-cooled very high-temperature reactor (LS-VHTR), and the molten salt reactor (MSR)
4) Performs advanced high-temperature reactor (AHTR) design analysis to extend initial design studies of the LS-cooled AHTR as a potential high-temperature heat source for electricity and power production

Figure 1 compares the latest modular pebble bed AHTR with the gas-cooled pebble bed modular reactor (PBMR).

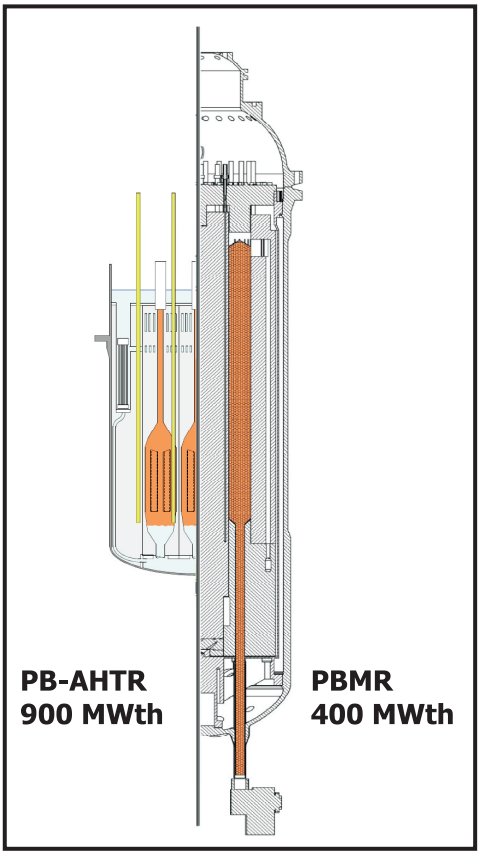

Figure 1. Scaled comparison of the modular 900 MW(t) AHTR and the 400 MW(t) PBMR.

Research Progress

Over the past year, researchers have made major progress both in supporting the reactor interface and intermediate loop development for the NGNP, as well as toward developing the LS-cooled AHTR.

The NGNP is a modular helium reactor (MHR) with an outlet temperature from 850 to 950°C. A major viability issue for the NGNP is the IHX, which transfers heat from the primary helium to an intermediate fluid. UCB achieved key progress in developing new tools to model the transient response of different IHX designs that will occur when the flow of the primary or intermediate fluid is abruptly changed or stopped. These simulations indicate that there may be unacceptable thermal stresses induced in compact plate type IHXs. The alternative is to use a conventional shell and tube design for the IHX, but for a helium-to-helium IHX, this would result in a massive and very costly IHX.

Researchers at UCB have studied the use of liquid salts as the NGNP intermediate fluid. They have proposed that the NGNP IHX use capillary tubes (inside diameter less than 2 mm) for the liquid salt, with sufficiently thick tube walls to keep compressive stresses below the values that would result in significant creep deformation. Figure 2 shows a scaled drawing of an initial capillary tube and shell IHX module design developed by UCB. This IHX design has been found to bring several benefits:

1) Excellent response to thermal stresses and thermal transients due to tube flexibility
2) Compact geometry with similar power density as a Heatric-type heat exchanger
3) An optimal geometry to resist high-temperature creep deformation of tubes
4) Capability to fabricate with an internal cladding material, or to apply nickel plating, to the internal surface of the tubes for corrosion resistance with liquid salt
5) A geometry that allows physical access to the outsides of the heat exchanger tubes for in-service inspection, which is not possible for diffusion-bonded (Heatric) heat exchangers
6) A geometry that allows a greater flow area for helium than a corresponding Heatric-type heat exchanger, allowing the potential for reduced pressure drop and helium recirculating power

UCB also made major progress in the development of the PB-AHTR. These advances have come since last year's decision to focus design and analysis on pebble fuels with a core outlet temperature of 704°C in order to allow the use of available American Society of Mechanical Engineers (ASME) Section III code qualified materials. The PB-AHTR then delivers heat at an average temperature of 652°C, the same average temperature as the gas turbine modular helium reactor (GT-MHR), and thus achieves the same power conversion efficiency of 46 percent. Economics scaling for the new 900 MWth modular PB-AHTR design, shown in Figure 1, indicates the potential for very large reductions in capital cost compared to MHRs.

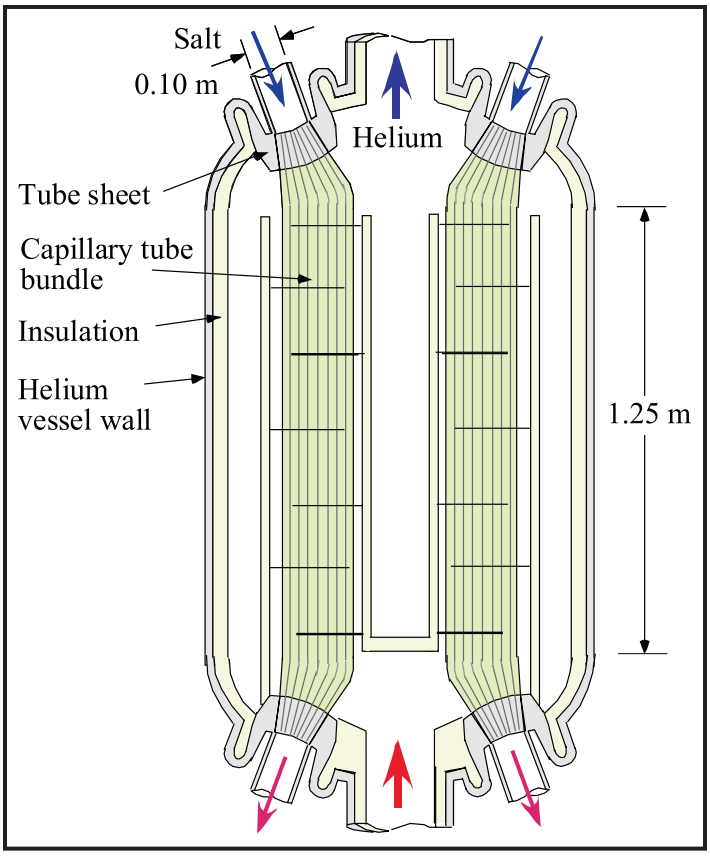

Figure 2. Elevation view of the capillary shell and tube IHX design developed by UCB for the NGNP.

Key progress on the PB-AHTR was reported at the Global 2007 Advanced Nuclear Fuel Cycles and Systems conference in September 2007. This included 1) the results of detailed neutronics analysis, verifying the capability to achieve negative void reactivity and high discharge burn up equivalent to or greater than MHRs; 2) transient analysis with RELAP5-3D showing excellent transient response with fuel and structural material temperatures remaining well below limits; and 3) additional results from the Pebble Recirculation Experiment (Figure 3) verifying the viability of pebble injection, circulation, and defueling.

Figure 3. The Pebble Recirculation Experiment (PREX-1) operating.

Planned Activities

Researchers are on track for completing the full work scope of this NERI project. Due to the large safety margins identified in the initial design, UCB is now focusing its research effort on a compact, 900 MWth modular PB-AHTR design (Figure 1) that introduces several attractive new design approaches and features and will include the development of a detailed program plan for remaining Viability Phase R&D. This would lead to the completion of a Nuclear Regulatory Commission (NRC) Pre-application Review Submittal package that would provide the basis for moving into Performance Phase development of the PB-AHTR.

Nuclear Energy Research Initiative

Development of Risk-Based and Technology-Independent Safety Criteria for Generation IV Systems

PI: William E. Kastenberg, University of California-Berkeley (UC Berkeley)

Collaborators: None

Project Number: 05-080

Project Start Date: March 2005

Project End Date: December 2008

Research Objectives

The objective of this project is to develop quantitative safety goals for Generation IV nuclear energy systems. These safety goals will be risk-based and technology independent. Researchers will develop a new operational definition of risk. They will also lay the foundation for a new approach to risk analysis that will 1) quantify performance measures, 2) characterize uncertainty, and 3) address a more comprehensive view of safety as it relates to the overall system.

Safety criteria are necessary for managing risk prudently and cost effectively. Results of this study will prove valuable for assuring the health and safety of the public as they manage, review, and approve advanced reactor designs.

Research Progress

Deployment strategies for future nuclear energy systems must consider multiple competing and incommensurable objectives. The multiplicity of nuclear energy system concepts offer differing sets of tradeoffs against these objectives and create ambiguity as to the best choice of system(s). The number and type of reactor systems deployed over time will likely require balancing competing objectives in the absence of a superior solution that simultaneously maximizes all objectives. Envisioning a larger set of alternative scenarios may suggest a path forward for nuclear energy research and development (R&D) to develop systems and institutions that achieve better outcomes.

Multiple studies have employed fuel cycle models with a scenario-based approach to assess outcomes, derive insights into system behavior, and establish R&D priorities. In contrast to a scenario-based approach, a multi-objective optimization framework has been developed that can identify a more complete set of deployment scenarios in response to a holistic set of selective pressures, such as those outlined in the Generation IV Roadmap. Within this framework, the influence of performance metrics and policy levers (i.e., selective pressures) on system response will also be assessed. For instance, a comparison could be made between a nonproliferation objective based on minimizing inventories of fissile material and an objective minimizing ambiguity as signaled by a state's technology choices.

Conventional multi-objective optimization approaches require a continuous cost function and/or a set of weights on incommensurable objectives and usually only return a single solution. When faced with complex models that are difficult to solve deterministically, meta-heuristic optimization techniques offer "good" solutions in reasonable time using intelligent search techniques. Multi-objective evolutionary algorithms (MOEAs) that mimic Darwinian evolution offer an approach to evolve a population of solutions along the tradeoff surfaces simultaneously (e.g., via Pareto dominance). These techniques have been demonstrated to be efficient and effective for complex multi-objective problems where conventional techniques fail to work well. Evolutionary algorithms offer the ability to 1) find a global optimum on a complex objective surface, 2) optimize a large number of continuous or discrete decision variables, 3) return a list of potential solutions and exclude inefficient and infeasible solutions, and 4) incorporate data obtained experimentally or analytically. MOEAs are also amenable to parallel computing to achieve convergence in less wall-clock time.

During this fiscal year, a fuel cycle model tracking mass flows and cognizant of various deployment constraints has been coupled to an MOEA algorithm as a proof-of-principle. Efforts led principally by the Department of Energy (DOE) have identified several viable advanced nuclear reactor

concepts, each with their own respective advantages. The first advanced reactor paper concept to see commercial success will have demonstrated, at a minimum, the following three inter-related attributes: 1) licensing feasibility, 2) reduction in construction time, and 3) investment risk commensurate with alternative base-load generation options. Fundamental design changes, such as single-phase working fluids, high-temperature refractory materials, and passive safety features, greatly reduce the complexity in assessing the risk associated with advanced reactors but also present a new set of licensing concerns.

The research proposed below is necessary to complete the project and will focus on assessing and reducing the uncertainty associated with the reliability of passive systems and developing a methodology for their inclusion in probabilistic risk analysis (PRA). A top-down approach is proposed starting with overall reactor safety criteria and working down to the sub-system and component performance level.

Planned Activities

Techniques developed in the chemical industry such as HAZOP and failure modes effect analyses will be used to determine an appropriate design basis envelope of considered events. Once identified, PRA techniques will be used to assess the frequency and consequences associated with each event. End states have already been defined as a function of frequency and dose release consequences with corresponding deterministic criteria and will be compared with the obtained PRA results.

A methodology for integrating passive system reliability into current PRA practice will be developed that reflects the true sensitivity of boundary and initial conditions experienced during different reactor transients. This methodology should be developed and implemented during the design phase in order to identify weak aspects of the system design.

Instead of repetitive reliability testing, a scaled integral effects facility will be constructed to explore system performance under various boundary and initial conditions. System response will be evaluated to determine overall weaknesses of the design in addition to validating the previously described reliability assessment methodology. Key thermal-fluid phenomena identified and ranked in previous research efforts will be experimentally verified in addition to assessing relative impact on overall system performance. Given the time scales associated with the passive system response, separate effects tests will have to be performed independently to determine longer-term failure mechanisms (i.e., corrosion, creep, etc.).

Nuclear Energy Research Initiative

Development of Modeling Capabilities for the Analysis of Supercritical Water-Cooled Reactor Thermal-Hydraulics and Dynamics

PI: Michael Z. Podowski, Rensselaer Polytechnic Institute

Collaborators: The Royal Institute of Technology (KTH), Sweden

Project Number: 05-086

Project Start Date: March 2005

Project End Date: March 2008

Research Objectives

In collaboration with KTH and the Korea Atomic Energy Research Institute (KAERI), this project will develop an experimental database for heat transfer in tubes and channels cooled by water and carbon dioxide (CO_2) at supercritical pressures. Researchers will develop mechanistic models of local turbulence-driven heat transfer in forced-convection flows of supercritical fluids experiencing strong variations of physical properties. The research team will test the proposed models using water and CO_2 as working fluids and will perform parametric analyses on the effects of different models of turbulence, including kinematic and, in particular, thermal aspects of turbulence. The new models will then be implemented in the NPHASE computational fluid dynamics (CFD) computer code, and researchers will perform model testing and validation against available experimental data for both water and CO_2. In addition, researchers will perform virtual experiments and use the results to develop simplified yet mechanistically based non-dimensional correlations for application in system codes and for future application in the analysis of supercritical water-cooled reactors (SCWRs) thermal-hydraulics. Finally, the team will perform numerical simulations of supercritical water system dynamics based on the NPHASE code. In particular, they will investigate transient response of a heated channel to power and flow variations. Researchers will analyze the effect of both heat transfer enhancement and heat transfer degradation.

Research Progress

It has been demonstrated that the property variations across the boundary layer play a critical role in the predictions of heat transfer in fluids at supercritical pressures. The variation of properties in this region is strongly nonlinear; therefore, further work is necessary to determine a more accurate method of precisely quantifying this effect in a mechanistic manner. Turbulence modeling in this region also plays a significant role in finding thermal, as well as kinematic, characteristics of the flow. A low Reynolds Number k-ε turbulence model, considered as the next step in the current research project, is expected to capture the effects of property variation in a more detailed manner.

The issue of heat transfer degradation (HTD) in forced-convection at supercritical fluids has been analyzed. It has been shown that the complexity of phenomena governing the combined kinematic and thermal phenomena in fluids experiencing dramatic changes in local physical properties makes it very difficult to develop acceptable predictive capabilities solely based on phenomenological models and correlations.

It has also been shown that a multidimensional approach based on CFD concepts is capable of properly capturing local effects that may lead to either heat transfer deterioration or enhancement. Additional work is still needed in order to develop fully mechanistic models applicable to different fluids and a broad range of operating conditions.

The results of analysis have been shown concerning the computational modeling of heat transfer in heated channels using supercritical CO_2 and water as working fluids. Two heater geometries have been investigated: flow in a tube heated from outside and an annulus with a central heated rod. Computer simulations have been performed using the NPHASE CFD code. The results of simulations have been compared against experimental data, empirical correlations, and the predictions by other computer codes. Typical results are shown in Figures 1a and 1b.

The effect of variable properties of supercritical water has been analyzed on the operating conditions of SCWRs. Selected thermal-hydraulic aspects of proposed future SCWR designs have been analyzed. Figure 2 shows that,

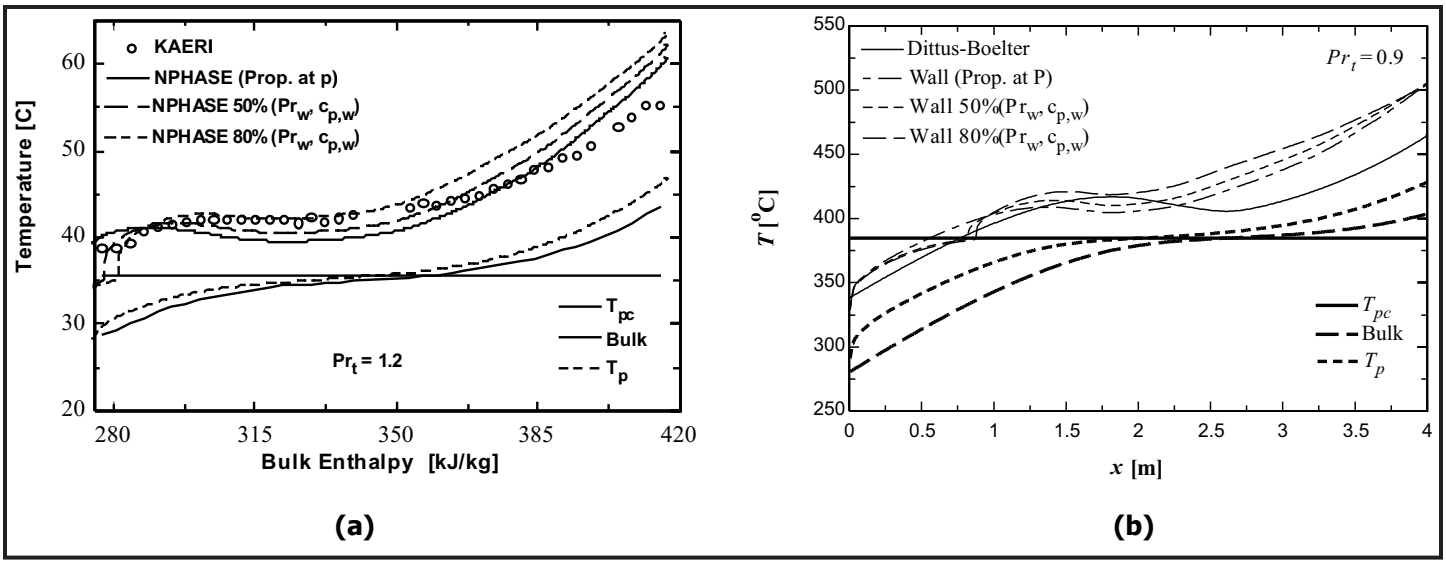

Figure 1. NPHASE predictions of fluid and heated wall temperatures at supercritical pressures: (a) CO_2 at 8.12 MPa and (b) water at 25 MPa.

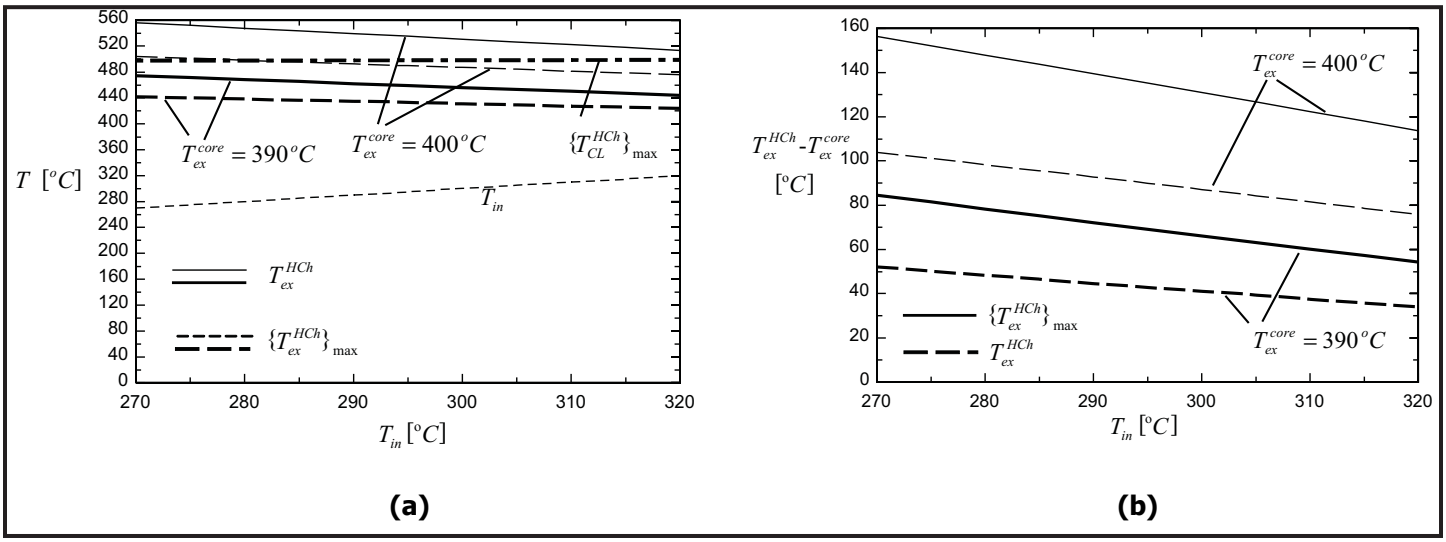

Figure 2. The effect of uncertainties in the evaluation of various SCWR parameters on the (a) maximum hot channel exit temperature and maximum cladding temperature and (b) maximum coolant temperature increase along the reactor core.

by modifying the reactor operating conditions and/or core design characteristics, significant improvements aimed at mitigating the effect of variable properties of supercritical water on the local non-uniform temperature distributions across the reactor core, and in particular, the exit coolant temperature, can be achieved.

Planned Activities

Following is a list of planned activities for the coming year:

- Complete the development of new mechanistic multidimensional models of turbulence and forced convection heat transfer for fluids at supercritical pressures
- Encode the new models in the NPHASE code, to perform model validation against available experimental data base for both water and CO_2, and to compare the results of model predictions against available phenomenological correlations
- Perform NPHASE-based virtual experiments and then use the results to develop scalable correlations and simple models for application in system codes
- Use the NPHASE code to perform numerical simulations of supercritical water systems corresponding to the anticipated designs of SCWR
- Continue the participation in the International Nuclear Research Initiative (I-NERI) collaboration, in particular with KTH and KAERI

Nuclear Energy Research Initiative

Novel Processing of Unique Ceramic-Based Nuclear Materials and Fuels

PI: Hui Zhang, State University of New York at Stony Brook (SUNY)

Collaborators: Brookhaven National Laboratory, Oklahoma State University (OSU)

Project Number: 05-110

Project Start Date: April 2005

Project End Date: August 2008

Research Objectives

The primary objective of this project is to develop high-temperature refractory ceramic materials for the fuel, in-core components, and control elements of gas-cooled fast reactors (GFRs). Refractory-based ceramics such as carbides, borides, and nitrides display a number of unique properties, including extremely high melting points, high hardness, high thermal and electrical conductivity, and solid-state phase stability. These unique properties make them potential candidates for a variety of high-temperature nuclear reactor components.

In this research effort, the team will demonstrate the feasibility of a novel process for fabricating mixed-carbide refractory composite materials based on pyrolysis of a mixture of preceramic polymers and submicron/nano-sized metal particles of uranium (U), zirconium (Zr), niobium (Nb), and hafnium (Hf). It will be carried out in a conventional oven under an inert atmosphere. This processing technique involves much lower energy requirements compared to hot isostatic sintering. It also provides the capability of fabricating net-shaped components and does not suffer from component size limitations, as does the chemical vapor deposition method.

This project will establish manufacturing processes for fabricating a variety of unique high-temperature ceramic materials and fuels, including metal ceramic carbides, mixed metal carbides, and unique metal silicon-carbides (SiCs). The resulting materials can be graded and will have a controlled microstructure (at both micron and nano levels), fiber-reinforced configurations, and a wide range of compositional control.

Research Progress

The research activities are broken into three primary tasks: 1) materials processing, 2) process modeling, and 3) nuclear transport. Each of these tasks is described below.

Materials Processing. During FY 2007, the team focused on the fabrication of SiC/uranium-carbide (UC) materials for nuclear fuel applications and on characterizing their physical and mechanical properties. Efforts of FY 2006 focused on fabricating SiC-UC materials for nuclear fuel applications, generating kinetics data, and characterizing structure-property relationships for precursor-derived SiC.

Materials processing was conducted at the new facility established at OSU. New equipment includes the acquisition of a new glove box and a new tube-furnace, both for enhanced environmental control. The pyrolysis of compacted specimens was carried out in the new tube furnace oven that was recently bought for better oxidation prevention. The oven was further modified with separate advanced oxygen and moisture traps with steel tubing at the receptor end to minimize any possibility of moisture and oxygen from the ultra-high purity argon supply. This resulted in successful pyrolysis and consolidation of each tried configuration so far. The pyrolysis temperature used during the current preparation was increased to 1,150°C (instead of the 900°C used at the Stony Brook Laboratory), which could be achieved in less time due to the enhanced capabilities of the oven.

The compositional matrix is nearly complete and materials have been fabricated to include both carbide and mixed-metal carbides based on Nb, Zr, and U, embedded in a SiC matrix. A total of 13 new material compositions

were fabricated and specimens were prepared for physical, mechanical, and thermal characterization. Measurement of density using pynometry, characterization of microstructure using scanning electron microscopy (SEM), determination of thermal conductivity, and measurement of mechanical strength using the ring-on-ring (RoR) test has been completed for all fabricated materials. Preliminary reaction kinetics data, using x-ray diffraction (XRD), has indicated the presence of in-situ, solid-state reactions. Figure 1 shows XRD data from materials fabricated using Nb nanoparticles incorporated into a SiC matrix. The unidentified materials, as shown in Figure 1, are suspected to be ternary carbides of Nb, Si, and C.

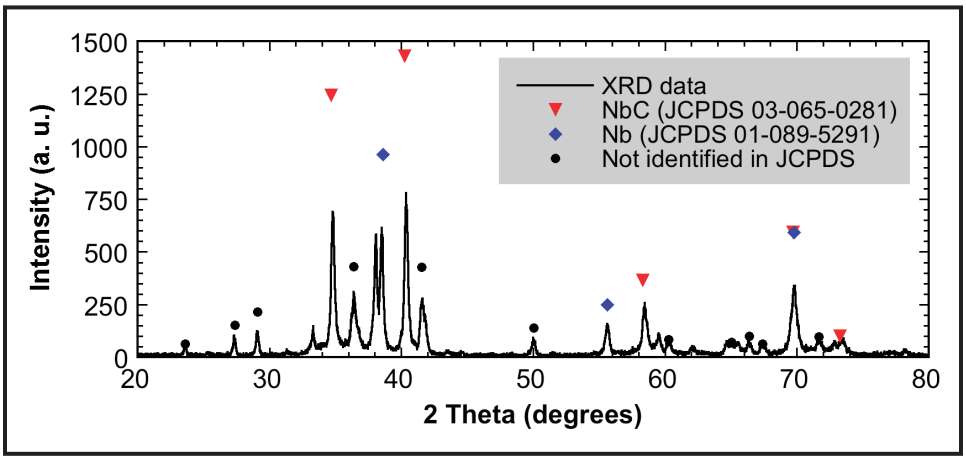

Figure 1. XRD data for Nb-rich regions in materials fabricated using Nb nanoparticles embedded in SiC showing the presence of NbC, free Nb, and some unidentified material(s).

In late FY 2007, researchers also initiated a comparison of SiC as fabricated using the polymer infiltration and pyrolysis (PIP) method and commercially available sintered SiC. This effort was initiated upon the request of Argonne National Laboratory (ANL) and seeks to compare the modulus, strength, and toughness of the two materials.

Process Modeling. During FY 2007, this task focused on further development of the "local process model" and the development of a "system model." The research team further refined and conducted studies on the microscale model developed in FY 2006. The microscale model is based on the smoothed particle hydrodynamics (SPH) method and focuses on the interaction between SiC matrix and filler particles, U_3O_8, or UC. First, the researchers have investigated the uncertainty associated with the random distribution of the filler particles in the microscale model, taking advantage of the mesh-free nature of SPH. The uncertainty is characterized by comparing the composition change of the filler for filler particles with the same particle size and volume ratio, but different random distribution. The reaction rates, heat and mass transfer, and composition changes of different components were also simulated, along with the effects of filler particle size on the microstructure and material properties of the final product. It was concluded that the production rate of both UO_2 and UC, as well as the microstructure of the product, is strongly dependent on the filler particle size. Also, the production rate of UC increases as the filler particle size increases. The effect of heating rate applied to the furnace on the composition evolution was also investigated, and it was concluded that the production rate of both UO and UC increases as the heat flux increases.

Nuclear Transport. During FY 2007, this effort focused on reactor design modifications for UC-SiC based fuels and initiated efforts for understanding the effects of other elements on the nuclear reactivity. Initially, researchers continued their investigation on the core configuration developed in FY 2006 that contained 271 pins per fuel assembly. This effort focused on the estimation of the requirements for fuel loading and the establishment of targets for the fuel development work. In FY 2007, it was found that a UC/SiC combination of 0.45/0.55 resulted in an acceptable beginning-of-life multiplication factor, a U density of 4.60 gm/cc, and an acceptably long core life to be practical. Later in FY 2007, the core configuration was further modified by increasing the number of pins per fuel assembly from 271 to 331. This change decreases the fuel power density from approximately 100 W/cc to 84 W/cc. This value is consistent with gas-cooled reactors; thus, heat removal under normal operating conditions and scrammed accident conditions should present no problems. The investigation then studied the sensitivity of the magnitude of the multiplication factor to various versions of the evaluated nuclear data files, as well as the size of significant feedback coefficients.

Finally, researchers investigated the reactivity effects of using fuel compositions based on NbC-UC-SiC, using the original core configuration. It was found that the multiplication factors show a significant drop when Nb is used in the core. This drop is due to the significant amount of resonance absorption that takes place in Nb.

Furthermore, adding U to the composition did not have the desired effect of significantly increasing the multiplication factor, since the Nb content is increased at the same rate. To alleviate this condition, two alternatives were investigated: varying the level of enrichment and using Zr instead of Nb.

Planned Activities

Materials processing will focus on the fabrication of two remaining compositions, completion of the materials property matrix (including comparison with commercially available sintered SiC), and the characterization of reaction kinetics in mixed metal carbides. The reaction kinetics data has been delayed due to instrumentation issues at OSU; however, once collected it will be incorporated into the process models. The process-modeling task will focus on efficient integration of the local and global models without losing information on porous structure, physics, chemistry, and variation. The integrated model will be compared with experimental measurements. The model can then be used to guide the design of the system and process of experiments. For instance, during the composite material fabrication, micro-cracks with various orientations/sizes may form. The optimal operating conditions to avoid such micro-cracks and to shorten the fabrication need to be obtained from the integrated model. The nuclear transport task will continue to investigate reactivity issues in mixed carbide fuels. This task will aid the effort in identifying compositions for the materials fabrication task.

Nuclear Energy Research Initiative

Real-Time Corrosion Monitoring in Lead and Lead-Bismuth Systems

PI: James Stubbins, University of Illinois at Urbana-Champaign

Collaborators: Los Alamos National Laboratory (LANL), Lawrence Livermore National Laboratory

Project Number: 05-114

Project Start Date: April 2005

Project End Date: March 2008

Research Objectives

The primary focus of this project is to address major corrosion issues associated with using lead (Pb) and lead-bismuth (Pb-Bi) liquid metals as working fluids in advanced nuclear systems. The approach to mitigate corrosion is to develop a persistent oxide film on the surface of internal structural components. The researchers will study material alloying and surface treatment approaches to form these protective films. If properly formed and maintained, the films can provide a useful barrier to inhibit the corrosive attack of liquid metal.

A central objective of this project is to further develop impedance spectroscopy (IS) for characterizing and monitoring corrosion in liquid metal systems. Researchers will use IS corrosion monitoring techniques to measure the kinetics and thermodynamics of the formation of oxide films on reactor structural materials. Use of this advanced real-time corrosion monitoring method to study scale formation on selected alloys will support the development of new corrosion-resistant alloy compositions and surface treatment techniques. Because the IS technology can measure oxide film formation in real time and is sufficiently compact, it can be deployed at numerous locations in an operating system to directly monitor local corrosion processes.

This project was designed to accomplish three major goals:

1) Develop the IS technique for Pb and Pb-Bi systems
2) Use enhanced IS techniques to measure the kinetics of oxide scale formation for a variety of materials and oxygen pressures at temperatures ranging from 200 to 700°C
3) Develop improved surface treatments and alloy compositions for enhanced corrosion resistance

Research Progress

The team conducted a number of IS scans again this year. Typically, the impedance responses were obtained by periodically scanning each sample over a range of signal frequencies from 100 kHz to 100 mHz. Figure 1 shows the impedance response of a typical sample of 316 stainless steel (SS) that was preoxidized for 48 hours. At the top of the figure is a complex plane plot, commonly called a Nyquist plot, which shows the imaginary impedance (reactance) versus real impedance (resistance). What is plotted is actually the negative of the imaginary impedance, since only capacitance, not inductance, is important for this project. These Nyquist curves show the impedance responses at several different times over an exposure period of nearly 10 days. The lower part of the figure shows the results of an equivalent circuit model which is used to characterize the behavior of the system. Randles equivalent circuit models typically portray the corrosion film and associated metal substrate and liquid metal fluid in terms of set resistance (impedance) and capacitance values. These values change with corrosion conditions, but are characteristic of the growth of the corrosion layer during exposure. The conditions shown in the model are those for the longest exposure, i.e., the largest curve in the experimental data at the top.

The corrosion responses simulated by the Randles equivalent-circuit model should provide some of the physical insight to the system which can be used to fit the experimental results. At overall large impedance magnitudes, however, the fit of the Randles model worsens, indicating that other, unknown electrochemical and physical processes may be taking place. In these cases, a constant phase element (CPE) seems to fit the data much more accurately. Values for the Randles

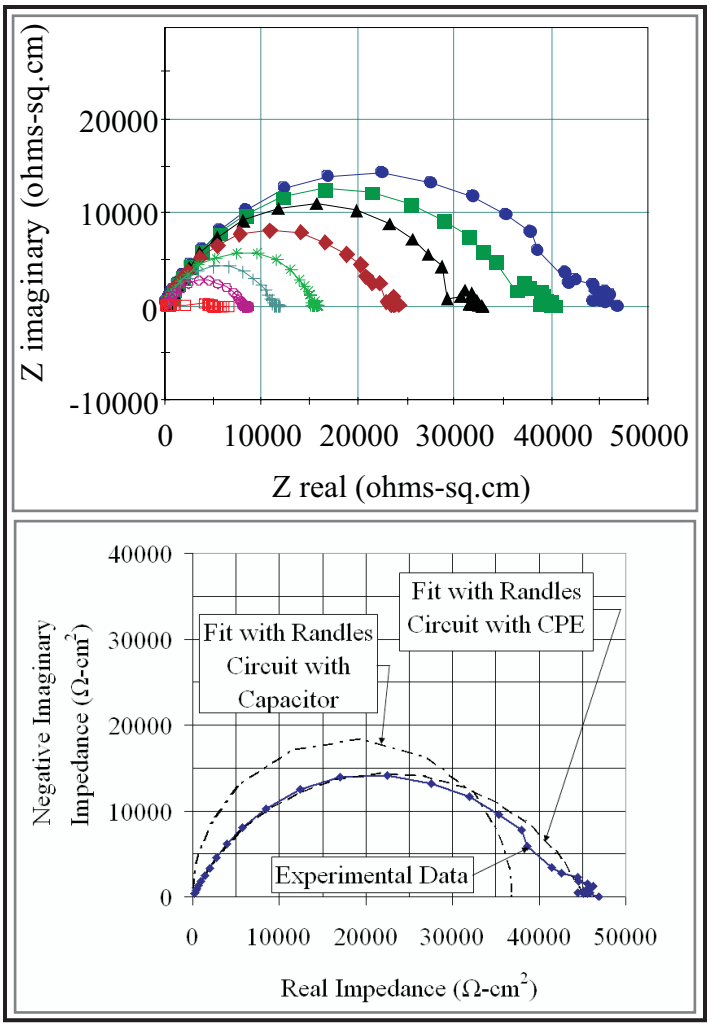

Figure 1. IS results for a single preoxidized sample of 316 SS in Pb-Bi eutectic (LBE) at 200°C. The measured Nyquist Plot is shown at the top and the Randles equivalent circuit model for the Nyquist plot is shown at the bottom.

equivalent circuit, including resistance, capacitance, and CPE, are shown in the following table. Note the large values of resistance which are typical of these films.

In addition to measurements on unperturbed films, a series of runs has been performed on films with microhardness indentations to establish the dynamics of oxide repair.

Sample	Fit	R_{oxide} (Ω-cm^2)	$(C \text{ or } T)_{oxide}$ (nF/cm^2)	CPE Exponent
A	With Capacitor	36800	6.5	1
A	With CPE	45200	160.7	0.722

Table 1. Randles Equivalent Circuit Values.

It was observed that the film repair characteristics and the IS response were essentially the same as the initial preoxidized condition. That is, after re-exposure to the LBE, the impedance grew rapidly after an initial incubation period, just as observed with undamaged specimens. A remarkable characteristic of the indented specimens was that the indentation depth was much greater than the film thickness. Despite this, the film remained intact, without noticeable cracking or delamination, as is shown in Figure 2.

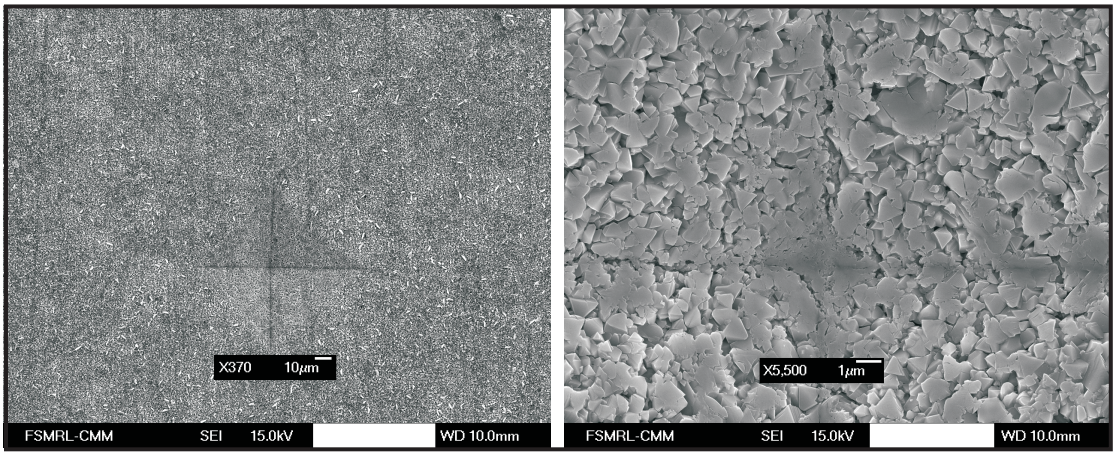

Figure 2. Two scanning electron microscopy (SEM) micrographs showing the microhardness indentation characteristics of the oxide film after exposure to LBE. The micrographs are of the same area at two magnifications.

Planned Activities

During the next year, the team plans to continue work on three research efforts: 1) verification and extension of a point defect model to liquid LBE corrosion, 2) experimental verification that heating and quenching the incoming gas can work around the kinetic limitations of oxygen control by gas dynamic equilibrium, and 3) experimentation to quantitatively determine the effect of mechanical integrity defects on the impedance response of oxide layers. In addition to these initial goals of the program, researchers plan to employ atomic force microscopy to measure film characteristics and relate these directly to the measured impedance properties of the films. This should provide a quantitative, physical basis for the resistance and capacitance properties using the Randles equivalent circuit approach. The team has been working closely with the group at LANL over the past nine months with a constant presence at the lab to advance various experimental parts of the program. Researchers plan to continue this close collaboration over the next year.

Nuclear Energy Research Initiative

The Effect of Hydrogen and Helium on Irradiation Performance of Iron and Ferritic Alloys

PI: James Stubbins, University of Illinois at Urbana-Champaign

Collaborators: Los Alamos National Laboratory (LANL); Lawrence Livermore National Laboratory (LLNL); Argonne National Laboratory (ANL); University of Michigan; Washington State University (WSU); the Belgian Nuclear Research Centre (SCK/CEN); Hokkaido University, Japan

Project Number: 05-116

Project Start Date: May 2005

Project End Date: April 2008

Research Objectives

The goals of this research project are to 1) develop a fundamental understanding of irradiation-induced defects on ferritic alloys, 2) understand the roles of hydrogen (H) and helium (He) in damage evolution, and 3) extend this knowledge to increasingly complex iron (Fe) alloy materials that are of interest for advanced reactor and accelerator-based applications. This information will be applied to the development of more irradiation-resistant alloys. Researchers will accomplish these goals through a combination of experiments and modeling.

Ferritic alloys are the prime choice for structural and component applications in several advanced reactor and accelerator-based system concepts. This class of alloy has relatively high irradiation resistance and retains good structural properties in temperatures ranging from 400 to 700°C. Existing irradiation performance data was developed for the fast breeder program, but this database represents fast fission neutron spectra.

This project addresses irradiation damage and effects in advanced reactor and accelerator-driven systems concepts. It will encompass substantial new developments in experimental analysis and high-speed computational modeling of the formation and evolution of defects in ferritic metals and alloys during radiation exposure. It will also focus on the influence and possible synergistic effects of H and He during defect production, clustering, and extended damage structures during irradiation. The experimental program will examine the evolution of point defects and defect structures as a function of radiation exposure, irradiation temperature, and H/He production in increasingly complex materials, ranging from the simplest single crystal iron, to polycrystalline iron and iron alloys, through advanced ferritic/martensitic steels.

The workscope consists of the following tasks:

- Perform microstructural and microchemical analyses for a set of irradiation exposure conditions. Materials include single crystal iron and increasingly complex binary, ternary, and commercial alloy systems, using ion irradiation to accurately control H and He levels and irradiation dose.
- Perform large-scale molecular dynamics and kinetic lattice Monte Carlo simulations to understand the effects of irradiation on material properties and damage processes.

Research Progress

The objective of the first two years of the research was to conduct and analyze proton and He irradiations in single crystal, body-centered cubic (BCC) iron and to extend the work to Fe-chromium (Cr) alloys. Irradiations of single crystal BCC Fe for both the protons and He were completed in year one. These specimens have been analyzed with positron annihilation spectroscopy (PAS) and transmission electron microscopy (TEM) to understand the effects of H and He on the damage microstructure. Simulations were also performed to emulate the experimental conditions utilized and to follow the defect evolution processes.

Specimens of single crystal Fe-14Cr and Fe-19Cr were obtained during the second year of the program effort. These single crystal specimens were prepared for ion irradiation in a matrix similar to that used for

the single crystal Fe specimens in the first program year. Currently, irradiations are performed in the ANL Intermediate Voltage Electron Microscope (IVEM)/Tandem Accelerator Facility to directly study and compare irradiation damage evolution between Fe and Fe-Cr alloys. The results of some of these studies are shown in Figure 1. Irradiations were carried out at 450°C with 150 keV Fe ions to simulate neutron-induced damage cascades. Doses up to about $1x10^{15}$ ions/cm^2 were attained. These doses are consistent with about 3.5 displacements per atom (dpa).

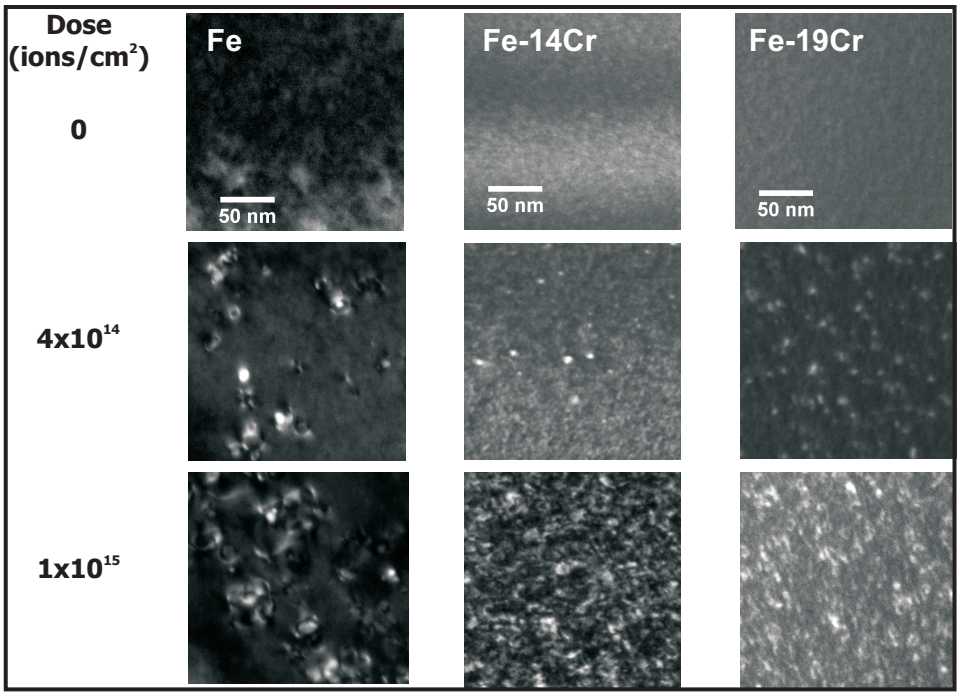

Figure 1. Damage evolution at 450°C in Fe and Fe-Cr alloys as a function of 150 keV Fe ion dose irradiated and imaged in the ANL IVEM/Tandem Accelerator Facility.

Other experimental work included PAS at WSU, synchrotron x-ray spectroscopy at APS-ANL, and electron microscopy at ANL and the University of Illinois to characterize defect structures in irradiated Fe and Fe-Cr alloys. In addition, experimental work to examine mechanical properties behavior of Fe-Cr alloys with a variety of carbon levels is ongoing. This work included modeling the approach to plastic instability due to the presence of second phase and grain reorientation, i.e., texture development, during post-yield deformation. This work is currently making use of electron backscattered diffraction techniques to understand the influence of grain structure reorientation during deformation. This year, several tests were run at APS-ANL to characterize the evolution of deformation during uniaxial straining of these materials. This will later be applied to understanding the influence of irradiation at various temperatures on the deformation dynamics in this class of alloys.

Irradiation damage modeling work with molecular dynamics (MD) cascade simulations and kinetic Monte Carlo (KMC) simulations of defect structure evolution has gone forward through collaborations with LANL, LLNL, and SCK/CEN. This work is being carried out with direct connection to the experimental irradiation damage program described above.

Planned Activities

During the next year, this project will focus further on the microstructural evolution caused by radiation damage in Fe and Fe-Cr alloys. The experimental techniques—TEM, PAS, and x-ray scattering—will continue to be employed for identifying and quantifying defects. The work with Fe alloys will examine how the alloying elements (i.e., chromium and carbon) affect the microstructural evolution when the system is exposed to proton irradiation and the presence of He. This work will also be carried out with both similar experimental and computational techniques. These results will be compared to that of pure Fe to understand the effects of the alloying elements.

Irradiations will be carried out on at least three different temperatures: 573, 723, and 823 K on the Fe-Cr single crystal materials (Fe-14Cr and Fe-19Cr) to fully understand the effect of Cr on the damage structure evolution. Once these samples are irradiated as described, they will be analyzed using PAS measurements. Positron annihilation lifetime spectroscopy (PALS) will be continued at WSU on the single crystal Fe and Fe-Cr specimens. Following all of the PAS experiments, the specimens will be analyzed via TEM.

Nuclear Energy Research Initiative

Alloys for 1,000°C Service in the Next Generation Nuclear Plant

PI: Gary S. Was, J. Wayne Jones, and Tresa Pollock, University of Michigan

Collaborators: Special Metals, Inc., Idaho National Laboratory, Oak Ridge National Laboratory

Project Number: 05-143

Project Start Date: April 2005

Project End Date: October 2008

Research Objectives

The objective of this project is to define strategies for improving alloys used for structural components in high-temperature helium reactors, such as the intermediate heat exchangers and primary-to-secondary piping. Specifically, the project will investigate oxidation/carburization from helium impurities, microstructural stability, and impact on creep behavior at temperatures between 900 and 1,000°C. The aim is to better understand the synergism among these critical processes and to provide data for long-term prediction of properties.

The design of the very high-temperature reactor (VHTR) proposed for the Next Generation Nuclear Plant (NGNP) project calls for outlet gas temperatures of up to 1,000°C. These are extremely challenging conditions for operating the metallic components in the intermediate heat exchanger and primary-to-secondary piping. Inconel 617, an advanced nickel-based alloy, has been identified as a leading candidate for such applications. However, its material properties in a high-temperature, impure helium environment are not sufficiently understood to qualify this alloy for service. Therefore, this study will also investigate alloy and microstructure modifications needed to enhance Inconel 617 properties.

Research Progress

Experiments on the behavior of alloy 617 in He-CO-CO_2 gas have been conducted for six gas mixtures in which the CO/CO_2 ratio varies between 7.2 and 1,320 and between temperatures of 850 and 1,000°C. The mixture with a CO/CO_2 ratio of 7.2 and temperatures of 950 and 1,000°C results in a net production of CO, while at temperatures of 900 and 850°C and at all CO/CO_2 ratios above 7.2, CO is consumed at all temperatures (Figure 1). Exposure of 617 to a CO/CO_2 ratio of 7.2 at 950 and 1,000°C causes oxidation and decarburization of the sample, indicated by an initial weight loss (Figure 2a). The lower temperatures at a ratio of 7.2 and all other temperatures at all other CO/CO_2 ratios resulted in oxidation and carburization, as typified by the plot for a CO/CO_2 ratio of 455 (Figure 1b). For CO/CO_2 ratios above 7.2, oxidation is characterized by the formation of a chromium-rich external scale, internal oxidation of aluminum to form alumina, and the formation of a thin discontinuous layer of alumina just below the external oxide scale at all temperatures (Figure 3). For all CO/CO_2 ratios above 7.2, the partial pressure of CO in helium is

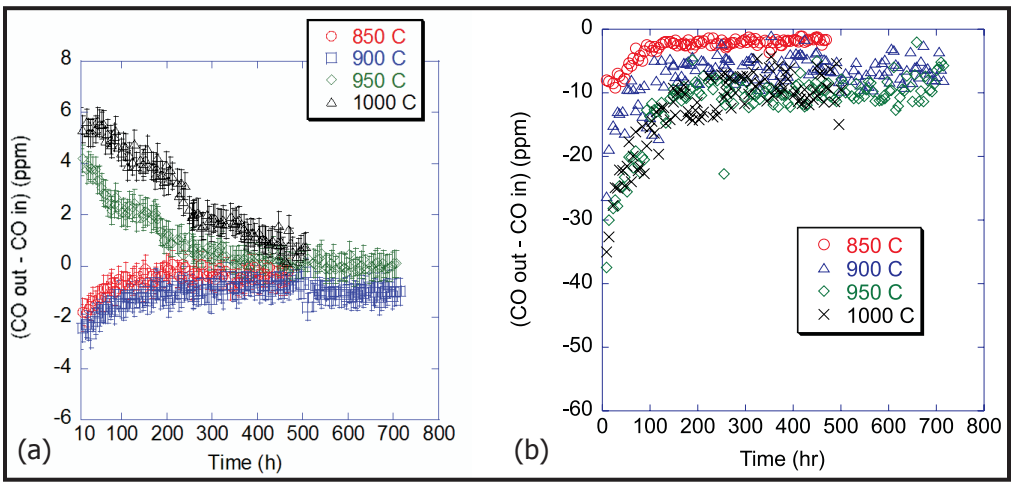

Figure 1. Plot of the difference between the CO concentrations at the outlet and inlet for (a) a CO/CO_2 ratio of 7.2 and (b) a CO/CO_2 ratio of 455 at 850, 900, 950, and 1,000°C.

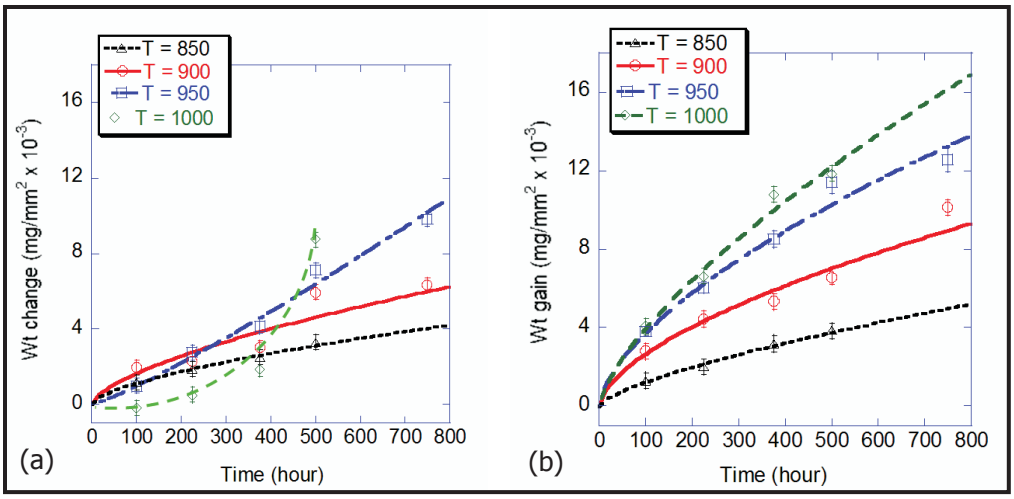

Figure 2. Weight change for alloy 617 over the temperature range 850–1,000°C in (a) a CO/CO_2 ratio of 455 and (b) a CO/CO_2 ratio of 7.2.

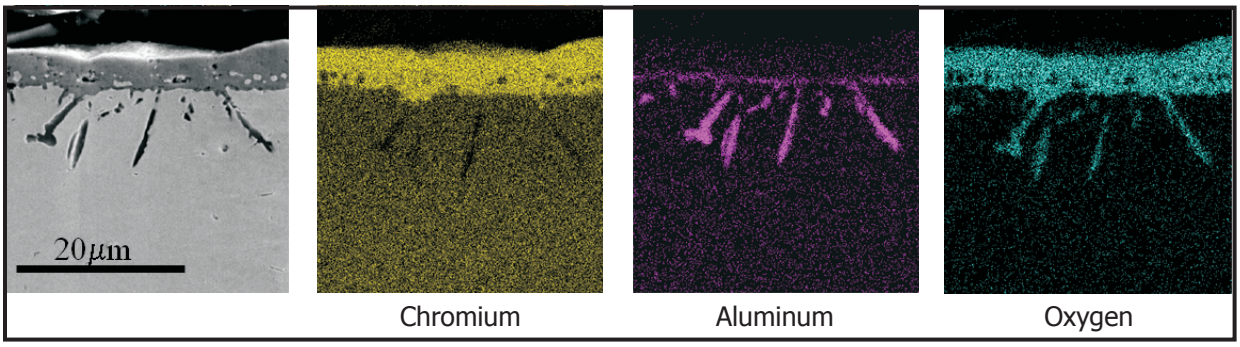

Figure 3. Scanning electron microscopy (SEM) image and corresponding x-ray maps for chromium, aluminum, and oxygen for a sample of 617 exposed to a CO/CO_2 ratio of 455 for 750 hours at 950°C.

high enough for the CO to react with Cr to form chromium carbide and chromium oxide over the temperature range 850-1,000°C, according to the following:

$$(27/6)\ Cr + CO \Leftrightarrow (1/6)\ Cr_{23}C_6 + (1/3)\ Cr_2O_3.$$

However, the partial pressure of CO in a gas mixture with a CO/CO_2 ratio of 7.2 and temperatures above 950 and 1,000°C is low enough to cause the reaction above to proceed in the reverse direction, resulting in decarburization and the release of CO, as observed.

The first set of experimental alloys (J-series) that exhibited potential in terms of oxidation resistance (weight loss/gain) and creep strength (in compression) at 1,000°C consisted of the compositions listed in Table 1.

Based on the oxidation results, the order or increasing oxidation resistance for the J-alloys listed in Table 1 is J2 < J7 < J8 < J6 < J9. The preliminary impure-helium exposure results for J-alloys in atmosphere #1 (CO/CO_2 approximately 7/1) at 1,000°C is shown in Figure 4. The alloys with Re addition exhibited decreased weight gain at

Alloy	Cr	Co	Mo	W	Re	Al	C	Wt. gain mg/cm^2	Compressive strength, MPa
J2	12	-	-	12	-	3	0.05	1.2	123
J6	15	12	2.7	5.3	7.6	2.3	0.05	0.175	133
J7	15	12	-3	8	6	2.3	0.05	0.92	113
J8	15	12	3	12	3	2.3	0.05	0.42	123
J9	12	12	3	8	6	2.3	0.05	0.08	123

Table 1. Composition of potential high-temperature Ni alloys from the J-series.

25 hours and 50 hours exposure compared to the Re-free J2 alloys. Additionally, the weight gain is seen to decrease with increasing Re between J8 (3 wt.% Re), J9 (6 wt.% Re), and J6 (7.6 wt.% Re) alloys, respectively. Evidently, the Re additions are affecting reactions at 1,000°C in this decarburizing atmosphere and exhibit potential for corrosion resistance in these atmospheres. The order or increasing corrosion resistance for the J-alloys under impure He exposure is J2 < J8 < J6 < J9, which is similar to the oxidation behavior. Preliminary x-ray diffraction analysis has shown that the presence of Re may discourage the formation of Cr_2O_3 compared to Al_2O_3. This is important because Cr_2O_3 becomes unstable at temperatures near or above 1,000°C compared to the stable Al_2O_3. Further analysis is currently underway.

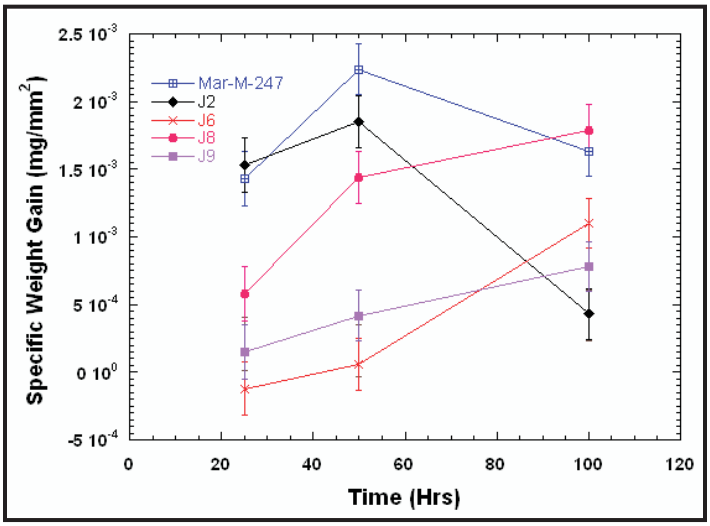

Figure 4. Specific weight gain of J-alloys containing Re during impure-He exposure at 1,000°C. With the exception of the J2 alloy, J6, J8, and J9 alloys contain 7.6 wt.%, 3 wt.%, and 6 wt.% Re, respectively.

Planned Activities

Exposure tests are planned to understand the mechanism responsible for the "microclimate" phenomenon that causes the reversal from decarburization to carburization with increasing temperature in CO/CO_2 = 7.2.

Experiments will also be conducted to determine the effect of water vapor on the kinetics of decarburization for alloy 617 in impure helium. Decarburization of alloy 617 above the critical temperature, which lies between 900 and 950°C, in a He-CO-CO_2 environment occurs via the following:

$$2\ Cr_2O_3 + Cr_{23}C_6 \rightarrow 27\ Cr + 6\ CO. \quad (1)$$

The presence of H_2O in the gas-mixture can increase the rate of decarburization as per the following reaction:

$$6\ H_2O + Cr_{23}C_6 \rightarrow 23Cr + 6CO + 6\ H_2. \quad (2)$$

In order to determine the effect of water vapor on the kinetics of decarburization, known amounts of H_2O will be added to the He-CO-CO_2 environment. The rate of decarburization in He-CO-CO_2 and He-CO-CO_2-H_2O will be compared to determine the effect of water vapor on the kinetics of decarburization.

To gain a better understanding of the solid solution strengthening effects of individual elements and multiple-solute alloys, fundamental studies on the strength of binary, ternary, and multi-component Ni alloys are currently underway. These include Ni-X binary, Ni-Cr-X ternary, and Ni-Cr-X-Y quaternary alloys, where X and Y solutes have been chosen from among molybdenum (Mo), tungsten (W), rhenium (Re), and ruthenium (Ru) elements. Several alloys with differing compositions of Mo, W, Re, and Ru are being prepared for compression testing at both low (25°C) and high temperatures (1,000°C) in order to obtain the critical solid-solution strengthening data for various additions of the most promising strengtheners from the 4d and 5d rows of the periodic table, namely Mo, Ru, W, and Re. This program is meant to provide support for the implementation of a second series of experimental alloys discussed below.

The strategy for the second experimental alloy set will explore Ru for solid-solution strengthening. Since Re is an expensive element, some of the experimental alloys will have minimum or no Re. Moreover, with W being the primary choice for maximum solid-solution strengthening in these single-phase Ni alloys, the new alloy set may contain 8-18 wt % W. Maximum W contents will be limited to that which produce only single phase Ni alloys. Results from the solid solution strengthening effects of individual solute additions will assist in refining the exact compositions and alloy modifications for this new alloy series.

Based on the outcome of the microstructural and mechanical tests, selection of compositions for two or three scale-up heats of 50 lbs will be made at Special Metals. Creep studies have begun using sheet specimens designed to maximize surface to volume ratio. A custom-built tensile creep system has been designed for creep experiments in controlled impure helium atmospheres at temperatures up to 1,000°C.

Nuclear Energy Research Initiative

Heat Exchanger Studies for Supercritical CO_2 Power Conversion System

PI: Akira Tokuhiro, Kansas State University (KSU)

Collaborators: Argonne National Laboratory

Project Number: 05-146

Project Start Date: January 2005

Project End Date: December 2007

Research Objectives

A gas turbine Brayton Cycle utilizing supercritical carbon dioxide (CO_2) working fluid is being considered for some Generation IV nuclear energy systems. This advanced power conversion technology is expected to increase efficiency and significantly reduce plant cost, size, and complexity. An added benefit is high-temperature operation suitable for hydrogen cogeneration. While such benefits derive from the unique thermo-physical properties of supercritical CO_2, these same properties also present technical challenges for the design of a regenerative heat exchanger.

To maximize the usefulness of the supercritical CO_2 (S-CO_2) power conversion system, researchers must design a compact heat exchanger and develop its basic performance data. The objectives of this project are to 1) establish heat exchanger performance under design conditions, 2) estimate performance for beyond design-basis accidents, and 3) compare different heat exchanger design options. The project will conduct the following activities:

- Design, construct, and operate an experimental facility for performance testing of compact heat exchangers for the supercritical CO_2 Brayton cycle recuperator/cooler application
- Obtain heat transfer and pressure drop data to evaluate performance of selected compact heat exchanger designs (e.g., printed circuit heat exchanger, or PCHE)
- Develop fluid flow and heat transfer simulation models and tools to support the evaluation of heat exchanger designs

Research Progress

During the past year, the planned CO_2/water heat exchanger tests have been completed using the Heatric PCHE. Along the way, the research team experienced a number of mechanical issues, such as suitability of pump seal materials and the malfunctioning of the resistance temperature detector (RTD). Figures 1 and 2 provide the CO_2/water loop schematic, a computer-generated solid model view, a top-down photo of the PCHE, and a photo of the loop.

Traditional heat exchanger analysis is based on a number of assumptions that are invalid under the current applications. In particular, the results to date indicate that the thermo-physical properties of CO_2 change throughout the heat exchanger. Researchers sought to understand these results from a number of perspectives. With respect to the water/water friction factor measurement, the team assumed that the hot and cold side friction factors are similar. For the purpose of calculating the convective heat transfer coefficients between supercritical CO_2 (SCO_2) and water, they also assumed that the heat transfer coefficients of water/water at a given Reynolds number is approximately equal. Using these assumptions and results from water/water tests, researchers calculated the heat transfer coefficient of water at given Reynolds numbers for the SCO_2/water tests. Equation 1 shows the calculation of the heat transfer coefficient of water using the traditional log-mean temperature method.

$$Q = UA\ln\Delta T_M \quad \frac{1}{U} = \frac{1}{h_h} + \frac{x}{k} + \frac{1}{h_c} \quad h_h h_c = h \quad \rightarrow \quad h \approx 2U \qquad (1)$$

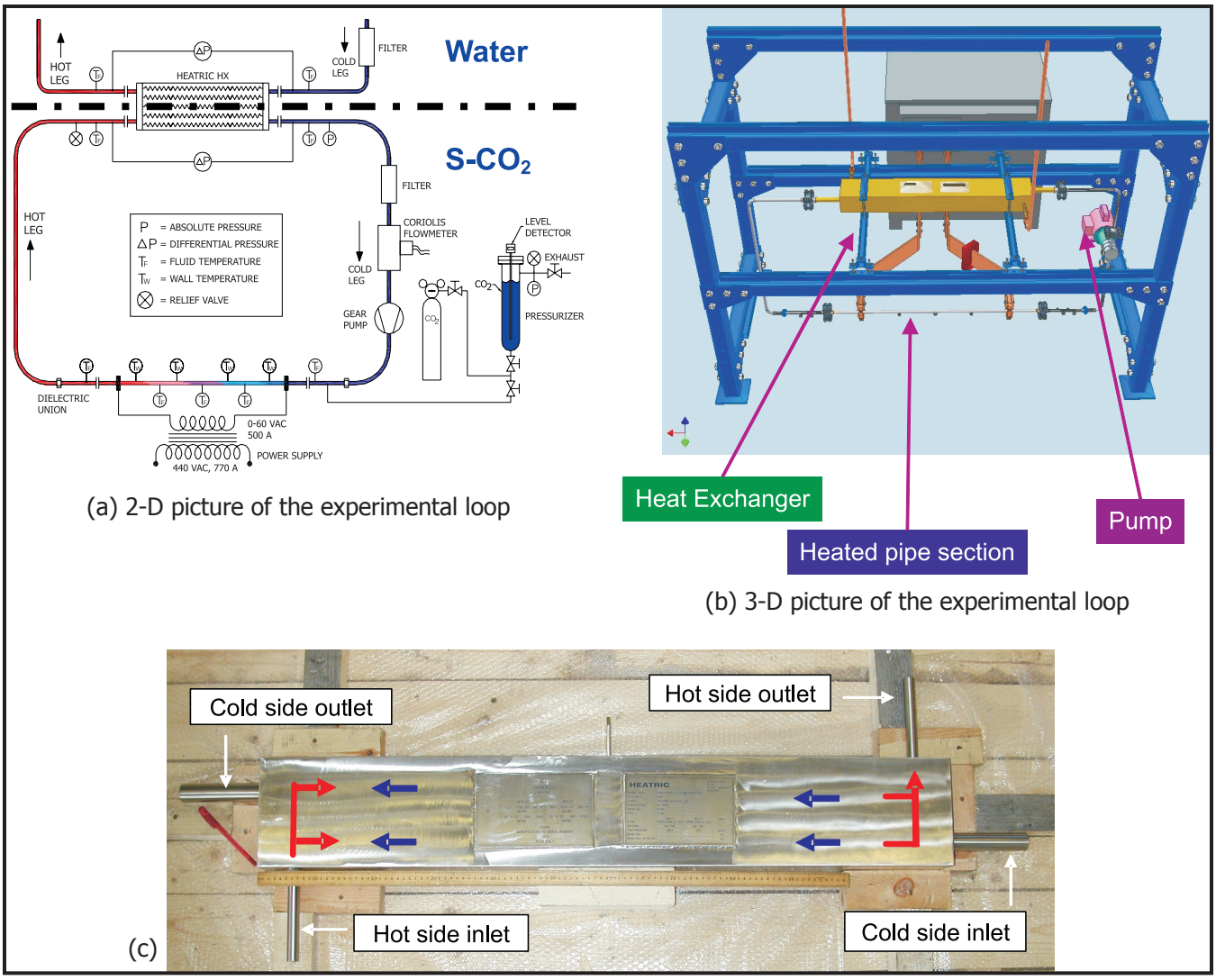

Figure 1. (a) Schematic of the CO_2/water PCHE test loop, (b) solid model of the loop, and (c) top-down view of the Heatric PCHE with inlet/outlet as indicated.

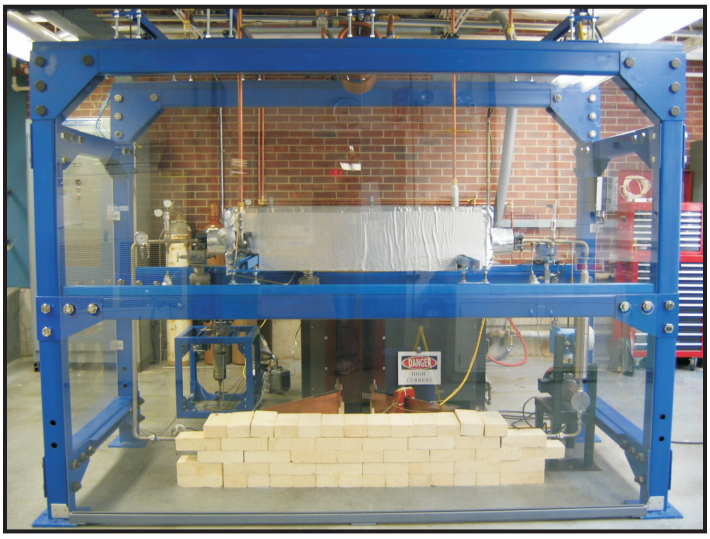

Figure 2. Frontal view of the CO_2/water PCHE test set-up. Item in center (silver) is the insulated PCHE.

Researchers noted that the heat transfer tests between SCO_2 and water were conducted at 75 and 85 Mpa—the 75 MPa test simulated the operating pressure of the STAR-LM pre-cooler. In order to contrast results at 75 MPa, they conducted a test at 85 MPa. The heat transfer coefficient of water for the CO_2/water test was calculated by measuring the water-side Reynolds numbers and that of SCO_2 using the equation above. Representative experimental results are presented in Figure 3.

Figure 3a shows that the temperature distribution along the PCHE heat exchange length described in "nodes" is non-linear on the CO_2 side relative to the water side. Further, in Figure 3b, for the two 7.5 MPa tests, there was no significant difference in the heat transfer coefficient, even though the outlet temperature for one run was closer to the pseudocritical point than the other run. While Figure 3b shows very little difference in this traditional representation, the difference in outlet condition commands careful consideration.

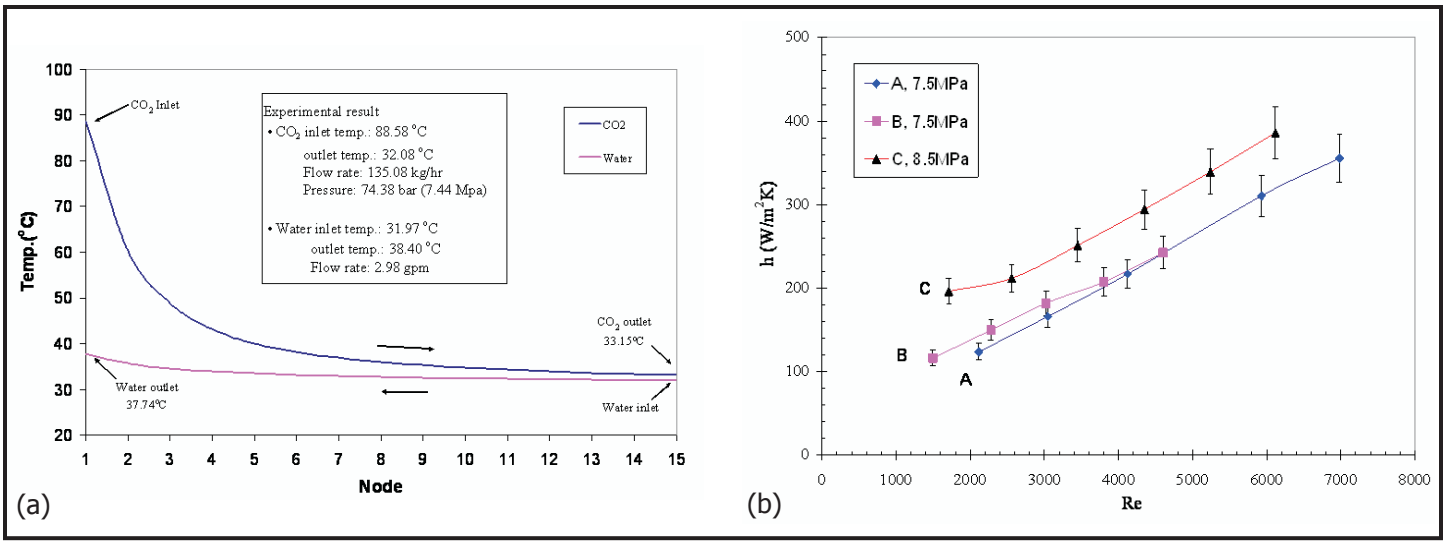

Figure 3. (a) Representative temperature distribution with the CO_2 and water channels of the PCHE, and (b) heat transfer coefficient versus Reynolds number (based on average flow) at 7.5 and 8.5 MPa, but with different outlet conditions.

Based on classical thermodynamic analysis of "lambda point" phase transition, like that experienced by CO_2 and, additionally, order of magnitude analysis (OMA) of the conservation equation, there is an alternative method whereby heat transfer data can be presented to reveal finer differences. Figure 4 shows just how peaked the "lambda" transition is for specific heat and (a decrease in) density.

Figures 5a and 5b depict the modified Nusselt number versus the non-dimensional temperature with respect to the critical temperature in Figure 5a and versus the Re and Pr-numbers with the exponential power dependence dictated by OMA. Note that the modified Nusselt is squared and typically has a small correction in terms of the Pr-number. This latter term essentially originates from consideration of both the axial and transverse gradients of the change in enthalpy of CO_2 in the energy equation. Figure 5b depicts experimental runs 1) at 75 bar with the outlet very close to critical conditions (red triangles), 2) at 75 bar with the outlet further from critical (blue diamonds), and 3) at 85 bar also with the outlet near critical. As the $RePr^{4/3}$ grouping can be dominated by the specific heat, C_p, contained in the grouping, the heat transfer does not increase as rapidly as at 85 bar where the C_p has a much smaller increase near the critical temperature. Also, if the outlet is close enough to the critical temperature (for the two 75 bar runs), the heat transfer does not increase as rapidly relative to operating the outlet further from critical. Finally, the linearity of the data presented appears to substantiate the validity of the analytical treatment.

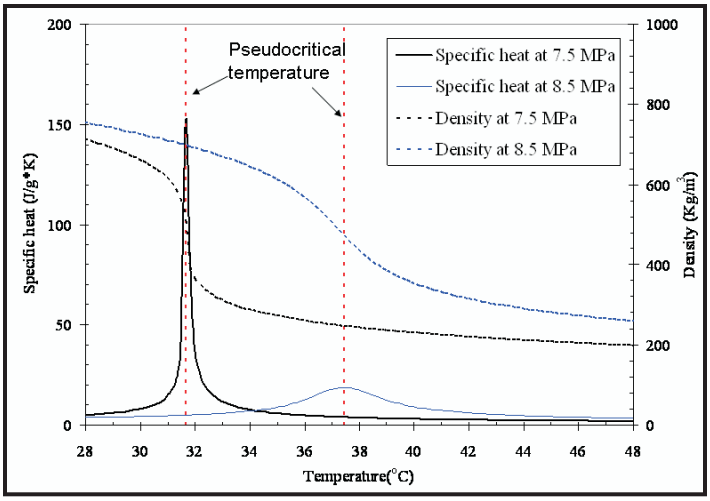

Figure 4. Change in specific heat and density of supercritical CO_2 at 7.5 and 8.5 MPa near the critical temperature.

Planned Activities

Upon completion of the CO_2/water PCHE tests, researchers modified the test facility to accommodate high and low pressure S-CO_2. The objective is to conduct PCHE (or similar heat exchanger) testing for higher pressure CO_2/lower pressure CO_2 heat exchange, simulating the low-temperature recuperator for the CO_2 Brayton cycle where the CO_2 temperature ranges from 85 to 150°C. Researchers plan to finish these tests as soon as possible and then move on to the second type of heat exchanger.

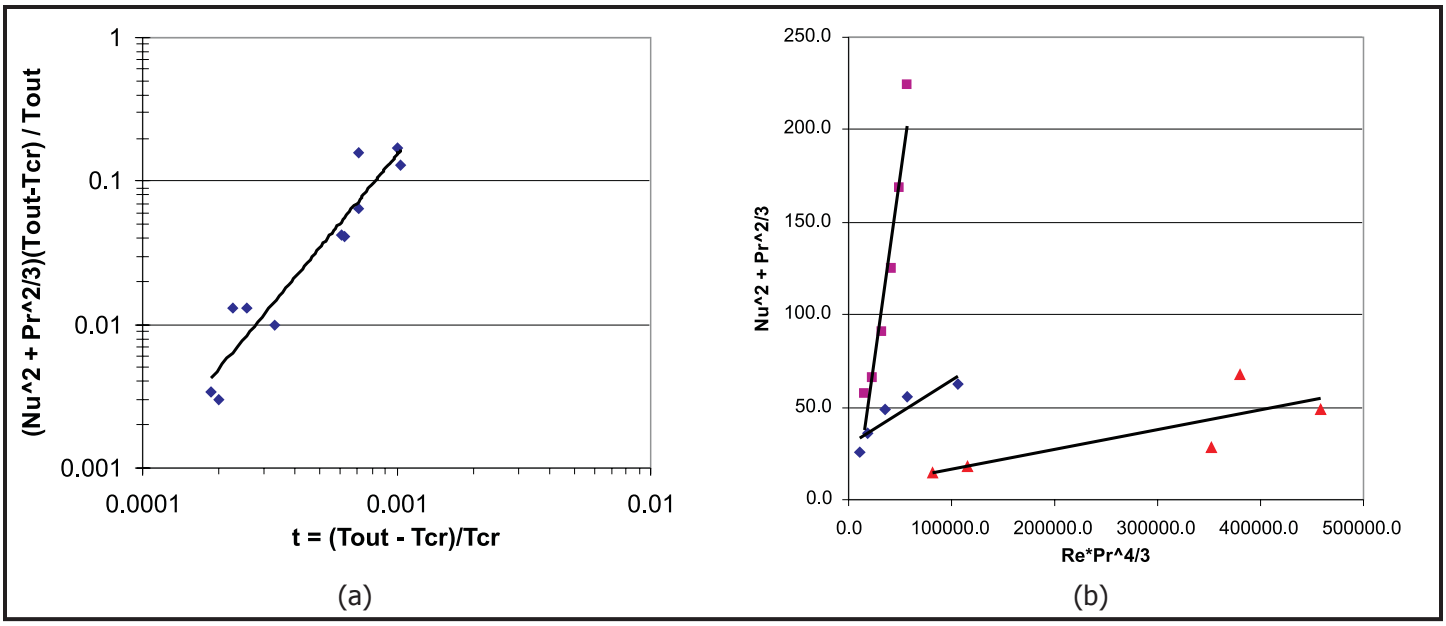

Figure 5 (a) and (b). Average hot side heat transfer coefficient for cooler conditions; water on the cold side and CO_2 on the hot side.

The team is continuing the modeling of the idealized compact heat exchanger using the CFD code, STAR-CD, with some results using a simplified four-layer, hot and cold channel heat exchanger model using FLUENT as a benchmark. With STAR-CD, the research team encountered meshing problems with a multi-layered PCHE model depicted in Figure 6a that were judged to be difficult to resolve. Therefore, researchers have restarted with a shortened PCHE model with a reduced number of hot-and-cold channel layers. In addition, the research team ran FLUENT simulations using the above simplified model and thermophysical property changes around the critical point modeled via (increased precision) polynomial curvefits. Figure 6b shows a representative isotherm from the team's FLUENT simulation.

Procurement of the second compact heat exchanger is still in progress with Heatric.

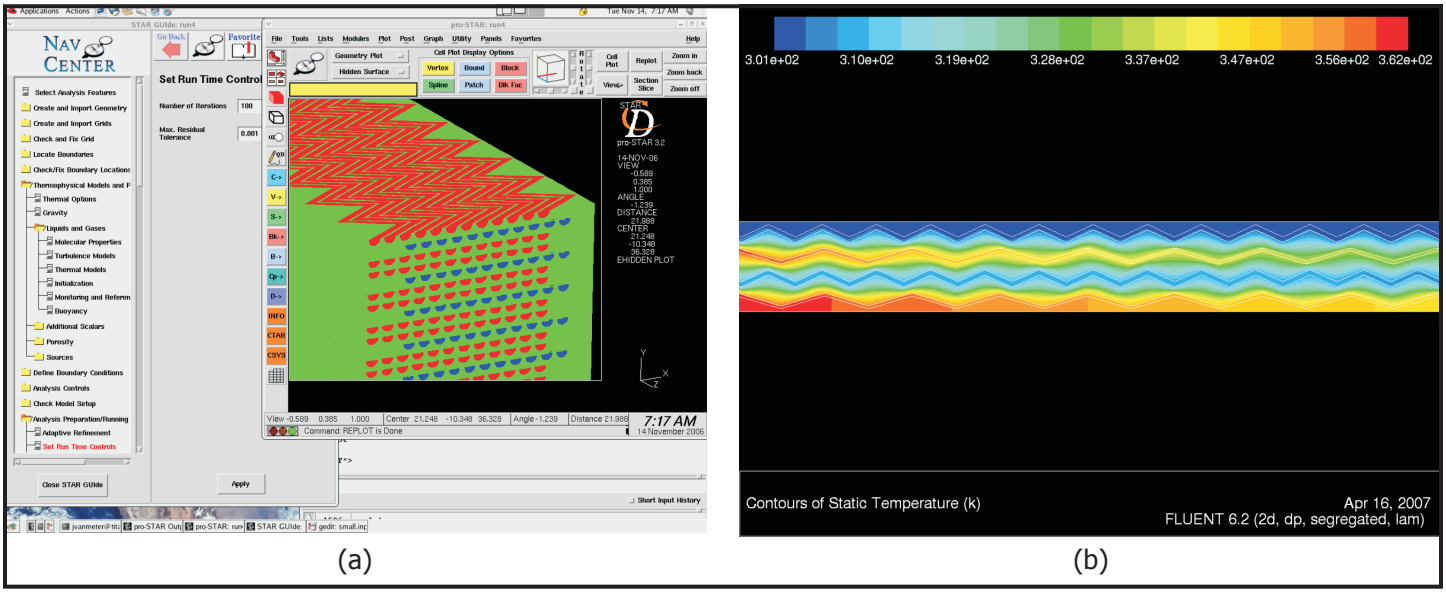

Figure 6. (a) Snapshot from the STAR_CD PCHE model working environment and (b) isotherms from FLUENT modeling of a four-layer heat exchanger model with two hot and two cold zigzag channels (angles 139° and 113°).

Nuclear Energy Research Initiative

Candidate Materials Evaluation for the Supercritical Water-Cooled Reactor

PI: Todd Allen, University of Wisconsin - Madison

Collaborators: University of Michigan

Project Number: 05-151

Project Start Date: March 2005

Project End Date: March 2008

Research Objectives

The supercritical water-cooled reactor (SCWR) system is being evaluated as a Generation IV concept. This system provides higher thermal efficiency and plant simplification than currently proven light water technology. However, because supercritical water (SCW) presents unique challenges to long-term performance, developing, testing, and selecting suitable materials for cladding and internal components are central to designing this reactor.

The objective of this project is to investigate degradation of materials in a SCW environment. First, researchers will study representative alloys from the important classes of candidate materials, including ferritic-martensitic (F-M) steels, austenitic stainless steels, and Ni-based alloys, to analyze their corrosion and stress-corrosion cracking (SCC) resistance in SCW at various temperatures, exposure times, and water chemistries. Second, emerging plasma surface modification and grain boundary engineering (GBE) technologies will be applied to modify the near-surface chemistry, microstructure, and stress-state of the alloys prior to corrosion testing. Third, researchers will examine the effect of irradiation on corrosion and SCC of alloys in the as-received and modified/engineered conditions by irradiating samples using high-energy protons and then exposing them to SCW.

Research Progress

Researchers conducted corrosion testing of the candidate alloys, including F-M steels, austenitic steels, and nickel-based alloys, in both subcritical and supercritical water at temperatures of 360°C, 500°C, and 600°C for times up to 1,026 hours and investigated the effect of oxygen concentration on corrosion behavior. Researchers applied surface modification and GBE treatment on selected materials and investigated the corrosion response. In addition to testing bulk samples, they are evaluating surface-modified steels using techniques such as shot peening and thermal spray coating.

For materials tested up to approximately 1,000 hours, weight gain due to oxidation in SCW is typically smaller and less predictable in austenitic stainless steels than F-M steels. Ni-based alloys show good corrosion resistance in the SCW environment but pitting occurs in most tested materials.

Oxygen concentration is one of the most important factors that influences or changes the corrosion behavior of materials in the SCW environment. Figure 1 presents the cross-sectional morphologies of austenitic alloy D9 after

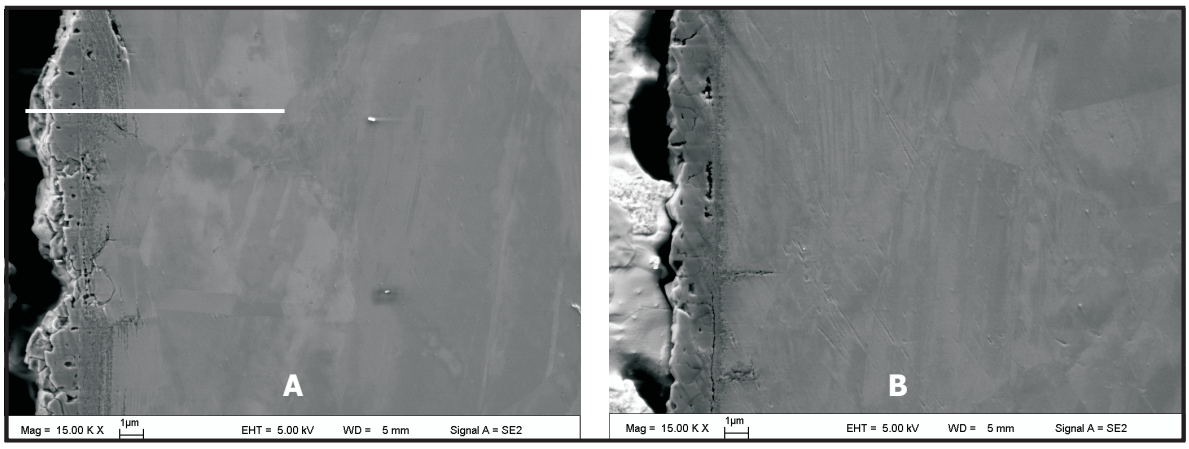

Figure 1. Comparison of cross-sectional morphologies of austenitic alloy D9 after exposure to 500°C SCW with a) 25 ppb dissolved oxygen content and b) 2,000 ppb dissolved oxygen content for approximately 505 hours.

exposure to 500°C supercritical water with inlet oxygen concentration of 25 ppb and 2,000 ppb dissolved oxygen contents, respectively. By comparing the cross-sectional scanning electron microscope (SEM) images, researchers observed that increasing the oxygen content to 2,000 ppb alters the microstructure and corrosion mechanism.

For low oxygen concentration exposure, the formed oxide scale on D9 is composed of an outer magnetite layer and an inner (Fe, Cr, Ni)$_3$O$_4$ spinel layer. Depending on the local microstructure and compositions of the bulk grains, the oxygen penetration depth in different areas varies, resulting in a nodular structure of the oxide scale and an uneven metallic/substrate interface. The region between two nodules is typically a Ni-enriched region. For high oxygen concentration exposure, however, the outward growth of the oxide scale and inward oxygen diffusion rate are homogenous and the scale thickness uniform.

Figures 2 and 3 present cross-sectional results from energy dispersive X-ray spectroscopy (EDS) and transmission electron microscopy (TEM) examination for D9 exposed to higher oxygen concentration. This data, along with the associated X-ray diffraction (XRD) and electron backscatter diffraction (EBSD) results (not shown), indicate that the oxide scale of D9 is a four-layer structure containing an outer hematite layer; an Fe, Cr, Ni oxide spinel layer; an oxygen depleted and approximately 400 nm amorphous layer; and an innermost layer with increased oxygen. The oxide scale developed on D9 in the high-oxygen-level environment was not stable and was prone to spallation. As shown in Figure 3, the weak interface appears to be the hematite/amorphous interface—where long cracking and delamination were found.

Loop temperature significantly influences the oxidation behavior of the tested alloys. Figure 4 shows the cross-sectional morphology of D9 after exposure to an inlet oxygen concentration of 25 ppb at 600°C for 1,000 hours. A non-uniform scale (with 10–40 µm in thickness) was formed. The oxide scale bonded well at the interface of the inner/outer oxide layers. Micron-sized cavities developed within the magnetite layer.

Thermo-mechanical processing (TMP) was employed on INCONEL alloy 617 for GBE purposes. The idea was to control the oxide development by changing the diffusion pathways in the bulk metal, purposely creating what are known as low-Σ coincidence site lattice boundaries (CSLBs). As-received samples were

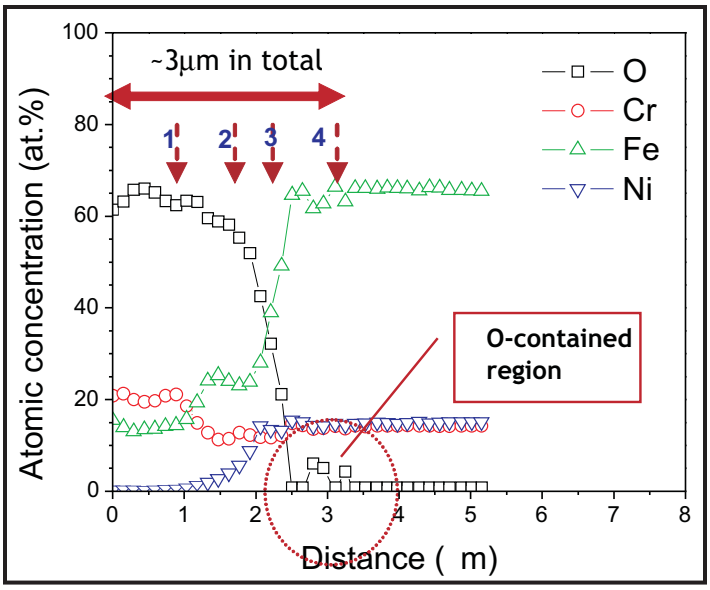

Figure 2. Composition profile across the oxide thickness for D9 after exposure to SCW with 2,000 ppb oxygen content.

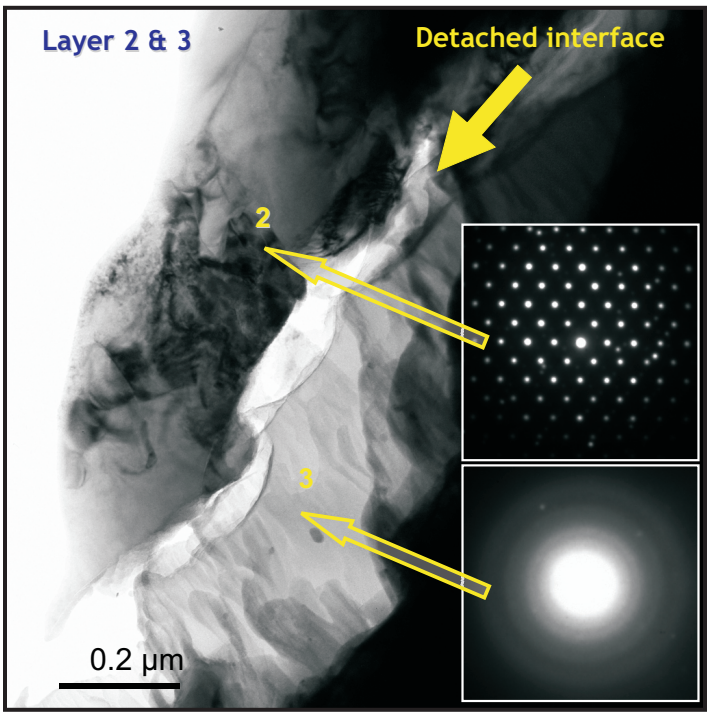

Figure 3. TEM/SAD examinations on the oxide layers 2 and 3 as indicated in Figure 1b in D9 after exposure to SCW with 2,000 ppb oxygen.

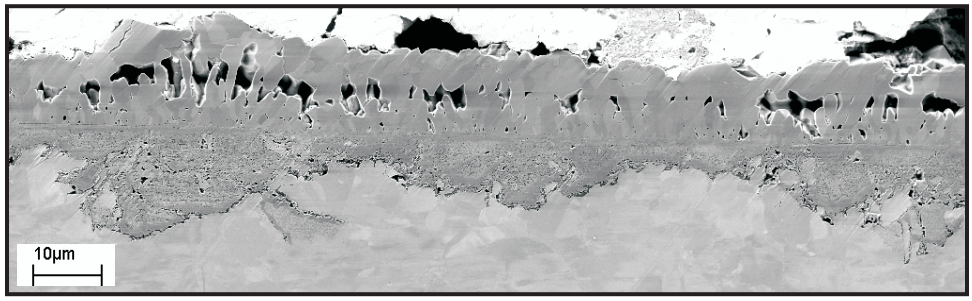

Figure 4. Cross-sectional SEM image of D9 alloy after exposure to 25 ppb oxygen concentration SCW at 600°C for 1,000 hours.

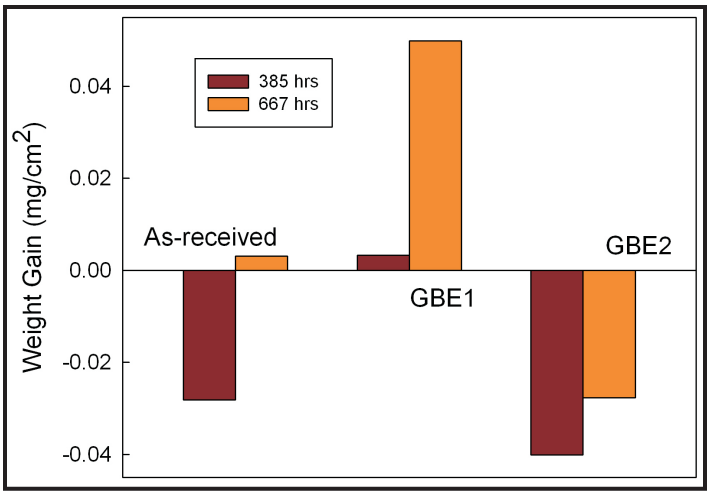

Figure 5. Weight gain of as-received and GBE-treated (GBE1 and GBE2) samples exposed to supercritical water at 500°C and 25 MPa for 385 hours.

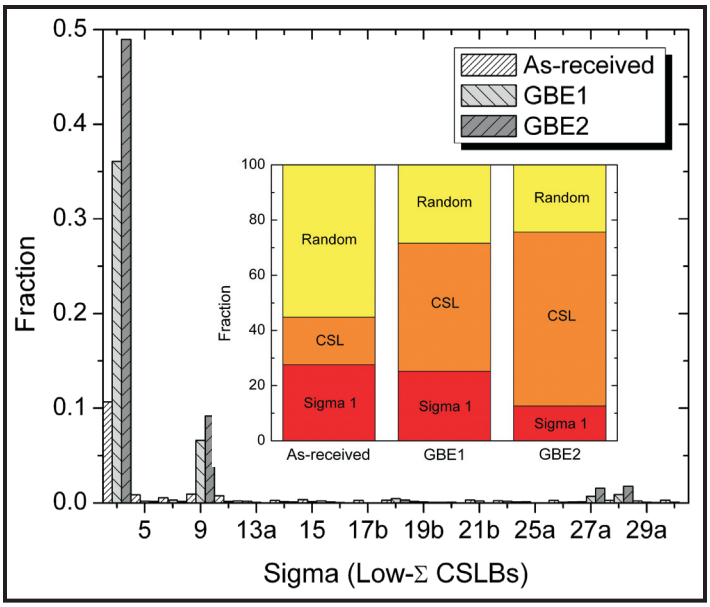

Figure 6. Fraction of low-Σ CSLBs of the as-received and GBE-treated samples, GBE1 and GBE2. The grain boundary character distribution (Σ1 boundaries, low-Σ CSLBs, and random boundaries) of these three samples is shown as an inset.

cold-rolled with an approximately 5 percent thickness reduction followed by annealing at 1,100°C for a variety of times. Two GBE-treated samples (labeled GBE1 and GBE2) were investigated. Both possess a similar low fraction of random boundaries (approximately 27 percent). The major difference is that sample GBE2 has an approximately 13 percent smaller fraction of Σ1 boundaries (or a higher fraction of low-Σ CSLBs) compared to sample GBE1.

The effect of GBE on oxidation behavior of Alloy 617 was studied by exposing the as-received and GBE-treated (GBE1 and GBE2) samples to SCW at 500°C and 25 MPa. The weight gain of the samples exposed for 385 and 667 hours is shown in Figure 5, which indicates a higher and a lower weight gain for GBE1 and GBE2, respectively, compared to the as-received sample.

The fraction of the low-Σ CSLBs of the two GBE-treated samples as well as the as-received sample is shown in Figure 6. The grain boundary character distribution of these three samples is shown as an inset in Figure 6 as well. It is clear that the fractions of $\Sigma 3^n$ (Σ3, Σ9, and Σ27) boundaries were greatly enhanced for GBE-treated samples, GBE1 and GBE2. The fraction of Σ3 boundaries of GBE1 and GBE2 increased to approximately 36 and 49 percent, respectively, compared to the approximately 11 percent for the as-received sample. The fractions of Σ9 and Σ27 boundaries of GBE1 and GBE2 were about 5–9 and 7–10 times that of the as-received sample, respectively. The increased fractions of $\Sigma 3^n$ boundaries indicate that significant twinning and multiple twinning events occurred during annealing after cold rolling to approximately 5 percent. This is desirable for property improvement of materials.

Stress corrosion cracking experiments were conducted on GBE tensile specimens that were strained to 15 percent in deaerated 500°C SCW to determine the effectiveness of special boundaries to resist cracking. Two alloys, each in two conditions, were tested: 316L, 316L GBE, 690, and 690 GBE. Analysis of the specimens indicated that the 316L GBE and 690 GBE specimens were more resistant to intergranular stress corrosion cracking (IGSCC) than the control specimens. The 316L GBE specimen had 93 percent less cracking than the 316L specimen, and the 690 GBE specimen had 55 percent less cracking than the 690 specimen. The cracking data was also normalized to account for differences in the grain sizes of the specimens. These normalized values also indicated that the GBE treatments mitigated IGSCC, thus confirming the effectiveness of the thermo-mechanical treatments. Analysis of the cracked boundaries indicated that the random high angle boundaries (RHABs) were more susceptible to IGSCC than the special boundaries, which included Σ3, Σ9, Σ27, and low angle boundaries (LABs). Further analysis on the 690 GBE specimen, however, showed that the Σ27 boundaries were not necessarily resistant to IGSCC in this environment.

The nature of the cracked boundaries on all four specimens was determined in order to verify that the increased fractions of special boundaries were responsible for the improvement in cracking behavior. Orientation imaging microscopy maps were correlated with SEM images to determine the boundary type as demonstrated in

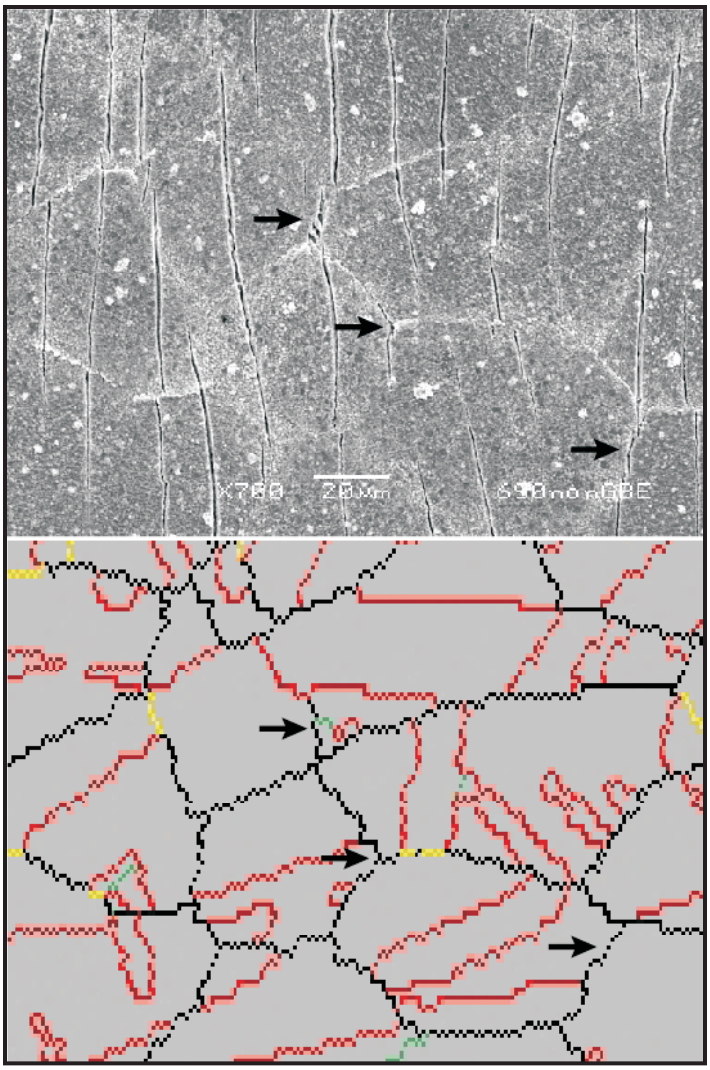

Figure 7. Identification of the nature of cracked grain boundaries in alloy 690. Black boundaries are RHABs, red boundaries are Σ3s, green boundaries are Σ9s, and yellow boundaries are LABs. Note that the only cracked boundaries in these images are RHABs.

Figure 7 for alloy 690. The percentages of the cracked boundaries that were RHABs were 94, 100, 89, and 73 for 316L, 316L GBE, 690, and 690 GBE, respectively. Comparing these values with the total length fractions of RHABs in each sample shows that the RHABs are more susceptible to cracking than are the special boundaries.

For example, while 62 percent of the grain boundaries in the 690 sample were CSL boundaries, only 11 percent of the cracked boundaries were CSL boundaries, as shown in Figure 8. It is important to note, however, that the initial boundary fractions noted in Figure 8 are the length fractions calculated from orientation imaging microscopy analysis, while the cracked boundary fractions are number fractions of grain boundary segments. This may be significant because not all boundaries have the same average length; therefore, these fractions cannot be

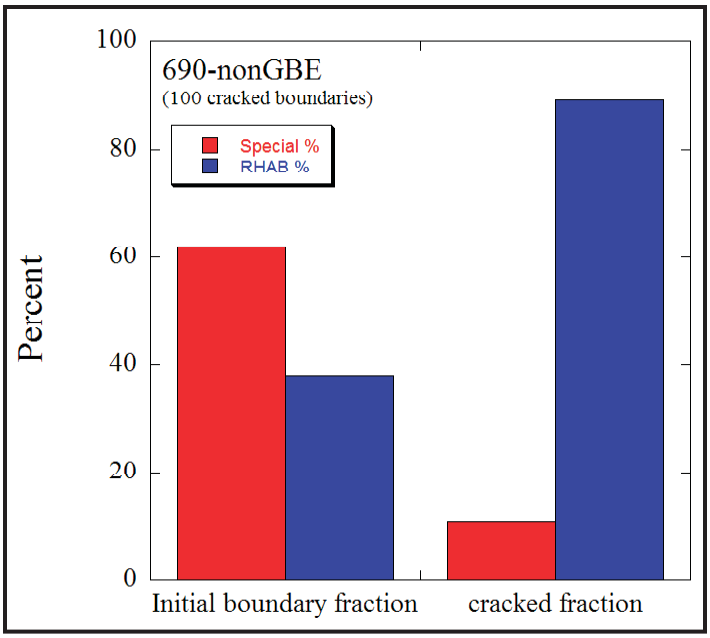

Figure 8. Percent of boundaries in alloy 690 that are CSL versus RHAB and the percent of each type that was observed to crack in 400°C water when strained to 15 percent in 500°C SCW.

directly compared. However, while the numbers may vary, the overall trends will remain the same.

Planned Activities

In the corrosion studies, researchers will continue screening new candidate materials. They will examine continued efforts to optimize corrosion performance through surface modification and grain boundary engineering. In the current phase, researchers are conducting a very short 500°C SCW corrosion test with the exposure times being set at 1 hour, 50 hours, and 100 hours as well as a long 500°C corrosion test with up to 3,000 hours. The examination of the short time run will help to understand the corrosion mechanism and initial evolution of different types of alloys; the long time run was designed to understand the scale stability of the candidate materials and investigate the possible failure mechanisms of the scales.

For the stress corrosion cracking studies, plans include an irradiation of alloys 316L and 690 at 400°C to 2, 4, and 7 dpa as well as an irradiation of alloys 316L, D9, 690, and 800H at 500°C to 7 dpa to determine dose and temperature dependence of cracking in SCW in subsequent Constant Extension Rate Testing (CERT) tests in 400 and 500°C water, respectively. An irradiation and CERT test is also planned on alloy 690 to determine the effectiveness of the CSL boundaries to resist stress corrosion cracking in the irradiation condition.

NUCLEAR ENERGY RESEARCH INITIATIVE

Validation and Enhancement of Computational Fluid Dynamics and Heat Transfer Predictive Capabilities for Generation IV Reactor Systems

PI: Robert E. Spall, Utah State University

Collaborators: Idaho National Laboratory (INL); Fluent, Inc.

Project Number: 05-160

Project Start Date: April 2005

Project End Date: April 2008

Research Objectives

Currently, two primary approaches exist for computational fluid dynamics (CFD) modeling of reactor systems. One approach is to use thermal/hydraulic analysis codes, such as RELAP, which model the entire plant using coarse nodes but cannot predict small-scale flow details. Another approach is to use traditional CFD codes, such as FLUENT, which are adept at detailed flow and temperature predictions, but only over specific regions. However, there are many unanswered questions regarding the ability of traditional codes to accurately model and predict complex flow patterns inherent in nuclear reactors, particularly turbulence. Turbulence is modeled either through direct numerical simulation (which is not practical for engineering design), large eddy simulation (LES), or Reynolds-averaged Navier-Stokes (RANS) equations. Because no single model can handle all geometries, research is needed to validate, modify, and improve CFD predictive capabilities.

This project will validate and improve CFD predictive methods for Generation IV nuclear reactor systems. Researchers will assess the ability of LES and RANS closure models, which are available in the FLUENT code, to predict flows for specific, fundamental geometries inherent in Next Generation Nuclear Plant (NGNP) reactors. Based on the results of the assessment, researchers will modify the closure models to improve predictive capabilities and obtain experimental data for relevant geometries to support code validation.

Research Progress

RANS Solutions. The effectiveness of five different turbulence models was assessed for the flow across a row of confined cylinders at a pitch-to-diameter ratio of 1.7 and at Reynolds numbers ranging from 2,621 to 55,920. Models examined include the one-equation Spalart-Almaras model; two-equation realizable $k - \varepsilon$, $k - \omega$, and shear stress transport (SST) models; and a four-equation $v^2 - f$ model. Quantities compared against published experimental data include minor loss coefficients, separation angles about cylinders, wake lengths behind cylinders, and streamwise velocity profiles at the periodic inlet/outlet boundaries. As shown in Figure 1 below, each of the models did a reasonable job in predicting the minor loss coefficient as a function of Reynolds number. With the exception of the $k - \varepsilon$ model, each was also able to predict the experimentally observed trend of decreasing wake and separation lengths with increasing Reynolds number. In addition, all models also predicted a local minimum in the separation angle about the inner cylinder as a function of Reynolds number, which has also been observed experimentally. Researchers concluded that the $v^2 - f$ model performed slightly better at predicting the experimental data than any of the other models examined.

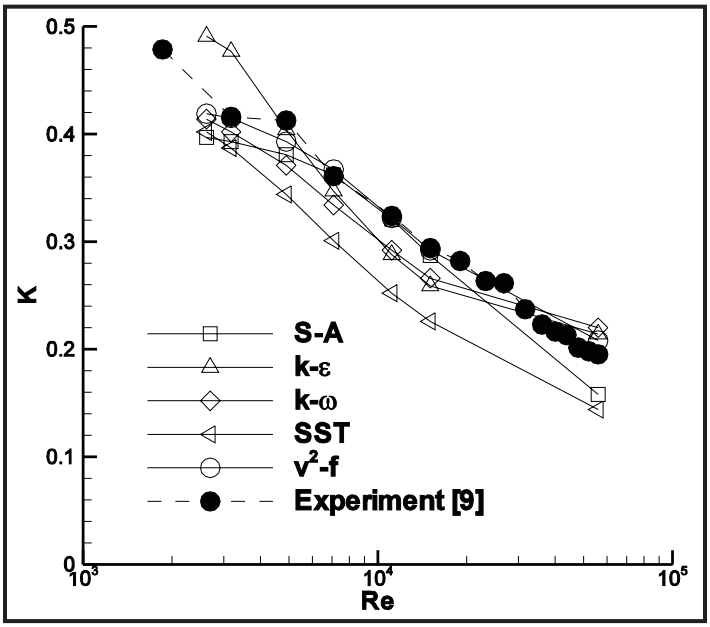

Figure 1. Minor loss coefficients as a function of Reynolds number.

Large Eddy Simulation Solutions. Four large eddy subgrid models were compared in their ability to predict the temperature distribution in the heated pipe. All LES models predict the mean velocity profile reasonably well. The root mean square (RMS) values of the Smagorinsky-Lilly model and the wall-adapting local eddy-viscosity (WALE) model show the same shape but different magnitude while the standard Smagorinsky model shows the maximum at a different location. The mean temperature profiles along the wall in the section with the prescribed heat flux are under-predicted by all LES models. Researchers have validated the resolution and are now looking at the energy spectrum, as shown in Figure 2. The spectrum shows a -5/3 slope but needs to be sampled over a longer time period.

The problems with the LES for the row confined cylinders configuration have been resolved with the help of Fluent, Inc. The non-iterative time advancement scheme does not work for this type of flow. Unfortunately, this makes an LES of the confined cylinders prohibitively expensive with Fluent, Inc. As an alternative, LES simulations have been started using OpenFOAM.

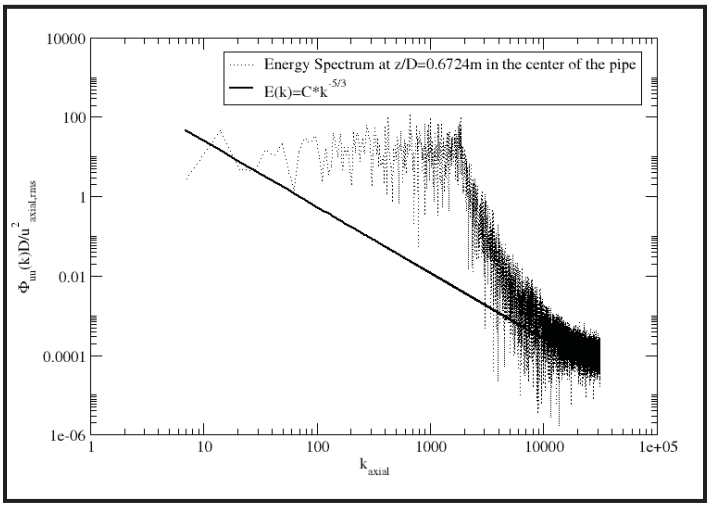

Figure 2. Energy spectrum for the heated pipe flow.

Experiments. Measurements of an array of 35 low-density (heated) jets spaced on equilateral triangles 2D apart using time-resolved particle image velocimetry (PIV) have begun. The measurement domain contains the center seven jets. Five planes of data were acquired for the unheated case and one heating value ($Ar = Dg\beta\Delta T/U^2 = 0.093$). The results demonstrate that the small amount of heating significantly enhances the interaction between the jets. In the event of a loss of flow accident, this effect will cause the jets impinging on the walls of the upper plenum to be better mixed. The mean flow vectors are shown for each plane in Figure 3.

The heated flow exhibits considerable unsteadiness compared to the unheated case. In the near field, large peaks in the streamwise fluctuation level corresponding to the shear layers of each jet are present, while in the farthest downstream plane for the heated case, these peaks merged, indicating that the potential core has ended by this station for this heating value.

The streamwise momentum flux was computed over the entire measured domain at each plane for both cases. While momentum is nearly constant for the unheated case, it increases considerably with downstream distance for the heated case.

Simultaneously to this effort, measurements of a jet with a rounded exit are ongoing in the INL Matched-Index-of-Refraction (MIR) Laboratory. Baseline measurements of a jet with a square edge have been acquired.

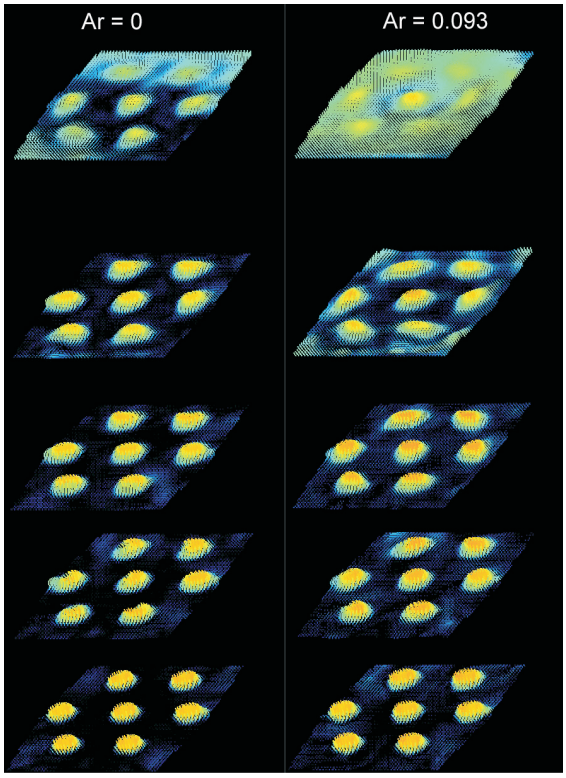

Figure 3. Time-averaged vectors of unheated (left) and heated (right) flow at x/D = 0.0, 0.5, 1, 2, and 4.

Planned Activities

RANS. During the final year of the project, researchers will be performing RANS calculations for the jet array experiments described on the next page. The results will concentrate on an array of three jets arranged in a triangular manner and will be obtained for both heated and unheated jets. Of primary interest is the ability of the CFD turbulence models to accurately predict the entrainment and subsequent merge points of the jets.

LES. Since the LES of the pipe cannot predict the wall temperature accurately, a discrete event simulation (DES) model with a turbulence model may be a better alternative, e.g., $v^2 - f$ might be a better approach. The research team will look into a derivation and implementation of such a model. They will also finish the highly resolved LES simulation of the heated pipe and continue the LES of the cylinder array with OpenFOAM.

Experiments. For the heated jet array experiment, one additional heating value will be acquired, and planes much farther downstream will be measured. Two-point correlations will be examined and compared for different heating values.

Nuclear Energy Research Initiative

Ab-Initio-Based Modeling of Radiation Effects in Multi-Component Alloys

PI: Dane Morgan, University of Wisconsin-Madison

Collaborators: None

Project Number: 06-006

Project Start Date: March 2006

Project End Date: March 2009

Research Objectives

The objective of this project is to develop a highly accurate, thermokinetic model for austenitic stainless steels based on fundamental quantum mechanical calculations. The model will incorporate the true temperature- and composition-dependence of the diffusion constants and provide missing information on interstitial motion.

In order to establish the critical data and computer programs to build the model, researchers will pursue the following specific objectives:

- Perform initial *ab-initio* calculations of atomic-scale properties of pure elements and alloys
- Develop iron-chromium-nickel (Fe-Cr-Ni) radiation-induced segregation (RIS) simulation and validation/refinement based on semi-analytic expressions for diffusion constants
- Develop Fe-Cr-Ni RIS simulation methods based on Monte Carlo techniques
- Perform validation/refinement by comparing analytical results to experiments
- Extend calculations and simulations to a preliminary ferritic Fe-Cr model

Research Progress

Over the past fiscal year, researchers focused on the dilute X concentration limits for Ni-X alloys (X = Cr or Fe). The following is a synopsis of the progress made for these systems.

Defect Energetics. The research team has calculated essentially all of the defect energies needed for analytical modeling of species-dependent diffusion within the dilute limit for the Ni-X alloys, for both vacancy and interstitial-mediated diffusion. The key highlights of this data are shown in Table 1 (all values are for dilute Cr or Fe in Ni) and their importance summarized below:

1) Vacancy migration barriers are ordered Cr < Fe < Ni, which will yield vacancy mediated diffusion constants in the order $D_{Cr} < D_{Fe} < D_{Ni}$. This difference in barriers is much greater than expected from previous fitting to experiments and will lead to Cr depletion at sinks during RIS.
2) Vacancy binding energies are all < 0.04 eV, implying that vacancy drag mechanisms considered in some previous studies will not be active.
3) Interstitial binding energies give a strong preference for Ni-Cr dumbbells, which will enhance Cr interstitial migration versus Ni and Fe.

Species	Vacancy Migration Energy (eV)	Interstitial Migration Energy (eV)	Vacancy-X Binding Energy (eV)	Ni-X <100> Binding Energy (eV)
Cr	0.82	0.08	0.04	-0.45
Fe	0.95	0.11	0.02	0.06
Ni	1.08	0.14	N/A	N/A

Table 1. Species dependence of vacancy and interstitial migration and binding energies in a Ni host.

Diffusion Kinetics. By combining with statistical models (Le Claire's 5-frequency model and a generalization for interstitials), the defect energetics can be used to calculate tracer diffusion constants as a function of temperature. The results for Ni-Cr are shown in Figure 1. Only ratios are given since they are relevant for RIS. Comparison to tracer diffusion constants fit to high-temperature experimental data shows that researchers' predicted values are in good agreement with experimental results. Similar results are obtained for Ni-Fe but with ratios closer to one. With respect to RIS, positive ratios lead to Cr depletion for the vacancy mechanisms and to Cr enrichment for interstitial mechanisms. The results demonstrate that, within this dilute approximation, both the vacancy and interstitial mechanisms will contribute strongly to RIS, but in opposite ways. This offers dramatic demonstration that interstitials are likely to play a major role in RIS and suggests that RIS in Ni-Fe-Cr alloys may be a balance of large vacancy and interstitial-driven contributions.

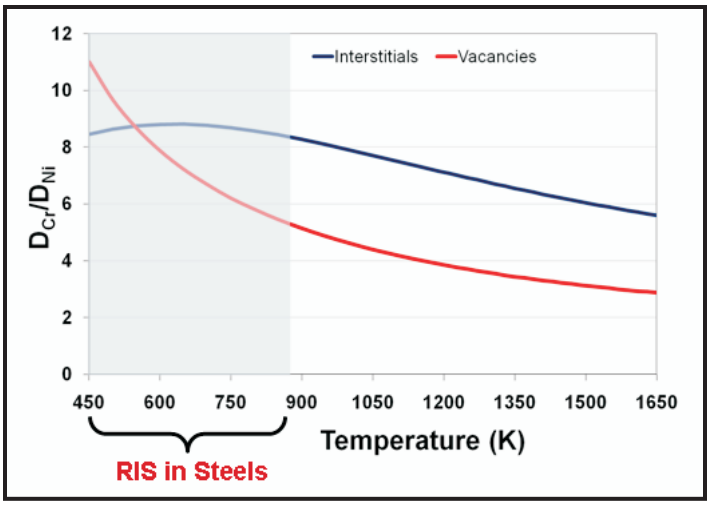

Figure 1. Predicted diffusion constant ratio for Cr to Ni for both interstitials and vacancies.

Planned Activities

Over the next fiscal year, researchers will continue their effort to refine the semi-analytic model for diffusion constants and develop a RIS model based on the values. This will be based on approximations of dilute solution in the Ni host and/or non-interacting solid solution models.

Researchers will also develop capabilities for modeling the more concentrated alloy. This will involve the continued development on kinetic Monte Carlo (kMC) codes and cluster expansions of the on-lattice and hopping energetics.

Through the remainder of the project, researchers will obtain full and accurate cluster expansions, complete the kMC codes, and combine them to derive improved diffusion constants. The temperature and composition-dependent diffusion constants will be used to study RIS in the Fe-Cr-Ni alloy.

Finally, researchers will further refine the models through comparison to RIS experiments, using the results to explore the effects of RIS on voids through void growth modeling. If time permits, researchers will extend their approach to Fe-Cr ferritic model systems.

Nuclear Energy Research Initiative

Managing Model Data Uncertainties in Simulator Predictions for Generation IV Systems via Optimum Experimental Design

PI: Paul J. Turinsky, North Carolina State University (NC State)

Collaborators: Argonne National Laboratory (ANL), Idaho National Laboratory (INL)

Project Number: 06-046

Project Start Date: March 2006

Project End Date: March 2009

Research Objectives

The objective of this project is to understand and manage the uncertainties in modeling and simulation software that are caused by the uncertainties in the software data itself, which is used to model the nuclear core of a proposed Generation IV reactor. In this project, researchers will optimize experiments by determining and quantifying the uncertainties of key design attributes and will use INL's Zero Power Physics Reactor (ZPPR) facility as a test basis to reduce model data uncertainties. The team will then complete a pseudo-ZPPR experiment for the optimum design via simulation to determine observable values and use these values to obtain adapted nuclear data.

The goal of this project is to produce the following methodologies and results, each of which has merit as a stand-alone method or can be used collectively to optimize experimental design:

1) A methodology to determine covariance matrices for responses of a complex engineering system and an experimental system
2) A methodology to interpret experimental system results via adaptive simulation
3) A methodology to optimize the experimental configuration most economically appropriate for reducing the uncertainties of the complex engineering system
4) A covariance matrix originating from nuclear data uncertainties for the key design attributes of a Generation IV nuclear core
5) Optimum experimental system properties for a ZPPR experimental facility which are most appropriate for reducing the uncertainties of the key design attributes of a Generation IV nuclear core

Research Progress

To test the experiment optimization portion of the methodology, researchers used a core simulator model approximating the ZPPR facility. The team has established detailed computer models of a ZPPR assembly using deterministic and probabilistic computer codes. They used the computer codes MCNP and REBUS to enable detailed 3D core analysis. The MC2**2 computer code was employed for the 15-group energy based cross-section generation.

For the MCNP modeling, two cases were considered: 1) the core was modeled as it is, that is, no simplification was made in modeling and all materials were taken at their original location and composition; and 2) in the second case, each drawer was homogenized with all constituents present initially and treated separately in the full core analysis. The MCNP5 simulation of the ZPR 6/7 assembly was performed with 100,000 neutrons per cycle for a total of 130 cycles, with the first 30 cycles skipped.

For the MC-2/REBUS modeling, cross sections were calculated for the ZPR 6/7 assembly using MC-2. Two different MC-2 models were established. For one model, the heterogeneous approach was used. In this, slab geometry was used and each plate in the drawer was distinctly represented. The core and blanket cross sections were calculated separately and then merged into a single cross-section library. For the second model, the homogenous approach was employed. All constituents of a drawer were homogenized to obtain the cross-section values. The MC-2 code system for calculating fast neutron spectra and multi-group cross sections is based on ENDF/B data (November 2000 Version).

Based on both the homogenous and heterogeneous approaches, the cross-section libraries were used in separate REBUS calculations. In REBUS, each drawer

Parameter	MCNP (As it is)	MCNP Homogenized	MC-2/ REBUS (Het.)	MC-2/ REBUS (Homo.)	Experimental	Ref(6)
k_{eff}	0.99931 (.00017)	0.98644 (0.00014)	0.99066	0.99883	1.0005 (.00003)	1.00662 (.00051)
$(\sigma_f\Phi)28/(\sigma_f\Phi)49$	0.027362	0.024918	0.0239	0.0177	0.02517	0.02703
$(\sigma_c\Phi)28/(\sigma_f\Phi)49$	0.14472	0.14938	0.139	0.143	0.144	0.1464
$(\sigma_c\Phi)28/(\sigma_f\Phi)28$	5.28914	5.99506	5.81	8.19	5.626	5.425

Table 1. Comparison of reaction rates and k_{eff} for ZPR 6/7 predicted by MCNP and MC-2/REBUS with experimental values.

was modeled separately unless two or more consecutive drawers of the same type in one row existed, in which case they were merged together.

The k_{eff} and reaction rates calculated by the various models employed are listed in Table 1. The experimental values and one set of published values are also listed for comparison.

The models described above were used to quantify core attributes' uncertainties for a ZPPR critical assembly. The team calculated uncertainties in the reaction rates of Pu-239, U-235, and U-238 for fission and capture for the 15 energy groups. The uncertainty was assumed to be zero for any cross section not included in the libraries.

Researchers conducted an adaptive simulation experiment, using the same core attributes for which the uncertainties were determined, to improve the fidelity of core simulator predictions by adjusting the 15-group cross sections. Their goal is to use efficient subspace method (ESM)-based algorithms to adapt core simulators to real plant data. For now, a virtual approach is employed where a design basis core simulator, denoted DC, is adapted to a set of virtual core attributes, denoted VC. The virtual core attributes are generated by perturbing the few-group cross sections in a statistically consistent manner with their prior uncertainties. In addition, the reaction rates were perturbed randomly by selecting them from Gaussian distribution with the standard deviation assumed to be 5 percent. In contrast to a real experiment, reaction rates for every spatial node in the REBUS model were assumed experimentally measured. In Figure 1, AC denotes the adapted core solution. The original difference <VC-DC/VC> was from 1.6 to 6.7 percent. The differences after adaption are denoted <VC-AC/VC>. The maximum error in reaction rates after adaption is about 0.6 percent. In terms of root-mean-square (RMS) mismatch between the virtual core and design core, the adaption reduces the mismatch by over a factor of 44.

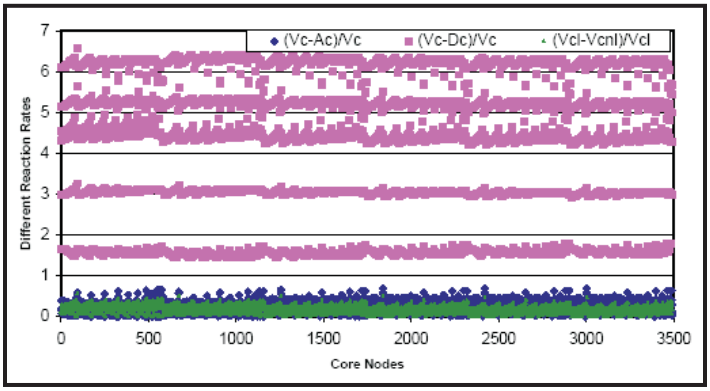

Figure 1. Adaption results based upon MCNP generated virtual core and MC-2/REBUS predictions.

The Generation IV core design concept selected for study was one of the ANL Advanced Burner Test Reactor (ABTR) pre-conceptual designs, specifically the metal fuel design with a conversion ratio of 0.6 to 0.7. The MC-2 and REBUS models for the ANL ABTR core design selected for this study, which were provided by ANL, were used unaltered to establish base models.

An extensive study of problem linearity of core reactivity and node-average power densities with respect to cross sections was successful. This was done using the principle directions associated with the singular value decomposition of the 15-group covariance matrix.

Having confirmed linearity, the uncertainty in reaction rates due to cross-section uncertainties was completed using ESM. Figure 2 is a plot of three graphs combined to show that using a subset of the singular vectors associated with ESM will produce the same standard deviation output that can be found from running the original perturbation matrix in REBUS.

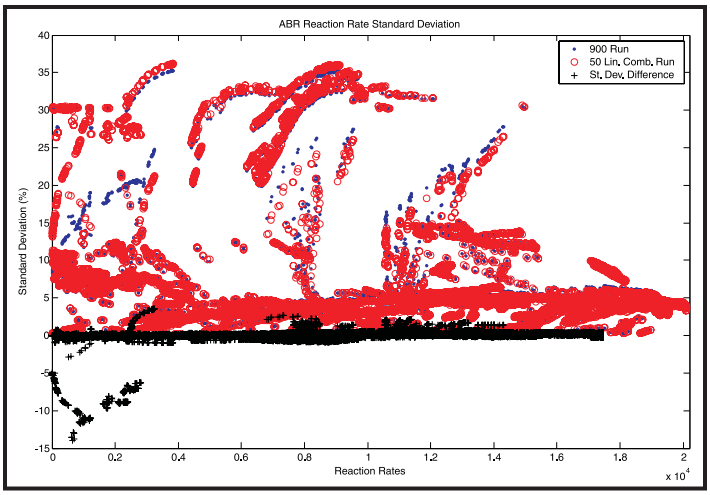

Figure 2. ABR reaction rate standard deviation.

The blue data represents the standard deviation that was calculated for all of the reaction rates by running a total of 900 principle directions in REBUS. The red data, which greatly overlaps the blue standard deviation data, is merely the standard deviation that was calculated for all of the reaction rates by running a linear combination of the first 50 principle directions in REBUS. It is also important to note that the standard deviation data presented in Figure 2 was ordered in ascending order to better grasp how the standard deviation data would match up depending on the reaction rate magnitude. Finally, the black data is the difference between the uncertainty data from the two cases presented in Figure 2. It can be seen that, as the reaction rate values increase, the discrepancy between the data sets decrease. There exists a small subset of data that produces a difference in standard deviation from 5 to 14 percent; however, the trend for the majority of the data is that the two data sets match within toleration.

Planned Activities

The investigation of the free design parameters and instrumentation options for a ZPPR core will continue. Cost models for Generation IV core margins and ZPPR experiments will be established, which will require the cooperation of the participating national laboratories and industry. The key design limiting responses of the Generation IV core will be identified and, subsequently, the capability to evaluate the sensitivity coefficients and covariance matrix of these responses will be developed. At that point, it will be possible to mathematically pose the optimization problem, i.e., to minimize Generation IV core margins due to uncertainties so as to reduce the cost at the expense of completing the optimized ZPPR experiments. This will require the introduction of a mathematical optimization capability.

Nuclear Energy Research Initiative

Uncertainty Quantification in the Reliability and Risk Assessment of Generation IV Reactors

PI: Karen Vierow, Texas A&M University (TAMU)

Collaborators: The Ohio State University

Project Number: 06-057

Project Start Date: March 2006

Project End Date: March 2009

Research Objectives

The goal of this project is to develop practical approaches and tools for dynamic reliability and risk assessment techniques that can be used to augment the uncertainty quantification process in probabilistic risk assessment (PRA) methods for Generation IV reactors. The objectives of the project are to 1) develop practical approaches and computationally efficient software to test event tree completeness for Generation IV reactors, 2) integrate a reactor safety code with PRA, and 3) assess and propagate plant state uncertainties in the PRA analysis.

This project involves generating a practical dynamic event tree (DET) tool and assessing and quantifying uncertainty propagation. In Phase 1, current software for DET generation will be modified and linked to a best-estimate computer code (such as MELCOR). Key modeling uncertainties will be identified via the Phenomena Identification and Ranking Table (PIRT) technique. The integrated software package will be tested on select, high-risk initiating events. In Phase 2, the computational efficiency will be improved by coupling the DET generation software with sampling software developed by Sandia National Laboratories (SNL). Finally, this new software will also be tested on select initiating events.

Research Progress

A computational infrastructure has been developed outside this NERI project that supports the generation of multiple DETs on a distributed computing architecture composed of a heterogeneous collection of computational and storage nodes. The DET generation is managed by a driver, called ADAPT (Analysis of Dynamic Accident Progression Trees), that 1) determines when branching is to occur, 2) initiates multiple restarts of system code analyses, 3) determines the probabilities of scenarios, 4) determines when a scenario can be terminated, and 5) combines similar scenarios to reduce the scope of the analysis.

A plant simulator (the MELCOR code) is used to follow the transient along each branch. Following an initiating event (or at any user-specified starting point during an accident progression), the Distributed Database Management System provides initiating conditions as well as the duration of the simulation (time parameters) to the plant simulator (SIM). The driver runs the simulator until a stopping condition is reached. The scheduler decides whether or not to branch depending on the information received from 1) the SIM on setpoint crossing, or equipment demand in general, and 2) the probability module on the branch probability. The PRA Database contains data to quantify the likelihood that branches will be generated upon meeting certain branching criteria (e.g., crossing set points).

The Distributed Database Management System, SIM, driver, and PRA Database have been successfully installed and configured to perform calculations on a computing system not associated with the development of the programs (Figure 1). This has allowed for the debugging of software, as well as clarification and improvement of the installation procedures. The graphical user interface (GUI) has been developed within the scope of this project. Following installation, usability issues concerning both the system interface and software performance are being addressed. The ADAPT server, database, and web-server are designed to run on any Linux environment while the GUI, since it is based in Java, can work on any operating system that supports the Java Runtime Environment.

Figure 1 shows the direction of information transfer for each component of the software. The driver, compute cluster, and database are in constant communication to facilitate the execution of the tree. The Java client

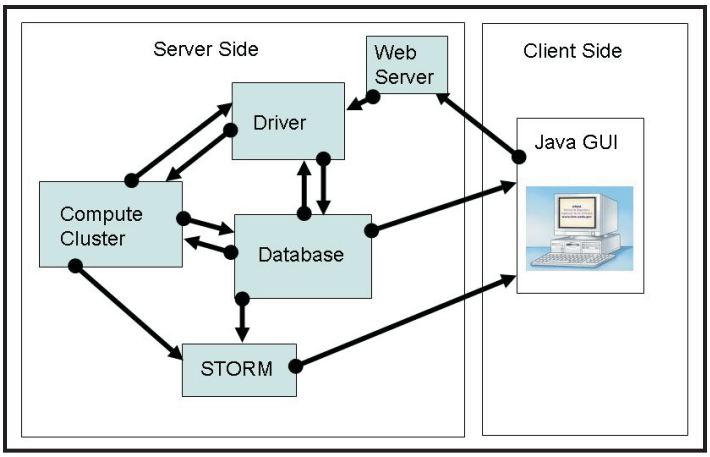

Figure 1. Diagram of information flow between different components in the ADAPT software.

communicates information to the web-server in order to have control of experiment execution. The client also downloads information from the database in order to display the tree as well as other information. However, the client never directly modifies the database. The STORM middleware is utilized to query the compute cluster file system and download plot data which is to be sent to the client. STORM attains the location of all branch data from the database and then downloads it from the compute cluster itself. The ADAPT GUI is a Java-based software that can be used on a user's local machine to launch experiments, display the event tree, and assist the user with more complex analyses of the generated event tree.

The previously developed MELCOR input deck for a pebble bed modular reactor has been successfully tested using the complete PRA system to confirm compatibility. This will enable the implementation and utilization of the PRA method for analysis of the Generation IV reactor and the simulation of modeling uncertainties.

Planned Activities

Following is a synopsis of the tasks the team plans to conduct over the next period:

- Complete determination of key modeling uncertainties
- Generate uncertainty input for the Pebble Bed Modular Reactor input deck
- Model key uncertainties for a representative Generation IV plant through best estimate code input
- Link the computational infrastructure with the input deck
- Test the software integration to consist of validation and verification exercises
- Prepare documentation for the user's manual
- Quantify modeling uncertainties for a reference Generation IV reactor
- Discuss software coupling with best estimate codes other than the demonstration code

NUCLEAR ENERGY RESEARCH INITIATIVE

An Advanced Neutronic Analysis Toolkit with In-line Monte Carlo Capability for VHTR Analysis

PI: William R. Martin, University of Michigan

Collaborators: Studsvik of America; Idaho National Laboratory; Los Alamos National Laboratory; General Atomics; Oak Ridge National Laboratory; TransWare Enterprises, Inc.

Project Number: 06-068

Project Start Date: March 2006

Project End Date: March 2009

Research Objectives

The goal of this project is to develop a lattice physics code for very high-temperature reactor (VHTR) neutronic design and analysis. The approach takes advantage of the highly developed capabilities available for light water reactor (LWR) neutronic analysis, in which lattice physics codes generate effective cross sections at the assembly level. Researchers can use these cross sections in nodal codes to efficiently calculate global flux/power distributions and effective multiplication (k_{eff}) as a function of fuel depletion and temperature.

This project will establish "proof-of-principle" by incorporating the Monte Carlo capabilities of the MCNP5 code directly into the lattice code, CPM-3. The team will accomplish code linkage through an interface that also enables extension to other cross-section generation codes. This will be demonstrated by linking MCNP5 to CASMO-4. The final package will inherit the substantial downstream capabilities of CASMO-SIMULATE, such as cross-section generation for global nodal analysis and depletion, systematic preparation of cross-section sets for accident analysis, and efficient fuel cycle analyses and assessment of alternative fuel management schemes. The final product will be a validated neutronics methodology for VHTR design and analysis, including cross-section generation, global reactor analysis, depletion, and fuel management.

The primary objectives are listed below:

- To develop an application program interface (API) to couple a collision probability code (CPM-3) and MCNP5 for analyzing VHTR configurations
- To demonstrate "proof-of-principle" of the coupled CPM-3/MCNP5 methodology by implementing and testing on a suite of selected benchmark problems
- To apply the coupled CPM-3/MCNP5 methodology to a Deep Burn configuration and assess its capability to treat low-lying resonances of plutonium isotopes and to adapt the methodology as needed to handle these important resonances
- To demonstrate the capability of using the API with a production lattice physics code by coupling MCNP5 and CASMO-4 and evaluating with the test suite
- To verify and validate the coupled CPM-3/MCNP5 methodology for simple VHTR configurations, critical experiments, and startup/operational data from Fort St. Vrain and Peach Bottom
- To assess the applicability of the coupled methodology to analyze pebble bed configurations

Research Progress

The research team has made significant progress toward meeting project goals during this past year. The key task has been successfully demonstrating that resonance cross sections from MCNP5 can be used within CPM-3 to allow CPM-3 to be used for the analysis of VHTR configurations, including an explicit treatment of the TRISO particle fuel. A brief summary of the key accomplishments is given below.

CPM-3/MCNP5 Coupling Methodology. The CPM-3 lattice physics code has been modified to incorporate problem-dependent cross sections for resonance nuclides that have been generated by MCNP5 using the same geometric and material specifications as in CPM-3.

A Fortran-90 code was implemented and embedded in the CPM-3 source code to couple CPM-3 and MCNP5. The Fortran-90 module prepares an MCNP5 input file to calculate 65-group resonance absorption and fission cross sections for all of the CPM-3 resonance materials in the fuel region.

The MCNP5 code is then executed and the resulting reaction rates are used to generate resonance absorption and cross sections for the resonance nuclides. These cross sections are communicated to CPM-3 for its subsequent analysis. For this initial coupling of MCNP5 and CPM-3, both codes were running simultaneously and the MCNP5 results were directly inserted into the corresponding CPM-3 data arrays.

LWR pin cell. The coupling methodology was tested on an LWR pin cell and the results are tabulated in Table 1. As can be seen, the k_∞ predictions by CPM-3 and MCNP5 agreed to within .095 percent prior to the incorporation of the MCNP5-generated cross sections into CPM-3, which reduced this difference to 0.07 percent, which is in the right direction. Since this is a LWR pin cell for which the CPM-3 calculation is considered quite accurate, the k_∞ difference between CPM-3 and MCNP5 may be due to other effects, including differences in the thermal models.

	Original CPM-3	Modified CPM-3	MCNP5
k_∞	1.343617	1.34137	1.34234
Difference (%)	0.095	0.072	

Table 1. k_∞ values predicted by CPM-3 and MCNP5 for LWR pin cell.

VHTR compact cell. A VHTR fuel compact cell consisting of a fuel compact surrounded by its share of the graphite in a fuel element was analyzed (Figure 1). The compact cell had reflecting boundary conditions. The CPM-3 model used homogenized fuel while MCNP5 explicitly resolved the TRISO fuel particles.

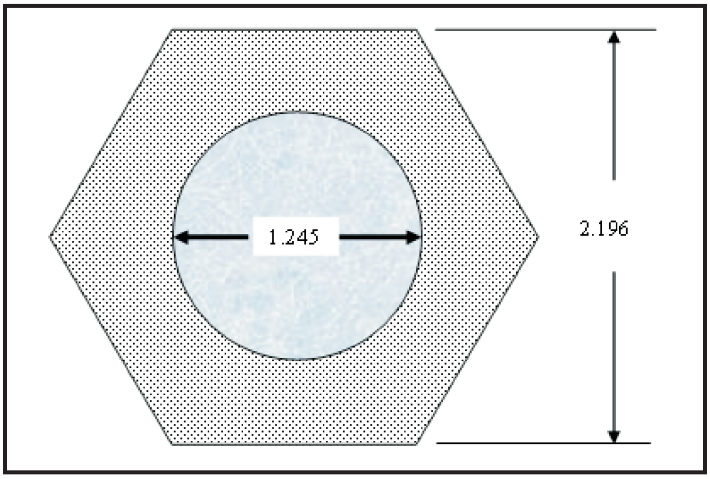

Figure 1. VHTR compact cell (dimensions in cm).

A comparison of the k_∞ values computed by MCNP5 and CPM-3 is presented in Table 2. These preliminary results are very encouraging, with CPM-3 agreeing to within 0.13 percent for k_∞ even though CPM-3 was analyzing homogeneous TRISO fuel. This indicates that CPM-3 with MCNP5-generated resonance cross sections can analyze TRISO fuel and account for the double heterogeneity.

Infinite Medium Multiplication Factor k_∞		
	Homogeneous	**Heterogeneous**
CPM-3 (original)	1.445165	N/A
MCNP5	1.439590	1.504610
CPM-3 (modified)	1.444911	1.502668
Relative Error (%)	0.369619	0.129070

Table 2. k_∞ values predicted by CPM-3 and MCNP5 for VHTR compact cell.

Planned Activities

Researchers plan to accomplish the following activities in the next period:

1) Work with Studsvik-Scandpower to couple MCNP5 with CASMO-5 using a code patch similar to what was done with CPM-3
2) Complete the development of the API, using the successful patch installed in CPM-3 to read and use MCNP5-generated cross sections for the resonance groups
3) Work with Studsvik-Scandpower to couple MCNP5 with CASMO-5 with the API
4) Set up validation test problems with General Atomic's assistance and perform MCNP5 benchmark calculations of these problems
5) Set up and run VHTR benchmark cases with MCNP5 and the coupled methodology

Nuclear Energy Research Initiative

Improving Corrosion Behavior in SCWR, LFR, and VHTR Reactor Materials by Formation of a Stable Oxide

PI: Arthur T. Motta, Pennsylvania State University

Collaborators: Westinghouse Electric Company, Los Alamos National Laboratory, University of Wisconsin, University of Michigan

Project Number: 06-100

Project Start Date: March 2006

Project End Date: March 2009

Research Objectives

This project is designed to establish a technical basis for corrosion protection of candidate materials for three different types of reactors: the supercritical water reactor (SCWR), the lead-fast reactor (LFR), and the very high-temperature reactor (VHTR). The materials to be studied include ferritic-martensitic steels, austenitic alloys, and nickel (Ni)-based alloys. In order to understand the mechanisms associated with corrosion behavior in these materials, a systematic study will be conducted on the nature of protective films formed during corrosion tests in simulated reactor environments.

The overall objective is to understand why certain alloys exhibit better corrosion behavior than others by examining the oxide microstructure. Alloys that resist corrosion develop a protective oxide layer that limits the access of corrosive species to the underlying metal, leading to stable oxide growth. The differences between a protective and a non-protective oxide are determined by the alloy chemistry and microstructure. Very small changes in microstructure can significantly affect corrosion rate.

The techniques to be used in this project are microbeam synchrotron radiation diffraction and fluorescence and cross-sectional transmission electron microcopy (TEM) on samples prepared using a focused ion beam. Examination by x-ray diffraction and fluorescence resolves the crystal structure, texture, and composition of oxide layers at the sub-micron level. By complementing the examination with TEM, researchers will precisely determine the structure of these layers and their impact on corrosion behavior of the alloys.

Research Progress

During the second year, detailed examinations were performed on the oxide layer structures using TEM, scanning electron microscopy (SEM), and microbeam synchrotron radiation diffraction and fluorescence. The oxide samples examined were produced by previously exposing various alloys to both supercritical water and lead-bismuth (Pb-Bi) environments.

An example of a TEM image, shown in Figure 1, is an oxide layer formed during exposure in Pb-Bi on model steel alloy #3 (91 wt% iron [Fe] and 9 wt% chromium [Cr]), labeled according to the phases present. Researchers continue to perform detailed TEM examinations on the various oxide layers.

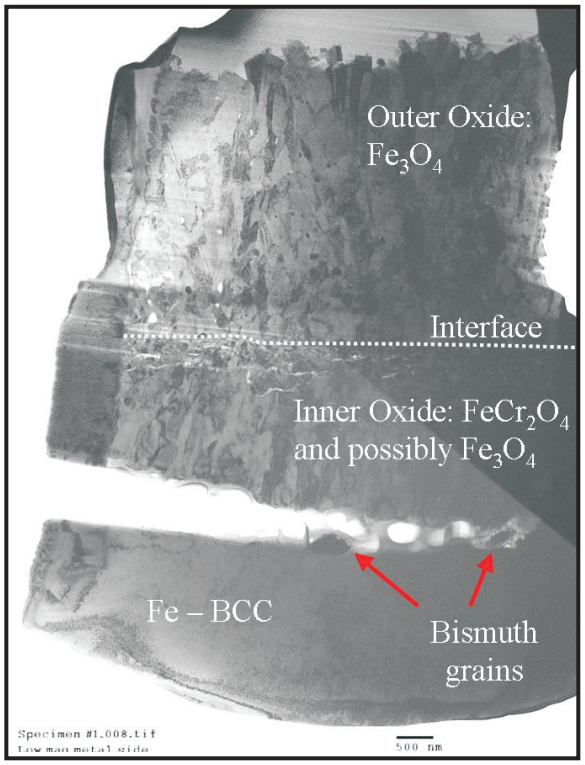

Figure 1. Bright field TEM image of Alloy #3 showing phase composition of the oxide layers as well as Bi grains found along the inner oxide/base metal interface.

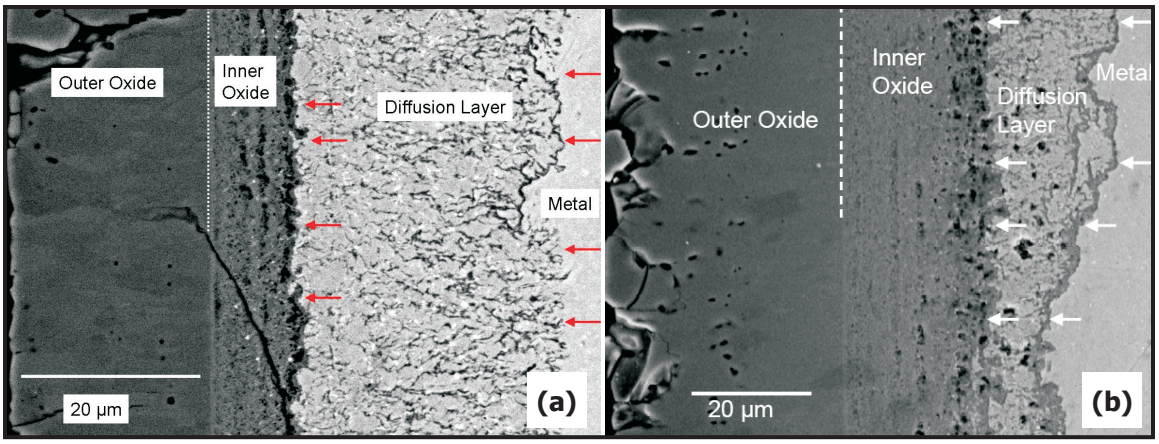

Figure 2. SEM images of 9Cr ODS after 600°C exposure in SCW for (a) 2 weeks and (b) 4 weeks.

Samples were also examined using microbeam synchrotron radiation diffraction and fluorescence as well as with SEM. Figure 2 shows two images showing the time evolution of oxide layers formed on 9Cr oxide dispersion strengthened (ODS) in supercritical water.

The dark band, which is well developed in the four week sample, has been determined to be Cr_2O_3, both by micro-diffraction and by SEM chemical analysis, as shown in Figure 3. The formation of this Cr_2O_3 band and the phases left behind during its progression are currently being investigated.

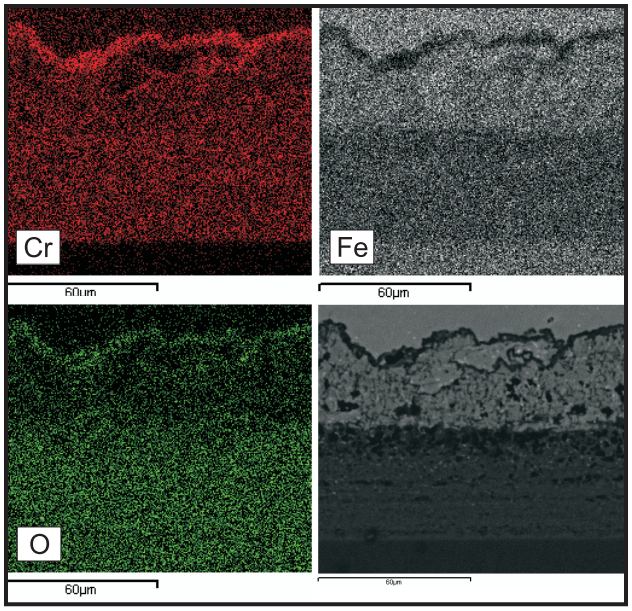

Figure 3. Energy dispersive x-ray map of oxide layer formed after four week exposure to supercritical water at 600°C.

For a more detailed analysis of elemental distribution in these samples, elemental mapping was performed using electron energy loss spectroscopy (EELS). EELS allows a qualitative overview of the elemental distribution at a fine scale. Typical EELS maps of Fe, Cr, and oxygen (O) are shown in Figure 4 with their corresponding bright field image for the metal/diffusion layer interface for 9Cr ODS 600°C at four weeks. The EELS maps confirm that the diffusion layer contains a mixture of phases of different composition, some Cr-rich and some Fe-rich. The Fe and O maps are almost complementary, showing that Cr oxidizes first in the low oxygen region.

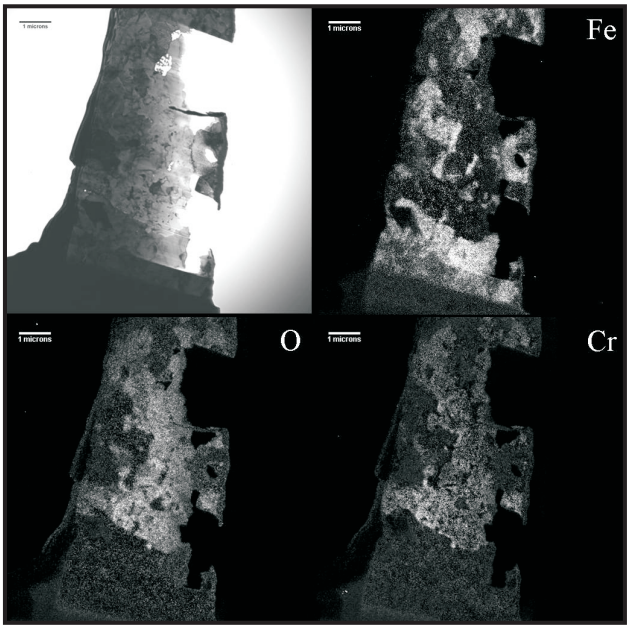

Figure 4. EELS maps of Fe, Cr, and O from the metal/diffusion layer interface of 9Cr ODS 600°C, four weeks.

Planned Activities

For the next year, researchers will continue the analysis of the oxide layers using both microbeam synchrotron radiation diffraction and fluorescence and TEM. The results will be cross compared and contrasted with weight gain behavior and with other characterization techniques in order to derive oxide growth mechanisms.

These results will be analyzed and correlated to the corrosion behavior to discern the mechanisms for protection and formation of stable oxide growth.

Nuclear Energy Research Initiative

Multi-scale Modeling of the Deformation of Advanced Ferritic Steels for Generation IV Nuclear Energy Systems

PI: Nasr M. Ghoniem, University of California-Los Angeles (UCLA)

Collaborators: California State University-Northridge (CSUN)

Project Number: 06-109

Project Start Date: March 2006

Project End Date: March 2009

Research Objectives

The objective of this project is to use the multi-scale modeling of materials (MMM) approach to develop an improved understanding of the effects of neutron irradiation on the mechanical properties of high-temperature materials (i.e., 650–700°C, compared to the current 550°C limit). Empirical potentials are not well developed for alloys and cannot easily adapt to local changes in chemistry caused by impurities.

In this project, researchers developed a hybrid *ab-initio*/continuum model to describe the core of dislocations in iron (Fe). The developed models allow studies of dislocation core structures in steels, without *ad hoc* assumptions of interatomic forces. The model is applied to determine the core structure of screw dislocations in Fe, as well as the interaction between dislocations and oxide and carbide precipitates, because they control the ductility and high-temperature strength of steels. Dislocation Dynamics models are developed to simulate the mechanical properties of radiation-damaged steels as a function of the neutron dose. Single dislocation interaction with nano-voids, precipitates, and self-interstitial atom (SIA) clusters during irradiation are developed. This information is used in a comprehensive rate theory model of radiation damage and in-reactor deformation. Predictions will be made for in-reactor deformation, with full microstructure information linked with the deformation field.

Research Progress

Researchers have developed a hierarchy of computational approaches to explore and determine the mechanisms responsible for the unusual dislocation core properties in body center cubic (bcc) materials and the effect of chemistry/precipitate.

The developed methods are listed below:

1) An *ab-initio*-based hybrid approach based on an extension of the parametric dislocation dynamics (DD) to bcc metals in which the dislocation core is non-planar where the dislocation spreading over multiple glide planes is explicitly accounted
2) A novel multiscale approach that allows the study of the core structure in straight dislocations in face center cubic (fcc) and bcc metals

***Ab-Initio* Hybrid Approach.** Most physical properties of crystalline materials are affected, to a greater or lesser extent, by the presence of dislocations. In many cases, this influence is dominated by the elastic strain field which, for distances more than a few atomic spacings from the center of the dislocation, is described well by linear continuum elasticity. However, the continuum description, which excludes the short-range details of the atomic lattice, cannot account for the intrinsic dislocation-lattice coupling, which is the source of the plastic anisotropy in bcc metals. This coupling has its origin in the dislocation core—the narrow, nonlinear region that surrounds the dislocation center and within which the crystal structure is the dominant influence.

Researchers have developed a hybrid approach that links parametric dislocation dynamics with *ab-initio* input for the generalized stacking fault energy surface (GSFES). This is an extension of the original Peierls-Nabarro (PN) model for planar core to the case of non-planar cores in bcc metals. The Burgers vector of the screw dislocation is divided into fractional dislocations which are allowed to spread into six glide planes—three (110) and three (112). The GSFES for these two sets of planes is calculated from *ab-initio* calculations. The research team takes into account both the screw and edge components of the dislocation

displacement field, satisfying a number of boundary conditions. This approach considers both the elastic interaction and the misfit energy. The codes have been developed and are currently being tested. The advantage of this hybrid approach is that it will allow for the study of kinks.

Concurrent Multiscale Approach. The two challenges to studying the interaction between dislocation and impurities are 1) proper treatments of the long-ranged elastic field and 2) reliable descriptions of atomic interactions in the framework of the density functional theory (DFT). Researchers have developed a new, concurrent, multiscale method that allows these difficulties to be overcome. In this approach, the whole system is divided into two regions: Region I, where detailed physics are relevant, and Region II, which serves as a large buffer environment. The energy of the combined systems can be written in the following form $E[I+II]=E_{DFT}[I]+E_{EAM}[II]+E_{int}[I,II]$. The total energy of the coupled system can be written in the form $E[I+II]=E_{EAM}[I+II]-E_{EAM}[[I]+E_{DFT}[I]$, where E_{EAM} and E_{DFT} are the energy of Region I in the absence of II obtained by DFT and EAM calculations, respectively.

Researchers have developed the code and have tested it for bcc Ta in order to compare it with previously published results using the first-principles Green function boundary condition, the Finnis-Sinclair potential, and the generalized pseudopotentials developed by Moriarty and co-workers in Livermore. The calculated core structure and Peierls stress are in excellent agreement with those of Woodward and Rao using the first-principles Green function boundary condition. The table below summarizes the results for the Peierls stress in GPa:

This Work	Rao	FP	Finnis-Sinclair	EAM	MGPT
1.8	1.8	1.7	4.3	1.8	0.6

The excellent agreement of the Peierls stress method with that of Rao/Woodward demonstrates the accuracy of this method. Currently, the research team is applying the results to understand the effect of tungsten (W) precipitates or substitutional impurities on the dislocation core properties in Ta.

Modeling the Core Structure of SIA Clusters. The core structure of self-interstitial loops in bcc iron and fcc copper was analyzed using an atomistic and continuum hybrid computer simulation method. The method was originally developed by Banerjee et al., based on the PN model and by the input of atomistic information prepared by separate *ab-initio* calculations. To enable a detailed, atomic-scale investigation of the core structure, researchers developed a method to derive the atomic arrangement from the hybrid simulation result. The resultant atomic arrangement is then compared to those obtained by the classical Molecular Dynamics (MD) method in order to show the similarity and difference between the results of the classical MD and the hybrid simulations. In the bcc Fe, the core structure has no dependence on the size of the self-interstitial loops and is almost identical to that of straight edge dislocation. On the other hand, in the fcc copper, the core structure has a strong dependence on the size of the self-interstitial loops. The core structure of partial dislocations of small self-interstitial loops is flat, and the width of the stacking fault between the partial dislocations is relatively narrow. As the size of the self-interstitial loop increases, the partial dislocations have a well-structured core and a wide stacking fault. The core structure of the self-interstitial loop with more than 441 SIAs has almost the same as that of the straight edge dislocation. The core structure of SIA clusters in bcc Fe is shown in Figures 1 and 2.

Constitutive & Crystal Plasticity Modeling. The objective of this research is to develop an understanding of the mechanical behavior and the dislocation microstructure evolution of single and polycrystals, as well as to delineate the physical and mechanical origins of spatially localized plastic deformation. Researchers developed a framework that combines both large-deformation kinematics and the physics of plastic instabilities. A rate-independent crystal plasticity model was developed to incorporate micromechanics, crystallinity, and microstructure into a continuum description of finite strain plasticity. A comprehensive dislocation density model based on rate theory is employed to determine the strain hardening behavior within each plastic slip system for the fcc crystal structure. Finite strain effects and the kinematics of crystal plasticity are coupled with the dislocation-density based model via the hardening matrix in crystal plasticity. ABAQUS/CAE is employed as a finite element method solver, and several users' subroutines were developed to model fcc crystals with 2 and 12 slip systems. The developed material models are applied to study single and polycrystal deformation behavior of copper. Interfaces between the ABAQUS users' subroutine UMAT and the ABAQUS main code are developed to allow further extension of the current method. Simulations carried out for polycrystals clearly illustrate the heterogeneous

nature of plastic strain, as well as the corresponding spatial heterogeneity of the mobile dislocation density. The origins of the spatial heterogeneities are essentially geometric as a result of constraints on grain rotation (finite strain effects) and geometric softening due to plastic unloading of neighboring crystals. The physical origins of plastic instabilities manifest themselves in the coupling between the dislocation densities and the localized kinematically induced softening.

Phenomenological rate theory models were used to study the dynamic behavior of defect interaction evolution. The models were explored for instabilities that may arise during their use. The research team used the concepts and techniques of nonlinear dynamics to study the material instabilities. Later, the team analyzed the spatial instabilities and, using dynamical systems methods, studied the instabilities in irradiated materials. Rich spatio-temporal dynamics that are exhibited by irradiated materials subjected to uniform tensile remain a challenging problem.

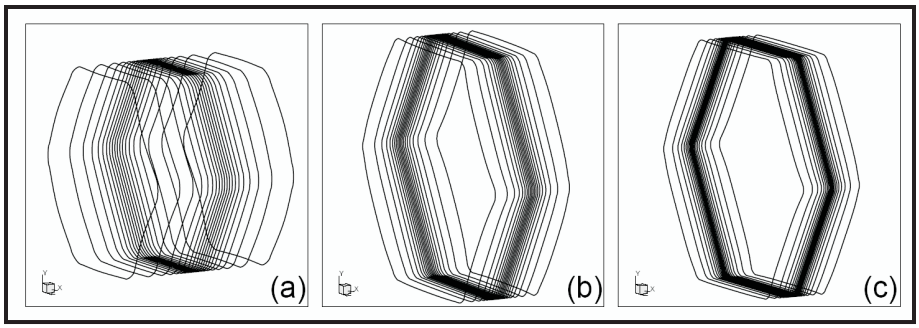

Figure 1. Core structures of self-interstitial loops with (a) 91, (b) 397, and (c) 919 SIAs in iron. The lines are the infinitesimal dislocations, which describe the displacements in the dislocation cores.

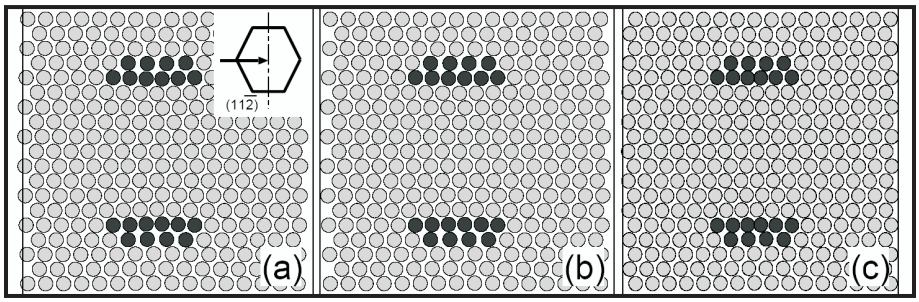

Figure 2. Atomic arrangements of core structure of dislocations on a (11$\bar{2}$) plane in iron obtained by the classical MD calculations with interatomic potentials developed by (a) Finnis and Sinclair, (b) Mendelev et al., and (c) the hybrid calculation. The colors are given based on coordination numbers. If the coordination number is eight, the atom is shown with gray color; if not, the atom is shown with black color.

Experimentally, it has been found that the instabilities arise in the deformation of irradiated materials. Detailed experimental investigation has shown that vacancy clusters generated as a result of irradiation (predominantly in the form of stacking fault tetrahedra [SFT]) play a dominant role in the inhomogeneous deformation. Here, researchers present a model for serration seen on stress-strain curves that are jerky under irradiation.

In the previous report, researchers outlined a new material model for the description of dislocation populations in irradiated materials. Presently, the model has three rate equations describing the density of mobile, immobile, and stacking fault tetrahedra. The rate equations are given below:

$$\frac{\partial \rho_m}{\partial t} = \theta v_m \rho_m - \frac{1}{2}\beta \rho_m \rho_s - \gamma \rho_m \rho_{im} + \lambda \rho_{im} + \frac{D}{\rho_{im}} \nabla^2 v_m \rho_m(x,y)$$

$$\frac{\partial \rho_{im}}{\partial t} = \beta \rho_m \rho_s - \gamma \rho_m \rho_{im} - \lambda \rho_{im}$$

$$\frac{\partial \rho_s}{\partial t} = \alpha - \frac{1}{2}\beta \rho_m \rho_s - \Delta \rho_s + \lambda f \rho_{im}$$

Researchers have performed a linear stability analysis of the model. The results of the analysis indicate that the stability range is very much dependent on the model parameters. Presently, researchers are focusing their attention on dislocation dynamics and Kinetic Monte Carlo in order to determine those parameters more precisely.

Planned Activities

Ab-Initio Modeling

- Develop formalism and codes for a Peierls-Nabarro model for bcc materials and the effect of impurities on the core structure
- Develop a hybrid *ab-initio* approach for the Cu-Fe interface and Cu precipitates
- Continue the development of the concurrent multiscale approach
- Study the formation of kinks on screw dislocations in Fe

Dislocation Dynamics Modeling

- Conduct DD simulations of the collective motion of large number (over several thousand) SIA clusters and moving dislocations to investigate SIA cluster patterns in irradiated iron
- Determine the effective velocity of dislocations as they interact with SIA cluster clouds

Modeling the Core Structure of SIA Clusters

- Compare the core structure of SIA clusters in copper and iron and document the findings of their research in a journal publication

Constitutive and Crystal Plasticity Modeling

- Further develop a rate theory model for dislocation populations in irradiated Fe
- Include spatial gradient effects in the rate theory model of dislocation populations
- Develop a crystal plasticity framework that includes dislocation populations in the finite element method (FEM) solutions
- Apply the crystal plasticity model to polycrystalline material deformation

Nuclear Energy Research Initiative

An Advanced Integrated Diffusion/Transport Method for the Design, Analysis, and Optimization of Very High-Temperature Reactors

PI: Farzad Rahnema, Georgia Institute of Technology (Georgia Tech)

Collaborators: Idaho National Laboratory

Project Number: 07-003

Project Start Date: July 2007

Project End Date: July 2010

Research Objectives

The main objective of this research is to develop an integrated diffusion/transport method to substantially improve the accuracy of nodal diffusion methods for the design and analysis of very high-temperature reactors (VHTRs). Due to the presence of control rods in the reflector regions in the pebble bed reactor (PBR-VHTR), traditional nodal diffusion methods will not accurately model these regions because the diffusion theory breaks down in the vicinity of high neutron absorption and steep flux gradients. The proposed integrated diffusion/transport (IDT) method will use a local transport solver based on a new incident flux response expansion method in the controlled nodes. Diffusion theory will be used in the rest of the core. This approach will improve the accuracy of the core solution by generating transport solutions of controlled nodes while maintaining computational efficiency by using diffusion solutions in nodes where this type of treatment is sufficient. The transport method will initially be developed and coupled to the reformulated 3-D nodal diffusion model in the PEBBED code for PBR core design and fuel cycle analysis.

This method will also be extended to the prismatic VHTR. It is expected that the new method will accurately capture transport effects in highly heterogeneous regions with steep flux gradients. The calculations of these nodes with transport theory will avoid errors associated with spatial homogenization commonly used in diffusion methods in reactor core simulators.

Research Progress

Between August 2007 and September 2007, researchers worked on developing the 2D(r,θ) response function-based transport method. The details are described in the following program:

Problems of Conventional Legendre Polynomial Expansion. The aim of this task is to develop a 2-D cylindrical transport method to generate response functions in terms of exiting partial currents, surface-averaged, and node-averaged scalar fluxes for non-multiplying regions, such as inner and outer reflectors (Figure 1), to couple with the diffusion method used in the fuel region.

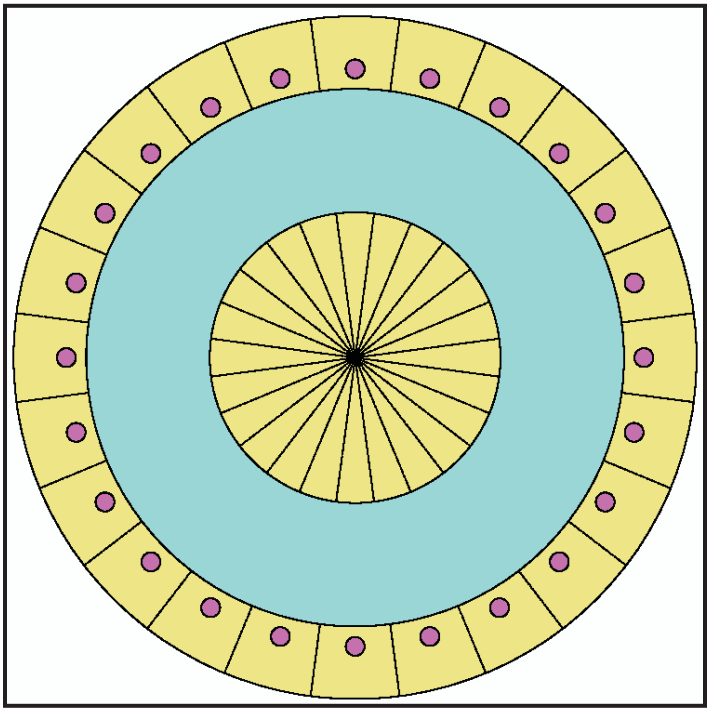

Figure 1. Geometric configuration of a 2-D PBMR400 PBR consisting of an inner reflector, an annular fuel region, and a controlled outer reflector.

To generate response functions for a coarse mesh, an approximation of neutron phase space distributions on the mesh boundaries must be made since the whole core solution is not known as priori. Conventionally, it is assumed that the interface angular current $_j(\vec{r},\hat{\Omega},E)$ can be expanded in terms of multi-products of Legendre

polynomials, as shown in Equation (1), and then response functions are calculated by solving each local fixed source problem with an incoming flux imposed on the mesh boundaries.

$$j^{\pm}(\vec{r},\mu,\varphi,E)=\sum_{lmnp} J^{\pm}_{lmnp} P_l(\vec{r}) P_m(\mu) P_n(\varphi) P_p(E) \quad (1)$$

or equivalently,

$$\psi^{\pm}(\vec{r},\mu,\varphi,E)=\frac{1}{\left(\vec{n}^{\pm}\cdot\hat{\Omega}\right)}\sum_{lmnp} J^{\pm}_{lmnp} P_l(\vec{r}) P_m(\mu) P_n(\varphi) P_p(E) \quad (2)$$

In the above equations, $\vec{r}$ represents spatial variable on the mesh interface; $\hat{\Omega}$ is the neutron direction; φ and μ denote the azimuthal and polar angle variables, respectively; E represents neutron energy; $\vec{n}^{\pm}$ is the outward or inward normal to the mesh interface at point; $\vec{r}$ $P_n(x)$ is the n-th order scaled Legendre polynomial; and $J^{\pm}_{lmnp}$ represents expansion coefficients or partial current moments.

Obviously, the 0th order expansion function represents a spatially uniform and angularly isotropic surface source with a flat energy spectrum. Accordingly, the 0th expansion moment is identical to the total partial current. Because of the orthogonalities of Legendre polynomials, a higher order expansion only changes the shape of the neutron distribution functions, while the total partial current still remains unchanged.

Though this expansion can guarantee that intra-nodal partial currents are conserved, it introduces singularities in scalar fluxes and consequently cannot be used by transport methods that couple to diffusion methods in which response functions, in terms of surface-averaged fluxes, are required. In thermal reactors, the angular flux in most regions is dominated by its isotropic component; it would be physically natural to require the 0th order angular expansion function to be equivalent to the isotropic angular flux.

Requirements of New Expansion Functions in 2D Cylindrical Geometry. Based on the discussion above, the following are the desirable characteristics of a new set of expansion functions:

1) The scalar flux resulting from the expansion is finite
2) Total partial currents remain unchanged after an expansion
3) The 0th angular expansion function is constant in angle (isotropic)

To avoid singularities introduced by an expansion, angular fluxes, instead of angular currents, should be chosen to be expanded in both the outward and inward hemispheres, as in the following form:

$$\psi^{\pm}(\vec{r},\hat{\Omega},E)=\sum_{i,j,k,l} c^{\pm}_{ijkl} f_{ijkl}(\vec{r},\hat{\Omega},E) \quad (3)$$

where $c^{\pm}_{ijkl}$ are expansion coefficients, f_{ijkl} represent expansion functions which satisfy the following orthogonality condition:

$$\int_S d\vec{r}\int dE \int_{\left(\vec{n}^{\pm}\cdot\hat{\Omega}>0\right)} d\hat{\Omega}\left(\vec{n}^{\pm}\cdot\hat{\Omega}\right) f_{ijkl}(\vec{r},\hat{\Omega},E) f_{i'j'k'l'}(\vec{r},\hat{\Omega},E) = A_{ijkl}\delta_{ii'}\delta_{jj'}\delta_{kk'}\delta_{ll'} \quad (4)$$

where S represents the mesh interface, δ is the Kronecker delta, A_{ijkl} are constants, and the factor $\vec{n}^{\pm}\cdot\hat{\Omega}$ is a weighting function. By using the above condition, the expansion coefficients $c^{\pm}_{ijkl}$ can be defined by the following relation with the angular flux $\psi^{\pm}(\vec{r},\hat{\Omega},E)$:

$$c^{\pm}_{ijkl}=\int_S d\vec{r}\int dE \int_{\vec{n}^{\pm}\cdot\hat{\Omega}>0} d\hat{\Omega}\left(\vec{n}^{\pm}\cdot\hat{\Omega}\right) f_{ijkl}(\vec{r},\hat{\Omega},E)\psi^{\pm}(\vec{r},\hat{\Omega},E) \quad (5)$$

It should be pointed out that the commonly used spherical harmonic functions cannot be used as the expansion functions in this research since they are defined in the whole 4π solid angle and do not satisfy the orthogonality condition (4). A new set of expansion functions satisfying the above requirements is expected to be developed in the upcoming year.

Planned Activities

For the upcoming year, researchers plan to complete the following activities:

- Develop a new set of expansion functions that are suitable to couple with diffusion approximations in 2-D cylindrical geometry (task 1.1)
- Develop a 2-D(r,θ) Response-Matrix Nodal Balance (RMNB) diffusion method (task 1.2)
- Integrate results of tasks 1.1 and 1.2 into the PEBBED code (task 1.3)
- Test the product of task 1.3 on an existing 2-D PBR benchmark problem

Nuclear Energy Research Initiative

Implications of Graphite Radiation Damage on the Neutronic, Operational, and Safety Aspects of Very High-Temperature Reactors

PI: Ayman I. Hawari, North Carolina State University (NCSU)

Collaborators: Idaho National Laboratory (INL), Oak Ridge National Laboratory (ORNL)

Project Number: 07-011

Project Start Date: June 2007

Project End Date: June 2010

Research Objectives

This project entails experimental and computational investigations to study the radiation effects of graphite in very high-temperature reactors (VHTRs). Researchers will use molecular dynamic and *ab-initio* molecular static calculations to 1) simulate radiation damage in graphite under various irradiation and temperature conditions, 2) generate the thermal neutron scattering cross sections for damaged graphite, and 3) examine the resulting microstructure to identify damage formations that may produce the Wigner effect.

In both the prismatic and pebble bed VHTR designs, the graphite moderator is expected to reach exposure levels of 10^{21} to 10^{22} n/cm^2 over the lifetime of the reactor, resulting in damage to the graphite structure. Studies of irradiated graphite show changes in the thermal conductivity and heat capacity at fluences less than 10^{21} n/cm^2. These properties depend on the behavior of atomic vibrations (phonons) in the graphite solid. It can be expected that any alterations in phonon behavior that would produce changes in these properties would impact thermal neutron scattering, with implications for the neutronic and safety behavior of the VHTR. Another important phenomenon pertains to published data showing that a high-temperature (>1,200°C) Wigner-like effect may exist in graphite. If confirmed, this effect would have direct implications on the safety behavior of VHTRs.

Research Progress

During the first quarter of this project, coordination was initiated with ORNL to discuss the availability of irradiated graphite samples for use in this project's structure studies, including the diffraction studies that will be performed at the NCSU PULSTAR reactor using the neutron powder diffractometer. Graphite neutron powder diffraction patterns have been reported in the literature. These measurements were performed using a highly crystalline graphite sample

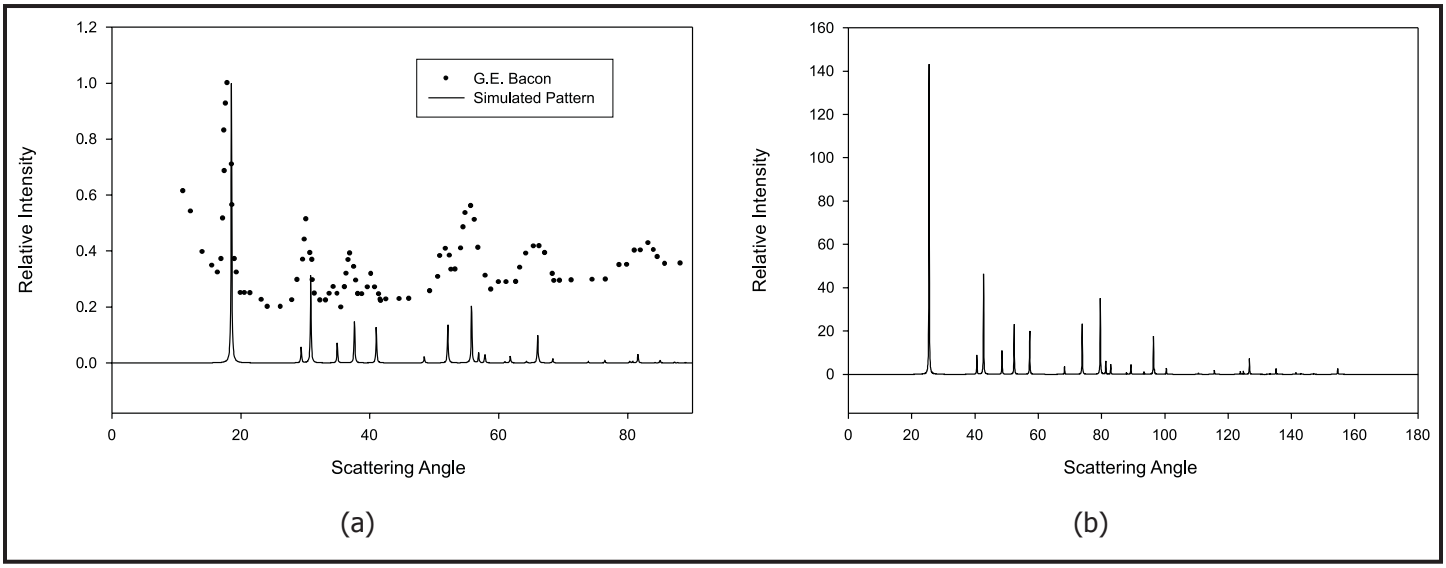

Figure 1. (a) Comparison between the Crystallographica simulation and data for crystalline graphite, and (b) simulated pattern for 1.478 Å neutrons.

and neutrons of wavelength 1.08 Å. To study these results and to predict the signal using the NCSU diffractometer, researchers used the software package Crystallographica to generate the expected diffraction pattern at this wavelength. Figure 1a shows the comparison between the simulated and experimental data. As can be seen from the figure, the data is consistent with the pattern generated assuming perfect unirradiated graphite. Figure 1b shows the predicted diffraction pattern for a 1.478 Å neutron beam, which is the wavelength that is extracted from the monochromator crystal at the NCSU diffractometer.

Reactor-grade graphite samples for neutron diffraction experiments have been prepared and experiments are expected to be underway shortly. The choice of the sample size is based on the desired count rate and the width of the diffraction beam. A larger sample size will give a larger count rate in the detector; however, a smaller sample size will decrease the width of the diffracted beam. Therefore, two samples of reactor grade graphite with different sizes were cut into rectangular prisms: one with sides of 3 mm and one with sides of 6 mm. Each prism is 5 cm tall and has a 0.5 inch hole drilled in the bottom so that it will fit snuggly on the sample holder. Figure 2 shows the sample holder and the two sample sizes.

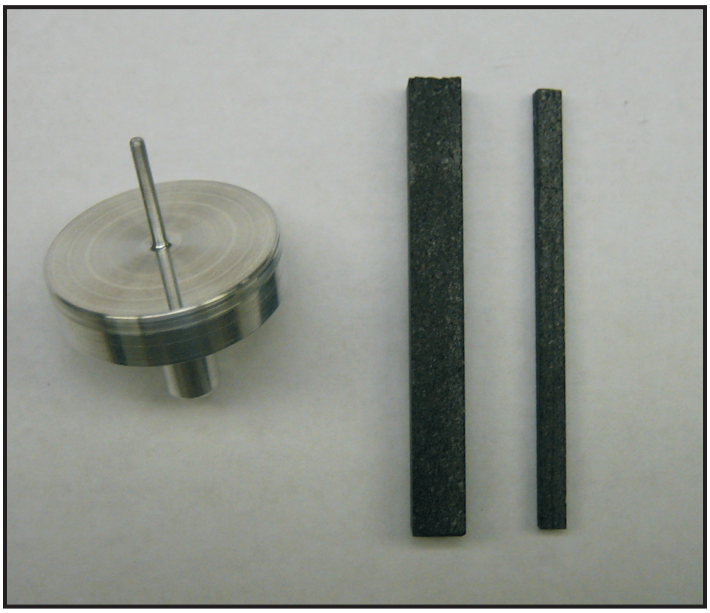

Figure 2. Graphite sample holder and samples for powder diffraction experiments at the NCSU PULSTAR reactor.

The computational effort for this project was initiated using the NCSU graphite molecular dynamics (MD) tools that have been developed over the past few years. The methodology developed earlier was validated for temperatures extending from a few degrees K to around 2,000°K, which includes temperatures relevant for the VHTR. In the current work, the MD methodology is being extended to enable calculating and extracting all the quantities that are relevant in thermal neutron scattering studies. One connection between MD and thermal neutron scattering lies in the dynamic pair correlation function, $G(\vec{r},t)$, which represents the probability of finding an atom at position $\vec{r}$ at time t. Under the Van Hove formulation, the Fourier transform of $G(\vec{r},t)$ in space and time gives the scattering law of the material $S(\vec{Q},w)=\frac{1}{2\pi\hbar}\int_{-\infty}^{\infty}\int_{-\infty}^{\infty}G(\vec{r},t)e^{i(\vec{Q}\cdot\vec{r}-wt)}d\vec{r}dt$, where $\vec{Q}=\vec{k}-\vec{k}'$; k and k' represent the magnitude of the wave vector of the incident and scattered neutron, respectively; *h* is the reduced Planck constant; and *ω* is the vibrational frequency. The advantage of the Van Hove approach described above is that it applies to both damaged and undamaged systems and includes all temperature anharmonic effects. In practice, the Fourier transform relating $G(\vec{r},t)$ to $S(\vec{Q},w)$ must be computed as a discrete Fourier transform since $G(\vec{r},t)$ is evaluated in discrete bins within the simulated space. Work is currently underway to integrate a routine for calculating $G(\vec{r},t)$ into the NCSU MD package. Very accurate interatomic forces will likely be needed in MD simulations of graphite in order to reproduce the phonon frequency distribution to a high degree of fidelity. To this end, it may be necessary to further refine the MD potential function through benchmarking to an ab-initio package, such as Vienna *Ab-initio* Simulation Package (VASP). A VASP model for graphite has already been developed and validated at NCSU. Thus, an ongoing task is to investigate the adjustment of the classical MD potential to better match the output from VASP, thereby improving agreement with the known frequency distribution of graphite.

Finally, communications have been initiated with INL to investigate the use of reactor benchmarks to study the impact of the new cross-section libraries in the VHTR design. It was agreed that once the cross sections are generated, they will be passed to INL for performing such studies.

Planned Activities

During the remainder of the first year for this project, researchers will focus on performing the diffraction measurements of various graphite samples at the NCSU PULSTAR reactor. In addition, they will transfer irradiated and unirradiated graphite samples from ORNL to NCSU and investigate these samples using neutron diffraction methods. The information revealed by these measurements will be integrated into the atomistic models that are currently being developed. Furthermore, the team will establish computational methods for extracting the scattering law from MD simulations. The MD simulations will then be used to model radiation damage in graphite and to produce early predictions of the scattering law for irradiated and unirradiated graphite.

Nuclear Energy Research Initiative

Advancing the Fundamental Understanding and Scale-up of TRISO Fuel Coaters via Advanced Measurement and Computational Techniques

PI: Muthanna Al-Dahhan, Washington University

Collaborators: None

Project Number: 07-017

Project Start Date: September 2007

Project End Date: August 2010

Research Objectives

The overall research objectives of this project are 1) to advance the fundamental understanding of the hydrodynamics TRISO fuel coaters by systematically investigating the effect of design and operating variables, 2) to evaluate the reported dimensionless groups as scaling factors, and 3) to establish a reliable scale-up methodology for TRISO fuel particle spouted bed coaters based on hydrodynamics similarity via advanced measurement and computational techniques. Researchers will develop an on-line, non-invasive measurement technique based on gamma ray densitometry (i.e., Nuclear Gauge Densitometry) that can be installed for coater process monitoring to ensure proper performance and operation and to facilitate the developed scale-up methodology.

To achieve these objectives, the research team will use the following research tools:

- Optical probes for solid and gas holdup and solids velocity distribution measurements
- Gamma ray computed tomography (CT) for measuring the solid and gas holdup cross-sectional distribution along the spouted bed height, spouted diameter, and fountain height
- Radioactive particle tracking (RPT) technique for measuring the 3D flow patterns and field, solids velocity, turbulent parameters, circulation time, and many others
- Gas dynamics measurement technique
- Pressure transducers

The team will then use the data and knowledge obtained as benchmark data to evaluate the computational fluid dynamics models and their closures to facilitate the developed scale-up methodology, to identify the conditions for hydrodynamics similarity, and to further investigate and optimize the process performance of TRISO coaters.

Research Progress

The following progress has been made since the project's initiation in September 2007:

- Designed a 6-inch and 3-foot high, 60 degree angle, conical-based spouted bed for future fabrication
- Identified three solid types of coaters that are expected to provide hydrodynamics similarity and mismatch in hydrodynamics similarity (based on the work of He et al., 1997)
- Assembled a ½ optical probe for a gas-solid system to be tested for gas and solids holdup as well as solids velocity measurements

Planned Activities

The following are planned activities for the coming year:

- Construct the 6-inch spouted bed coater with 10 ports along its height for the optical probe and pressure transducers measurements
- Design and construct a 3-inch spouted bed
- Assess the ½ optical probe measurements
- Develop a new, small-size, optical probe technique with its needed data acquisition system and algorithm/programs for data processing to obtain gas/solid holdup and solids velocity
- Use the optical probe and the gas dynamics technique to assess the hydrodynamics similarity of the identified solids and the 6-inch and 3-inch spouted beds
- Based on the results, evaluate the reported dimensionless groups as scaling factors
- Select and acquire the proper pressure transducers
- Prepare and initiate the gamma ray CT and the development of the Nuclear Gauge Densitometry

NUCLEAR ENERGY RESEARCH INITIATIVE

Fission Product Transport in TRISO-Coated Particle Fuels: Multi-Scale Modeling and Experiment

PI: Izabela A. Szlufarska, University of Wisconsin-Madison

Collaborators: None

Project Number: 07-018

Project Start Date: June 2007

Project End Date: June 2010

Research Objectives

The objective of this project is to develop a multi-scale computational model of transport of fission products through tri-isotopic (TRISO)-coatings. The model will build on 1) the strength of massively parallel molecular dynamics simulations to provide a full atomistic picture of silicon carbide (SiC) microstructural features (e.g., grain boundaries), 2) quantum mechanical approaches to determine highly accurate diffusion barriers in these structures, and 3) continuum level theories to determine diffusion rates in macroscopic samples. Experiments will be performed to provide input for simulated microstructures (e.g., information about typical grain boundary textures) and to validate modeling predictions. The developed model will be employed to determine mechanisms of fast diffusion of silver (Ag) through SiC coating.

Research Progress

Up to this point, researchers have focused on quantum mechanical calculations of Ag defect energetics in SiC, which will form the foundation of bulk diffusion for Ag in SiC, and on microstructural analysis of SiC and constructions of diffusion couples.

Defect Energetics. The first step in the *ab-initio* work was to determine accurate simulation parameters needed for the SiC calculations. Researchers are performing the calculations with the Vienna *Ab-Initio* Simulation Package (VASP), a plane wave density functional theory-based code. The key parameters consist of the reciprocal space k-point mesh, which is used for numerical integration, and the plane wave energy cutoff, which determines the size of the basis used to represent the wave functions. In both cases, the goal is to use values high enough to get well-converged results (here represented by energy), but no higher since larger values slow the calculations. Based on their calculations, the research team chose a 6x6x6 k-point mesh and an energy cutoff of 600 eV.

Researchers are currently studying Ag and SiC defects in order to determine which Ag defects are energetically favorable. This will allow the research team to calculate diffusion coefficients for Ag diffusion through bulk SiC. At the time of this writing, researchers have found the following defects to have stable configurations: C vacancy; Si vacancy; Si on C site (Si_C); C on Si site (C_{Si}); C on Si site and Si on C site (antisite defect, Si_CC_{Si}); Ag substituting Si (Ag_{Si}); Ag substituting C (Ag_C); Ag in center of C tetrahedral region ($Ag_{I\text{-}Ctet}$); Ag in center of Si tetrahedral region ($Ag_{I\text{-}Sitet}$); and an Ag-Si <110> dumbbell ($Ag_{I\text{-}110}$).

Researchers have calculated how defect formation energies ΔE_f for Ag on Si, Ag on C, and Ag interstitials change as a function of the chemical potentials, which can range in value depending on the environmental conditions. If it is assumed that the Si and C will form bulk stable phases of the pure elements or SiC to the extent they are able, the values of μ_{Si} and μ_C are constrained to the shaded region in Figure 1.

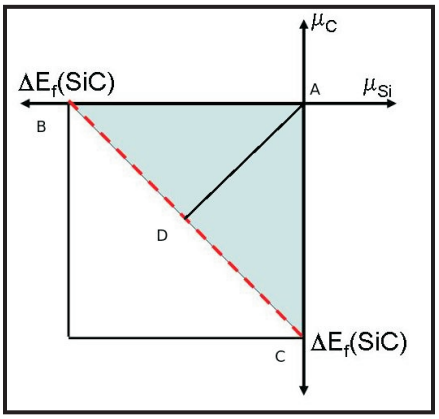

Figure 1. The acceptable values of μ_{Si} and μ_C based on the stability of the solid SiC. ΔE_f(SiC) is the formation energy of SiC. The letters A, B, C, and D are references used in Figure 2.

Figure 2 shows ΔE_f for Ag_{Si}, Ag_C, (lowest energy tetrahedral Ag interstitials–the dumbbells are still being analyzed) as we move along the path ABCAD in Figure 1. In general, all Ag interstitials have about the same formation energy on this scale, so one line in the figure is suitable for visualizing it in relation to the other defects.

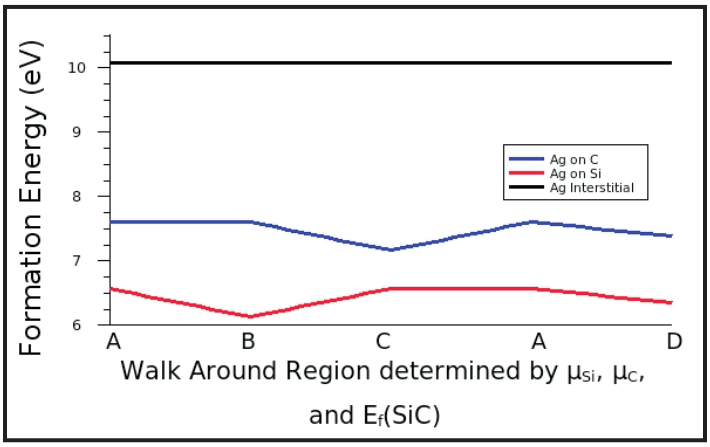

Figure 2. How the formation energy of the defects change as the chemical potential of Si and C changes within the values given in Figure 1.

Figure 2 shows that, of the Ag defects, Ag_{Si} is the most energetically favorable, regardless of chemical potentials of Si and C. It also shows that the Ag interstitials are unlikely as the formation energy for them is so much more than Ag substitutional defects. Based on these formation energies, researchers are now working to calculate concentrations of these defects. They will then calculate diffusion coefficients for Ag through bulk SiC.

Experimental Analysis of SiC. The microstructure of the chemical vapor deposition (CVD) β-SiC obtained from Rohm and Hass is similar to that found in TRISO fuel particles. Scanning electron microscopy (SEM) analysis shows columnar grains along the deposition direction with equiaxed grains observed on a plane-view of the sample. Raman spectroscopy of the as-received SiC produced a strong Raman shift at 796 cm^{-1}, confirming the β-SiC phase. Raman spectroscopy of the fracture surface on an as-received sample shows a strong shift at 796 cm^{-1} and smaller peaks around 200 cm^{-1} and 970 cm^{-1}. These less pronounced shifts suggest the possibility of free Si on the grain boundary. Further analysis is needed to confirm the presence of Si at the grain boundary.

Diffusion Couple Construction. The design for diffusion couple experiments required the SiC/Ag to be sealed in a diffusion barrier under vacuum to avoid Ag loss due to vaporization. Molybdenum (Mo) was chosen as the canister material as it has a low solubility for Ag and Si and high temperature stability. The surface normal to the growth direction of the CVD-SiC was polished and placed in a pellet press and loaded with Ag powder, pumped down to remove as much gas as possible, then pressed into a pellet resulting in a diffusion couple which fit into the Mo canister with good tolerance. E-beam welding of the Mo canisters was conducted by SWS-Trimac, Inc. The integrity of the weld was tested by measuring weight loss of the diffusion couple after a 24-hour soak at 1,200°C. With the success of the weld, the diffusion couple construction was validated and an additional set of diffusion couples systems was sent out for welding. Future work will examine diffusion couple systems exposed at varying temperatures.

Planned Activities

Molecular dynamics (MD) simulations have been performed to determine the structure of a number of grain boundary types in SiC. Future activities will be focused on the development of an empirical potential for the interaction of SiC with Ag. Parameters of the potential will be fitted to more accurate *ab-initio* calculations. MD simulations will be performed at elevated temperatures (in the range of high-temperature reactor [HTR] normal operating conditions) to determine diffusion constants of Ag through relevant grain boundary structures of SiC.

Researchers will also determine diffusion constants of Ag through SiC bulk and selected grain boundaries using full *ab-initio* simulations. Diffusion constants will be determined from Kinetic Monte Carlo simulations combined with *ab-initio* calculations of barriers for Ag motion. The frequently intractable problem of exploring complex grain boundaries with *ab-initio* will be overcome by using grain boundary structures and suggested diffusion paths predicted by the potential-based MD simulations.

Capabilities will be developed to study Ag transport in the experimental structures. These models will be based on solving diffusion equations on digitized experimental micrographs with diffusion constants informed by atomistic simulations.

In the experimental part of the project, researchers will focus on full characterization of SiC samples and on carrying out diffusion couple experiments to determined concentration profiles of Ag in SiC. Experimental diffusion profiles will be compared to modeling predictions to validate the developed models.

Nuclear Energy Research Initiative

Emissivity of Candidate Materials for VHTR Applications: Role of Oxidation and Surface Modification Treatments

PI: Kumar Sridharan, University of Wisconsin-Madison

Collaborators: None

Project Number: 07-020

Project Start Date: April 2007

Project End Date: March 2010

Research Objectives

The objectives of this project are to 1) evaluate emissivities of candidate materials for the reactor pressure vessel (RPV) and internal components of the very high-temperature reactor (VHTR) in air and helium environments from 300 to 900°C; 2) study the effects of emerging and commercial surface treatments on emissivity after exposure in air and helium environments at elevated temperatures; 3) develop a comprehensive understanding of the relationships between emissivity, oxide characteristics, and surface treatments by characterizing surface oxides that form on untreated and surface modified alloys after elevated temperature exposure; and 4) develop an integral separate-effects emissivity database for potential candidate materials and surface modification treatments.

The thermal radiation of heat from the outer surface will partially cool the RPV and internal components of the VHTR. With an unexpected increase in temperature, thermal radiation becomes a significant mode of heat dissipation because of its fourth power temperature dependence, according to the Stefan-Boltzmann equation. Since oxidation will inevitably occur at these higher temperatures, it is clear that material emissivity is intricately related to the chemical, physical, and mechanical characteristics of the oxide scales that form on the surface, including their chemical composition, grain morphology, topography, and porosity. The growing field of surface modification provides opportunities for achieving high emissivities at high temperatures by changing topography and grain orientation or inducing controlled surface compositional changes.

Research Progress

The design of the system for measurement of spectral emissivity of various candidate materials and coatings in air and VHTR purity helium has been finalized. Critical components for this system have either been procured or are in the process of procurement; construction of the system is underway. The design for this system will consist of a cylindrical isothermal block of monolithic silicon carbide about 6" in diameter and 8" in height. Silicon carbide has been selected on account of its high emissivity and high thermal conductivity, as well as its environmental stability in air at high temperatures. Eight holes or cavities, approximately 0.25" in diameter, are being machined circumferentially in this block, 1" from the circumference of the block. Seven of these holes or cavities will be approximately 0.25" in depth and will hold the material test samples for emissivity evaluation. The eighth hole will be approximately 1.5" in depth and will serve as the black body reference. By selecting a material with high emissivity and using geometrical considerations to further enhance the emissivity, researchers will ensure that this cavity closely approaches the desired emissivity value of close to unity.

A commercial U.S. vendor has been identified who will supply this machined block of silicon carbide as per the requirements. The block will be placed in a furnace through which air or VHTR purity helium will be circulated during testing at temperatures up to 900°C. Two 6" diameter aluminum-oxide top covers will be used to sequester the radiant heat in the furnace experimental system. A shutter system will allow researchers to selectively expose any one given sample at a time for emissivity measurements. A periscope will guide the radiation to a Fourier Transform Infra Red (FTIR) spectrometer through a CaF2 window, which will be used to measure emissivity values in the temperature range of 300 to 900°C (or higher if necessary) in the infrared through ultraviolet spectral range. The furnace holding the sample/isothermal block will be operated in conjunction with a gas chromatograph, which will allow for the assessment of inlet and outlet

gas compositions. This is particularly important in the experiments in both air as well as VHTR helium, which will react with the sample surface. A comparison of the inlet and outlet gas compositions will enable the research team to achieve the broader goals of correlating emissivity with materials corrosion, in conjunction with separate materials characterization work. Figure 1 illustrates the design of the emissivity measurement system.

A state-of-the-art FTIR (Bruker Optics Vertex-70 FTIR) has been procured for spectral emissivity measurements at high temperatures and initial calibrations of this instrument have been performed. The FTIR will collect the digital signal of an interferogram emanating from the sample via photo detectors and, through a series of fast mathematical transformations, convert this signal to a wavelength plot. This is a crucial element of the system. Unique features of this system include gold-coated internal optics, KBr Beamsplitter, MCT Liquid N2-cooled detector, and a spectral range approximately 1 to 25 microns. The FTIR will automatically scan over the entire spectrum with a high-resolution response to even weak signals and will allow for measurements over a wide range of temperatures and wavelengths. Figure 2 shows the progress in construction of the emissivity measurement system.

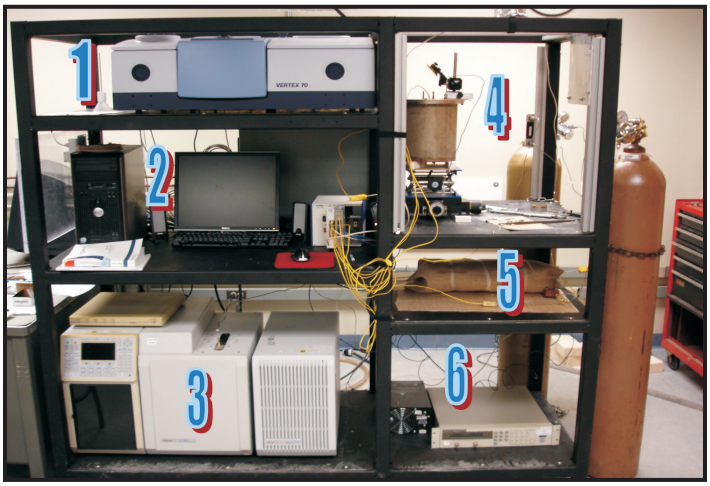

Figure 2. Status of the construction of the emissivity measurement system: (1) FTIR spectrometer; (2) data acquisition system; (3) mass spectrometer/gas chromatograph; (4) location of furnace with isothermal silicon carbide sample holding block; (5) gas preheating coil; (6) voltage sources for gas preheater and valves.

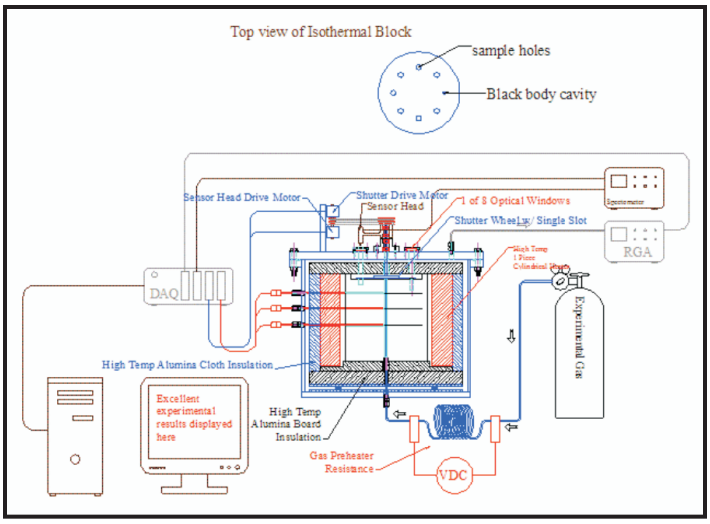

Figure 1. Illustration of the design of the experimental system that will be used for emissivity measurements in this research.

Planned Activities

Emissivity evaluations will be performed on three ferritic steels (T91, SA508, and T22) and four austenitic steels (Incoloy 800H, Haynes 230, Inconel 617, and 304 stainless steel). Samples of these materials are presently being cut by the EDM technique into 0.5”x0.5” test flats for emissivity measurement experiments. These materials have been selected based on their direct relevance to RPV and other components of VHTR. Emissivity measurements will be performed at 300, 500, 700, and 900°C after exposure durations of 10, 100, and 200 hours in air (with known humidity) and VHTR purity helium. The composition of the VHTR helium will be decided based on consultations with personnel at Idaho National Laboratory and will be procured in cylinders with pre-mixed compositions. Surface treatments to be investigated include shot peening and xenon ion bombardment for physical topographical surface modification as well as diamond-like carbon, hafnium-oxide, chromium-oxide, and silicon carbide coatings. Detailed characterization of surface oxides and corrosion products will be performed using scanning electron microscopy, Auger electron spectroscopy, and x-ray diffraction in order to correlate surface chemistry changes to changes in emissivity.

Nuclear Energy Research Initiative

Materials and Design Methodology for Very High-Temperature Nuclear Systems

PI: James Stubbins, University of Illinois

Collaborators: Stress Engineering Services, Idaho National Laboratory (INL), Massachusetts Institute of Technology (MIT), Boise State University, University of Nevada-Las Vegas

Project Number: 07-024

Project Start Date: May 2007

Project End Date: April 2010

Research Objectives

The objective of this research project is to address major materials performance and methodology issues for the design and construction of high-temperature and very high-temperature nuclear systems. This work will provide a synergy between the development of simplified, but robust, design rules for high-temperature systems and materials testing, along with performance and improvement of these systems. Such systems will have to deal with time-dependent materials properties (creep, creep-fatigue, high-temperature corrosion) in components with complex stress states, long intended service lives, and aggressive operating environments. Because routine mechanical properties data and current high-temperature design methodology do not provide adequate information for long-term, robust system design, this project will address these issues. In addition, high-temperature materials testing in relevant corrosive environments (such as low oxygen, partial pressure with substantial carbon activities) will be performed to support further code qualification of existing alloys and the development of emerging alloys.

Research Progress

Work to date has concentrated on the development of experimental facilities for high-temperature corrosion testing, including the layout of the experimental equipment to produce helium (He) atmospheres with controlled levels of impurity gasses (such as O_2, H_2O, CH_4, CO, CO_2, etc.) to provide oxygen partial pressures and carbon activities consistent with VHTR reactor environments. Additionally, the team has initiated acquisition activities for the pressurized tube creep specimens.

The program has also started various activities in association with researchers at INL, MIT, Boise State University, and the University of Nevada-Las Vegas. These activities are aimed at investigating crack initiation and growth behavior at elevated temperatures in controlled atmospheres. Test specimens are currently being fabricated for this joint research effort.

Activities associated with the development of high-temperature design guidelines are also currently in progress.

Planned Activities

During the next program year, work will commence on activities associated with mechanical properties testing in controlled atmospheres at very high temperatures, development of high-temperature design guidelines which account for properties-based materials performance characteristics, and assessment of joint activities on high-temperature crack initiation and growth behavior. The corrosion testing facilities will also be completed.

Nuclear Energy Research Initiative

Experimental and CFD Analysis of Advanced Convective Cooling Systems

PI: Victor M. Ugaz and Yassin A. Hassan, Texas Engineering Experiment Station

Collaborators: None

Project Number: 07-058

Project Start Date: June 2007

Project End Date: May 2010

Research Objectives

The objective of this project is to study the fundamental physical phenomena in the reactor cavity cooling system (RCCS) of very high-temperature reactors (VHTRs). One of the primary design objectives is to assure that RCCS acts as an ultimate heat sink capable of maintaining thermal integrity of the fuel, vessel, and equipment within the reactor cavity for the entire spectrum of postulated accident scenarios. Since construction of full-scale experimental test facilities to study these phenomena is impractical, it is logical to expect that computational fluid dynamics (CFD) simulations will play a key role in the RCCS design process. An important question then arises: To what extent are conventional CFD codes able to accurately capture the most important flow phenomena, and how can they be modified to improve their quantitative predictions?

Researchers are working to tackle this problem in two ways. First, in the experimental phase, the research team plans to design and construct an innovative platform that will provide a standard test setting for validating CFD codes proposed for the RCCS design. This capability will significantly advance the state of knowledge in both liquid-cooled and gas-cooled (e.g., sodium fast reactor) reactor technology. This work will also extend flow measurements to micro-scale levels not obtainable in large-scale test facilities, thereby revealing previously undetectable phenomena that will complement the existing infrastructure. Second, in the computational phase of this work, numerical simulation of the flow and temperature profiles will be performed using advanced turbulence models to simulate the complex conditions of flows in critical zones of the cavity. These models will be validated and verified so that they can be implemented into commercially available CFD codes. Ultimately, the results of these validation studies can then be used to enable a more accurate design and safety evaluation of systems in actual nuclear power applications (both during normal operation and accident scenarios).

Research Progress

Since formal establishment of the project in mid-year, research activities have focused on establishing the foundation for design and construction of the test facility that will be used to perform proposed studies of the convective flow phenomena. On the experimental side, researchers began by performing background literature reviews in order to become familiar with relevant work in the field. They then started work to determine the relevant scaling parameters that will enable them to construct a lab-scale test facility that best duplicates the underlying physical phenomena in a conventional full-scale RCCS system (see Figure 1). As a starting point,

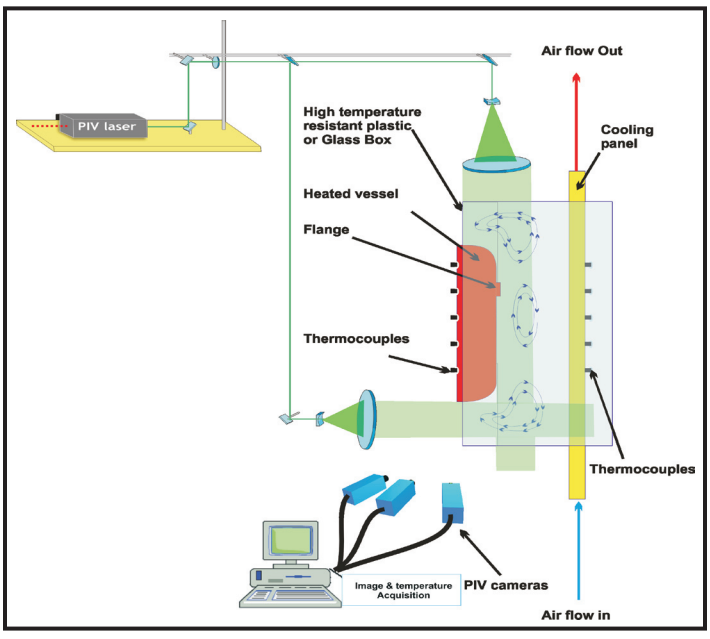

Figure 1. Illustration of proposed experimental setup for simultaneous coordinated flow velocity and temperature field measurements.

researchers will simultaneously match the Reynolds and Rayleigh numbers, combined with the dimensionless flow chamber aspect ratio (height to diameter) using the fluid properties and characteristic length scales corresponding to both the conventional and lab-scale geometries as adjustable parameters. The scaling process is not entirely straightforward due to the multiplicity of spatial and temporal scales associated with the flow phenomena.

As a starting point, the research team will initially choose the Rayleigh number based on the temperature difference between opposing vertically oriented heated surfaces as the primary parameter and adjust the temperature difference between the surfaces in order to obtain a match between length scales. Researchers will then estimate the corresponding Reynolds numbers and iteratively adjust the design in order to achieve the best possible match. This will reveal the combination of fluid properties and temperature conditions needed to construct an appropriately scaled model system. Once this scaling has been completed, the design and construction of the test facility should proceed smoothly.

On the computational side, researchers have begun investigations to identify the most suitable commercial CFD software package to use as a vehicle for computational development. So far, they have investigated STAR-CD, FLUENT, and CFX software. These are leading CFD packages and are all available to the team; however, researchers are working to determine how to obtain versions compatible with the multi-node parallel supercomputer cluster available at Texas A&M University (TAMU). A planned upgrade to the cluster hardware scheduled for installation in January 2008 should allow all three of these packages to be used, thereby providing a unique platform to simultaneously co-evaluate the predictions from these packages to determine their suitability in modeling RCCS phenomena.

Planned Activities

The primary tasks associated with the experimental |and computational phases of the project are listed below. These tasks are in line with the proposed schedule status and milestones.

Experimental Phase:

- Continue dimensional analysis combined with preliminary computational calculations for the RCCS prototype test geometry.
- Explore new seeding materials that can be used in order to 1) serve as tracers that will enable the flow field within the flow system to be directly visualized and 2) serve as indicators of the local temperature within the flow.
- Draw up plans for and begin construction of the test section.
- Develop experimental test plan, identify flow conditions, and assess instrument uncertainty.
- Perform calibration of particle image velocimetry (PIV) setup and obtain initial measurements to identify key phenomena.

Computational Phase:

- Begin assessment and validation studies over a range of flow conditions in order to support the dimensional analysis studies for test facility design.
- Begin investigation of techniques to accurately model temporal and spatial flow structure. Large eddy simulation (LES) will provide the temporal and spatial flow regimes under turbulent, transitional, and laminar conditions. Turbulence phenomena of the turbulent coherent structure will be identified. These flow patterns will help in developing/refining turbulence models and global correlation for RELAP system code.
- Compare computational results with preliminary experimental data.

NUCLEAR ENERGY RESEARCH INITIATIVE

Establishing a Scientific Basis for Optimizing Compositions, Processing Paths, and Fabrication Methods for Nanostructured Ferritic Alloys for Use in Advanced Fission Energy Systems

PI: G. R. Odette and Takuya Yamamoto, University of California-Santa Barbara

Collaborators: None

Project Number: 07-069

Project Start Date: August 2007

Project End Date: July 2010

Research Objectives

The objective of this research is to further the development of high-performance fuel cladding, duct, and internal structural material systems for a variety of future fission reactors, including advanced fast burner reactors envisioned in the Global Nuclear Energy Partnership (GNEP), Generation IV (GEN IV), and Advanced Fuel Cycle Initiative (AFCI) programs. The objective for alloy performance centers on attaining a combination of 1) high-temperature creep strength, 2) thermal and radiation stability and resistance to other sources of in-service degradation permitting long lifetime (high burn-up) operation to doses of 200 displacements per atom (dpa) or more, 3) corrosion resistance and compatibility in advanced reactor coolant environments, 4) a good balance of mechanical properties, and 5) favorable neutronic characteristics and life cycle costs.

Achieving these ambitious objectives in a practical alloy system requires a combination of alloy design optimization, closely coupled with the development of compatible processing, fabrication, and joining paths. Research will focus on a newly developing alloy class that has shown a very high promise of achieving all of these objectives—nano-structured dispersion strengthened ferritic alloys (NFAs). The proposed work consists of the following tasks:

- ***Developing a Deformation Processing Database***, which involves a science-based approach to dealing with a major current limitation in directionally worked product forms in NFAs which have anistropic microstructural and strength properties; constructing a deformation database that will map out recrystallization regimes that lead to more isotropic behavior; and examining strain, strain rate, and temperature regimes that may allow superplastic deformation resulting in fine, stable grain structures that can be optimized for creep strength and a good balance of properties
- ***Solid State Joining***, which includes mapping regimes of efficient diffusion bonding guided by the understanding previously developed for the thermal stability of NFA microstructures, including the nm-scale strengthening features
- ***Alternative Alloys and Alloy Optimization***, which involves a semi-combinatorial approach to optimizing NFA compositions to enhance a variety of performance indices, such as corrosion resistance, as well as exploring new approaches to utilizing $\gamma-\alpha$ phase transformation routes to achieving equiaxed microstructures to reduce the strength and fracture toughness penalties associated with dispersion strengthened martensitic steels
- ***Identification and Optimization of the Nanometer-sized Feature (NF)***, which involves filling a missing element in alloy design, namely the basic character of the nanofeatures in NFA, thus providing a basis of understanding for property optimization
- ***Target of Opportunity Irradiations, Post-Irradiation Examinations, and Modeling,*** which includes additional best effort mechanical testing to provide additional low-cost information of the use of NFAs in severe nuclear environments; modeling

Research Progress

NFAs are processed by ball milling to mechanically alloy (MA) metallic iron-chromium-titanium-tungsten (Fe-Cr-Ti-W) powders with Y_2O_3, effectively dissolving the yttrium (Y) and oxygen (O) into the ferrite matrix. Hot extrusion or hot isostatic pressing (HIP) precipitates the dissolved Y,

O, and Ti as 2-6 nm sized features or complex oxide phases. One challenge facing NFA development is producing a uniform dispersion of Ns, which is responsible for the material's remarkable high-temperature properties and radiation damage resistance. The non-uniformity results in grain growth and dislocation recovery in regions of low NF concentrations, producing a bimodal grain size. The objective of the current research is to systematically investigate mechanical ball milling and alloying processes to optimize the NF distribution. The milling conditions investigated include changing ball mass to charge ratio, ball diameter, milling time, elemental powder sizes, and the milling order and procedure.

Scanning electron microscopy (SEM) characterization of the grain structure is used as an indirect measurement of NF distribution; large grains (>1 micron) representing areas of low NF concentration and small grains (<1 micron) representing areas of high NF concentrations. Each SEM sample is prepared using the following sequence of steps. First, a pre-alloyed, rapidly solidified Fe14Cr3W0.4Ti powder is mechanically alloyed with Y_2O_3 powder using a SPEX shaker mill. The powder is subsequently annealed at 1,150°C in dry helium (He) and mounted in a phenolic conductive polymer. After polishing, the powder is etched using a 3:1:1 solution of hydrochloric, nitric, and acetic acids to reveal the grain structure. The area fraction of small grains and large grains is evaluated to determine the effect of milling parameters on the NF distribution. Large grains are outlined in blue and regions of small grains are outlined in green and red. Red labels the region of small grains whose size can be easily determined and green signifies rough-appearing areas whose grain boundaries are not easily distinguished. An example showing an SEM image and equivalent red-green-blue (RGB) grain designation image is shown in Figure 1.

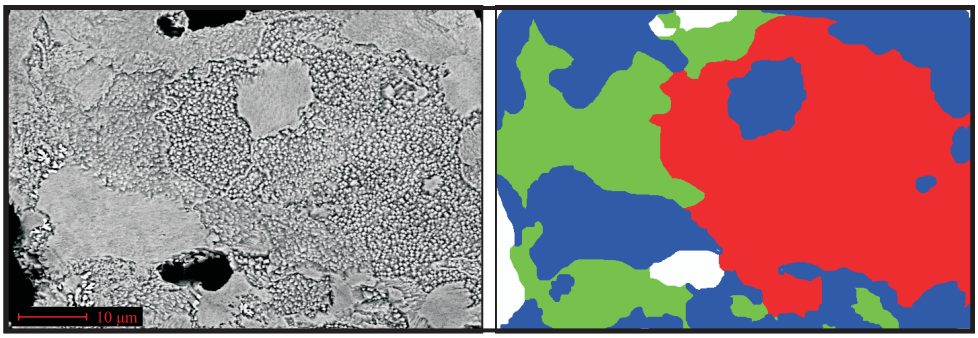

Figure 1. Left: SEM image of etched powder particle; Right: RGB image designating large and small grain areas.

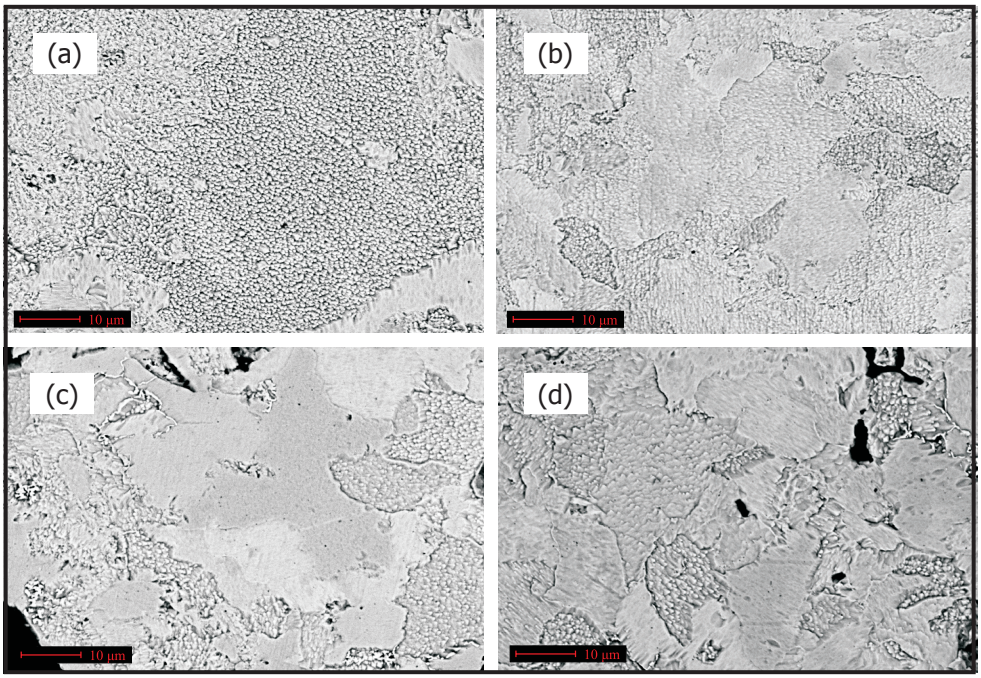

Figure 2. (a) 5:1 ball mass to charge ratio; (b) 5 hour increment mill with yttria additions; (c) Re-mill-anneal of pre-milled-annealed powder; (d) 15:1 ball mass to charge ratio using 50g of 8 mm and 100g of 11 mm diameter balls.

Each mechanically alloyed powder is a variant of the following baseline milling condition: 10g of -100 +300 mesh pre-alloyed, rapidly solidified Fe14Cr3W0.4Ti powder blended with 0.03g of <10 µmY_2O_3 powder; 10:1 ball mass to charge ratio; 9.5 mm diameter hardened steel milling balls; and 10 hours of continuous mill. The milling matrix explored to date is shown in Table 1. A check mark (✓) indicates that the powders have been mechanically alloyed, and the number in parenthesis indicates the small grain fraction observed for the conditions that have been fully characterized. Many of the samples have been milled and their grain structure measured, but further analysis is required to determine the small grain fraction.

The SEM images in Figure 2 qualitatively demonstrate that different milling parameters have significant effects on the grain structure of NFAs. Preliminary results show that smaller milling balls and lower ball mass to charge ratios

Mass/Charge Ratio		Milling Time		Ball Diameter	
✓	5:1 (.74)	✓	8 h	✓	6 mm
✓	15:1	✓	12 h	✓	8 mm (.76)
		✓	14 h	✓	11 mm (.44)
		✓	16 h		
		✓	30 h		

Mixed Milling Ball Sizes	
✓	6 mm and 8 mm (50g/50g)
✓	8 mm and 11 mm (50g/50g)
✓	8 mm and 11 mm (50g/100g) (.57)
✓	8 mm and 11 mm (50g/100g) 2 h increment (.55)

Milling Sequence	
✓	Remove-declump material from canister walls in 5 h increments
✓	Remove-declump material from canister walls in 2 h increments
✓	Remove-declump material from canister walls with two 0.015g yttria additions in 5 h increments (.74)

Miscellaneous	
✓	< 1 micron Y_2O_3 powder
	-100 +325 mesh W elemental powder
	1-5 micron W elemental powder
	-60 +100 mesh Ti elemental powder
	-325 mesh Ti elemental powder
✓	Re-milling/annealing pre milled-annealed powders
✓	Milling higher Y_2O_3 concentration with Fe14Cr3W0.4Ti and diluting in 2 h increments (.55)

Table 1. Milling matrix.

increase the small grain area fraction. Periodic removal of clumped material from the canister walls during milling and incremental additions of Y_2O_3 also produce a higher fraction of small, nm grains compared to the baseline process.

The research team has been preparing a small batch of NFA with Al additions to improve their corrosion resistance as part of a collaborative effort with Los Alamos National Laboratory (LANL). Consolidated alloys will be provided to LANL in early 2008.

Finally, small angle neutron scattering (SANS) and local electrode atom probe (LEAP) tomography studies have been carried out on various NFAs to identify the character of the NF.

Planned Activities

The baseline ball milling matrix will be completed and the combination of the most promising methods will be explored to optimize the NF and grain size distribution. Additional studies will include MA in hydrogen (H) and cryomilling. The optimized consolidated powders will be characterized by a variety of microstructural techniques, including SEM, transmission electron microscopy (TEM), and SANS. The strength and toughness of the optimized alloys will also be characterized.

Studies of thermo-mechanical processing to mitigate microstructural-mechanical property anisotropy in extruded NFAs will be initiated in early 2008. These studies will map the relation of deformation temperature, strain rate, strain, annealing time, and temperature regimes to grain structures to identify routes, including superplastic deformation that result in fine, stable isotropic grain structures, optimized for creep strength and a good balance of properties.

Diffusion bonding studies on MA957 will also be initiated in early 2008.

Nuclear Energy Research Initiative

A Research Program on Very High-Temperature Reactors (VHTRs)

PI: Sudarshan Loyalka, University of Missouri-Columbia

Collaborators: North Carolina State University (NCSU), Washington University-St. Louis

Project Number: 08-043

Project Start Date: September 2007

Project End Date: September 2010

Project Description

Prismatic and pebble bed VHTRs are very attractive both from a thermodynamic efficiency viewpoint and hydrogen-production capability. This project addresses numerous challenges associated with the VHTR fuel cycle, materials, and complex fluid dynamics and heat transfer. The effort will also lead to graduate student research training at the participating universities and possible practicums on VHTR technology at the national laboratories.

Workscope

Consortium members will perform the following tasks in support of this project:

- Conduct physical experiments for fission product transport phenomena in the overcoating and compact structural graphite and transport through TRISO coating layers
- Develop improved sorption measurement techniques to measure the accumulation of condensable radionuclides ("plateout") in the VHTR primary coolant circuit; obtain representative data
- Develop advanced computations of charged, radioactive dust (aerosol) transport in the VHTR coolant circuit and confinement by exploring DSMC techniques for deposition and resuspension; conduct experiments to verify computational predictions
- Develop a program to measure emissivity for various VHTR component materials, both bare and oxidized, and obtain extensive data
- Develop an experimental program to characterize gas, fission product, and particle flows in the complex geometries of PBMRs and help improve computational approaches and computer programs through experimental understandings

Nuclear Energy Research Initiative

Cladding and Structural Materials for Advanced Nuclear Energy Systems

PI: Gary S. Was, University of Michigan

Collaborators: Alabama A&M University, Pennsylvania State University, University of California-Berkeley, University of California-Santa Barbara, University of Wisconsin-Madison

Project Number: 08-055

Project Start Date: September 2007

Project End Date: September 2010

Project Description

The goal of this consortium is to address key materials issues in the most promising advanced reactor concepts that have yet to be resolved or that are beyond the existing experience base of dose or burnup. The research program consists of three major thrusts: 1) high-dose radiation stability of advanced fast reactor fuel cladding alloys, 2) irradiation creep at high temperature, and 3) innovative cladding concepts embodying functionally-graded barrier materials.

Following are the objectives of this research:

- Develop an understanding of the high-dose radiation stability of candidate sodium fast reactor (SFR) cladding and duct alloys under the expected range of temperatures and dose, using a closely integrated program that combines targeted charged particle and neutron irradiation, in-situ irradiation, and computer simulation of defect microstructure
- Determine the stability of oxide dispersion strengthened (ODS) steel and ultrafine, precipitation-strengthened (HT-UPS) austenitic steel
- Characterize and understand the mechanisms for irradiation creep in silicon carbide (SiC) in TRISO fuel, ferritic-martensitic (F-M) alloys, and ODS and HT-UPS steels
- Develop barrier layers for protection of F-M alloys from fuel-clad chemical interaction and of Alloy 617 from attack by coolant impurities in the intermediate heat exchanger of the Very High-Temperature Reactor
- Develop modeling tools to explain the behavior of F-M steels under irradiation, and predictive tools to extend the reach of understanding beyond the experimental database

Beyond scientific achievements, this consortium is expected to provide substantial long-term benefits that will be crucial for success of the advanced reactor program, including establishing pathways for the incorporation of data into the ASME codes and standards.

Workscope

The major tasks comprising this program are as follows:

- High-dose radiation stability of advanced fast reactor fuel cladding and structural materials
  1) Formation and characterization of irradiated microstructures
  2) In-situ ion irradiation
  3) Simulation and microstructure evolution
  4) Characterization of neutron irradiation effects
- Irradiation creep at high temperatures
  1) Irradiation creep of candidate materials for high-temperature application
  2) Transmission electron microscopy study of the creep and strengthening mechanisms
- Innovative cladding concepts embodying functionally graded barrier materials
  1) Barrier layer process development
  2) Barrier layer durability

Nuclear Energy Research Initiative

6.2 Advanced Fuel Cycle Research and Development

There are 50 NERI research projects currently being performed that closely relate to the research goals of the Advanced Fuel Cycle R&D program: 17 awarded in FY 2005, 13 awarded in FY 2006, 12 awarded in FY 2007, and 8 new NERI-C projects in FY 2007.

As described in Section 3, AFCI is a wide-ranging research and development program whose mission is to develop and exhibit technologies that facilitate the conversion to an environmentally, socially, politically, and economically acceptable advanced fuel cycle. The chief goals are to 1) achieve a significant reduction in the amount of toxic and heat producing high-level radioactive waste requiring geologic disposal, 2) significantly reduce accumulated plutonium in commercial spent fuel, and 3) extract more useful energy. This will be accomplished by developing advanced fuel, cladding, waste forms, separations, and disposal technologies that separate long-lived, highly radiotoxic material and facilitate their recycle, allowing the recovery of valuable energy from the spent fuel.

During FY 2007, a number of research projects targeted the separation of actinides and lanthanides by several techniques (aqueous process with redox, aqueous process with soft donor atoms, and UREX+). Much work is taking place in the advanced fuel development area. Projects involve analytical studies and modeling techniques, developing and optimizing materials, developing fuel processing and fabrication techniques, and improving fuel coatings. Transmutation projects are targeting alloys for the ABR, TRU transmuters, and minor actinide recycling with boiling water reactors. Systems analysis projects are developing and optimizing computer models for fuel cycle analysis, using those codes to evaluate different scenarios, and conducting fuel cycle economic evaluations. Two new projects are improving SFR simulation methodology and measurement techniques.

In FY 2007, the program was refocused to support R&D on the most promising technologies developed to date. Under GNEP, DOE tested the UREX+ separations process and designed an Advanced Fuel Cycle Facility for R&D on advanced separations and fuel manufacturing technologies. Over the course of the year, NE collaborated with international and private parties to refine GNEP and gauge interest in a demonstration of sodium-cooled reactor technology, which would serve as the fast ABR.

Planned NERI research efforts under the newly awarded FY 2007 consortia projects related to the AFCI program will focus on separations systems and analysis; fuel performance, measurements, and radiation effects; risk informed analysis and computational tools; and small export reactors.

An index of the research being performed under this program follows, along with a summary of each project.

Nuclear Energy Research Initiative

Project Summaries and Abstracts

FY 2005 Project Summaries

FY 2006 Project Summaries

NUCLEAR ENERGY RESEARCH INITIATIVE

FY 2007 Project Summaries

FY 2007 NERI-C Project Abstracts

Nuclear Energy Research Initiative

Nuclear Energy Research Initiative

Determination of Basic Structure-Property Relations for Processing and Modeling in Advanced Nuclear Fuels: Microstructure Evolution and Mechanical Properties

PI: Pedro D. Peralta, Arizona State University

Collaborators: Los Alamos National Laboratory (LANL)

Project Number: 05-001

Project Start Date: March 2005

Project End Date: March 2008

Research Objectives

The objective of this project is to investigate a strategy for fuel development based on experimental work on surrogate materials. Fuel development under the Global Nuclear Energy Partnership (GNEP) and the Advanced Fuel Cycle R&D (AFCI) program will rely heavily on modeling physical mechanisms to predict performance, rather than on conducting direct experimentation on nuclear materials or on empirical relationships derived from experimental data. In this project, researchers will study the structure-property relationship of nitrides and oxides in solid solutions using surrogate elements in order to simulate the behavior of inert matrix fuels, emphasizing zirconium-based materials. The goals are to 1) provide insight into processing fuel that has better performance and greater structural reliability during manufacturing and service and 2) develop structure-property relations that can be used as input for fuel performance models.

Researchers will explore three key aspects of these materials: 1) microstructure, measured through global texture evolution and local crystallographic variations; 2) mechanical properties (including fracture toughness, compression strength, and hardness) as a function of load and temperature; and 3) structure-property relations. This research will use crystallographic information to evaluate fuel performance and incorporate statistical variations of microstructural variables into simplified models of the mechanical behavior of fuels.

Following are the primary tasks of this project. In conjunction with these activities, the research team will also carry out work with actual fuel materials.

- Develop processing procedures for pellet fabrication and characterize their properties
- Establish appropriate plutonium (Pu) surrogates, fabricate samples, and optimize processing
- Translate techniques from surrogate processing to actual fuel; fabricate and characterize
- Establish models for high-temperature behavior, characterize properties, perform testing and analysis

Research Progress

Microstructure plays an important role on the thermomechanical behavior of materials typically used for nuclear fuels; therefore, the characterization of this microstructure and the formulation of models of fuel behavior that account explicitly for it are of particular interest to further the current understanding of fuel behavior. Current efforts of this project are concentrated on 1) continuing work towards optimizing the microstructure and mechanical properties of sintered zirconium nitride (ZrN) and (Zr,Ti)N in order to investigate the effects that sintering temperatures and composition have on structural integrity and 2) translating characterization and modeling techniques developed for ZrN to oxides, particularly yttria stabilized zirconium oxide (YSZ), which is a potential material to be used as a matrix for inert and low fertility fuels.

Uniaxial compression testing was performed on ZrN and (Zr,Ti)N pellets sintered at either 1,375°C, 1,475°C, or 1,600°C. Testing was performed in an ultra-high purity argon (Ar) atmosphere at two temperatures: 25°C and 800°C. Post-Mortem fractography was performed using scanning electron microscopy (SEM) as shown in Figures 1 and 2. In most cases, elevated temperature testing resulted in the following: a reduction in compression strength by nearly 50 percent, an increase in compressive strain, and an introduction of non-critical cracking prior to catastrophic failure as compared to "identical" samples tested at

room temperature. It was determined that (Zr,Ti)N solid solution samples have similar or higher specific strength (strength divided by density) when tested at intermediate temperatures as compared to pure ZrN samples due to their smaller grain size, higher porosity, and increased crack arrest mechanisms and elastic energy dissipation sites. In addition, researchers performed compression testing of YSZ samples which were either sintered conventionally or with a mixed mode microwave (MMMW) sintering technique at both 25°C and 800°C. Initial analysis indicates a 40 percent increase in compressive ultimate strength of the MMMW sintered samples compared to conventionally sintered samples when tested at 800°C.

Hardness values in ZrN and (Zr,Ti)N solid solutions display the same trends observed during compression tests. Hardness values were lowest for samples sintered at the lowest temperature (1,375°C), peaked at intermediate temperatures (1,475°C), and decreased for pellets sintered at high temperatures (1,600°C). This was attributed to the following: low densities at lower temperatures for the low hardness, the achievement of peak density and small grain size at the intermediate temperature for the largest hardness value, and the larger grain size and longer intergranular cracks at the higher temperature for the decrease in hardness. Hardness testing as a function of position indicated a slight tendency for hardness to be heterogeneous, with values changing between the center and the edges of the pellets, which can be attributed to wall and edge effects during cold pressing and sintering.

Proof-of-principle secondary electron imaging and orientation imaging microscopy (OIM) measurements were carried out on sintered pellets of cubic ZrO_2 to establish appropriate electron microscopy procedures to perform measurements in sintered YSZ pellets as well as depleted uranium oxides without the need to coat the samples or use low-vacuum imaging techniques (e.g., water vapor).

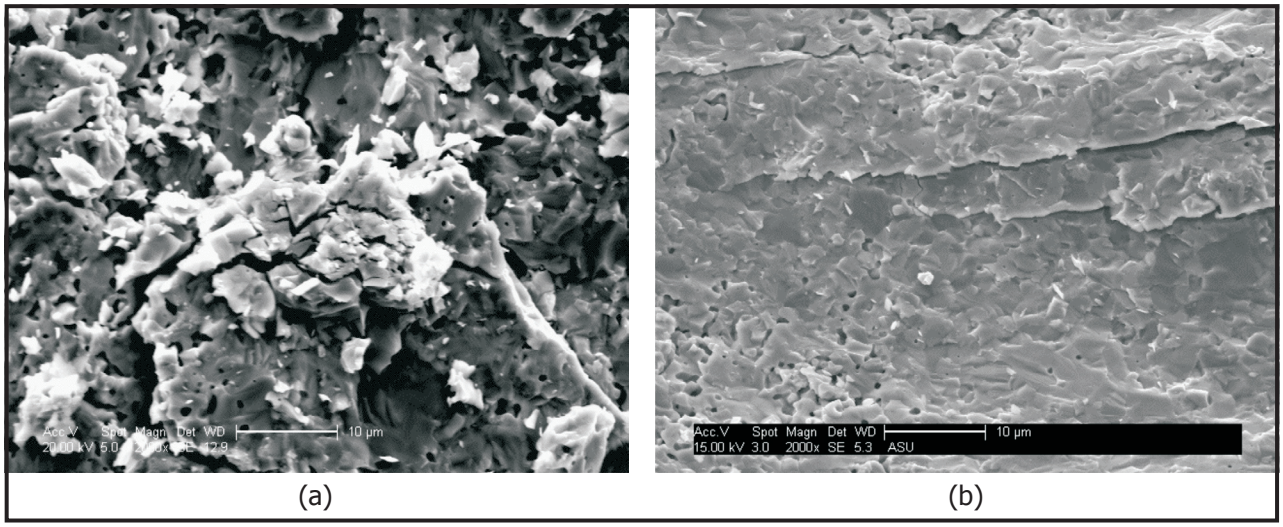

Figure 1. Compression test fracture surface of 1,475°C (Zr,Ti)N: (a) 25°C test, 2,000x, 10µm scale; (b) 800°C test, 2,000x, 10µm scale.

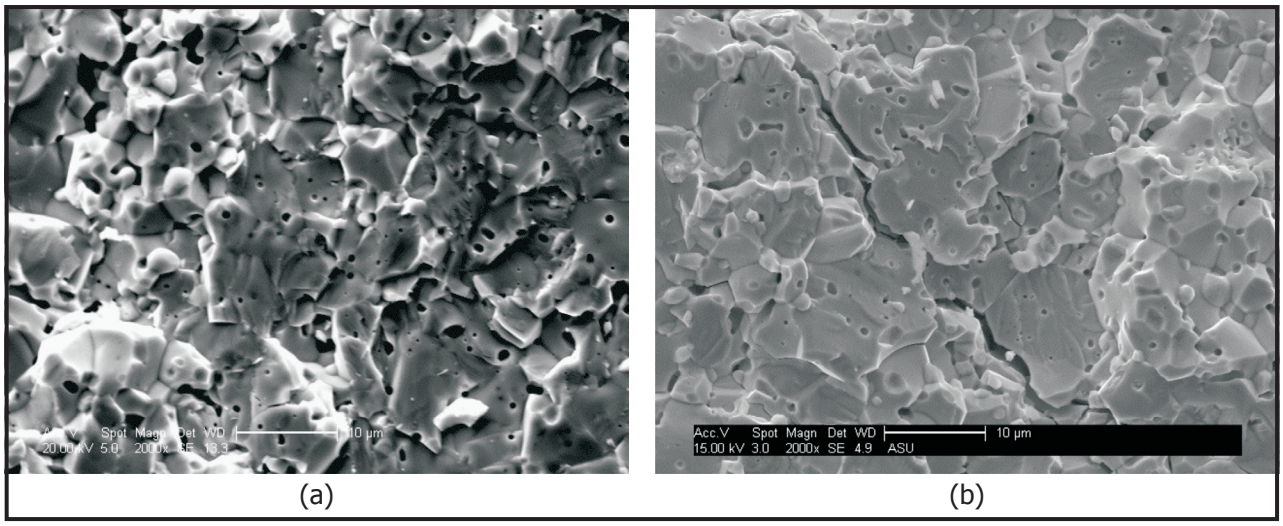

Figure 2. Compression test fracture surface of 1,475°C ZrN: (a) 25°C test, 2,000x, 10µm scale; (b) 800°C test, 2,000x, 10µm scale.

Pertaining to modeling efforts, a serial sectioning technique was used to develop a three-dimensional (3D) representation of the microstructure of a dense ZrN pellet sintered in Ar at 1,600°C. Twenty-five two-dimensional (2D) images of the microstructure obtained by imaging with an optical microscope at 200X (slides spaced 2μm apart from each other) were used as a basis for reconstructing the 3D microstructure of the ceramic for modeling using Finite Elements (FE). This representation allows the quantification of the spatial distribution of porosity in the samples as well as the creation of a 3D finite-element model (FEM) that accounts for the presence of pores. Also, another model was obtained using 3D Computer Aided Design (CAD) software to observe stress-strain behavior of the reconstructed volume subjected to tensile stress and to look at critical regions of interest (Figure 3). Correlations of the 3D models with existing 2D models and experimental results obtained at LANL show that the pellet density is very well correlated between the 2D, 3D, and experimental results. What can also be seen is that the highest concentration of stress occurs at the grain boundaries in both 2D and 3D models.

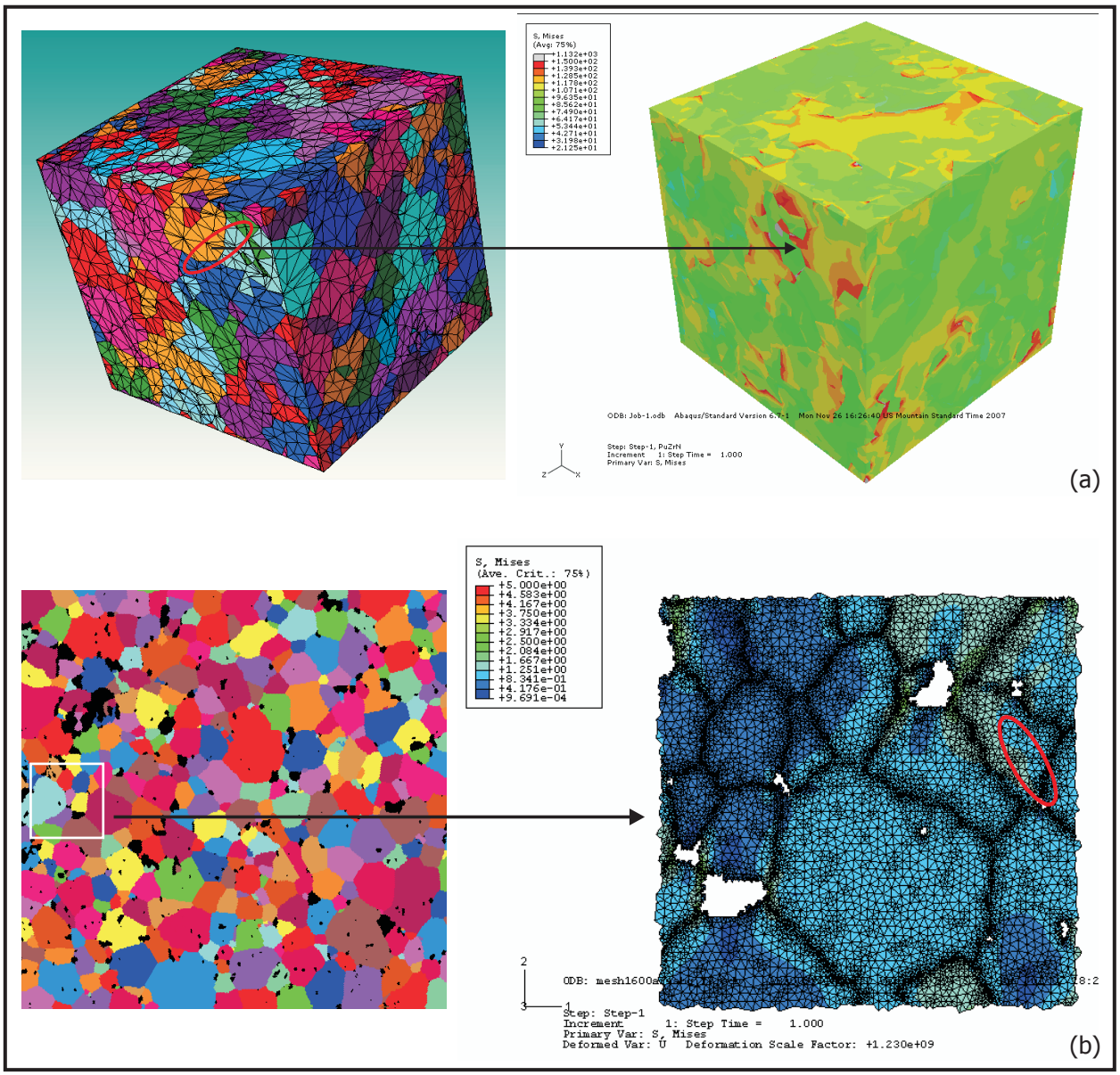

Figure 3. Von Misses Stresses for (a) 3D and (b) 2D model for uni-axial stress simulation.

Planned Activities

Pertaining to characterization efforts, the time remaining for this project will be devoted to high-temperature (1,200°C+) compression testing of ZrN, (Zr,Ti)N, and YSZ pellets to conclude the temperature dependent testing. Transmission electron microscopy (TEM) is currently being performed on fractured ZrN and (Zr,Ti)N compression samples in order to see if dislocation motion is a contributing factor of elevated temperature compressive failure. In addition, a study has begun that will attempt to establish mechanical properties of ZrN sintered at 1,600°C on a sub-micron scale with respect to specific crystallographic grain orientations. Nano-indentation will be used to determine plasticity variations and make small cracks in different grains of a dense ZrN sample for chosen grain orientations. Grain selection was based on crystallographic orientation determined via electron backscatter diffraction (EBSD), and micromachining of fiducial marks on the sample was performed via focused ion beam (FIB) in order to find a desired location using atomic force microscopy (AFM).

The continuation of modeling efforts will include using the 3D modeling techniques that have been developed while working with ZrN, and developing a model of an YSZ pellet sintered at 1,500°C using both conventional and MMMW sintering techniques. Technique refinements will include using a FIB to mill and image each layer of the microstructure in the hopes of speeding up and refining the serial sectioning process. Initial FIB-based serial sectioning work indicates that high-quality serial section layers as small as approximately 40 nm are possible on non-conductive samples such as YSZ and should also be possible on depleted uranium oxide samples as well.

Nuclear Energy Research Initiative

The Application of Self-Propagating High-Temperature Synthesis (SHS) to the Fabrication of Actinide-Bearing Nitride and Other Ceramic Nuclear Fuels

PI: John J. Moore, Colorado School of Mines

Collaborators: Idaho National Laboratory (INL)

Project Number: 05-013

Project Start Date: January 2005

Project End Date: December 2008

Research Objectives

The major research objective of this project is to determine the fundamental self-propagating high-temperature synthesis (SHS) processing parameters for ceramic fuel materials. Researchers will first use manganese (Mn) as a surrogate for americium (Am) to produce dense Zr-Mn-N ceramic compounds. They will then transfer these fundamental principles to the production of dense Zr-Am-N ceramic materials at INL.

Due to the high vapor pressures of Am and americium nitride (AmN), there is concern about producing nitride ceramic nuclear fuels containing Am. Sintering results in retention problems of Am and adversely affects the synthesis of a consistent product with desirable homogeneity, density, and porosity. Similar difficulties experienced during laboratory-scale process development for producing metal alloys containing Am have led researchers to abandon compact powder sintering methods and to investigate other synthesis methods, such as SHS.

A further objective of this research program will be to generate fundamental SHS processing data for the synthesis of Pu-Am-Zr-N and U-Pu-Am-N ceramic fuels, again using surrogate materials first. Cerium (Ce) will be substituted for plutonium (Pu), Mn for Am, and depleted uranium (DU) for uranium (U). The sequence for SHS synthesis of these ceramic fuels will be as follows:

Pu-Am-Zr-N, using Ce as the surrogate for Pu and Mn as the surrogate for Am:

1) $(Ce_{0.5}Mn_{0.5})N$
2) $64wt\%[(Ce_{0.5}Mn_{0.5})N]$-$36wt\%ZrN$

U-Pu-Am-N, using DU as the surrogate for U, Ce as the surrogate for Pu, and Mn as the surrogate for Am:

1) $(DU_{0.5}Mn_{0.5})N$
2) $(DU_{0.5}Ce_{0.25}Mn_{0.25})N$

As before, once sufficient fundamental data have been determined for these surrogate systems, the results will be transferred to INL for synthesis of Pu-Am-Zr-N and U-Pu-Am-N ceramic fuels.

Research Progress

Researchers have produced zirconium (Zr), Mn, and nitrogen (N) compounds and initiated the quantification of Mn losses using an Induced Coupled Plasma (ICP) process. Minimal to no loss of Mn is expected. They have begun investigating the production of lanthanide-nitrides as surrogates for actinide-nitrides, considering praseodymium (Pr) as a potential surrogate for Am, Ce for Pu, and DU for U. They will utilize a densification process with a Gleeble 1500 as a preliminary step to using an induction hot press.

Manganese nitride (Mn_3N_2) powder has been made by employing auto-ignition combustion synthesis. The powder that is produced will be used in the production of dense nitride pellets. Researchers have optimized the time and temperature for the reaction. Further work is being conducted to optimize and to expand the process in order to produce lanthanide-nitrides as surrogates for actinide-nitrides using the elements stated above. Efforts are also underway to maximize the conversion to nitride powder and remove impurities from the powder.

Researchers have nearly completed the laboratory setup to accommodate DU experimentation following completion of the Zr, Mn, and N reactions. For the next phase, they will use Pr as a surrogate for Am and dysprosium (Dy) for Pu in the DU experimentation to produce homogeneous pellets. Various fuel chemistries will be incorporated to demonstrate flexibility in the process.

Planned Activities

Following is a synopsis of the tasks the team plans to conduct over the next period:

- Initiate additional surrogate studies using Pr and Dy
- Optimize auto-ignition combustion synthesis (AICS) production of Mn-N, Pr-N, and Dy-N powders
- Optimize SHS-consolidation of dense Zr-Mn-N compounds
- Optimize Am-N and Zr-Am-N SHS systems
- Conduct differential thermal analysis (DTA) of Am-N and Zr-Am-N SHS systems
- Optimize SHS-consolidation of Zr-Am-N systems

Nuclear Energy Research Initiative

Minor Actinide Doppler Coefficient Measurement Assessment

PI: Nolan Hertel, Georgia Institute of Technology (Georgia Tech)

Collaborators: Education, Research and Development Association of Georgia Universities; Los Alamos National Laboratory (LANL)

Project Number: 05-024

Project Start Date: April 2005

Projected End Date: December 2007

Research Objectives

The objective of this project was to assess the viability of measuring the Doppler coefficient of reactivity in minor actinides (MAs). Using a series of calculations, the researchers estimated the change in reactivity resulting from a change in the operating temperature of small quantities (approximately 1-10 grams) of pure MAs. The team used this data to design experiments for measuring Doppler coefficients.

As part of the Advanced Fuel Cycle R&D (AFCI) program, transmutation of waste using advanced fast reactors and accelerator-driven systems have shown the ability to reduce the amount of plutonium (Pu) and transuranic (TRU) materials for disposal. In order to conduct safety assessments of transmutation systems for fuel with significant MA content, researchers require the Doppler coefficients for each isotope. Several isotopes of Pu, neptunium (Np), americium (Am), and curium (Cm) were studied, including Np-237, Pu-239, Pu-238, Pu-241, Am-242m, Am-243, Am-241, and Cm-244.

Using the radiation transport code MCNP5, researchers performed extensive scoping calculations as a function of five parameters: 1) isotope, 2) sample quantity, 3) operating temperature, 4) critical assembly, and 5) data library. With these calculations, they determined the quantity of MA material needed to cause a 10^{-5} change in reactivity due to a 200°C change in sample temperature (e.g., from 800 to 1,000°C). They used the resulting data to develop experiments for measuring the Doppler coefficient of each isotope. For this work, the team used the FLATTOP and COMET assemblies at the LANL Critical Experiments Facility.

Research Progress

The initial phase of the project was designed to run a total of 960 individual MCNP calculations to determine the viability of the critical assemblies in question. The first step was to create Doppler broadened cross section for each of the eight isotopes at the temperatures of 800, 900, 1,000, and 1,100°C from the latest versions of the ENDF/B, JEFF, and JENDL cross sections. These new Doppler-broadened cross sections were created using the NJOY computer code. Initially, it was thought that the FLATTOP assembly would be the assembly to conduct the experiments on, and initial calculations were made to determine the possible mass ranges for each of the eight isotopes. The ranges determined for the FLATTOP assembly were between 6 and 22 grams for Np-237 and Pu-239 and between 2 and 18 grams for the other six. Using the determined ranges and the Doppler-broadened cross section sets, an entire suite of 120 calculations for the ENDF/B cross sections were made. However, due to the fast spectrum of the FLATTOP assembly, it was not possible to statistically determine a Doppler coefficient for any of the isotopes.

For the second phase of the project, the scope of the remaining calculations was limited to determining the viability of using the COMET assembly for Np-237, Pu-239, Pu-241, and Am-241 for the latest resonance cross section data only. Since there are several possible configurations for the COMET assembly, calculations were made to compare the neutron spectrum for the advanced burner reactor (ABR) for various configurations. Calculations were made using several highly enriched uranium (HEU)/Graphite and HEU/Iron configurations of the Zeus critical experiment series.

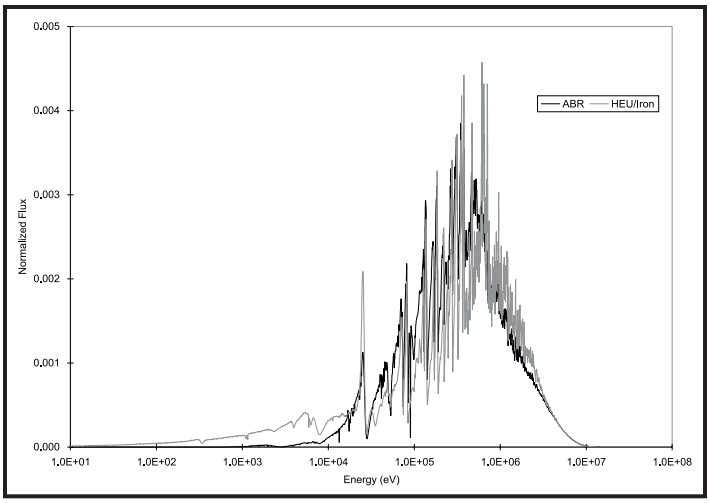

Figure 1. Normalized ABR spectrum versus HEU/Iron spectrum.

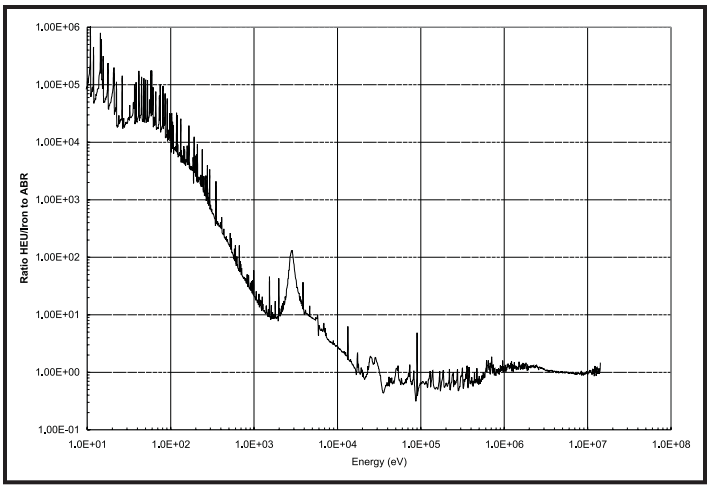

Figure 2. Ratio of HEU/Iron spectrum to ABR spectrum.

The normalized neutron flux spectrum results from various HEU/Graphite and HEU/Iron configurations were compared to the normalized spectrum for the ABR. The HEU/Iron configuration that was the closest match in the resonance and fast energy range consisted of 11 fuel units. Each fuel unit consisted of a 19.05 cm radius x 0.30 cm thick fuel plate stacked between four 0.30 cm thick iron plates and one 0.30 cm thick polyethylene plate. Figure 1 displays the calculated ABR spectrum versus the calculated HEU/Iron spectrum while Figure 2 displays the ratio between the two spectrums. It is noted that there are large differences between the spectrums under 1E4 eV; however, the neutrons in this range represent less than 10 percent of the total.

After determining the configuration on the COMET assembly, initial scoping calculations were run to determine the 2 or 3 masses to run the final calculations for the four isotopes. From these scoping calculations, the masses were set at 6, 14, and 22 g for Pu-239 and Np-237 and 2, 10, and 18 g for Pu-241 and Am-241. With the determined masses, 24 input files were created using three different masses and two different temperatures for each of the four second-phase isotopes. At the end of FY 2007, 14 of these final input files were run on clusters at Georgia Tech.

Planned Activities

This project is complete. During the final months, the remaining 10 COMET assembly input files were run and the data analyzed to determine if the COMET assembly could be used for Doppler coefficient measurements.

NUCLEAR ENERGY RESEARCH INITIATIVE

Plutonium Chemistry in the UREX+ Separation Processes

PI: Alena Paulenova, Oregon State University

Collaborators: Argonne National Laboratory (ANL), University of Nevada-Las Vegas (UNLV)

Project Number: 05-062

Project Start Date: April 2005

Project End Date: March 2008

Research Objectives

The objective of this project is to examine the chemical speciation of plutonium (Pu) in the UREX+ (uranium/tributyl phosphate) extraction processes for advanced fuel technology. Researchers will analyze the change in speciation of Pu in aqueous and organic phases and incorporate kinetic and thermodynamic data into existing computer modeling codes. The research team will examine the different oxidation states of Pu to find the relative distribution between the aqueous and organic phases under various conditions, such as different concentrations of nitric acid, total nitrates, acetohydroxamic acid, or actinide ions. Researchers will also utilize several spectroscopic techniques, including x-ray absorbance spectroscopy and small-angle neutron scattering, to determine Pu and uranium speciation in all separation stages.

The following tasks have been accomplished during this reporting period:

- The experimental work on distribution ratios of Pu(IV) as a temperature dependence was initialized for a range of different concentration ratios of acid:salt (HNO_3:$LiNO_3$).
- The team has employed eight different ratio systems with a constant nitric acid, varied nitrate, with and without acetohydroxamic acid (HAHA), and at four different temperatures (Task II).
- UV-Vis-nIR spectra of Pu(IV) in the nitric acid/tri-n-butylphosphate (TBP) extraction phases relevant to the UREX-process at 25°C has been collected (Task II).
- The modeling program, FITEQL, has been employed to model the speciation of Pu(IV) using extraction and spectroscopic data (Task III).
- With the assistance of collaborators from ANL, the measured data were incorporated into the AMUSE code prior to the summer 2007 demonstration experiment; modeling work continues, incorporating the temperature factor to the AMUSE code (Task III).

Research Progress

Extraction of Pu(IV) in the presence of HAHA. Figure 1 displays the sharp decrease of extraction yields of tetravalent plutonium (Pu-239) from 1 M HNO_3 by 1.1 M TBP (30 volume percent) in *n*-dodecane upon the addition of HAHA. A very small addition of HAHA rapidly reduces extraction yields of Pu due to the formation of a strong Pu-acetohydroxamate complex in the aqueous solution. At a concentration of [HAHA]>0.1 M, extraction yields of Pu decrease slightly. Even at [HAHA] = 0.8 M, a still reasonable amount of Pu is extracted to the organic solvent. The extracted Pu species are believed to be solvates of plutonium tetranitrates and ternary plutonium-acetohydroxamato-nitrates $[Pu(AHA)_x(NO_3)_{4-x}].(TBP)_2$. A similar co-extraction of uranyl-acetohydroxamato-nitrates and molybdenyl-acetohydroxamato-chlorides solvated with tributyl phosphate was also observed.

Speciation of Pu(IV) in aqueous phase. The speciation of Pu(IV) (Pu-242, 2.26×10^{-3}M) was investigated spectroscopically for 1 M nitric acid and various concentrations of acetohydroxamic acid (2.5×10^{-4}-0.8)M HAHA using Vis-NIR Ocean Optics spectrometer. To study the speciation of Pu with acetohydroxamic acid under acidic conditions (HNO_3), hydrolytic degradation of HAHA and the reduction of Pu(IV) to Pu(III) by HAHA should also be considered. As shown earlier, the reduction of Pu(IV) to Pu(III) by HAHA is very slow and several hours are needed for complete reduction; therefore, during the short time period (2-3 minutes), the effect of hydrolysis

of HAHA on the stability of Pu(IV)-acetohydroxamato-nitrates under acidic conditions is negligible. However, to minimize changes of conditions due to hydrolytic and redox reactions, all Vis-NIR spectra were taken immediately after the addition of HAHA.

Addition of acetohydroxamic acid to the aqueous solution of Pu(IV) leads to the formation of Pu-acetohydroxamate species and significant changes in absorption spectrum in the Vis-NIR region. In general, complexation of Pu(IV) by acetohydroxamic acid in the nitric acid matrix can be expressed as the following:

(1) $Pu(IV) + xHAHA + yNO_3^- = [Pu(AHA)_x(NO_3^-)_y]^{(4-x-y)+} + xH^+$

where HAHA denotes protonated (non-dissociated) acetohydroxamic acid. For conditions where [Pu(IV)] and $[HNO_3]$ are constant, it can be assumed that the variations in absorbance are attributed to the variation in the Pu(IV) distribution among $[Pu(IV)]_{free}$ (non-complexed with HAHA) and Pu(IV)-mono-, di-, and tri-acetohydroxamate species. The mass balance for total concentration, $[Pu(IV)]_{tot}$, in aqueous solution is then written as the following equation:

(2) $[Pu(IV)]_{tot} = [Pu(IV)]_{free} + [Pu(IV)(AHA)_1] + [Pu(IV)(AHA)_2] + [Pu(IV)(AHA)_3]$

Because all Pu(IV) species on the right side of equation (2) contribute to the absorption spectra, the absorbance of Pu solution for given wavelength at variable [HAHA] and constant $[HNO_3]$ and [Pu(IV)] concentrations can be expressed as the following:

(3) $A_{(ij)} = \varepsilon_{Pu(free)(i)} \bullet [Pu]_{free(j)} + \varepsilon_{Pu(L1)(i)} \bullet [PuL_1]_{(j)} + \varepsilon_{Pu(L2)(i)} \bullet [PuL_2]_{(j)} + \varepsilon_{Pu(L3)(i)} \bullet [PuL_3]_{(j)}$

where $A_{(ij)}$ is the absorbance of the system at the wavelength *i* and concentration of ligand *j* and ε is the extinction coefficient for particular absorbing species in solution.

Plutonium(IV)-acetohydroxamate species were resolved from the experimental data obtained by absorption spectroscopy using the chemical equilibrium modeling software FITEQL 4.0. Through calculation of the sum of squares of residuals between the experimental complexation data and predictions made with initial estimates, values of extinction coefficients (ε) for Pu-AHA, $Pu\text{-}AHA_2$, and $Pu\text{-}AHA_3$ complexes at λ=423 nm were determined for the complexation reactions specified (1).

Using chemical equilibrium modeling and stability constants determined for Pu-AHA complexes by S. Sinkov [PNNL], distribution of Pu species was determined. It was found that the formation of three Pu-acetohydroxamate species is possible in 1 M HNO_3 and the studied range of HAHA concentration (Figure 2). Under conditions of lower HAHA concentrations, mainly the non-acetohydroxamate and mono-acetohydroxamate species of Pu are formed. At 0.1 M concentration of HAHA and higher, which is more relevant to UREX process conditions, the di-acetohydroxamate complex of Pu becomes predominant and also the concentration of Pu-tri-acetohydroxamate species grows. Values of log ε for Pu-AHA, $Pu\text{-}AHA_2$, and $Pu\text{-}AHA_3$ calculated by FITEQL 4.0 at 423 nm are 2.29, 2.72, and 2.80 $dm^3 \cdot mol^{-1} \cdot cm^{-1}$, respectively.

Figure 3 compares experimental absorbance of Pu(IV) at λ=423 nm with absorbance calculated from equation (3) as a function of [HAHA, free]. In this case, [HAHA, free] denotes the concentration of non-complexed protonated ligand, which was calculated from pK_a and given concentrations of HAHA, Pu, and HNO_3 using FITEQL. Extinction coefficients for Pu-AHA, $Pu\text{-}AHA_2$, and $Pu\text{-}AHA_3$ species determined by FITEQL are in very good agreement with the experimental data and calculated values of absorbance.

The effect of nitric acid concentration on the speciation of Pu in 0.4 M HAHA was fitted by the Hyperquad Simulation Speciation program (HYSS). The presence of Pu-acetohydroxamate complexes, even at a very high concentration of nitric acid, was identified by Vis-NIR spectroscopy (Figure 4). The changes in spectra due to the formation of Pu-acetohydroxamate species with a maximum at 423 nm observed at high nitric acid concentration confirm a very strong complexation power of HAHA toward Pu(IV).

Planned Activities

In the next period, researchers will focus on the following tasks:

- To continue the extraction experiments with Pu and to measure the distribution between aqueous and organic phases under various conditions such as different concentrations of nitric acid, total nitrates, and temperature
- To investigate Pu and neptunium (Np) speciation in both the aqueous and organic phases for different concentrations of HAHA and nitric acids, using UV-Vis-NIR, FTIR, Raman, and ESI-MS spectroscopy
- To examine the redox kinetics and complexation speciation of actinides (Pu and Np) with various concentrations of nitric acid and nitrates, utilizing modeling programs for both the ionic equilibrium (FITEQL 4.0) and reaction kinetics (GlobalWorks). Data will be incorporated into the AMUSE modeling program.

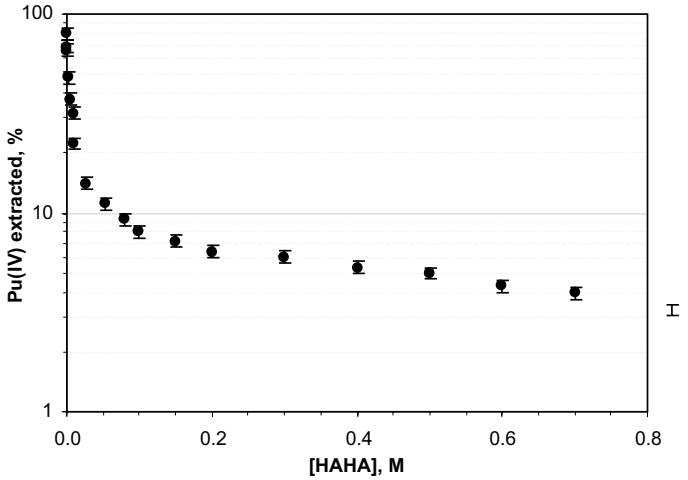

Figure 1. Dependence of extraction yield of Pu(IV) on concentration of HAHA. Organic phase: 30 percent TBP in n-dodecane; aqueous phase: 1 M HNO_3.

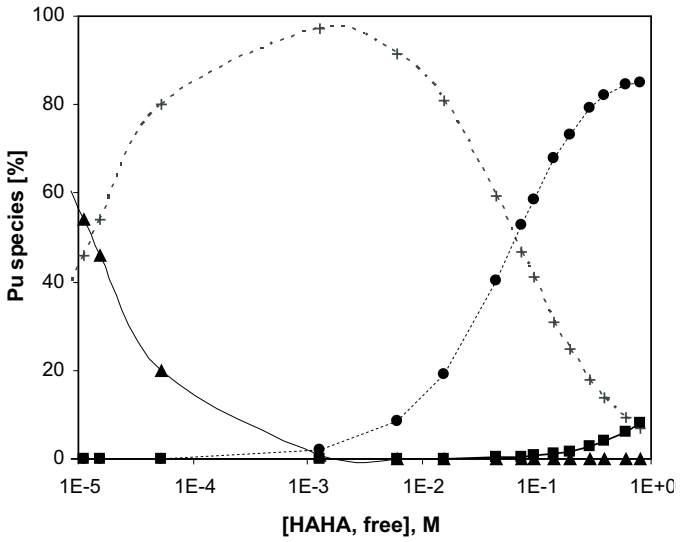

Figure 2. Speciation diagram for Pu(IV)–HAHA system calculated for total [Pu(IV)]=2.26x10^{-3}M, 1 M HNO_3 and various concentrations of HAHA: (▲) Pu, free (non-complexed with HAHA); (+) Pu-mono-acetohydroxamate species; (●) Pu-di-acetohydroxamate species; (■) Pu-tri-acetohydroxamate species.

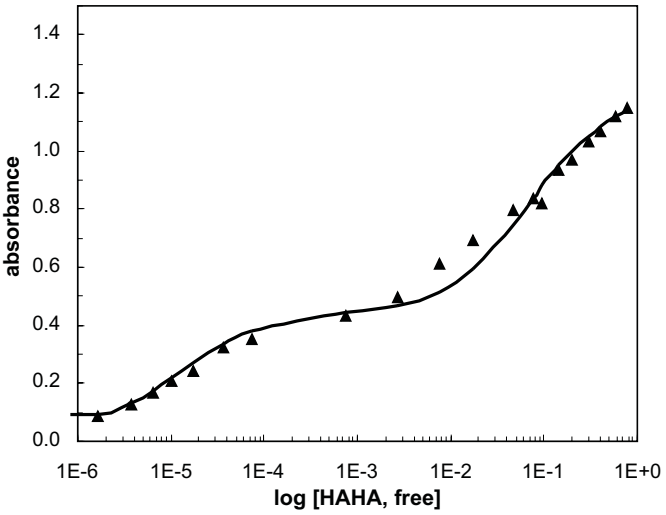

Figure 3. Experimental (▲) and calculated (line) data on absorbance of aqueous solution of Pu(IV) at λ=423 nm as a function of free concentration of HAHA (non-complexed with Pu).

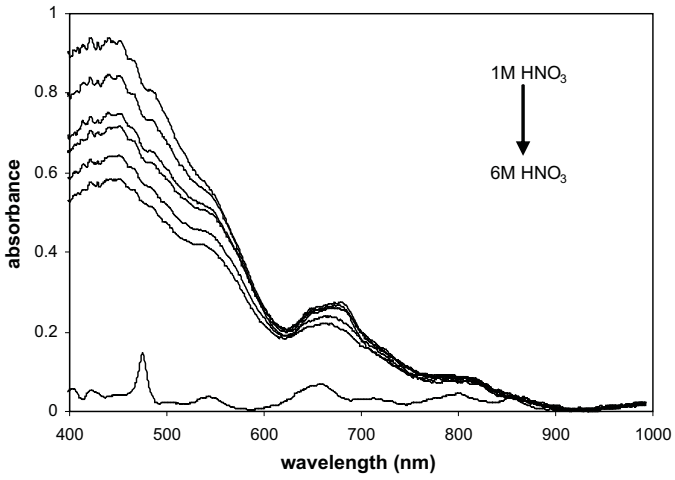

Figure 4. Absorption spectra of Pu(IV)-acetohydroxamate complexes in 1-6 M HNO_3 and 0.4 M initial concentration of HAHA. Spectrum on the very bottom belongs to Pu(IV) in 1 M HNO_3 without presence of HAHA.

Nuclear Energy Research Initiative

Development of an Engineered Product Storage Concept for the UREX+1 Combined Transuranic/Lanthanide Product Streams

PI: Sean M. McDeavitt, Texas A&M University

Collaborators: Purdue University; University of California-Berkeley; Argonne National Laboratory

Project Number: 05-066

Project Start Date: April 2005

Project End Date: July 2008

Research Objectives

The U.S. Department of Energy is developing next generation processing methods to recycle uranium and transuranic (TRU) isotopes from spent nuclear fuel. The objective of this project is to develop near-term options for storing TRU oxides isolated through the uranium extraction (UREX+) process. More specifically, a Zircaloy matrix cermet has been developed as the storage form because it has the ability to serve as an inert matrix TRU-burning fuel form after intermediate storage. The goals of this research are 1) to develop the processing steps required to transform the effluent TRU nitrate solutions and the spent Zircaloy cladding into a zirconium matrix cermet storage form and 2) to evaluate the impact of phenomena that govern durability of the storage form, material processing, and TRU utilization in fast reactor fuel.

Research Progress

The UREX+ reprocessing methods incorporate sequential aqueous solvent extraction schemes with optional ion exchange methods to separate uranium, selected fission products, and TRU elements from dissolved spent nuclear fuel. A significant amount of Zircaloy cladding is removed and cleaned for waste disposal after the chop and dissolve step; a typical pressurized water reactor (PWR) fuel assembly contains approximately 115 kg of Zircaloy. At the other end of the process, a relatively small volume of TRU-bearing solution is recovered from the fuel; the same hypothetical fuel assembly contains 5 to 10 kg of TRU. As a result, there is an abundance of Zircaloy waste in the process and the Zircaloy recycle process does not need to be 100 percent efficient. The process development portion of this project has focused on three processes: 1) the sol-gel formation of mixed oxide microspheres, 2) the recycle of Zircaloy cladding via hydride-dehydride methods, and 3) the cermet fabrication via hot extrusion.

The TRU conversion process is designed to follow the pattern of UO_2 microsphere production by the internal gelation (or sol-gel) method used for TRISO fuel kernel fabrication. For UO_2 production, a broth solution is prepared containing uranyl nitrate ($UO_2[NO_3]_2$), HMTA ($[CH_2]_6N_4$), and urea ($[NH_2]_2CO$) to form low-temperature (0°C) precursors such as $UO_2(NO_3)_2$*2$(NH2)_2CO$. This solution is inserted into warm (90°C) silicone oil as spherical droplets to induce a sequence of self-consuming reactions that break up the complexes, consume the reaction products, and gel into product microspheres of ammonium diuranate ($[NH_4]_2U_3O_7$) which are then fired to form and sinter into UO_2 microspheres.

The process that researchers are studying uses mixed uranyl nitrate and cerium nitrate solutions to examine the co-gelation of mixed oxides as an analog to this process. The primary questions relate to the relative stability of the complexes that form in the broth and how efficient the system is at forming mixed oxide precursors. The ultimate goal is to define the chemistry required to form $(U,Ce)O_2$ ceramic microspheres. Figure 1 shows a photo of cerium

Figure 1. Cerium oxide microspheres fabricated via internal gelation.

oxide microspheres produced in the sol-gel system built for this project.

The Zircaloy recycle process is based on existing technology applied in a new way. The underlying principle is that zirconium readily reacts with hydrogen to form zirconium hydride (ZrH_2). This is the same reaction that produces performance limiting ZrH_2 formations in reactor cladding. During reactor service, this embrittlement is considered negative. In the present application, this is the enabling phenomenon since cladding may be completely embrittled and the density changes from approximately 6.5 g/cm^3 to 5.6 g/cm^3, causing the sample to crumble. This enables rapid milling to fine powder. Once the alloy is pulverized into powder, hydride powder may be reduced by raising the temperature to about 900°C and reducing the ambient pressure to dehydride the ZrH_2 to metallic Zr.

Researchers have completed a fundamental rate study for hydride formation temperatures ranging from 440 to 640°C. There is an eutectoid reaction in the Zr-H system that occurs at approximately 540°C. Processing above 540°C is very rapid, but the β-Zr phase has a high hydrogen solubility and the resulting product is relatively tough. Processing below 540°C is slower, but more effective since the α-Zr phase has low hydrogen solubility and the resulting product is brittle and crumbles without mechanical action. Temperature-time correlations have been developed for hydride formation in α-Zr and β-Zr and an all-in-one process system has been designed and assembled to fully demonstrate this recycling process. The system incorporates a heated mill within a controlled atmosphere chamber.

The hot extrusion process for Zr matrix cermets builds on experience gained during the development of a similar cermet system for the thorium fuel cycle. The experimental setup features an extrusion die fabricated from high-temperature superalloys from Haynes International. The system has been described in other publications, but its operations are currently being refined. Final tests using sol-gel microspheres and dehydrided Zircaloy will be completed this summer.

Regarding the second major goal of this project (i.e., TRU utilization in a fast reactor), many neutronic and Zr/TRU cermet fuel parameters have been calculated following the same protocols used in the development of a U-TRU metal fueled core. Parameters of specific interest are the TRU consumption rate and the reactivity feedback coefficients which affect the operability of the core.

The first two parameters considered were the full core fuel mass and TRU consumption rate. As shown in Table 1, there is a slightly lower TRU loading in the cermet fueled core. In addition to this, the heavy metal loading of the cermet core, which is the same as the TRU loading, is significantly lower due to the absence of uranium. The cermet core can maintain criticality with the lower heavy metal loading due to much better fuel utilization caused by the absence of the parasitic absorption in U-238. A secondary effect of the absence of U-238 is a higher net TRU consumption rate. U-238 primarily acts as a neutron absorber and TRU breeder, reducing the overall consumption rate. This is also the reason why the burnup reactivity loss is higher for the TRU core, that is, 6.6 percent versus 4.3 percent for the metal fueled core. The higher TRU consumption rate could be good or bad depending on the goals of the Global Nuclear Energy Partnership (GNEP). If the goal is to quickly and efficiently burn TRU, the cermet fueled core performs better by burning the TRU isotopes more rapidly. If the goal is long-term sustainability of the fuel cycle, the metal fueled core performs better by breeding some new TRU to offset some of what is lost.

	Cermet	Metal
BOC TRU Loading (kg)	2219	2250
Net TRU Consumption (kg/yr)	269	189.3

Table 1. Comparison of cermet and metal TRU masses.

The next parameters of interest in comparison between the two cores are the reactivity feedback coefficients. Again, the same coefficients that were considered for the metal core are calculated. These values include delayed neutron fraction, sodium void worth, and axial and radial expansion coefficients. Table 2 summarizes the comparison of these values.

	Cermet	Zr Metal
BOC Beta (pcm)	234.7	263.3
BOC Sodium Worth	$3.37	$3.97
EOC Beta (pcm)	236.6	256.7
EOC Sodium Worth	$4.20	$5.05
Axial Expansion (c/K)	-0.18	-0.35

Table 2. Reactivity feedback comparison of metal and cermet fueled cores.

Three significant differences in reactivity coefficients are worth noting. The first difference is that the effective delayed neutron fraction for the metal fueled core is

consistently higher than that of the cermet core. This is due to the presence of U-238 in the metal fuel, which has a much higher delayed neutron fraction when it undergoes fission than does TRU. The next apparent difference between the reactivity feedback coefficients of the two cores is the lower sodium void worth of the TRU cermet core. There is a 31 percent decrease in the BOC sodium void worth and a 24 percent decrease in the EOC sodium void worth in terms of dollars. The smaller delayed neutron fraction of the cermet fueled core somewhat skews the data, meaning the difference in the feedback in terms of change in eigenvalue is even larger. The differences when only delta k is considered are 38 percent and 30 percent for BOC and EOC, respectively.

The final difference between the two cores is the smaller axial feedback coefficient. The immediate cause of this difference is not as evident. One possibility for the difference is the smaller fuel fraction in the Cermet fuel, that is, 38 percent without TRU in the cermet fuel versus 75 percent without U-TRU in the metal fueled core. An expansion of the core in the axial direction would affect the number densities of fissile isotopes much less in the cermet fuel, which could cause the reactivity feedback to be smaller.

Planned Activities

This project is nearly complete and the final outcomes are still being analyzed. The discussion above reflects the current status of the project and the projected completion date has moved to the summer of 2008. The following activities are planned for this summer:

- Fabricate a cermet pin using dehydrided Zircaloy and sol-gel mixed oxides
- Demonstrate the all-in-one Zircaloy recycle system
- Complete the evaluation of mixed oxide internal gelation
- Perform final core design and compare TRU-burning performance to the baseline metal fuel in a sodium fast reactor
- Compile and publish the final report

Nuclear Energy Research Initiative

Selective Separation of Americium from Lanthanides and Curium by Aqueous Processing with Redox Adjustment

PI: Kenneth L. Nash, Washington State University (WSU)

Collaborators: Idaho National Laboratory (INL)

Project Number: 05-082

Project Start Date: March 2005

Project End Date: April 2008

Research Objectives

The objective of this project is to investigate oxidation state adjustment and control methods to achieve selective partitioning of americium (Am) from lanthanides and curium (Cm) using conventional aqueous separations methods and materials. Increased application of mixed oxide (MOX) fuels and longer burnup times of conventional fuels will produce greater amounts of the trans-plutonium actinides Am and Cm in spent nuclear fuel. Because the half-lives of the Am isotopes (432 years for ^{241}Am and 7,370 years for ^{243}Am) are significantly longer than the half-lives of Cm, berkelium (Bk), and californium (Cf) or most fission product lanthanides, isolating Am is a rational approach to integrating transmutation into advanced nuclear fuel cycles. In addition, the selective separation and transmutation of Am isotopes from other actinides and lanthanides could significantly reduce the long-term radiotoxicity of the residues from spent fuel or from spent fuel reprocessing.

The chemistries of trivalent lanthanides and actinides under aqueous processing conditions are similar, making selective separation of Am extremely challenging. This project is investigating oxidation state adjustment (and control) methods to achieve selective partitioning of Am from lanthanides and Cm using conventional aqueous separations methods and materials. Oxidized Am species are not expected to be inherently stable, but transient stability may be adequate for isolating Am. A key requirement of this strategy is to minimize contact with readily oxidized species.

The goal of this research is to develop strategies for adjusting the oxidation state and demonstrating a successful separation based on the oxidation of Am. Detailed studies are being conducted on the most promising candidate process identified. The work scope is defined by the following three tasks:

1) Investigate application of conventional aqueous separation processes to Am in non-standard oxidation states
2) Develop methods and operational conditions under which the upper oxidation states of Am can be stabilized for an adequate period of time to isolate it from Cm and lanthanides
3) Investigate use of unconventional media, such as room temperature ionic liquids and organic or inorganic micellar/colloidal media (e.g., non-ionic surfactants or polyoxometallates), for Am oxidation state adjustment and control

In Task 1, researchers will gain insight from studying the chemical separations behavior of redox stable analog ions like thorium (Th^{4+}), neptunyl (V) (NpO_2^+), and uranyl (VI) (UO_2^{2+}). Task 2 will emphasize the influence of kinetics and the use of chemical oxidants to maintain oxidized Am species long enough to allow the separation. Task 3 will focus on reducing the influence of readily oxidizable reagents on Am instability while considering the need for short contact times.

Research Progress

A new milligram actinide facility was established at WSU to facilitate this program. Actinide isotopes have been provided by the collaborators at Pacific Northwest National Laboratory (PNNL) and by the Radiochemistry Engineering Development Center (REDC) at Oak Ridge National Laboratory (ORNL). A separate facilities grant from the U.S. Department of Energy (DOE) Office of Basic Energy Sciences has provided support for instrumentation of this new facility. Equipment acquisitions include an ozone generator, which is needed for clean preparation of oxidized Am species, upgraded glovebox facilities for actinide handling and inert atmosphere operations, conventional

instrumentation, and radioanalytical counting equipment. This laboratory has become operational. Other experiments have been done at INL.

Researchers 1) are conducting studies on the effect of nonionic surfactants on actinide chemistry, 2) are conducting studies on the behavior of ionic liquids in biphasic separations systems relevant to this problem, 3) have completed studies of some conventional solvent extraction approaches to this separation challenge, 4) have conducted fundamental studies on the electrochemical properties of selected room temperature ionic liquids (RTILs), and 5) are examining solid-liquid separations of lanthanides from oxidized Am species. On the question of RTILs, they have ruled out a simple solvent-substitution approach because other work has established that this system is too complex to provide a workable solution to the problem. However, the electrochemical properties of RTILs would make them an attractive medium for investigating facile preparation of oxidized Am species. The nonionic polyelectrolyte approach has a number of positive features to recommend it for further studies, including diminished content of reducible components due to the minimization of organic solvents. Researchers are exploring a connection between electrochemical oxidation of Am in an RTIL with subsequent selective isolation of the oxidized Am from the RTIL phase. A promising sequential extraction process has been recently discovered and is under investigation. A convenient connection to an industrial supplier of extractants and less expensive ionic liquids has been made. Researchers are also examining detailed approaches to the recovery and recycle of RTIL components for this application. Finally, researchers have conducted exploratory studies of polyoxometallate systems and of lanthanide/actinide separations in carbonate/bicarbonate media.

Planned Activities

The carbonate chemistry approach is seen as a means of increasing the lifetime of oxidized Am species to a regime that is suitable for conventional aqueous separations techniques. The approach researchers are taking complements work being done at Los Alamos National Laboratory (LANL) on a similar system, taking a somewhat different approach to separating Am from fission product lanthanides from the LANL work. This line of investigation is unconventional, but could develop a variety of new options for selective separation of Am with variation in redox control parameters. A principal advance that could arise from this line of research would be improved radiation stability in the separation system. The initial experiments have provided encouraging evidence that this approach could result in an important breakthrough in Am-lanthanide separations efficiency. Several reports in the literature indicate that alkaline solutions could have a useful impact on creating and retaining oxidized Am species. Researchers can significantly advance this activity through studies of redox stable species of uranium and neptunium, such as U(VI) and Np(V). They are also examining the chemistry of plutonium, in the form Pu(VI), as a spectrophotometric probe of the hexavalent oxidation state in this system.

Nuclear Energy Research Initiative

Selective Separation of Trivalent Actinides from Lanthanides by Aqueous Processing with Introduction of Soft Donor Atoms

PI: Kenneth L. Nash, Washington State University (WSU)

Collaborators: Pacific Northwest National Laboratory (PNNL)

Project Number: 05-083

Project Start Date: March 2005

Project End Date: April 2008

Research Objectives

A closed loop nuclear fuel cycle requires mixed oxide (MOX) fuels that utilize plutonium (Pu) as the primary fissile component. The use of MOX fuel, combined with longer irradiation times, increases the production of trans-plutonium actinides, most significantly isotopes of americium (Am) and curium (Cm). Furthermore, in long-term storage fuels, β- decay of ^{241}Pu steadily increases the amount of ^{241}Am in the fuel and in spent fuel dissolvates. Because the presence of these isotopes significantly impacts the long-term radiotoxicity of high-level waste, it is important to develop effective methods for their isolation and/or transmutation. Whether by thermal reactor, fast spectrum reactor, or accelerator irradiation, transmutation is most efficiently done in the absence of lanthanide fission products, as some of the lanthanides are significant neutron poisons.

Lanthanide content is 100-fold higher on a molar basis than Am or Cm in freshly dissolved spent fuel; therefore, it is very important to develop effective procedures for their mutual separation. Assuming that lanthanides are to be separated from the predominantly trivalent trans-plutonium actinides Am and Cm, the most useful and versatile separations of these species are accomplished using reagents containing donor atoms that are "softer" than oxygen (O) and that interact more strongly with actinides than lanthanides. Nitrogen (N) and sulfur (S) are particularly suited and the chloride ion (Cl-) has been used as well. Several reagents that have been advanced in recent years show promise, but suffer various weaknesses, many relating to their instability in a radiation field or strongly acidic solutions.

This project investigates new chemical methods (and improvement of existing methods) for selective separation of trans-plutonium actinide isotopes from fission product lanthanides using the proven techniques of aqueous processing—specifically those processes that employ soft donor atoms (N, Cl-, and S). The overall work scope for this project includes the following elements:

- Investigate selective partitioning of trivalent Am and Cm from fission product lanthanides using ammonium thiocyanate and concentrated chloride solutions
- Adapt the basic philosophy of the TALSPEAK process (using water soluble aminopolycarboxylate complexants) to these extractant systems in various classes of solvent extraction systems
- Explore radiation protection methods based on the removal of radiolytic degradation products (largely free radicals, introducing radical scavengers) from the extractant or the aqueous phase

Research Progress

Research initially focused on 1) solvent extraction studies from thiocyanate media using conventional extractant molecules and 2) the design, synthesis, and characterization of new formulations of polyaza-extractants and aqueous complexing agents. At present, the team has suspended most activities on chloride and thiocyanate systems in favor of a more focused effort on the TALSPEAK system complemented by a continuing study of polyaza ligands. Ongoing research addresses the kinetics of lanthanide interactions with aminopolycarboxylate complexants in lactate media and the impact of temperature, pH, and lactate concentration on basic TALSPEAK performance. Several publications are in preparation to describe these results.

Results of rate studies indicate that kinetic limitations in process chemistry must result from chemistry occurring in the interfacial region of the phase transfer system

rather than in the aqueous phase. This knowledge could contribute to a different engineering solution to TALSPEAK processing problems based on slow kinetics.

Researchers have received actinide isotopes from PNNL and improved their infrastructure to enable the safe handling of these materials at the milligram level. The delivery of isotopes was delayed unexpectedly by additional paperwork required by the State of Washington Department of Health regarding airborne release permitting for the research facility. Researchers have worked out some materials handling issues with the WSU Radiation Safety Office (RSO) and have commissioned new laboratory space to conduct these studies. A $289K equipment grant from the Department of Energy (DOE) Office of Basic Energy Sciences has been used to modernize the instrumentation in this special-purpose laboratory.

Researchers have also synthesized several new polyaza extractant molecules and are presently evaluating their coordination chemistry and separations potential. The ligands that have been targeted for synthesis are polyaza donor systems bearing structural similarity to ethylenediamine-tetramethylpyridyl complexants, which are under investigation at the Tokyo Institute of Technology. This class of compounds should be inherently resistant to radiolytic degradation. The polyaza extractant synthesis studies have progressed from investigating a combination amine-amide donor system to investigating a multiple amine donor extraction system. These extractant species employ some degree of preorientation of donor groups to enhance interaction strength and emphasize conditions for actinide selectivity. A significant portion of this study has been conducted in hot lab facilities at PNNL. Several publications are in preparation based on these results as well.

Planned Activities

The research team will continue to investigate the chemical details of the TALSPEAK process until the end of this project—profiling the temperature dependence of this process, pH dependence, and assessing the details of lactate partitioning between the TALSPEAK phases. These investigations are designed to assist the team in optimizing the operational characteristics of TALSPEAK. The other primary task to be completed is the completion of the numerous open literature publications that are in progress.

NUCLEAR ENERGY RESEARCH INITIATIVE

Development of Nanostructured Materials with Improved Radiation Tolerance for Advanced Nuclear Systems

PI: Xinghang Zhang and K. Ted Hartwig, Texas A&M University

Collaborators: Los Alamos National Laboratory (LANL)

Project Number: 05-088

Project Start Date: April 2005

Project End Date: April 2008

Research Objectives

This project explores the fundamental mechanisms through which interfaces in the nanolayered structures and grain boundaries of bulk nanomaterials attract and eliminate point defects and unwanted foreign species. Candidate materials include nanostructured multilayer composites synthesized by magnetron sputtering (a bottom-up approach) and structural bulk nanomaterials produced by severe plastic deformation, equal channel angular extrusion (a top-down approach), or ECAE.

This project will have a profound and broad impact on understanding the fundamental science behind improving radiation resistance by inducing interfaces and grain boundaries in nanomaterials and by designing and engineering structural nanomaterials for advanced nuclear reactors. Data from this study will be used for estimating defect capture rates and lifetimes of multilayered structures and bulk nanomaterials in conditions that would seriously degrade conventional microstructures. Researchers expect this project to benefit a broad spectrum of DOE programs associated with fission technology research and development.

Research Progress

Steels processed by equal channel angular pressing (ECAP) at high temperature. Researchers processed another batch of bulk T91, HT9, 316L, 316L powder, and 304 in the form of can material alloys. They varied the extrusion temperatures from 500–700°C to study the influence of extrusion temperatures on the refinement of microstructures. As-received bulk T91 LA1 (hardness = 250 HV) alloys were annealed for one hour at 1,050°C and ECAP-processed in nickel cans for one pass at 700°C and 2B at 600°C. Samples for transmission electron microscopy (TEM), microhardness/annealing, ion implantation, and tensile testing were extracted via wire electro-discharge-machining (EDM). X-ray diffraction (XRD) examination revealed no phase changes in the material and peak broadening was not sufficient for grain refinement estimation.

Figure 1a shows the microstructure of the LA1 1,050°C annealed specimen. After annealing and rapid cooling, the specimen transformed almost entirely into martensites, indicated by approximately 200 nm platelets, with high texture as shown by the inserted diffraction pattern. ECAP processing of this specimen at 700°C has an effect of both extrusion and tempering. As a result, the average grain size seems to be larger, approximately 1μm, and martensite seems to transform to ferrite during processing, as shown in Figure 1b. Specimens (LA1 1,050°C annealed) processed via ECAP at 600°C have a much smaller average grain size, approximately 300 nm, which is also shown in Figure 1b. In this case, martensite has been transformed to ferrite during tempering, followed by significant grain refinement due to extrusion, as shown in Figure 1c.

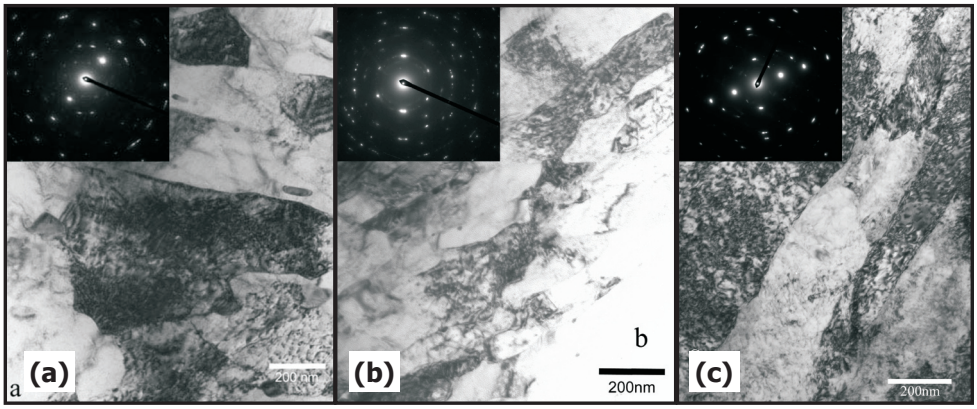

Figure 1. TEM micrographs of T91 alloys: (a) LA1 1,050°C annealed specimens, (b) LA1 1,050°C annealed specimens followed by ECAP processing at 700°C/1pass, and (c) LA1 1,050°C annealed specimens followed by ECAP processing at 600°C/2 passes.

Tensile testing was performed on T91 coupons in order to obtain a more detailed mechanical behavior data set. The results are presented in Figure 2. Note the unusual necking behavior in the annealed sample. In general, the variation of yield strength and ultimate tensile strength with processing (annealing) condition is very consistent with the variation of specimen hardness. Specimens with higher hardness have higher yield and ultimate tensile strength. ECAP-processed LA1 specimens at 600°C have a combination of high strength and considerable ductility.

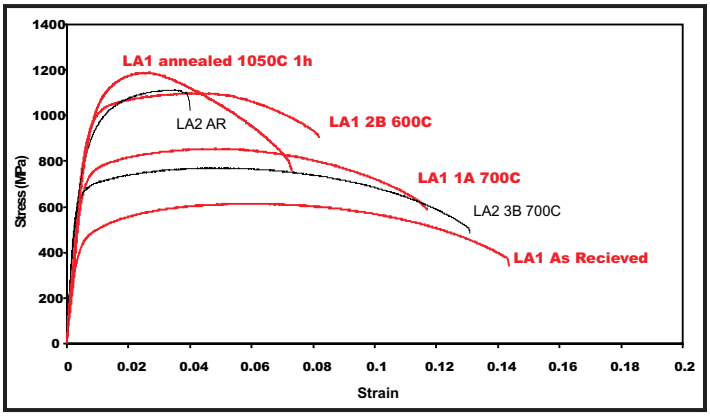

Figure 2. Comparison of the tensile properties of T91 alloys ECAP-processed at various conditions subjected to uniaxial tensile test.

Fracture surfaces of tensile specimens were examined by SEM. The as-received material has river patterns, indicating that ductility is conserved in specimens. Sharp edges and clear outlines of many elongated features also indicate that inter-granular fracture may have occurred and could be related to the limited ductility of as-received specimens. Fracture surface of the ECAP process specimens shows a more complicated morphology. Researchers observed many pits with a 5–10 micron diameter, probably due to the pulling out of materials during tests. The research team will attempt to use wavelength dispersive spectrometry (WDS) to quantify the phase of these spheres.

Some of these ECAP-processed specimens have been tested for corrosion resistance in the Delta loop at LANL, which simulates an environment similar to a Pb-Bi-cooled reactor. These processed materials will be implanted with He ions at the Ion Beam Materials Laboratory at LANL.

Sputtered Cu/Nb, Cu/V, and Fe/W nanolayers with improved ion irradiation tolerance. A series of sputter-deposited Cu films and Cu/Nb multilayers with a total film thickness of 240–500 nm were implanted at room temperature by either 33 keV He^+ ions with a dose of 6 x $10^{16}/cm^2$ or 150 keV He^+ ions with a dose of 1 x $10^{17}/cm^2$. Helium bubbles with a 2–3 nm diameter were observed in 500 nm thick Cu films irradiated with 33 keV He ions at a dose of 6 x $10^{16}/cm^2$. A magnified image of the box in radiated Cu100/Nb100 nm multilayers (Figure 3a) is shown in Figure 3b. The selected region is expected to have peak He concentration as indicated by SRIM calculation. Helium bubbles were observed in both Cu and Nb layers and their concentration appeared to be higher along layer interface as indicated by dense packing of He bubbles along interfaces. Similar radiation experiments were performed in Cu2.5/Nb2.5 nm multilayer films. Surprisingly, such irradiation conditions did not seem to generate He bubbles in this case, as shown in Figure 3c. Furthermore, the layer structure remains unchanged.

The studies reveal that Cu/Nb multilayer films with a few nm layer thickness have remarkable He and defect storage capabilities compared to their bulk counterparts. The size of Helium bubbles in these fine multilayers, if any, is below the bubble detection limit of current TEM microscope (approximately 0.5 nm). Further studies will focus on the identification of critical layer thickness that may suppress the nucleation of He bubbles.

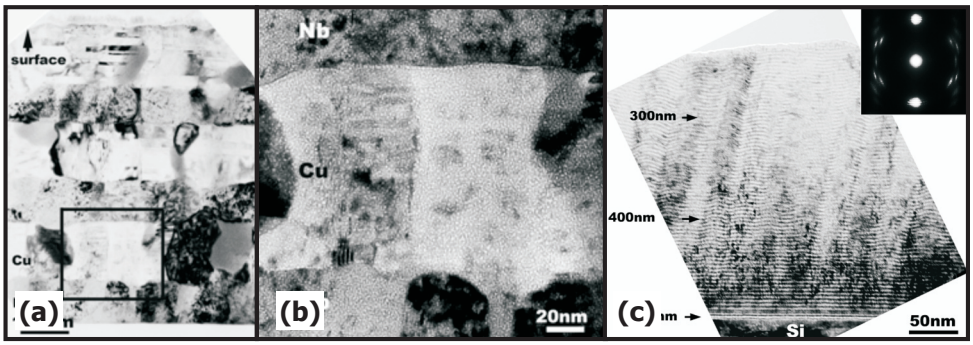

Figure 3. (a) Low magnification XTEM micrograph of Cu100/Nb100 nm multilayer films ion irradiated with He ions at 150keV/1 x $10^{17}/cm^2$. (b) Magnified image (small box in Figure 3a) shows a large number of He bubbles in Cu and Nb layers with a larger bubble concentration along layer interfaces. (c) Cu2.5/Nb2.5 nm multilayer films subjected to the same He ion irradiations. No He bubbles were detectable. Microstructure remains unchanged, i.e., layer interfaces are still continuous and Cu and Nb are unmixed after ion irradiation.

A series of Cu/V multilayer films with different individual layer thickness (2.5–100 nm) were irradiated by He ions with an ion energy of 50 keV and a dose of 6 x 10^{16} ions/cm^2. XRD studies show that, after ion irradiation, peak intensity is decreased, indicating the disordering of crystalline structures due to ion irradiation. Peak shifts to lower angle in most cases, presumably as a result of lattice expansion by entrapment of He ions and generation of vacancies.

Figure 4a shows XTEM micrographs of He ion irradiated Cu 5/V 5 nm nanolayers. Region 1 close to the film surface is anticipated to be a less radiated region. Region 2, 150–250 nm underneath film surface, is anticipated to be a heavily radiated region. The magnified XTEM micrograph of region 1 (Figure 4b) shows a clear interface between Cu and V without the observation of a large number of defects. Careful examination of Figure 4b shows that, close to the bottom of region 1, some white dots start to appear. These white dots are typical signatures of He bubbles as a result of radiation. In region 2, shown in Figure 4c, He bubbles are distributed throughout the specimen. The average diameter of He bubbles is 1–2 nm. Yet, Cu/V layer interfaces are still clearly visible, indicating that the incorporation of He bubbles in these small nanolayers did not destroy the integrity of the layer structure. This is the region with the highest density of He bubbles, consistent with the prediction of SRIM simulation.

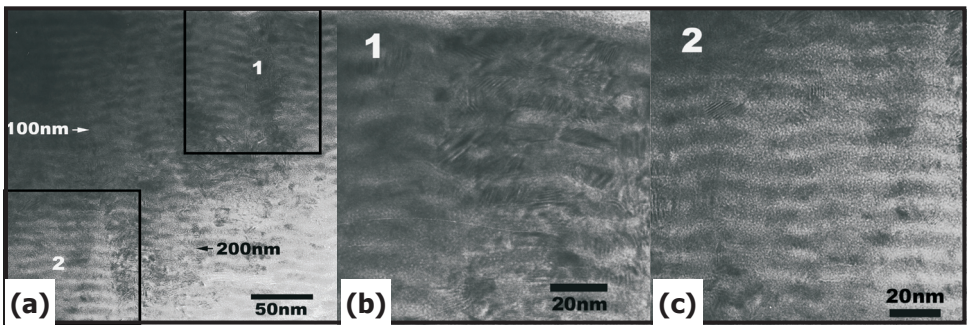

Figure 4. (a) XTEM images of ion-irradiated Cu/V 5 nm multilayer films with indication of two regions located at different positions relative to the film surface. (b) Magnified view of region 1 shows the multilayers are essentially intact after ion irradiation with some signs of He bubbles at the bottom of the region. (c) Magnified view of region 2 shows a very high density of bubbles formed throughout the region. The average diameter of He bubbles is 1-2 nm in diameter. The integrity of Cu/V layer interface remains with the incorporation of He bubbles inside layer structure.

The indentation hardness of as-deposited and ion-irradiated Cu/V multilayers was determined from a nanoindentation test. Figure 5 shows the change of hardness between the as-deposited and irradiated Cu/V samples as a function of $h^{-1/2}$, where h is individual layer thickness. Blue and red data are specimens subjected to the same dose with slightly different energy. Such energy difference was shown (by SRIM calculation) to generate

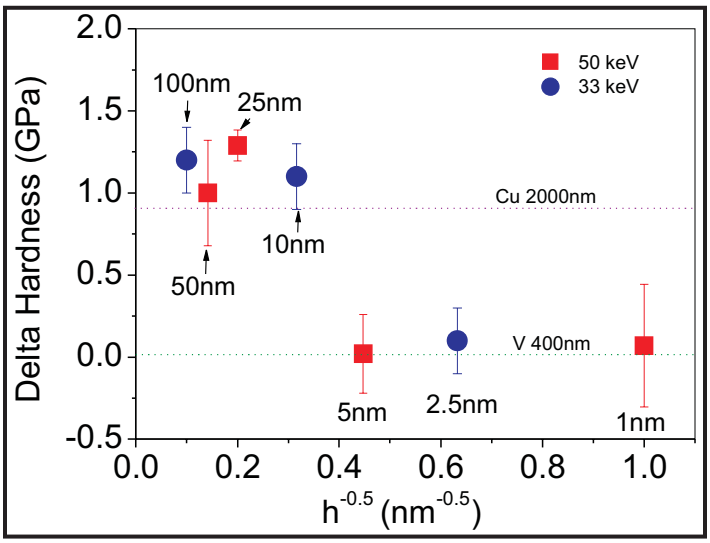

Figure 5. Variation of hardness versus $h^{-0.5}$, where h is individual layer thickness, in Cu/V multilayers after He ion irradiation. Significant hardening is observed in multilayer with 10 nm or greater layer thickness, whereas hardnesses barely change in Cu/V with smaller layer thicknesses. Dash lines indicate hardness variation for single layer Cu and V films.

slight offset of He peak concentration. In general, radiation induced significant hardening, approximately 1 GPa, in multilayers with a layer thickness of 10 nm or greater. It is anticipated that the formation of point defects (vacancies and interstitials) will impede the movement of dislocations during the deformation. Orowan type mechanisms may have led to the strengthening in radiated multilayers, as has been seen in bulk metals subjected to He ion irradiation. Surprisingly, there is a negligible increase of film hardness in ion-irradiated multilayers with 5 nm or less layer thickness.

The phenomenon of abrupt contrast in hardness variation in ion irradiated Cu/V nanolayers raises a fundamental scientific question: Is the radiation-induced strengthening mechanism very different at a few nm layer thickness? Recent Molecular Dynamics simulations at LANL have shown that vacancy and interstitials are trapped by Cu/Nb layer interface and that the vacancy-interstitial recombination rate has significantly increased. As a result, radiation-induced defect concentration is significantly reduced at a few nm length scale. In the current study, a large quantity of He bubbles, 1–2 nm, are still visible in Cu/V 5 nm films. It is puzzling why such He bubbles do not contribute to the hardening of multilayer films. Further investigations are underway.

Similar ion irradiated studies have been performed in Fe/W nanolayers. Fe/W has a bcc/bcc crystal system with incoherent interface. In general, ion irradiation has shown He bubbles intermixing along interface in Fe/W nanolayers.

Planned Activities

The team will perform more microstructural and chemical analysis to understand the evolution of hardness of phases during annealing and the ECAE process. They are studying thermal stabilities of T91 alloys using differential scanning calorimetry (DSC) and a high vacuum annealing furnace. They are also working on systematic ion irradiations of ECAP-processed T91 alloys. They will use CINT (Center of Integrated Nanotechnology, operated by Los Alamos and Sandia National Laboratories) to access their ion implantation facilities and are in the process of examining the microstructure, density, and mechanical properties of a series of specimens processed by ECAP. These include HT-9, 316L SS, consolidated 316L SS powders, and 304 SS. In parallel, various corrosion tests will continue both in the Delta Loop at LANL and at the supercritical water reactor at the University of Wisconsin-Madison. Preliminary studies show that ECAP-processed materials are more corrosion resistant.

Results on radiation damage in nanolayers have been submitted for publication. Collaborations with LANL on molecular dynamics simulations will help researchers understand the fundamental mechanisms of interface-defects interaction at the molecular level. To date, the project has led to the publication of 9 journal articles, 9 presentations at conferences or workshops (including several invited talks), and 5 manuscripts submitted or in preparation.

Nuclear Energy Research Initiative

Utilization of Minor Actinides as a Fuel Component for Ultra-Long-Life VHTR Configurations: Designs, Advantages, and Limitations

PI: Pavel V. Tsvetkov, Texas A&M University

Collaborators: None

Project Number: 05-094

Project Start Date: March 2005

Project End Date: March 2008

Research Objectives

The objective of this project is to assess ultra-long-life very high-temperature reactor (VHTR) configurations utilizing minor actinides (MAs) as a fuel component. Researchers will analyze the capabilities of pebble bed and prismatic core designs with advanced actinide fuels (fuels with high quantities of MAs) to operate in a single-batch mode without intermediate refueling. Researchers are developing long-life VHTR systems and are analyzing them, focusing on control, dynamics, safety, and proliferation-resistance during autonomous operation. The autonomous single-batch operation of VHTRs should improve their marketability worldwide. Utilizing MAs in VHTRs facilitates the development of new fuel cycles and supports nuclear fuel supply sustainability leading to nuclear power sustainability as an energy source.

To support the overall focus on VHTRs with transuranics (TRUs), particularly with MAs, there are several project tasks to be completed:

- Develop whole-core/system models with explicit multi-heterogeneity treatments
- Develop benchmark test problems to compare with experimental data
- Validate and verify the VHTR models
- Analyze uncertainty effects on VHTR performance characteristics
- Analyze configuration variation capabilities to achieve ultra-long operation without refueling, maximize burn-up levels, and minimize reactivity swings
- Complete control, dynamics, safety, and proliferation-resistance studies of ultra-long-life VHTR configurations with advanced actinide fuels

To assure a comprehensive, realistic assessment of the VHTR design and operation targeting passive safety confirmation, the adequacy of computational methods and models used to compute performance characteristics is being supported by comparisons with experimental data covering appropriate ranges of conditions. The code-to-experiment benchmark evaluations from the first year of the project confirmed the chosen analysis approach.

Since both the pebble bed and prismatic block core designs permit flexibility in component configuration, fuel utilization, and fuel management, it is possible to improve the fissile properties of MAs by neutron spectrum shifting through configuration adjustments. The principal mechanism for achieving long-life VHTR configurations is enhanced involvement of self-sustaining compositions based on spent light water reactor fuel. Figure 1 illustrates the envisioned VHTR system consisting of the VHTR fueled with low enriched uranium (LEU) and TRU from pressurized water reactors (PWRs) and the corresponding fuel cycle components, including the spent fuel repository.

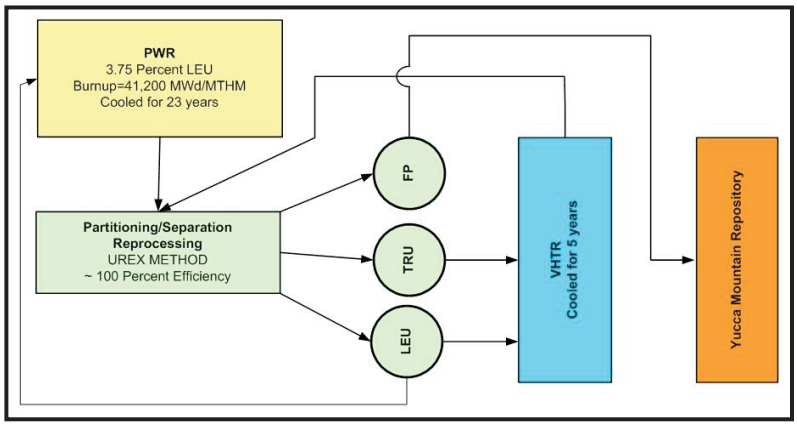

Figure 1. LEU-and TRU-fueled VHTRs within the LWR-VHTR fuel cycle framework.

Researchers have adopted a hybrid methodology for coupled neutronics-thermal hydraulics design studies of VHTRs that combines Monte Carlo and deterministic approaches. High-fidelity 3-D coupled neutronics and thermal-hydraulics VHTR models with multi-heterogeneity treatments are being developed and implemented. The analysis takes into account uncertainty effects and error propagation. As illustrated in Figure 1, the results describe the performance of the entire power system with TRU-fueled VHTR and its fuel cycle components as well as support conclusions regarding feasibility, performance, and possible directions for further development.

Research Progress

The Next Generation Nuclear Plant (NGNP) concept envisions an advanced, efficient, next-generation nuclear reactor designed for electricity generation and hydrogen production. One of the six Generation IV concepts, VHTR is specifically intended for this application but could also serve as a high-temperature heat source for other industrial applications such as sea water desalination and various petrochemical applications. The VHTR design originates from high-temperature gas-cooled reactors (HTGRs), which have successfully demonstrated their feasibility. The VHTR concept has been proposed in two design configurations: a prismatic core consisting of fuel and graphite blocks and a pebble bed core composed of thousands of fuel and graphite spheres. Prototypes of each of these configurations exist as the high-temperature test reactor (HTTR) in Japan and the high-temperature test module (HTR-10) in China. The NGNP/VHTR technology is expected to enter commercial energy markets after 2030. Apart from hydrogen production, the VHTR technology is being seriously considered as one of the thermal neutron transmutation approaches for TRU nuclides incineration. Researchers at General Atomics, Los Alamos National Laboratory (LANL), and Oak Ridge National Laboratory (ORNL) proposed a deep-burn transmutation in the HTGR prismatic cores.

This NERI project considers TRU vectors as potential fuel components that could enhance performance characteristics of power units with VHTRs by prolonging their operation on a single fuel loading. It also considers optimized transmutation of TRUs by completely recovering their energy value.

During this research period, researchers performed a literature survey to develop a database of actinide fuels and material properties in order to establish realistic VHTR configurations with advanced materials. They completed the analysis of existing uncertainty effects on VHTR performance characteristics, focusing on the effects of nuclear data and design parameters. This was followed by a reliability evaluation of VHTR modeling. Results of model validation and verification and sensitivity/uncertainty analysis agree with available data and confirm the validity of the chosen analysis approach. The sensitivity/uncertainty analysis is the basis of ongoing studies of configuration variation capabilities. Researchers are evaluating methods to optimize a physically achievable system lifetime, taking advantage of self-sustainable fuel compositions with higher actinides. The design target is an autonomous operation with minimized required control interventions.

A Monte Carlo-deterministic analysis methodology has been implemented for coupled design studies of VHTRs with TRUs using the ORNL SCALE 5.1 code system. Figure 2 shows applied 3D whole-core model structure accounting for 3D temperature distributions corresponding to prototypic operation conditions. The modeling adequacy is confirmed by a performed series of experiment-to-code benchmark evaluations.

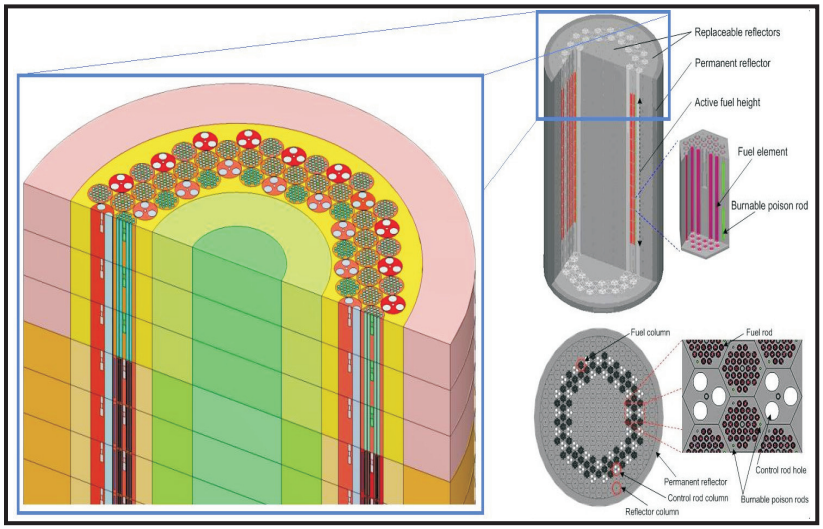

Figure 2. 3D whole-core VHTR model (prismatic block system).

Up-to-date studies demonstrate significant differences between the LEU- and TRU-fueled VHTR configurations. Figure 3 illustrates the differences between LEU- and TRU-fueled systems and shows neutron spectra in the TRU-fueled VHTR prismatic cores for several carbon-to-heavy metal (C/HM) atom ratios.

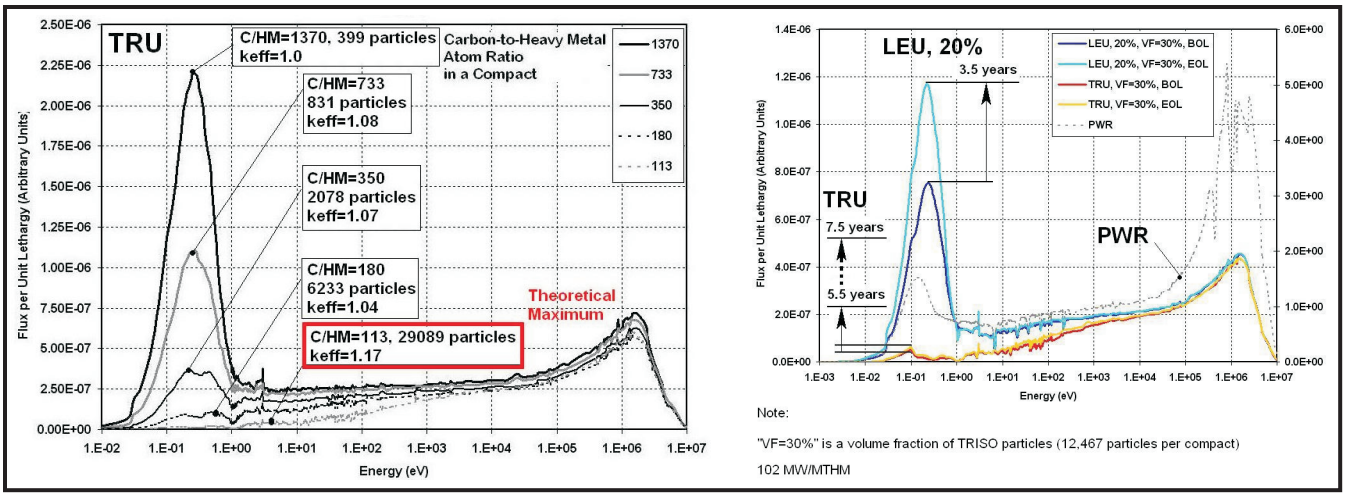

Figure 3. Spectra in TRU-fueled VHTRs (prismatic block system).

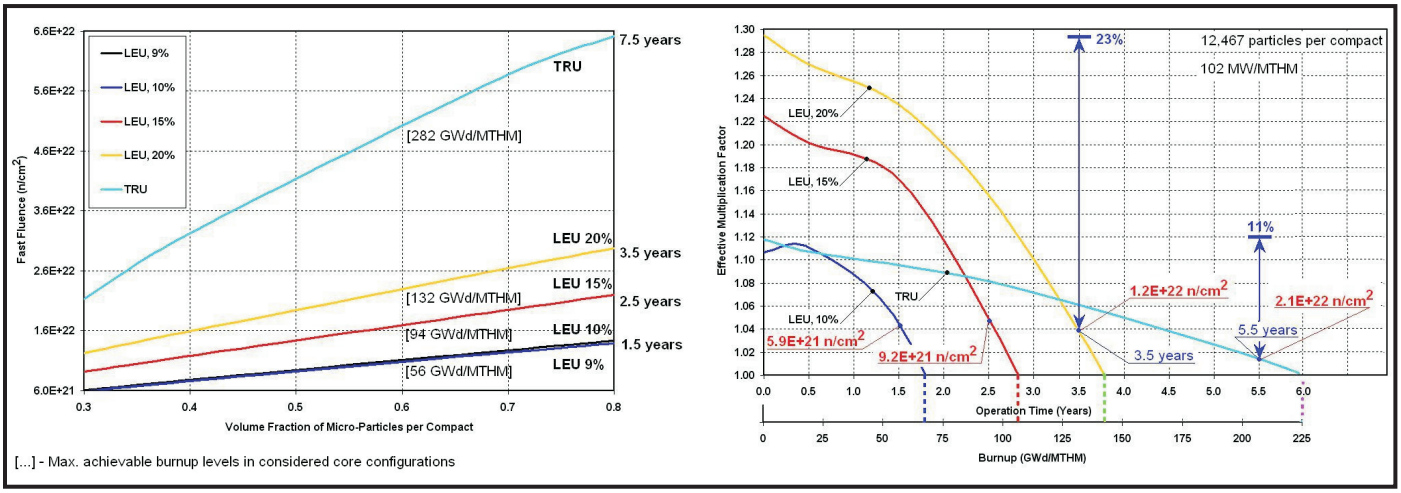

Figure 4. Lifetime of LEU- and TRU-fueled VHTRs operating without refueling (prismatic block system).

As illustrated in Figure 4, the TRU-fueled VHTR cores can potentially sustain longer refueling intervals than the corresponding LEU-fueled traditional VHTR cores. The extended operation of the TRU-fueled VHTRs is also characterized by smaller lifetime reactivity swings due to the self-sufficiency of advanced actinide compositions. The extended batch mode operation without refueling can be prolonged further by decreasing power densities in the TRU-fueled VHTR cores to reduce fast fluences. Figure 4 demonstrates limiting fast fluences that will force power density reductions and use of advanced materials. These limitations will ultimately define performance domains of VHTRs with advanced actinide fuels.

The extended-lifetime approach could reduce the technical need for additional repositories and should improve marketability of the Generation IV VHTR designs as small-to-medium internationally deployable energy sources for electricity generation and industrial heat applications. The TRU-fueled VHTRs offer performance characteristics that would be difficult to achieve in analogous LEU-fueled systems:

- Almost a decade-long batch mode operation without intermediate refueling
- Significant reductions of initial excess reactivity levels (smaller lifetime reactivity swings)
- Inherently higher achievable burnup levels

At the same time, the presented results clearly illustrate that use of TRU vectors as a fuel inherently facilitates the development of specially designed VHTRs with core materials withstanding performance conditions of systems optimized for fuel loading with TRUs:

- Limiting fast fluences and larger resulting radiation damage effects
- Significant core physics differences due to spectral shift effects towards harder neutron spectra with substantially reduced neutron populations at thermal energies

Planned Activities

This project is currently within its third year of performance. Results are in agreement with the available data and confirm the chosen approach. Although indicating some technical limitations and challenges, studies of VHTRs with MAs definitely suggest promising performance and possibility to utilize the core configurations with MAs gaining prolonged operation and self-sustainability. The ongoing studies are the central, most time consuming and information-intense part of the project. These detailed studies account for key aspects of the developed VHTRs with MAs.

In the remaining period, the following efforts are being completed, fulfilling the objectives of the project:

- VHTR optimization for autonomous operation without intermediate refueling
- Feasibility of long-life VHTRs with MAs
- Long-life VHTRs and transmutation
- Dynamics, safety, and control of VHTRs with MAs
- Fuel cycle of long-life VHTRs with MAs
- Proliferation-resistance of long-life VHTRs

Nuclear Energy Research Initiative

Ambient Laboratory Coater for Advanced Gas Reactor Fuel Development

PI: Duane D. Bruns, University of Tennessee, Knoxville (UT)

Collaborators: Idaho National Laboratory (INL), Oak Ridge National Laboratory (ORNL), Iowa State University

Project Number: 05-118

Project Start Date: January 2005

Project End Date: December 2007

Research Objectives

The objective of this project was to develop a physics-based understanding of the spouted bed coaters presently used to coat tristructural-isotropic (TRISO) nuclear fuel particles. The goal was to scale-up the coaters from research scale (50 mm ID) to production dimensions (>150 mm) using a combination of intensive experimental efforts and detailed model development to guide (and accelerate) the scale-up program.

The physical characteristics and properties of the particles, bed, and fluidizing gas interact, affecting the hydrodynamics in the fluidization processes. The hydrodynamics drive the heat, mass, and momentum transfer both locally and globally in the unit operation. Presently, there are no reliable design procedures to scale-up the fluidization process, let alone specialized spouted bed reactors.

Researchers collected experimental measurements from four coaters operating at temperatures up to 500°C (50, 83.5, 95, and 150 mm), in addition to a 50 mm hot surrogate coater, a 50 mm uranium coater, and a 150 mm BWXT coater. The latter has more sophisticated distributors than the typical conical bottom. The data collected included the high-speed (1,000 Hz) differential pressure time series of the fluidizing gas from the bed inlet to exit.

Researchers used fast response sensors to capture dynamic behavior, such as a 3-D positioning system with feedback control and pitot tube to measure average local velocities. They controlled relative humidity to mitigate electrostatic effects. If the coater provided optical access, the team recorded digital images for later analysis. The time scale of the bed dynamics allowed visual observation to provide insight into the physics of the process. In addition, the advanced computational fluid dynamics tools for granular flow simulations in MFIX allowed researchers to interactively conduct experiments and simulations. The excellent overall agreement between experiments and simulations provided additional insight into the complex interactions between the gas and particles in the spouted beds. Researchers have reported that existing correlations for minimum spouting velocity give poor values; therefore, this project's new correlations should be of immediate value.

This research included the following tasks:

- Designed and fabricated fluidized beds with changeable nozzles and distributors
- Developed LabVIEW software for operation, data collection, and feedback control
- Studied parameters important to scale-up and developed correlations for minimum fluidization velocity, minimum spouting velocity, bed pressure drop, and spout shape in shallow spouted beds with high density and spherical particles
- Collected high-speed pressure measurements and images and conducted image analysis; developed new measurement techniques for flux and momentum distributions
- Supported instrumentation and control and measurements in coating temperatures to 2,000 K
- Applied chaos and nonlinear dynamics concepts for feedback control

Research Progress

These coaters are highly nonlinear, sensitive to boundary conditions, and exhibit idiosyncratic behaviors such as complex transients, unstable hydrodynamics, and chaos, which contribute to scale-up issues.

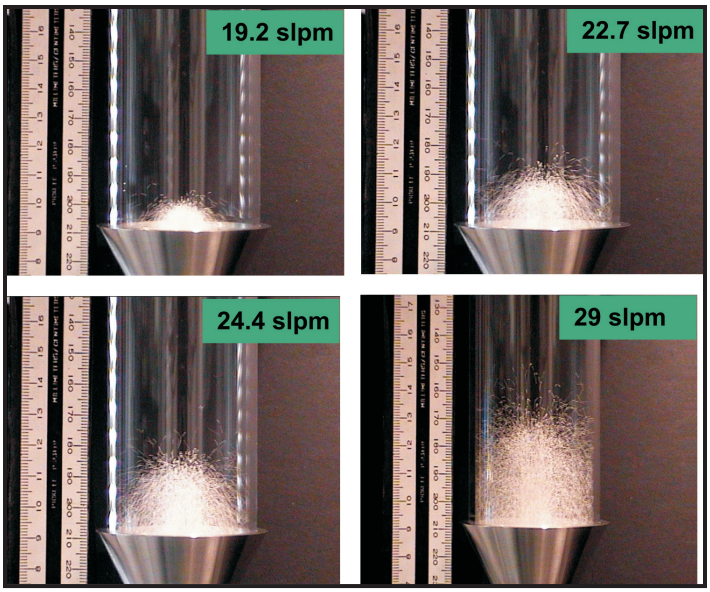

Figure 1. High-speed photographs of ZrO_2 particles in 60°, 50 mm spouted bed.

The images in Figure 1 show the profiles produced by 53.9 g of 500 µm zirconium oxide (ZrO_2) particles in the 50 mm spouted bed with a 60° cone at four different flow rates. Simulated local gas velocities tracked the experimental values taken with a small Prandtl tube. Figure 2 shows the experimental gas velocities plotted for eight different heights from the cone inlet. The model output compares well dynamically to lab data in terms of the Power Spectral Density (see Figure 3). These plots generally show transitions from one spout pinching or modulating amplitude peak to two peaks, which indicates both spout pinching and entering "bubbles" and then to one "bubbling" or pockets of fluidizing gas entering the bed amplitude peak as the gas velocity is decreased from a high to low flow rate. This demonstrates that bifurcations occur in the chaotic process. This result has major implications for the operation of coaters and deserves additional investigation.

The methodology for extracting quantitative spout height and diameter is illustrated in the series of images shown in Figure 4. The image on the left is single frame, the center is an average over many contiguous experimental frames, and the right-hand frame shows a time-averaged MFIX simulation for a vertical cross section through the center of the bed. The time-averaged images from the experiment and MFIX model agree very well.

Quantitative Definition of U_{ms}. The procedure to measure the minimum spouting velocity (U_{ms}) is similar to determining minimum fluidization velocity (U_{mf})—except visual observations are used. Starting from a fully spouting state, the gas flow rate is slowly decreased; U_{ms} has been reached when the observed particle movement stops.

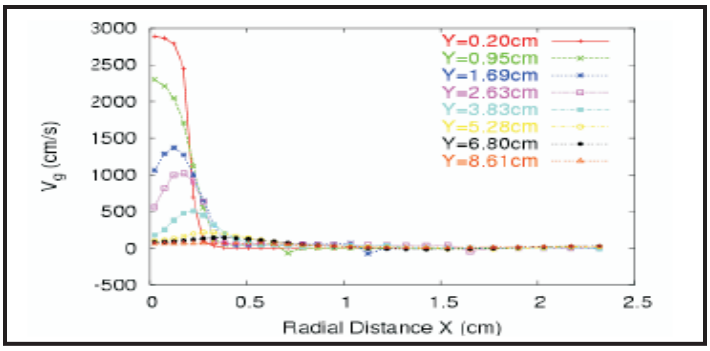

Figure 2. Experimental gas velocities as a function of radial distance and height.

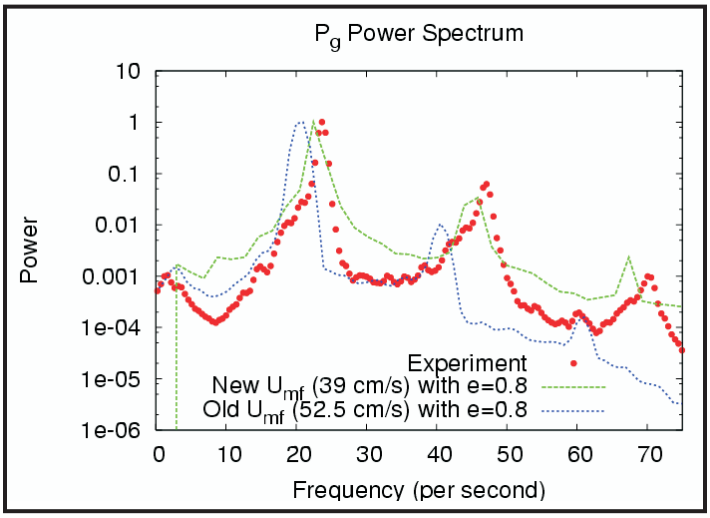

Figure 3. Experimental versus model power spectral density.

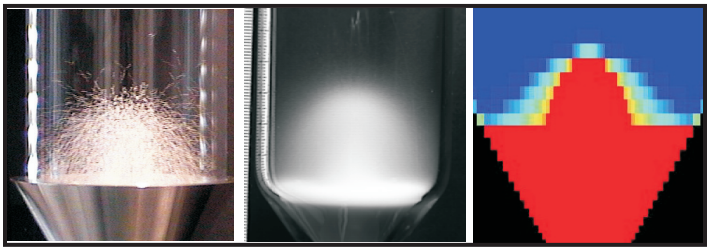

Figure 4. Methodology for extracting spout parameters: (a) 1/30th second, single-frame image; (b) average over many contiguous frames; (c) MFIX simulation.

Researchers have developed a new quantitative technique to define U_{ms}. Lowering the gas flow rate in discrete steps while measuring differential pressure (ΔP) yields a smoothly decreasing ΔP curve until it reaches a minimum value. Then, it increases sharply as gas flow is lowered further. The velocity corresponding to this minimum point is U_{ms}. Figure 5 shows an example for 53.9 g of 0.5 mm ZrO_2 in a 60° spouted bed. Here, U_{ms} occurs at a flow rate of 12.0 SLMP. This method is more reproducible than visual observations; generally, the particles appear to have stopped moving slightly before reaching the minimum ΔP.

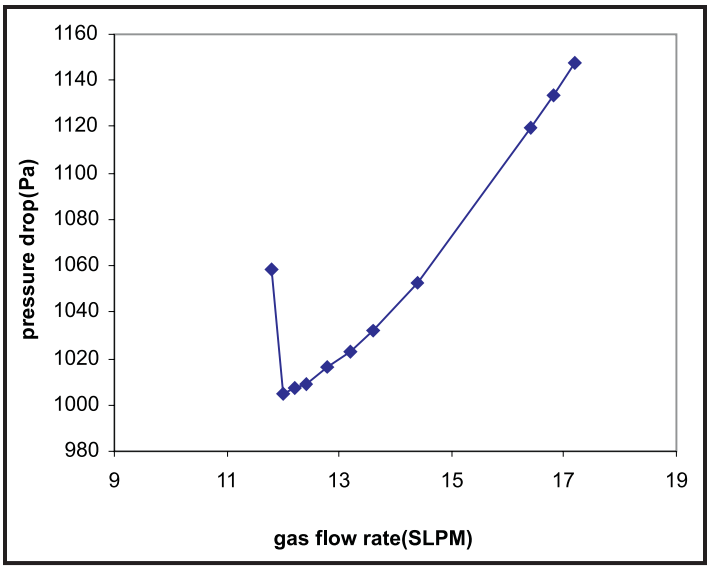

Figure 5. Quantitative measurement of U_{ms} for 53.9 g of 0.5 mm ZrO_2 in a 60° spouted bed.

Hydrodynamic Correlations. The spouted beds used for nuclear fuel particle coating are very different from those published in fluidization literature, as the nuclear coaters have very shallow beds (ratio of particle height to bed diameter < 1) and very dense particles (U specific gravity ≈ 13; ZrO_2 ≈ 7). However, the very narrow particle size distribution and nearly spherical shape make the process ideal for modeling.

The experimental matrix covers the following set of variable parameters: 1) ZrO_2 particle diameters (Dp) from 300–1,000 µm, 2) cone angles (γ) from 15–75°, 3) static particle height $0.5<H_0<1.1$ and less than cone height, and 4) fluidizing gas velocity $0.9 < U/U_{ms} < 2.5$. Fixed conditions include a 500 mm bed column diameter (Dc), 0.04 mm throat diameter (Dt), and use of ambient air at 35 percent relative humidity as the fluidization gas. Measurements of U_{mf} for ZrO_2 particles agree very well with predictions.

The U_{ms} correlation is $Re_{ms} = 0.0015\ Ar^{0.86}\ (Ho/Dc)^{0.59}\ \tan(\gamma/2)^{0.87}$.

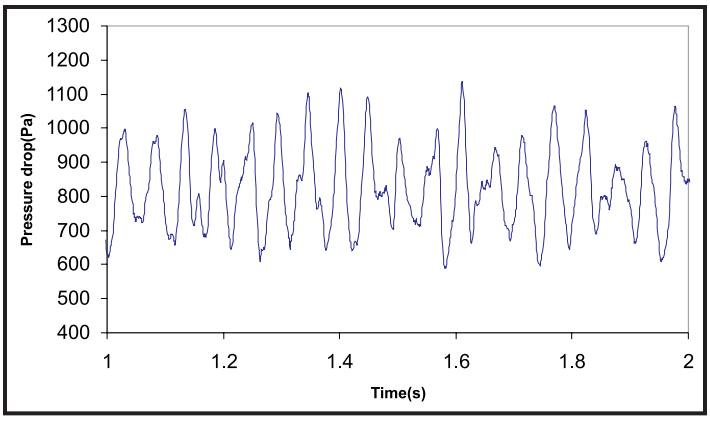

Figure 6. Fluctuations in pressure drop measured across spouted bed.

The gas pressure drop across the spouted bed fluctuates around its mean value. Figure 6 illustrates the time series for a sample case (53.9 g of 500µm ZrO_2 in 60° bed at $U/U_{ms} = 1.5$). The average ΔP is obtained by averaging data collected at 1,000 Hz over one minute.

Researchers studied the effect of all parameters in detail for the example problem. Figure 7 shows plots of ΔP versus U/U_m and log(ΔP) versus log(Ho/Dc). The following is the resulting ΔP correlation:

$$\frac{\Delta P_s}{\rho_p H_0 g} = 0.15\left(\frac{D_p}{D_c}\right)^{-0.208}\left(\frac{H_0}{D_c}\right)^{0.02}\left[\tan\left(\frac{\gamma}{2}\right)\right]^{-0.039} \qquad r^2 = 0.99$$

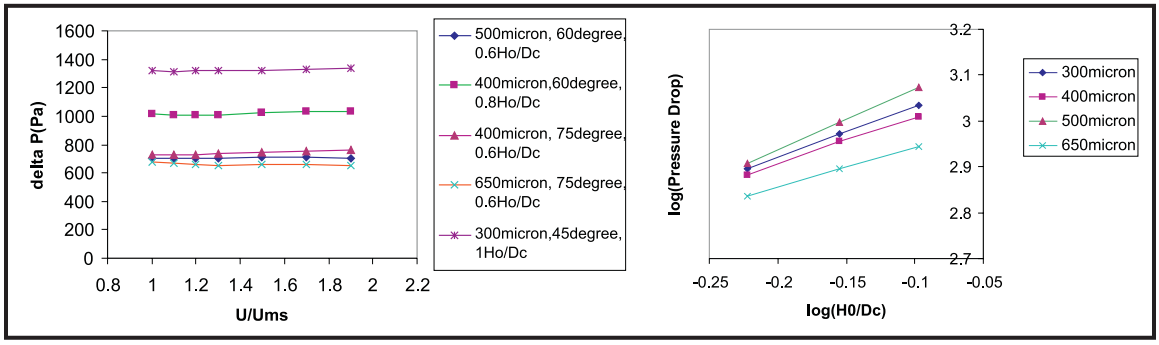

Figure 7. Pressure plots as a function of input parameters (e.g., particle size, spout angle, velocity).

The hydraulic bifurcations related to "pinching" and "bubbling" are found with respect to most process inputs. This is an important key to controlling spouted bed coaters.

Planned Activities

This project has been completed.

Nuclear Energy Research Initiative

Uncertainty Analyses of Advanced Fuel Cycles

PI: Laurence Miller, University of Tennessee

Collaborators: Argonne National Laboratory (ANL)

Project Number: 05-123

Project Start Date: March 2005

Project End Date: March 2008

Research Objectives

The objectives of this research focus on the evaluation of a variety of issues that influence the sustainability of power generated by nuclear energy. Some of these objectives are as follows:

1) Design and analyze advanced fuel cycles for light water reactors (LWRs), including boiling water reactors (BWRs)
2) Determine the effect of nuclear data and technological uncertainties on fuel cycle evaluations and evaluate the feedback of nuclear data requirements
3) Identify and assess the repository benefits of advanced fuel cycles
4) Determine the effect of uncertainties on repository benefit assessments
5) Conduct dynamic fuel cycle scenario studies to develop an understanding of the issues in the transition from thermal reactor to a mixed thermal/fast reactor fleet, or a fleet in which the majority of reactors are fast and/or accelerator-driven
6) Optimize the use of key resources, e.g., repository capacity and uranium ore, in the long term for advanced fuel cycles
7) Evaluate the optimal use of fast reactors and accelerator-driven systems from both technological and market perspectives

Researchers will model various fuel cycle options and strategies for implementation through the use of a versatile computer program, DANESS, which was developed by personnel from ANL. This code is capable of calculating numerical values of parameters that relate directly, or indirectly, to the endpoints listed in the project objectives. In addition, uncertainties in the input data will be propagated through dynamic and equilibrium fuel cycle models to determine distributions of values for the desired results. Thus, the quality of results can be evaluated and understood, and the lack of knowledge that contributes to the uncertainty of results can be identified. This will enable researchers to understand where improvements in knowledge are needed and where additional resources should be invested.

Research Progress

Significant accomplishments during the past year include the following:

1) Improvements and updates of DANESS
2) Completion of an expert elicitation to facilitate improved uncertainty analyses
3) Generation of cross-section libraries for fast reactors for determination of time-dependent isotope-specific decay heat release in a repository
4) Determination of time-dependent isotope-specific decay heat release in a repository
5) Simulations of symbiotic fuel cycles with LWRs and fast reactors with DANESS
6) Uncertainty in economics of alternative fuel cycles
7) Uncertainty assessment of equilibrium fuel cycles which includes plutonium (Pu) recycle
8) Development a neural-network-based fuel cycle simulation and optimization system

Uncertainty analyses incorporated into simulations of reactor fuel cycles were performed for LWRs and for a mixed fleet of fast reactors (FRs) and LWRs. Some of the variables considered in these simulations include the following:

1) Burnup
2) Growth rates
3) Ratios of thermal to fast reactors
4) Enrichment of fuel
5) Type of fuel cycle
6) Enrichment of fuel

Simulations that modeled mixed fleets of LWRs and FRs were completed for the following:

1) Fixed and varying numbers of LWRs with three different growth rates of FRs
2) Different initial amounts of Pu
3) Varying times of introduction of FRs

Uncertainty analyses for reactor fleets with time-dependent ratios of FRs and LWRs were simulated to determine uncertainties in inventories of Pu and minor actinides (MAs) in the overall system and in reactor cores. Results from these simulations show that expected inventories of Pu and MAs may vary by about a factor of two. Results from economic analyses show that the once-through fuel cycle is the least expensive with the least uncertainty in expected costs, while the mixed oxide (MOX) recycle in LWRs is the most expensive with the most uncertainty in expected costs. Costs, and uncertainty in costs, for mixed fleets of LWRs and FRs are intermediate to the once-through and MOX recycle in LWRs. Expected heat loads on the repository depend on assumptions of how MAs are handled.

So far, development of a neural-network-based fuel cycle simulation code has been used to provide probability density functions of integral decay heat loads and isotopic masses for a variety of reactor parameters. Future optimization routines will focus on using the previous neural network code as part of a larger graphical environment for performing quick uncertainty analyses with a flow layout according to Figure 1. The neural-network-based optimization system is shown in terms of two potential fuel cycles: the common once-through and a hybrid LWR-FR cycle with reprocessing. Each of the blocks in the previous diagram corresponds to a page in the graphical user interface (GUI) that allows the user to define parameters relevant to that stage of the fuel cycle, giving the user an intuitive way to design a fuel cycle rather than a list of inputs. The code designed for use with the GUI may also be called from the command line such that a user may run input files without navigating the GUI.

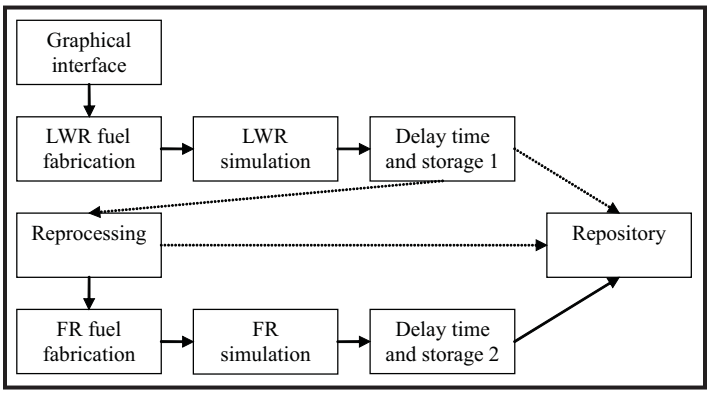

Figure 1. Flow layout of future optimization routines.

Planned Activities

Objectives for the remainder of the third fiscal year will include the completion of a system for rapid evaluation of alternative fuel cycles, incorporation of gas and molten salt reactors into the fuel cycle, and calculation of isotopic content of gas reactor fuel for use in dynamic and direct cycle fuel cycles.

Using Matlab as a foundation, a GUI will be created to define fuel cycle characteristics, outputs, and parameter distributions for use in the neural-network-based model. Within the graphical environment, a user will be able to quickly design a fuel cycle and perform an uncertainty analysis using user-selected parameters and distributions. Optimization routines within the GUI will contain three built-in cases: reduction of isotopic inventory, minimization of fuel cycle cost, and minimization of repository heat load. Each of the cases contains separate criteria that define the optimization function. For the isotopic reduction and heat load minimization cases, similar genetic algorithms will be used to find the optimal fuel cycle and reactor parameters to achieve each of the respective goals. The economic optimization case will contrast the previous physical cases in preference to capital, transportation, and storage costs associated within steps of the fuel cycle. In each of the cases, certain parameters (such as delay times in which spent fuel resides at the reactor site before it proceeds to the next step in the fuel cycle) are changed within the genetic algorithm such that an optimization of the goal is achieved with those parameters.

Assessments that include gas and molten salt reactors into reactor fleets will require additional neutronic calculations to obtain isotopic composition in spent fuel for decay heat calculations, similar to that accomplished for LWRs and FRs. These results will be used for DANESS simulations and for direct fuel cycle analyses.

Nuclear Energy Research Initiative

BWR Assembly Optimization for Minor Actinide Recycling

PI: G. Ivan Maldonado, University of Tennessee (UT)

Collaborators: Exelon Nuclear, Oak Ridge National Laboratory (ORNL), Los Alamos National Laboratory (LANL), Westinghouse Electric Corporation

Project Number: 05-125

Project Start Date: March 2005

Project End Date: March 2008

Research Objectives

The primary goal of this project is to design advanced boiling water reactor (BWR) fuel assemblies for the recycling of minor actinides (MAs), applying and extending the latest advancements in light water reactor (LWR) fuel management optimization. Two specific objectives for this project are listed below:

1) Develop a new methodology for the direct coupling between the pin-by-pin control variables and the core-wide (bundle-by-bundle) optimization objectives
2) Extend this new methodology into a new application that includes control variables, objectives, and constraints designed to maximize targeted MA incineration

The first objective is expected to uncover considerable dormant thermal margin, while the second is expected to consume some of this uncovered margin. Therefore, researchers will optimize improvements in fuel cycle efficiency to offset potential losses in efficiency associated with the recycling of MAs.

This project implements an Advanced Fuel Cycle R&D (AFCI) program initiative to investigate spent fuel treatment and recycling options for current generation LWRs, and supports the Department of Energy's technical assessment of a second high-level waste repository. The general work scope entails the following:

- ***Within-bundle activities.*** Define candidate MAs; specify control variables, objectives, and constraints at the bundle level; and generate families of lattices and bundles as a function of relevant parameters (exposure, void fraction, etc.)
- ***Core-wide activities.*** Define bundle-to-core coupling, generate families of core loadings and corresponding operational strategies (control rod patterns, core flow), and validate diffusion theory analyses via transport theory benchmarks
- ***Global integration of the project.*** Verify proper functioning of models and generate optimized advanced BWR bundles and associated fuel cycle strategies

Research Progress

A key result generated using the SCALE ORIGEN-ARP code is shown in Figure 1, which reveals the overwhelming contribution of americium (Am)-241 to the total heat load within the 100 to 1,000 year time period of LWR spent fuel in a repository environment (brown line). This expected trend has directed recent research toward Am-241 targets (in blended or heterogeneous form) for recycling purposes in a BWR thermal neutron environment.

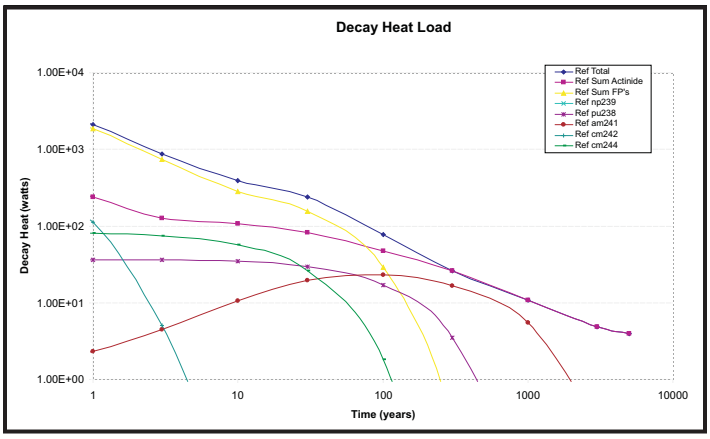

Figure 1. Decay heat load in LWR nuclear waste.

Recent work has focused specifically on combining lattice loading optimization capabilities with the new ability to test lattice designs in a 3D BWR core-wide environment. Therefore, at the lattice physics level, the optimization algorithm adjusts the concentration and location of all material loading, while pursuing objectives (e.g., power peaking minimization and/or enrichment maximization) and satisfying specified constraints (e.g., k-infinity profile versus burnup).

Figure 2 illustrates a sample optimization result that displays six classic simulated annealing "cooling cycles" (high-to-low objective function trajectories) in addition to the corresponding objectives and constraints applied. In this example, the algorithm was forced to seek higher contents of Am loading by modifying the lower constraint of Am in FORMOSA-L after each cooling cycle step. Figure 3 shows the pin arrangement and loadings in a 10x10 optimized lattice arising from this optimization, in which the Am-241 w/o is highlighted by asterisks within the shaded cells.

A general tendency observed has been the reduction of the beginning-of-cycle (BOC) uranium (U)-235 loading within the spiked pins by an average of approximately 2 w/o in order to maintain equivalent reactivity with the pre-loaded Am. This enabled the Am content to increase to more than 6.0 w/o, because the underlying intent was to eliminate larger quantities of Am, if possible, while satisfying reactivity and operational constraints. Also noticeable is the large fraction of pins which capped at or very near the five percent U-235 enrichment limit to compensate for the decrements in the spiked pins.

Once a lattice is designed, the standard process in industry is to use the lattice physics data to assemble a full 3D bundle that can be tested within a core-wide environment. This step is generally difficult, which is where the collaboration with Westinghouse Electric Corporation has been crucial to the success of this project—their software tools are designed exactly for that purpose (i.e., to design real cores).

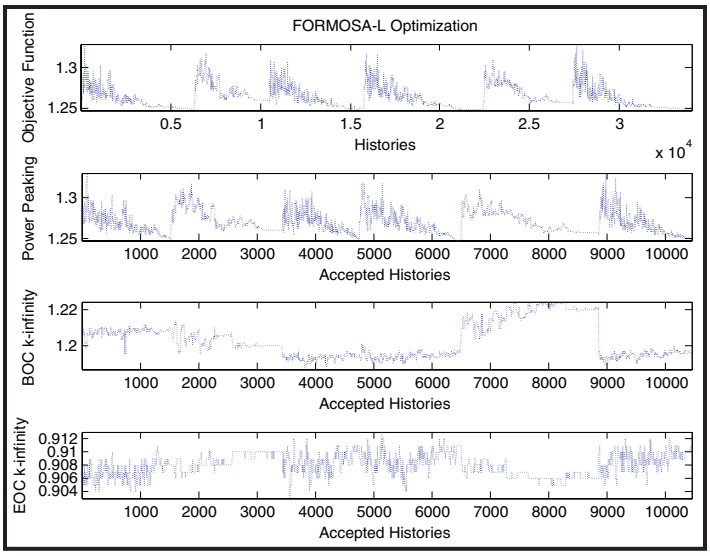

Figure 2. FORMOSA-L lattice loading optimization results.

	A	B	C	D	E	F	G	H	I	J
1	3.36	2.91 *6.01	4.21	2.70 *6.51	5.00	4.98	4.98	4.98	2.91 *6.01	3.50
2	2.91 *6.01	5.00	3.49	3.49	4.98	5.00	5.00	5.00	2.80 *6.96	2.91 *6.01
3	4.12	5.00	4.98	4.98	5,00	4.97	4.98	5.00	5.00	4.98
4	2.70 *6.51	5.00	4.97	-	WR	4.97	5.00	4.98	5.00	4.98
5	4.97	4.97	5.00	-	-	3.36	4.97	4.97	5.00	4.98
6	4.98	4.97	5.00	5.00	3.36	-	WR	5.00	4.98	5.00
7	4.97	5.00	5.00	5.00	5.00	-	-	4.98	3.49	2.70 *6.51
8	2.70 *6.51	4.97	5.00	5.00	5.00	5.00	4.97	4.98	3.49	4.21
9	3.00 *6.10	2.70 *6.51	4.97	4.98	4.97	4.97	5.00	5.00	5.00	2.91 *6.01
10	3.50	3.00 *6.10	4.98	4.97	5.00	4.97	2.70 *6.51	4.12	2.91 *6.01	3.36

Figure 3. Optimized Am-spiked lattice.

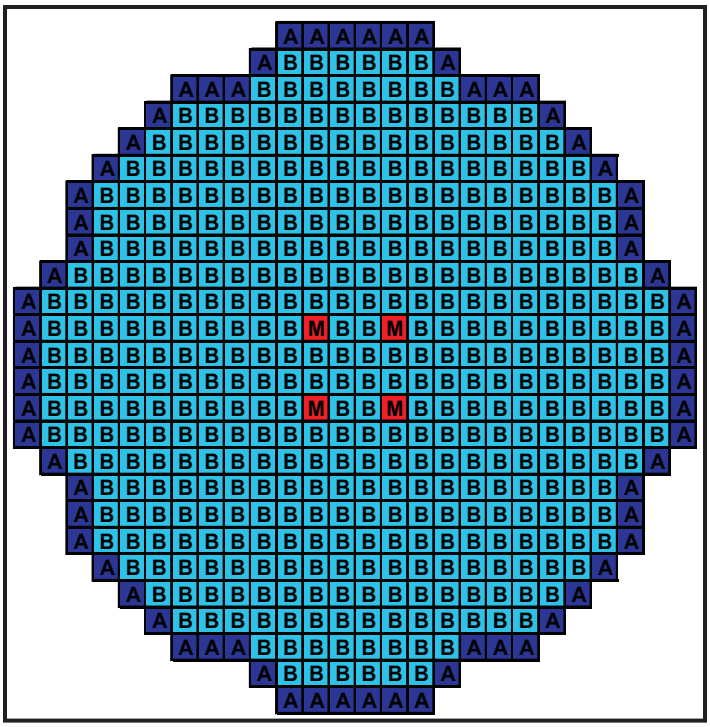

Figure 4. Core map showing location of spiked bundles.

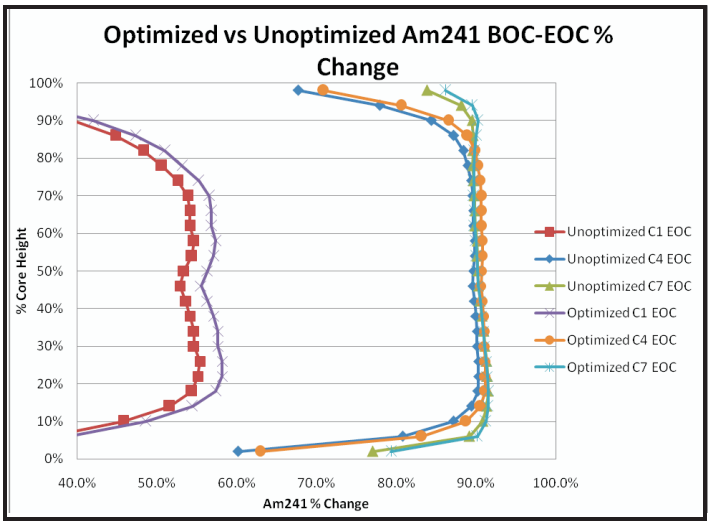

Figure 5. Axial profiles of preloaded Am-241 incineration in spiked bundles.

The approach to achieve high bundle burnup in a core-wide environment was carried out with sample reference (initial) core available with the delivered software. Researchers placed the Am-spiked bundle of interest in four symmetric locations near the central region of the core. These bundles are highlighted in "red" within Figure 4. Researchers then proceeded to simulate multiple cycle depletions, including the off-loading and reloading of all fuel, except the four Am-spiked bundles which were reinserted into each cycle in the same locations. This process was repeated for several cycles to mimic high burnup levels of up to 80,000 megawatt days per metric ton of uranium (MWD/MTU).

Using the same test core, the optimized bundle was also compared to an unoptimized bundle, one with pin arrangements and Am loadings in which the Am transmutation and power peaking was not optimized by the FORMOSA-L code at the lattice level. This bundle was then placed in the core in the same fashion as described above and the results were compared to those obtained with the optimized bundle placed in the core. Figure 5 shows the results of this comparison. First, what is noted is that the percentage change appears to reach some equilibrium value at high burnups (approaching 60-80,000 MWD/MTU); however, at lower burnups, the optimized bundle preferentially destroys the Am-241. These results serve as an illustration of the benefit of the optimization scheme, as there is an approximate three percent difference at the end of Cycle 1.

Planned Activities

The latest research results presented in this report show a new implementation of lattice loading optimization of Am-spiked bundles subjected into a core-wide BWR 3D environment. Transmutation rates of planted Am-241 exceed 90 percent incineration levels at high burnups in a fairly uniform manner along the axial length of the bundles, indicating the viability of LWRs to efficiently destroy certain MAs.

Currently, the test cases performed utilized hypothetical/sample core designs, though more realistic core-wide environments than any previously employed. Researchers are currently in the process of implementing a full core model for a more realistic test bed that uses a Quad Cities Unit 2 Optima-2 Equilibrium Cycle. This has been possible, again, by the collaboration with Westinghouse, but also due to the participation of Exelon Nuclear.

Nuclear Energy Research Initiative

Optimization of Oxide Compounds for Advanced Inert Matrix Materials

PI: Juan Nino, University of Florida

Collaborators: Imperial College of Science, Technology, and Medicine (U.K.); Idaho National Laboratory (INL)

Project Number: 05-134

Project Start Date: April 2005

Project End Date: March 2008

Research Objectives

The objective of this project is to develop oxide ceramics with optimal thermophysical properties for use as inert matrix fuel (IMF) in the current generation of light water reactors (LWRs). The approach, entailing a combination of computation and experiment, focuses on the materials science of oxide compounds and composites that exhibit minimal radiation swelling, high thermal conductivity, excellent hot water corrosion resistance, and reprocessing compatible with UREX+ processes.

An important benefit of using optimized IMF materials, rather than conventional uranium oxide (UO_2) fuel, is that their higher thermal conductivity will considerably reduce the fuel centerline temperature and minimize the impact of a loss-of-coolant accident. In addition, using IMF will avoid formation of transuranic fission products by neutron capture, thereby allowing higher fuel burnup and reducing waste. Finally, the improved corrosion resistance will ensure that the IMF is compatible with the coolant under cladding breach accidents.

Research Progress

Five different processing methods have been utilized to synthesize several magnesium oxide (MgO)-$Nd_2Zr_2O_7$ (NDZ) cercer composite batches. Pellets have been formed and sintered and the microstructure variation among same batch samples and between the batches is being characterized. The characterization of composites synthesized in the sintering kinetics study also continues. Thermal diffusivity, specific heat capacity, and thermal expansion measurements have been performed on the composites and have begun on the constituent phases. Preliminary results indicate that the 70 vol% MgO composite is coarsening-resistant due to the dual-phase interpenetrating microstructures. Because of the coarsening-resistant nature of this composite, there is a negligible effect on the thermal diffusivity between the composites sintered in the 1,450°C isothermal series and between composites sintered in the four-hour isochronal series. The average thermal conductivity of the composites is approximately 11 $Wm^{-1}K^{-1}$ at 800 K. The different processing methods have a small effect on the thermal conductivity, with a difference of approximately 2 $Wm^{-1}K^{-1}$ between the ball milled composite with the highest thermal conductivity and the Turbula mixed composite with the lowest thermal conductivity. The primary effect of processing has been on the degree of measurement dispersion between composite pellets synthesized from the same batch. Ball milling, Spex milling, and Turbula mixing have relatively small standard deviations when the diffusivity data from the three pellets of the same batch are compared, while magnetic bar mixing and mortar

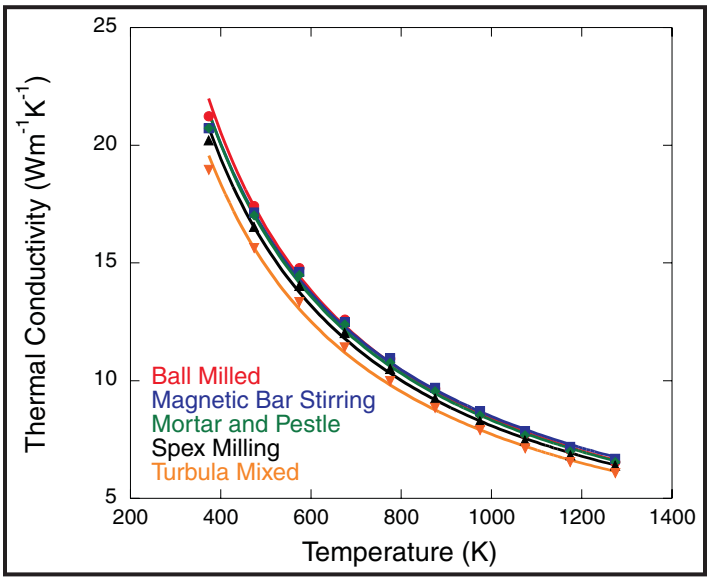

Figure 1. Experimental thermal conductivity of $Nd_2Zr_2O_7$-MgO composites (30:70 by volume) as a function of temperature for the different processing techniques investigated. Results based on laser flash thermal diffusivity and calorimetry and thermal expansion data.

and pestle have relatively large standard deviations. This indicates that processing does not necessarily have a significant effect on the average thermal conductivity of the composite, but rather on the consistency of the data over a larger number of samples. A summary of the thermal conductivity curves is presented in Figure 1.

Kr was chosen as the irradiation source to simulate the fission fragment effects due to its better penetration effect. Magnesium tin oxide (Mg_2SnO_4) was irradiated at 50 K, 150 K, and 300 K. The amorphization dose for Mg_2SnO_4 is determined as $5\text{-}10^{19}$ ions/m^2 at 50 K and 10^{20} ions/m^2 at 150 K. The irradiation dose reached $5\text{-}10^{19}$ ions/m^2 for Mg_2SnO_4 at 300 K, but there was no sign of amorphization. Even though the exact amorphization dose for Mg_2SnO_4 at 300 K is currently unknown, the value should be greater than 10^{20} ions/m^2, suggesting Mg_2SnO_4 is a very irradiation-resistant material. Irradiation tests were also performed for magnesium oxide aluminum oxide ($MgO{\cdot}2.0Al_2O_3$) at 50 K and 300 K. The final dose is $1.5\text{-}10^{19}$ ions/m^2 for the irradiation test conducted at 50 K and $3\text{-}10^{19}$ ions/m^2 at 300 K, but neither of the specimens became amorphous after irradiation. Therefore, the amorphization doses for $MgO{\cdot}2.0Al_2O_3$ at 50 K and 300 K should be greater than the final doses, but the exact values are still unknown.

For the reprocessing task, hot water corrosion tests on the MgO-NDZ composite pellets continued and were performed at multiple temperatures on different composite compositions to investigate the thermal nature of the hydration process. It was found that the hydration process is thermally activated (follows Arrhenius behavior) with a calculated activation energy of 52 kJ/mol for the 60 vol% MgO composite, 44 kJ/mol for the 50 vol% MgO, and 40 kJ/mol for the 40 vol% MgO. The corroded pellets were examined using scanning electron microscopy (SEM) and a representative microstructure is presented in Figure 2. The presence of plate-like residual magnesium hydroxide ($Mg[OH]_2$) as a residual byproduct is clearly observed.

For the computational simulation, an analysis based on anharmonicity and the Grüneissen parameter was carried out to assess the quality of the interatomic potentials used for the simulations of the thermal conductivity of both MgO and NDZ. It was found that these potentials should yield thermal conductivities of MgO and NDZ that are 1.02 times and 1.61 times their experimental counterpart, respectively. The simulation study of the temperature dependence of

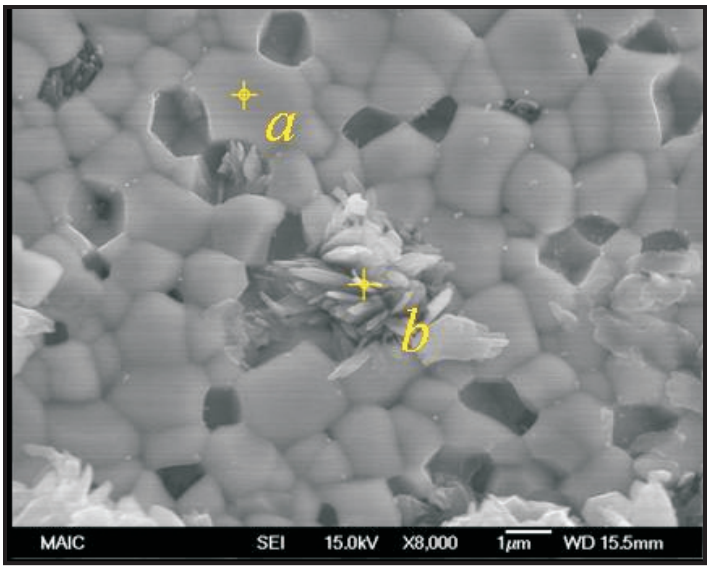

Figure 2. SEM of the MgO pyrochlore composite where $Mg(OH)_2$ platelets (hydration corrosion byproduct) are observed.

the thermal conductivity of NDZ polycrystal was completed. A new code to generate MgO-NDZ composites of various connectivities and compositions was developed. The temperature dependence of the thermal conductivity of $MgAl_2O_4$ spinel has been determined. To address the role of cation antisite disorder, researchers built 50 percent inverse and 100 percent inverse $MgAl_2O_4$ structures. Determination of their thermal expansion coefficients is ongoing.

Planned Activities

In accordance with the project's objectives and timeline, the team will continue quantification of the microstructures synthesized by the different processing methods and the sintering kinetics study. Thermal diffusivity and thermal expansion measurements of the composite will also be completed. Composite pellets will be synthesized from the stabilized slurry by gel casting and the microstructure of the composite will be characterized by SEM and hydrothermal corrosion. Chemical composition analysis will be carried out for the irradiated Mg_2SnO_4 by using energy dispersive spectroscopy (EDS) in order to evaluate the chemical stability. As part of the thermophysical property simulation component, MgO-NDZ nanocomposites will be built. Finally, the thermal-transport properties of the MgO-NDZ composite and $MgAl_2O_4$ spinel with differing degrees of inversion will be simulated.

Nuclear Energy Research Initiative

Synthesis and Optimization of the Sintering Kinetics of Actinide Nitrides

PI: Darryl P. Butt, Boise State University

Collaborators: University of Florida

Project Number: 05-135

Project Start Date: August 2005

Project End Date: July 2008

Research Objectives

The primary objective of this project is to develop processing models and to perform an economic analysis on the synthesis of nitride-based nuclear fuels. Such fuels, particularly those based on uranium-nitride (UN) and plutonium-nitride (PuN), are candidates for the Advanced Fuel Cycle R&D (AFCI) program. Nitride-based fuels have a combination of higher uranium loading and higher thermal conductivity compared to other fuel forms, thus lower enrichment can be used. It is also possible to produce inert matrix fuels because of their compatibility with candidate matrices, such as zirconium-nitride (ZrN) and refractory metals. Although several processes have been developed for synthesizing powder and monolithic forms of actinide nitrides, the sintering kinetics and mechanisms are not fully understood. Having a quantitative understanding of the mechanism and kinetics of densification and grain coarsening is critical to ensure both satisfactory product performance and favorable economics of any ceramic fabrication process. Through optimized processing conditions, sintering temperatures and equipment size can be greatly reduced, production rates can be increased, and properties can be improved and more precisely controlled.

In this study, researchers will synthesize actinide and surrogate powders of varying morphologies and particle size. They will thoroughly characterize the powders and press them into fuel forms. Detailed sintering studies will be conducted in order to assess the specific rate equations and kinetics models as a function of time and temperature, grain size, and other processing variables. By applying these fundamental models and combining microstructural characterization, the researchers will determine rate-limiting and process-controlling mechanisms for comparing transport properties (including solid state diffusion and gas transport). An end result of these studies will be a processing model and economic analysis that will enable fuel processing to be done at lower temperatures, shorter times, and with less costly infrastructure.

Research Progress

Research conducted for this NERI project has advanced the understanding and feasibility of nitride nuclear fuel processing. In order to perform this research, necessary laboratory infrastructure was developed, including basic facilities and experimental equipment. Notable accomplishments from this project include the synthesis of UN, dysprosium-nitride (DyN), and cerium-nitride (CeN) using a novel low-cost, room temperature, mechanical method; the synthesis of phase-pure UN, DyN, and CeN using thermal methods; and the sintering of UN pellets from phase-pure powder that was synthesized in the Advanced Materials Laboratory at Boise State University. To date, this work has been shared in the form of two scientific journal submissions and six conference presentations on the following subjects:

- **Novel Ball-Milling Synthesis Route:** This route was demonstrated by nitriding pure uranium metal filings from ingot, 99.9 percent pure dysprosium metal filings, and 99.9 percent pure cerium metal filings at room temperature for 24 hours, yielding U_2N_3, DyN, and CeN, respectively. Shown in Figure 1a is the ball milling jar with pure uranium metal filings and yttria stabilized zirconia (YTZ) milling media. Figures 1b and 1c show the resultant nitride powder and the x-ray diffraction (XRD) pattern showing the formation of phase-pure U_2N_3.
- **Uranium Nitride Pellet Sintering:** The sinterability of UN was studied by sintering two 13 mm diameter pellets with different binders, namely Polyvinyl Butyral and Polyethylene Glycol.

- **Direct Nitriding Route:** This route was demonstrated by nitriding 99.9 percent pure dysprosium metal filings at 1,300°C, yielding a phase-pure DyN powder with an oxygen content of 0.33 percent.
- **Hydriding prior to Nitridation Synthesis Route:** This route was demonstrated by the synthesis of UN, DyN, and CeN. Pure uranium metal ingot produced an estimated 92 percent pure UN. Very high-purity DyN and CeN with 0.043 and 1.4 percent oxygen contents, respectively, were produced by 99.9 percent pure dysprosium and cerium metal filings.
- **Carbothermic Reduction prior to Nitridation Synthesis Route:** This route was demonstrated by the synthesis of UN, DyN, and CeN. The carbothermic reduction of UO_2 has proven to provide the largest amount of phase-pure UN for other related studies. Also, this route has been utilized to produce low-quality DyN and CeN.
- **Oxidation Kinetics of DyN:** Thermal gravitational analysis has been performed from room temperature to 800°C to identify a suitable oxidation range for isothermal studies. Ten isothermal gravitational analysis runs have been made for 6 hours to describe the weight change of the DyN as it converts to Dy_2O_3. Further analysis of the data needs to be completed to correlate it to the kinetics of oxidation and to identify a mechanism.
- **Iodide Route:** This route may also be used in the future as a possible synthesis route for UN at very low temperatures. However, more experimental detail is needed to achieve optimum conditions for nitride synthesis, especially regarding the solubility of uranium iodide in a suitable organic solvent.
- **Sintering/Hot Pressing:** The optimum conditions for sintering pure ZrN were determined and the maximum density achieved was approximately 83 percent theoretical density. Therefore, hot-pressing was used to achieve higher densities. The results of the ZrN-DyN hot-pressing clearly show that DyN does not form a complete solid solution with ZrN.

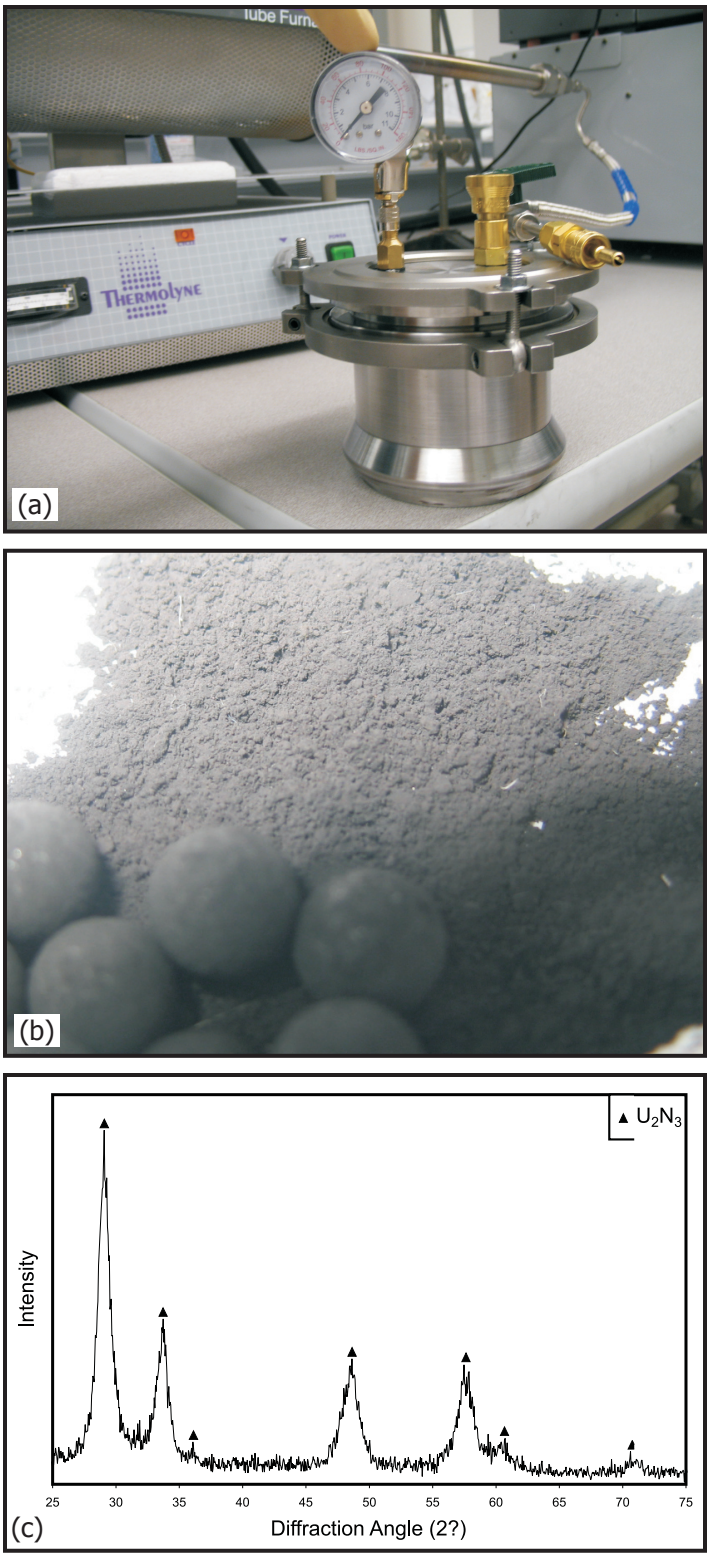

Figure 1. Uranium nitride produced at room temperature by mechanically induced gas-solid reaction method. After a detailed literature review, the work of synthesizing uranium nitride, or any other actinides or lanthanides, at room temperature by the use of a ball mill has never been published. This work is very promising due to the extremely low cost of synthesis and its applicability to synthesizing actinide nitrides. (a) Planetary ball mill container that allows for multiple charges/purges to 420 kPa with oxygen-gettered UHP N_2 during the milling process. (b) Photograph of the powder formed after 24 hours of ball milling pure uranium metal filings. (c) X-ray diffraction pattern distinguishing phase-pure U_2N_3 powder.

Planned Activities

The future work of this project will focus on the following two areas:

- Sintering UN with and without additives (DyN and CeN)
- Refining the novel nitride synthesis routes

To begin, it would be reasonable to perform the UN sintering study using the highest purity nitride powders. Based on the quality of the nitrides produced, the hydride-nitride route will be used to produce DyN and CeN and the carbothermic reduction route will be used to produce UN for the sintering studies. Researchers will continue optimizing the sintering cycle of pure UN by controlling the particle size, pressing conditions, overall sintering profile, and atmosphere (vacuum or argon). Once the UN sintering process is optimized, they will begin to study the effects of additives on the process. DyN, in concentrations up to 50 percent (equivalent to the americium-nitride [AmN] concentration in the proposed inert matrix nitride fuel), will be the first binary system studied. Thermo-gravimetric analysis (TGA) and differential scanning calorimetry (DSC) analysis will be conducted to understand the phase changes, oxidation rates, and volatility of the UN and DyN systems, separately. This information will be used to design the UN-DyN sintering cycle for optimum density and microstructure. Based on the success of the UN-DyN study, researchers will begin to study the UN-CeN system.

Regarding the refinement of the nitride synthesis routes, the results shown in this report indicate that many nitride routes can be used to produce high-purity UN, CeN, and DyN powders. However, due to the economic feasibility and potential for drastically reducing the processing facility footprint, the team will focus on refining the novel routes, specifically the mechanical gas-solid reaction and direct nitridation routes. In particular, they will focus on characterizing the nitride powders produced by the novel routes using available characterization techniques to determine particle sizes, morphologies, and purity levels. The ultimate goal is to optimize processing parameters to produce the highest purity nitrides possible using the most economically feasible approach.

Nuclear Energy Research Initiative

The Development of Models to Optimize Selection of Nuclear Fuel Materials through Atomic-Level Simulation

PI: Simon Phillpot, University of Florida

Collaborators: Los Alamos National Laboratory

Project Number: 05-136

Project Start Date: April 2005

Project End Date: April 2008

Research Objectives

The objective of this project is to develop an advanced fuel performance calculational platform, based on the FRAPCON code, using databases to provide detailed nuclear material properties input. Currently, all fuel performance codes are based on correlations derived from experimental data. However, these correlations cannot be extrapolated to operating conditions beyond the experimental points on which the correlations are based, nor can they be used for materials lacking experimental data.

Figure 1 provides a schematic of the key tasks of this work. Researchers will evaluate the possibility of extending performance codes to new materials based on databases developed from state-of-the-art electronic-structure, thermodynamic, atomistic, and first principles calculations. They will use these databases to create a prototype of a new generation of advanced fuel performance codes. Pertinent inputs include material composition, temperature, density, closed porosity, surface roughness, fuel grain size, sintering temperature, and fractional cold work of the cladding. The code, based on "first principles," will reduce costs associated with fuel development programs—transforming the current selection process, which relies on costly and time-consuming experimentation, into a process based on modeling, simulation, and analysis that requires only confirmatory irradiation testing.

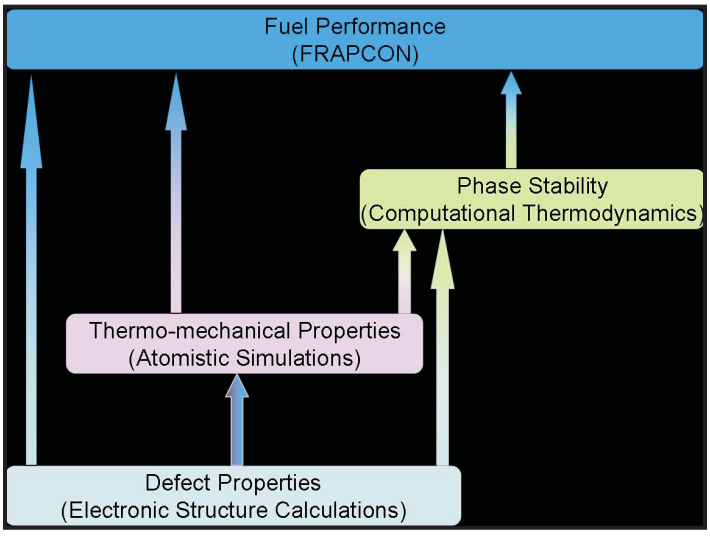

Figure 1. Key tasks of the project and connections among them.

Research Progress

The FRACON code has been modified to accept input for the thermal conductivity and thermal expansion of unirradiated uranium dioxide (UO_2) from the first-principles simulations. Strong agreement between the hard-wired FRAPCON results and FRAPCON with input from molecular-dynamics simulations was obtained for the temperature profile through a pellet and for pellet expansion at beginning-of-life (BOL), as shown in Figure 2.

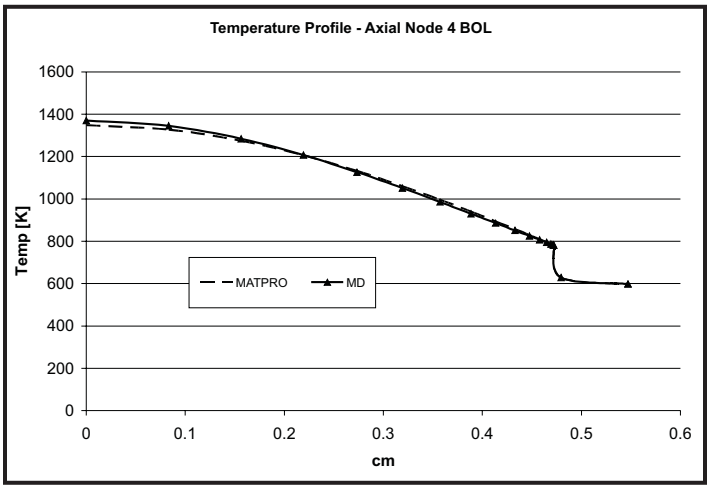

Figure 2. The temperature profile through a fuel pellet at BOL, as calculated with the thermal conductivity calculated from the *ab-initio* simulations, is in excellent agreement with that determined from the model built into the FRAPCON code.

A systematic analysis of the effects of polycrystalline microstructure on the thermal conductivity of UO_2 has been performed and analyzed. It was found that the presence of grain boundaries has a very significant effect on the thermal conductivity in the sub 0.1 μm grain size region, but is not important for grain sizes above 1 μm. The effects of off-stoichiometry in UO_2 on the thermal conductivity have been analyzed. As Figure 3 shows, even relatively small deviations from stoichiometry can have a significant effect. Interestingly, for large degrees of off-stoichiometry, the thermal conductivity is essentially temperature independent over the temperature range of interest to operating reactors. This arises from the very short mean free paths of the vibrational excitations in these systems. The methodologies required for radiation damage simulations have been developed and fully validated. These include thermostatting procedures for the simulation cell; the development of a completely new and efficient method for dynamically adjusting the time step; and the implementation of Ziegler, Biersak, and Littmark potential, which is needed to describe short-ranged interatomic interactions for radiation damage simulations.

Electronic structure calculations within Vienna *Ab-Initio* Simulation Package (VASP), using spin-polarized LDA+U, have given researchers high-quality data for the energetics of the formation of intrinsic defects in UO_2. As Figure 4 illustrates, a detailed thermodynamic analysis shows how the defect energetics depends on temperature and on the chemical environment (oxidative vs. reducing).

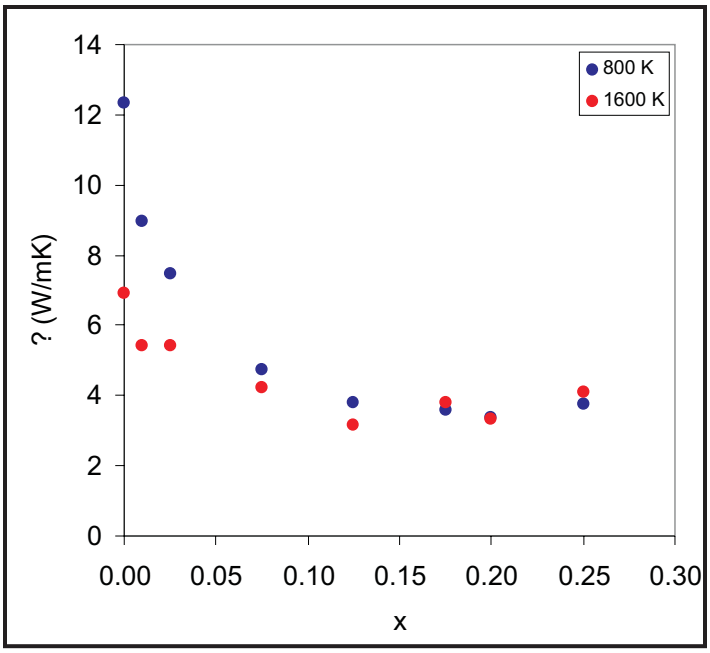

Figure 3. The thermal conductivity of UO_{2+x} only depends on temperature and stoichiometry for near-stoichiometric compositions.

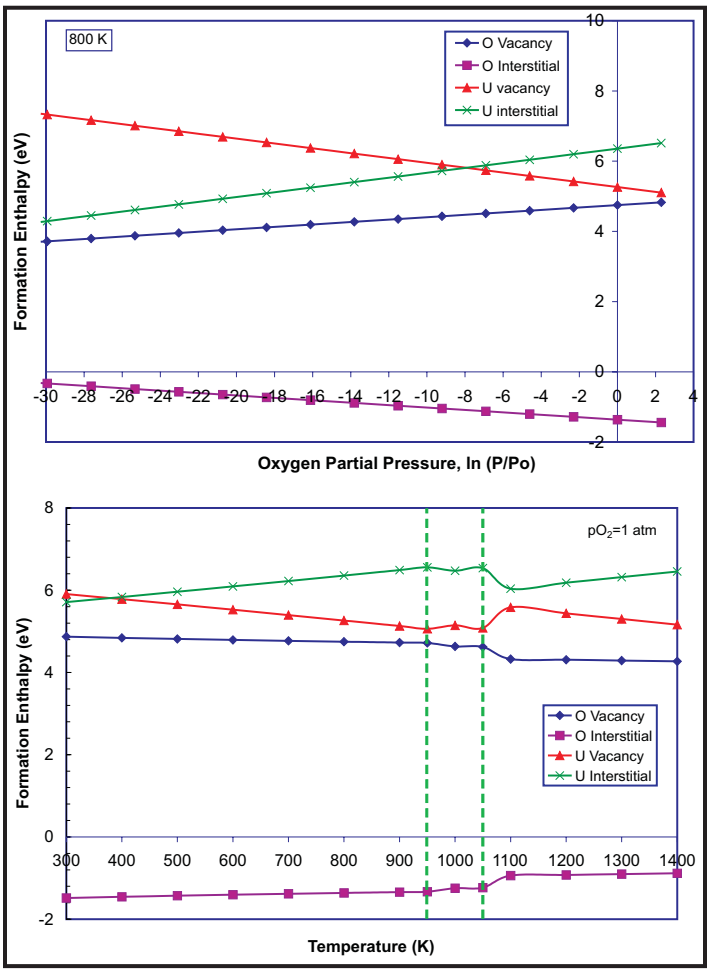

Figure 4. The oxygen partial pressure and temperature can have significant effects on the formation energies of intrinsic point defects in UO_2.

Planned Activities

The remaining few months of this project will focus on completing analysis and publication of the key results from the research performed. This will include papers on the following:

- The performance of the FRAPCON code with input from *ab-initio* simulation results
- The simulation of the thermal-transport properties of off-stoichiometric UO_2
- The detailed characterization of the methodology for the simulation of radiation damage in UO_2
- The analysis of the thermodynamics of intrinsic point defects in UO_2

Nuclear Energy Research Initiative

Development of TRU Transmuters for Optimization of the Global Fuel Cycle

PI: John C. Lee, University of Michigan

Collaborators: None

Project Number: 05-142

Project Start Date: April 2005

Project End Date: March 2008

Research Objectives

The objective of this project is to develop advanced fuel cycles for the transmutation of transuranic (TRU) elements in irradiated nuclear fuel from light water reactors (LWRs). Researchers will use a systematic, integrated approach to evaluate diverse fuel cycles and energy production systems in order to optimize the global fuel cycle.

This project will study deployment of fast-spectrum transmuters, together with LWRs and advanced reactors, to minimize the risks associated with disposing and storing irradiated nuclear fuel in underground repositories. Such risks include radiological toxicity, proliferation, and radiological dose of the irradiated fuel. Researchers will develop an equilibrium fuel cycle methodology to consistently compare LWR transmuter performance with other designs. Key objectives include the following:

- Develop an optimization methodology that could systematically optimize core configurations both for LWRs and sodium-cooled fast reactors (SFRs)
- Study synergistic deployment of LWRs and SFRs for global fuel cycle optimization as envisioned in the Global Nuclear Energy Partnership (GNEP)

Research Progress

During the first year, researchers developed an equilibrium search algorithm to systematically compare the performance of diverse fuel cycles in order to conduct global fuel cycle analysis. The algorithm is similar to the REBUS-3 fast reactor methodology, but with macroscopic depletion capabilities typically employed for LWR analysis. To illustrate the usefulness of the LWR equilibrium methodology, and to explore ways to efficiently transmute legacy plutonium in spent nuclear fuel, the researchers studied the use of thorium in an alternate pressurized water reactor (PWR) fuel cycle.

During the second year, researchers focused on developing an optimization methodology that can account for constraints in the overall fuel cycle. They developed a basic formulation, applicable to both LWR and SFR core configurations, using the calculus of variations. The algorithm uses a direct adjoining approach to optimize various fuel cycle objective functions in a few iterations, while explicitly and rigorously representing the power peaking inequality constraint. An initial effort was made to obtain optimal burnable absorber (BA) and fuel loading patterns for PWR configurations, successfully demonstrating the feasibility of obtaining fuel configurations that offer better performance than reported in the AP600 Standard Safety Analysis Report (SSAR). The optimal core design, systematically obtained, yields a lower power peaking factor with fewer BA rods and extends the cycle length.

During the current year, significant effort has been made to extend the fuel cycle optimization methodology to SFR configurations by incorporating the algorithm into the DIF3D/REBUS package. The optimization algorithm for a SFR core consisting of hexagonal fuel assemblies with a G-group, N-nuclide microscopic depletion structure, requires a $(2G+N+3)$-dimensional system vector. The capability of the algorithm for optimizing TRU loadings in a representative SFR design is illustrated by comparing the optimized and unoptimized power maps in Figure 1. Together with a reduction of the peak-to-average power density (i.e., the power peaking factor) from 1.75 to 1.25, the optimized core decreases the reactivity swing over the cycle from 3.34 to 2.72 $\%\Delta K/K$. This compares favorably with a reference SFR transmuter design from the Argonne National Laboratory (ANL) that indicates a power peaking factor of 1.35 and reactivity swing of 2.94 % $\Delta K/K$. The optimization is achieved in a few iterations and provides physical insights to the optimization process itself.

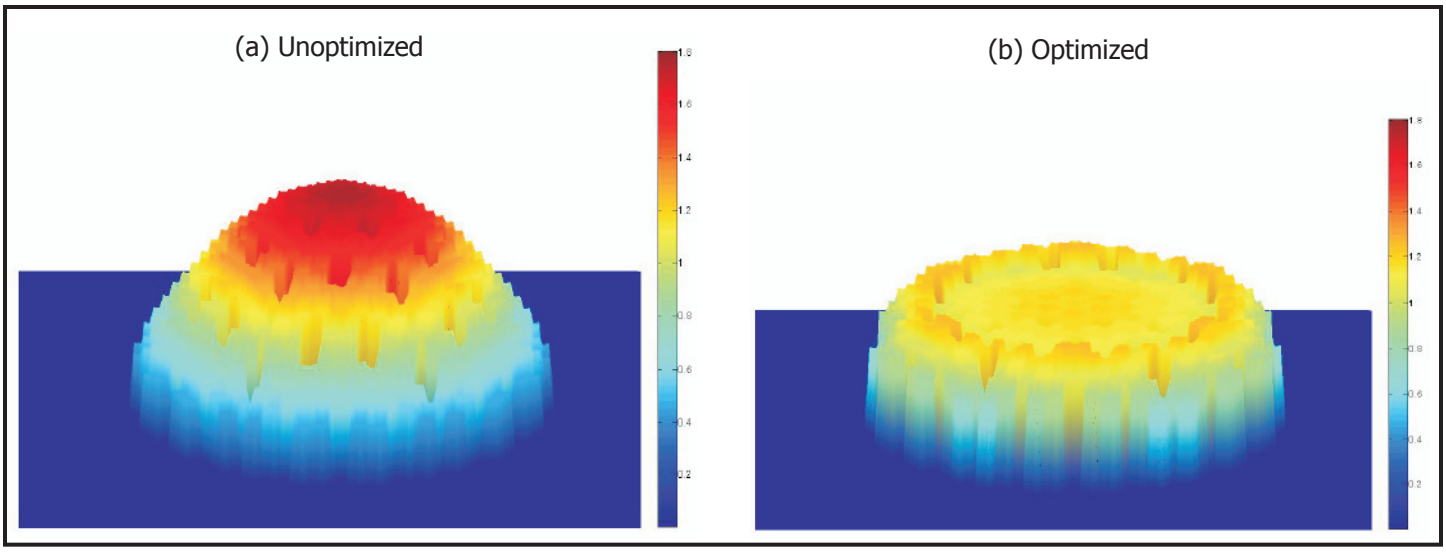

Figure 1. Comparison of unoptimized and optimized power distributions for an SFR configuration, illustrating a significant reduction in the power peaking factor.

In an effort to evaluate diverse nuclear fuel cycles, researchers have developed an equilibrium TRU management scheme that could provide sufficiently accurate calculations of the heavy metal (HM) inventory and fuel cycle economics. The Equilibrium Operation Fuel Cycle Model (EO-FCM) is an Excel-based script that provides a simple calculation of key fuel cycle parameters using an equilibrium operation (EO) approximation for a nuclear park scenario consisting of two reactor types. By matching the total electricity generated in the nuclear park, the EO model tracks, with good accuracy, the transition operation (TO) mode that the VISION code and other dynamic fuel cycle models represent. EO-FCM calculations have been performed for once-through and mixed oxide (MOX) cycles for LWRs and for TRU fuel cycles for SFRs.

Planned Activities

Researchers will perform the following tasks during the remainder of this project:

- Study optimized LWR fuel cycles by extending the capability of 2-D fuel cycle optimization algorithm to include alternate objective functions
- Optimize SFR transmuter performance by incorporating heterogeneous core designs and optimal placement of TRU target assemblies using the new optimization algorithm developed in a modified DIF3D/REBUS code
- Further develop the capability of the equilibrium-operation fuel cycle model for efficient TRU management and fuel cycle economics
- Formulate simplified models to provide physical insights and guidance for evaluating diverse fuel cycles, in parallel with developing optimal cycles

Nuclear Energy Research Initiative

The Adoption of Advanced Fuel Cycle Technology Under a Single Repository Policy

PI: Paul P. H. Wilson, University of Wisconsin-Madison

Collaborators: Argonne National Laboratory (ANL)

Project Number: 05-157

Project Start Date: April 2005

Project End Date: March 2008

Research Objectives

This project will develop models to study the impact of a policy that retains a single spent fuel storage repository at Yucca Mountain. An increasing amount of technology-driven analysis is being done to determine how reprocessing and separation technologies can improve the loading of Yucca Mountain while maintaining the same general design concept and licensing basis. However, little policy-driven analysis has been conducted to study the adoption of new reprocessing and separation technologies assuming that only one repository is constructed. Given the current mismatch between the legislative capacity limit at Yucca Mountain and the expected spent fuel inventory from the existing reactor fleet, a single-repository policy would likely improve the economic attractiveness of advanced fuel cycle technologies. In addition, this project will study the relationship between fuel cycle advances driven primarily by repository performance and those advances necessary for a transition to a sustainable fuel cycle that is both economical and feasible. It will support the Department of Energy's evaluation of additional geologic repositories for spent nuclear fuel (beyond Yucca Mountain), which is one of the near-term goals of the Advanced Fuel Cycle Initiative.

Research Progress

The most advanced fuel cycle modeling tools include VISION, developed primarily by Idaho National Laboratory (INL), and DANESS, developed primarily by ANL. Through collaborations with these labs, researchers have studied the capabilities of these tools with respect to economic modeling of repository benefit. The repository models for VISION and DANESS did not include the necessary features to support economic repository benefit calculations. Most importantly, both tools simply tracked the accumulation of waste mass, whether spent nuclear fuel or high level waste (HLW), with no consideration for how the different waste streams consume different amounts of space in the repository. Whereas VISION did not consider repositories by mass or volume, DANESS offered an interface that suggests finite-sized repositories and the need to construct additional repositories, just as it does for other fuel cycle facilities. However, the default behavior of DANESS is to not allow the construction of additional repositories; hence, DANESS simply overfills the available repository. Furthermore, even after minor modifications to allow the construction of repositories, there is no feedback of the cost of a repository (known or assumed) into the total fuel cycle costs.

A repository capacity model has been implemented that will allow systems to express the quantity of waste in terms of the required repository space (length of drift tunnel) rather than in terms of mass. This is a critical step in eventually determining an economic repository benefit of reprocessing, distinct from the technical repository benefit. This model is based on the repository thermal analysis performed by Wigeland, Bauer, et al., at ANL. Three important limiting cases were previously identified for the Yucca Mountain design basis and a simplified model was developed for each case. A thermal response is determined for each of the isotopes tracked by VISION and linear superposition is used to determine the response for a given waste stream by weighting the isotopic response by its mass fraction. For the drift wall limits, the thermal response is an effective decay power, taking into account the change in power over the thermal time scale of the near-field host rock. At emplacement, the effective decay power is a linear combination of the initial power and the power at 0.3 years. At closure, the decay power is changing so slowly that the instantaneous decay power at closure suffices. For the mid-drift temperature limit, the thermal response is the mid-drift temperature change per unit mass. While

strict superposition does not hold for this response, testing showed that 1) it was valid in the limit of very high thermal loadings, and 2) a maximum error of 7.6 percent was considered reasonable for the high-level systems analysis application of the model.

It is important to be able to consider the amount of energy that has been delivered by a particular waste stream. With the potential for many recycles and materials flowing in many streams, the simple notion of fuel burnup as a measure of delivered energy is no longer practical. This work will concentrate more on the theoretically available fission energy (embodied potential energy [EPE]) and the expended fission energy (embodied delivered energy [EDE]). The simplest approach is to ascribe roughly 180 MeV of EPE to every remaining actinide atom and roughly 90 MeV of EDE to each fission product atom. This results in approximately 1 MWd_{th}/g of EPE for actinides and a similar quantity of EDE for fission products. This concept is directly related to the already demonstrated repository benefit of recycling spent nuclear fuel. The variable cost of constructing a deep geologic repository is dependent on the length of the tunnels and is independent of the EDE being disposed in those tunnels.

It is useful to formulate a repository loading and costing model based on the available space in the repository. However, the total cost of waste disposal is best expressed in units of cost per unit energy. A model that permits both of these goals is proposed in equation where *C* is the disposal cost per unit of energy generated [$/MWh], *U* is the unit cost of space in the repository [$/m], ρ_{limit} is the limiting waste loading density [kg_{HLW}/m], α is the fraction of the HLW that is composed of fission productions [kg_{FP}/kg_{HLW}], and *E* is the amount of generated energy per unit mass of fission products [MW h/kg_{FP}].

$$C = \frac{U}{\rho_{limit} \alpha E} \quad (1)$$

In addition to the quantity *C*, the denominator of (1) can be considered as an energy loading factor, measured in MWd_{th}/m. Both measures may be necessary to satisfy a combination of technical and political limits as well as the ability to track the initial mass of heavy metal that can be attributed to the HLW stream. Repository loading metrics were added to the model, including the overall mass loading factor, measured in tonnes/m, and the energy loading factor (ELF), measured in MWd_{th}/m. The ELF is a meaningful metric for the comparison of the repository impact of different fuel cycle choices because it effectively provides normalization for the total energy generated in the nuclear system.

The full suite of base cases provided in VISION 1.5 was tested with this model with a simple separations efficiency of 99.8 percent. With this model, 99.8 percent of the recycled TRU is sent to the recycle stream and the remainder is sent to the repository in HLW. Meanwhile, 0.2 percent of the fission products are sent to the recycle stream with the remainder sent to the repository. Following this, some sensitivity studies were done to examine the impact of improved separation efficiency, increased time between emplacement and closure, and the impact of cesium (Cs) and strontium (Sr) removal.

The best ELF among the base cases was only about 2 times better than the once-through fuel cycle, primarily because of the short time between emplacement and closure for material generated late in the fuel cycle combined with the presence of Cs and Sr in the HLW. Separation of Cs and Sr increased the ELF values for the best cases to approximately 300 times the value for the once-through fuel cycle. Delaying repository closure also allowed improvements in the ELF, with the best case being about 4 times larger than the once-through fuel cycle.

Using the repository loading model described above, the team performed a detailed analysis of the impact of separation efficiency on repository size across a set of characteristic fuel cycle options selected from the VISION base cases. Ten cases were selected to provide a number of illustrative comparisons. All cases use the same total nuclear energy demand curve as their input, but supply that demand with different combinations of reactor technology. In addition to comparing the impact of different fuel cycle types (once-through vs. LWR MOX vs. fast reactors vs. two-tier), this analysis considered the impact of timing (early transition vs. late transition). Case 1 represents a standard business-as-usual once-through fuel cycle.

Although currently an active area of model improvement in VISION, only a very simple separations model was implemented in the version used here. In the separations module, each isotope is separated into two streams: one that goes to the repository labeled as HLW and one that returns to the fuel cycle. A single separations efficiency, *e*, was defined to represent the partitioning of all elements. Three different separation efficiencies were compared: 0.9, 0.99, and 0.999. In some cases, an additional waste

stream was added to the VISION model for the separation of Cs and Sr. In these cases, a separate loss fraction was defined, l_{CsSr}, and that fraction of the Cs and Sr was sent to the repository while the same fraction was returned to the fuel cycle, with the remainder being placed in a separate storage location. Three different loss fractions were considered: 0.001, 0.01, and 0.1.

Based only on the thermal loading limits for the 10 cases considered here, a number of fuel cycle choices can realize substantial repository capacity benefits (ELF improvement > 8), even with modest separation efficiencies. In any scenario that includes an early transition to an advanced fuel cycle and the recycling of Am in the fuel cycle, a factor of 8 improvement in the ELF is realized with an actinide separation efficiency of 0.99 and a Cs/Sr loss fraction of 0.01. In all cases that include curium (Cm) recycling, there is an additional benefit realized by improving the actinide separation efficiency. However, given other limitations on repository loading (e.g., dose limits, stability of waste forms, etc.), it is not clear that this additional loading benefit can be realized (more results can be found in the paper presented at GLOBAL 2007).

Planned Activities

Remaining activities are focused on examining the economic impact of this repository model on the overall fuel cycle economics. Using the VISION.ECON sub-model in the newest version of VISION, the first step will be to generate a back-end fuel cycle cost based on the length of repository space used rather than on the mass of material that can then be combined with other costs to develop a distribution of possible fuel cycle and electricity costs. Finally, with these costs in place, different pricing/costing strategies for repository space can be compared to determine how they have an effect on the economic performance of the overall system.

In addition to these economic analyses, extensions to the repository loading model are being considered, including accounting for dose/source term in the repository loading constraints and/or allowing for alternative repository geometries in the loading models.

Nuclear Energy Research Initiative

Radiation Stability of Candidate Materials for Advanced Fuel Cycles

PI: Todd Allen and James Blanchard, University of Wisconsin-Madison (UW)

Collaborators: None

Project Number: 06-007

Project Start Date: March 2006

Project End Date: March 2009

Research Objectives

This project will use proton irradiation to further understand the microstructural stability of those ceramics being considered as matrix material for advanced fuels. Following are the specific goals for this work:

- To determine the radiation stability of candidate materials in response to proton irradiation at temperatures between 600–900°C. Following irradiation, researchers will examine samples using transmission electron microscopy (TEM) to understand the effect of radiation on lattice stability, phase change, void growth, and other microstructural features.
- To determine the effect of radiation on hardness and fracture toughness in response to proton irradiation at temperatures between 600–900°C. Estimates of the relative changes in fracture toughness as a function of radiation will be made using crack length propagation following Vicker's indentation.
- To perform structural analysis using finite element analysis to determine the limiting performance of these ceramic fuel matrices, identify promising candidate materials for advanced reactors, and identify pressing data needs.

Researchers will test the following materials: titanium carbide (TiC), zirconium carbide (ZrC), titanium nitride (TiN), zirconium nitride (ZrN), magnesium oxide (MgO), magnesium oxide-zirconium dioxide ($MgO\text{-}ZrO_2$), and magnesium oxide-zirconium dioxide-dierbium trioxide ($MgO\text{-}ZrO_2\text{-}Er_2O_3$).

Research Progress

To provide a basis for comparing the unirradiated and irradiated microstructures, researchers characterized the as-received materials using scanning electron microscopy with energy dispersive spectroscopy (SEM EDS), X-ray diffraction (XRD), TEM, and microhardness. Researchers used XRD and glancing incidence XRD (GIXRD) to characterize the lattice parameters of the investigated materials. The measured lattice parameters of as-received materials agree very well with the values reported by other researchers. The microstructures of unirradiated materials were also characterized using TEM for ZrC, TiC, ZrN, and TiN. The materials are generally free from a high density of defects, although ion milling during sample preparation can introduce some damage on the surface of the specimen, which can be differentiated from proton irradiation damage based on size and structure. Microhardness tests were performed with a Buehler Micromet 2003 Microtester and indentations were used for the fracture toughness analysis.

Proton irradiations were performed using the UW Tandem Accelerator Facility and High Temperature Radiation Stage. This accelerator is a 1.7 MV machine capable of accelerating protons up to 3.4 MeV. Samples are irradiated in the form of 3 mm diameter disks coupled to a metallic stage through a graphite foil that can provide enough compliance to ensure that samples of slightly varying thickness are coupled to the stage for adequate temperature control. Fifteen different samples can be irradiated simultaneously and temperature is monitored and controlled through beam heating and stage temperature controller. The rastered irradiation beam is centered on the target via an aperture system with total beam current measured to provide a measure of the radiation dose. The parameters of the first irradiation as well as the accumulated damage of the specific materials involved

Proton Energy		2.6 MeV	
Temperature		800 ± 8°C	
Materials		CERCOM	French CEA
Accumulated Damage	ZrN	0.7 dpa, 1.5 dpa	1.5 dpa
	ZrC	0.7 dpa, 1.5 dpa	
	TiC	0.47 dpa, 1 dpa	
	TiN	0.47 dpa, 1 dpa	1.0 dpa 0.5 dpa
	SiC	0.6 dpa	

Table 1. Irradiation parameters and accumulated doses.

(i.e., ZrN, ZrC, TiC, TiN, and SiC) are listed in Table 1. Two sources of samples are in the test program. Samples from the U.S. program came from CERCOM. Additional samples from the French program came from the Commissariat a l'énergie atomique. The samples and irradiation conditions are listed in Table 1.

Proton irradiation at 800°C to a dose of 1.5 dpa on ZrC produces a high density of Frank loops, with most sizes smaller than 10 nm. Figure 1 plots the loop size distribution for ZrC as a function of dose. Lattice expansion was observed in the irradiated ZrC to different doses. Incremental changes were found for both the microhardness and fracture toughness properties of irradiated ZrC. No irradiation-induced defects were found in the irradiated ZrN to a dose of 1.5 dpa. There is approximately 0.07 percent of lattice expansion in the irradiated ZrN with a dose of 1.5 dpa, as determined using XRD.

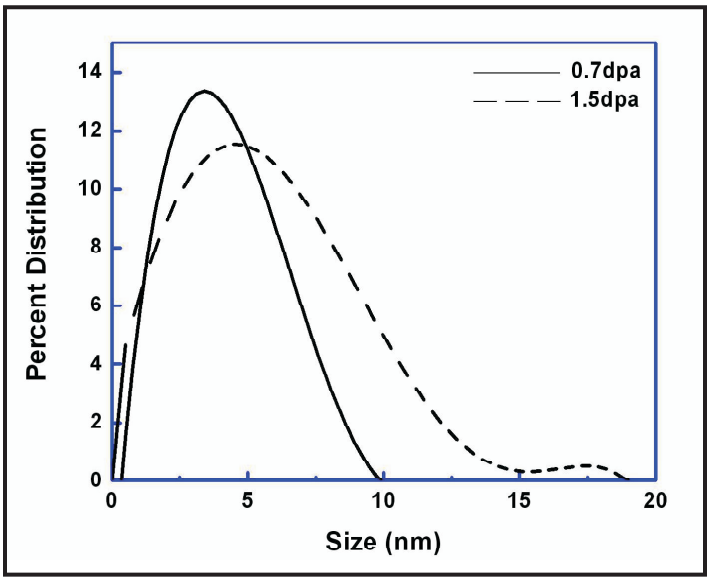

Figure 1. Loop size distribution for ZrC irradiated at 800°C.

For the TiC, a similar dislocation structure as ZrC was observed in the sample with a dose of 1 dpa. An approximately 0.06 percent lattice expansion was found for the irradiated TiC with a dose of 1 dpa. The associated hardness and toughness properties were also measured and estimated, with a 6 percent increase of microhardness and a 7 percent increase of fracture toughness. The XRD results do show a slight lattice expansion for the irradiated TiN. A summary of the lattice expansion for ZrC, ZrN, TiC, and TiN as a function of irradiation dose is provided in Figure 2.

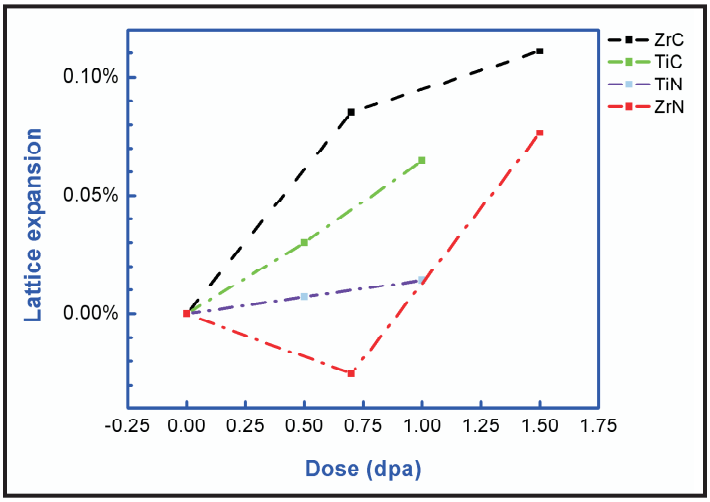

Figure 2. Lattice expansion as a function of dose for samples irradiated at 800°C.

Regarding the inert matrix fuel (IMF) materials, the microhardness of unirradiated MgO was evaluated and structures of Mgo-ZrO_2 were examined using SEM and XRD. The synthesis of materials has been attempted using ball milling followed by cold pressing and sintering, and the parameters will be optimized for achieving denser bulk material. A heavy ion irradiation of MgO was performed at Los Alamos National Laboratory to study and test the experimental process. The post-irradiation analysis is still in process. Additionally, the nanoindention analysis began with single crystal Li-doped MgO (110) and the Berkovich indenter area function was obtained.

Planned Activities

For the upcoming research year, researchers will perform more proton irradiation experiments at various temperatures and doses. Then they will examine microstructural evolution using TEM to study the lattice stability, phase change, void growth, and other microstructural features. Ultimately, correlations between the microstructural changes and radiation temperatures and doses for different materials will be developed and related to bulk properties. A systematic evaluation of the effect of radiation on hardness and fracture toughness in response to different irradiation conditions will also be conducted.

Nuclear Energy Research Initiative

Solution-Based Synthesis of Nitride Fuels

PI: Ken Czerwinski and Dan Rego, University of Nevada-Las Vegas (UNLV)

Collaborators: Los Alamos National Laboratory (LANL), Argonne National Laboratory (ANL), Savannah River National Laboratory

Project Number: 06-012

Project Start Date: September 2006

Project End Date: August 2009

Research Objectives

The objective of this project is to develop a solution-phase process for synthesizing actinide nitrides for use in nuclear fuels. The current process entails carbothermic reduction from the oxide to the nitride, based on a step-wise process of solid-phase reactions from the metal oxide, to the carbide, and finally the nitride. This high-temperature, solid-phase synthesis process is plagued by impurities in the final nitride product and difficulties in production, creating major drawbacks in using nitride fuels for advanced reactor designs. Direct synthesis of the nitride by a solution route could eliminate or minimize the impurities and other synthesis problems. The proposed solution route to nitride has the added benefit of providing several adjustable parameters that would allow control over the properties of the final solid product.

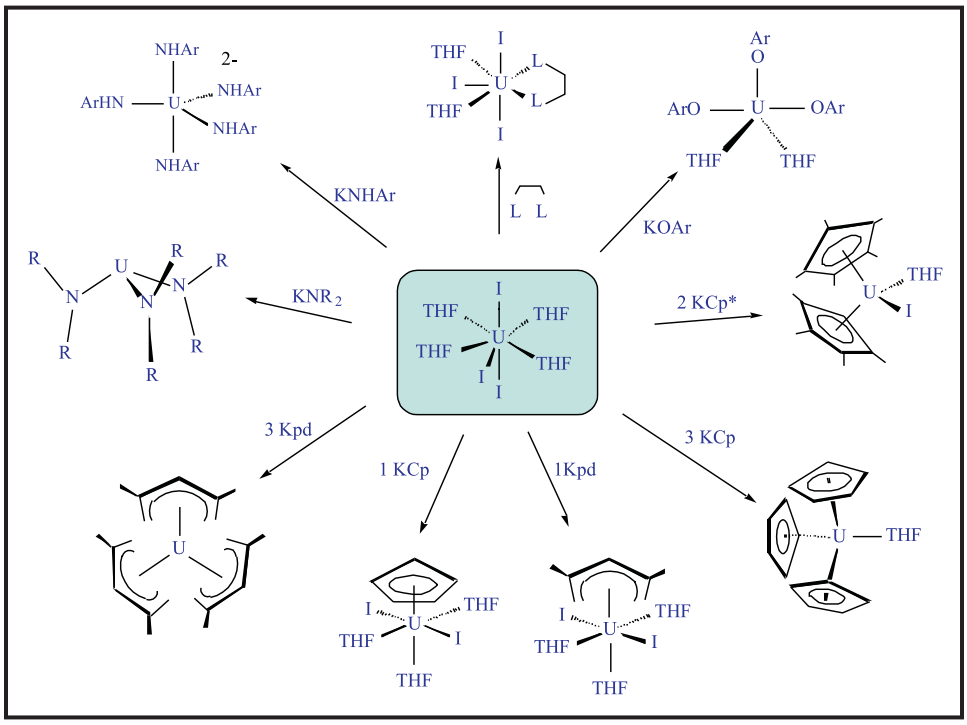

Figure 1. Low valent UI_3 reactions.

Recent work by LANL collaborators has investigated amido reactions in non-aqueous solvents:

$$AnI_3(solv)_4 + 3\ NaNR_2 \rightarrow An(NR_2)_3 + 3\ NaI + solv$$

From this result, the following is a plausible route for the synthesis of nitride fuels:

$$AnI_3 \xrightarrow[NH_3(l)]{} AnI_3(NH_3)_4 \xrightarrow[3NaNH_2]{} An(NH_2)_3 \xrightarrow{\Delta,-2NH_3} AnN$$

where An is an actinide fuel (uranium, neptunium, plutonium, or americium). The non-aqueous synthetic route based on amido chemistry potentially provides property control over the nitride product similar to the sol-gel methods for actinide oxides. The resulting nitride product should be free of the impurities inherent in the carbothermic reduction technique.

Research Progress

As stated above, the objective of this project is to develop a solution-phase process for synthesizing actinide nitrides for use as nuclear fuels. The basis reaction involves the use of UI_3 starting material, as a number of reactions can be performed with this starting material (Figure 1). The emphasis at UNLV will be on evaluating experiments with UI_3 for the formation of UN prior to progressing to studies with transuranic elements.

During this reporting period, work involved the synthesis of $UI_3(NH_3)_4$ in liquid ammonia and resulted in low yield. The cause for the low yield is uncertain, but is possibly due to unreactivity in liquid NH_3. The synthesis was redirected to use literature methods for the preparation of $UI_3(THF)_4$ (THF=tetrahydrofuran) with the substitution of iodide with amido-ligands. This shift of focus is based on work previously performed by ANL and LANL collaborators and is done under their advisement. This redirection involves the development of synthetic capacities to perform the initial reaction of U metal and I_2 in THF solvent. Once formed, the $UI_2(THF)_4$ moiety will be reacted with $NaNH_2$ in liquid ammonia. It is expected that this synthesis will occur in the first part of 2008.

Planned Activities

The project is divided into three primary tasks:

1) Perform non-aqueous coordination chemistry, involving the development of amido coordination with uranium, neptunium, and transneptunium actinides
2) Develop and characterize uranium nitride, neptunium nitride, and transneptunium nitrides from amido species
3) Develop methods for the synthesis of actinide nitrides
    - Identify crucial parameters of the solution-based synthesis of uranium nitride, neptunium nitride, and transneptunium nitride
    - Compare solution synthesis for uranium and neptunium nitride and identify required methods for solid-solution synthesis
    - Perform experiments on the synthesis of uranium-neptunium solid solutions if large variations are identified

Nuclear Energy Research Initiative

The Development and Production of Functionally Graded Composite for Lead-Bismuth Service

PI: Ronald G. Ballinger, Massachusetts Institute of Technology (MIT)

Collaborators: Los Alamos National Laboratory

Project Number: 06-038

Project Start Date: April 2006

Project End Date: April 2009

Research Objectives

The objective of this project is to produce materials that meet both the corrosion and structural requirements of liquid lead and supercritical water systems at temperatures up to 700°C in a neutron flux environment. Use of lead and lead-bismuth (Pb/Pb-Bi) eutectic as coolants in advanced liquid-metal-cooled fast reactor and transmutation systems is limited by their corrosive effects on fuel cladding and structural materials. In addition, the existing upper temperature limit of approximately 550°C for operation of these systems, dictated by corrosion concerns, is insufficient.

A new series of iron-chromium-silicon (Fe-Cr-Si) alloys provide several advantages: 1) formation of a protective film over a wide range of oxygen potentials; 2) minimal solubility in liquid metals, which may occur in crevices or other oxygen-depleted areas; and 3) resistance to corrosion in Pb/Pb-Bi eutectic at temperatures up to 700°C. Initial testing indicates that these materials are resistant to stress corrosion cracking degradation in supercritical water systems and the formation of a Cr-Si-based dual oxide layer provides a high degree of protection.

In this work, researchers will produce functionally graded composites, consisting of a corrosion-resistant layer on a structural alloy, in two forms of tubing suitable for either pipe or fuel cladding applications. Two structural alloy systems will be used for each product form: 1) quenched and tempered and 2) oxide dispersion strengthened (ODS), resources permitting, which will be fabricated using standard commercial practice. The researchers will test the materials produced for corrosion resistance and structural properties. The clad alloy can also be fabricated in the form of welding wire for use as an overlay for more complex shapes.

Research Progress

During this year, the team focused on the following areas:

1) Producing the tubing and pipe preform extrusion billets that will then be processed into the final tubing form
2) Producing the weld wire that will be used as the overlay for the extrusion billets; the overlay weld will then be processed with the extrusion billets into the final product form
3) Diffusion studies to evaluate the long-term diffusion of Si in T91, the structural material chosen for the project

Extrusion Billets. With the support of several vendors, the extrusion billets have been produced. T91 material was melted and then machined to form the extrusion billet form. Three extrusion billets were produced: one that will be weld overlaid on the outer diameter (OD), a second that will be weld overlaid on the inner diameter (ID), and a third that will be co-processed without overlay as a part of a collaboration with the Idaho National Laboratory (INL) to produce baseline tubing material. Figure 1 shows a photograph of the finished extrusion billets.

Figure 1. Extrusion billet photograph.

Weld Wire. The weld wire billets have been melted and processed into extrusion billets. The initial ingots were melted and then sent to be processed into extrusion billets. The extrusion billets will then be processed into rods that will then be additionally processed into weld wire for the overlay process. The extrusion billet processing is currently being done as follows:

1) Machine/grind surface of the material to prepare for bar and wire mill rolling
2) Process material from a nominal 4.5" diameter round to a nominal .250" diameter coil
3) Annealed and pickle prior to shipment

The 0.025" diameter wire will then be processed further to 0.035" diameter weld wire.

Diffusion Studies. The composite system will achieve its corrosion resistance via the presence of a high Si layer on the surface exposed to the environment. For this layer to remain protective, the Si concentration must be maintained above approximately 1.25 weight-percent. However, the Si concentration of the underlying structural layer will be much less a requirement for radiation damage resistance. At the expected upper operating temperature of 700°C for the fuel cladding product form, there will be a potential for dilution of Si in the protective layer due to mixing by diffusion. Because of this possibility, the research team has initiated a task to evaluate the diffusion process.

Six diffusion couple "blanks" have been produced and are now undergoing an aging process. After aging, the degree of mixing of the Si will be evaluated. If possible, actual diffusion couples coefficients will be measured.

Planned Activities

During the coming year, the program will focus on the following areas:

- Producing the composite fuel cladding and pipe forms
- Corrosion testing of both archive and new material from the composite program:
  - Weld wire used for the overlay
  - T91 base material
  - Composite material
- Initiating the diffusion studies program
- Completing the thermally driven loop design
- Commissioning the supercritical water experimental facility

Nuclear Energy Research Initiative

Flexible Conversion Ratio Fast Reactor Systems Evaluation

PI: Neil E. Todreas and Pavel Hejzlar, Massachusetts Institute of Technology (MIT)

Collaborators: None

Project Number: 06-040

Project Start Date: March 2006

Project End Date: March 2008

Research Objectives

The objective of this project is to design a flexible conversion ratio fast reactor system that enables time-dependent management of fissile inventories and higher actinides. The goal is to produce a single reactor design capable of being configured to achieve both 1) conversion ratios near zero in order to transmute legacy waste and 2) conversion ratios near unity for operation in a sustainable closed cycle.

Candidate liquid coolant core designs—lead and liquid salt—will be developed and cross-compared against each other and two other reactor designs: 1) the supercritical carbon dioxide cooled reactor being developed through another MIT project and 2) the sodium-cooled reactor being developed at Argonne National Laboratory (ANL). This will help decision makers select the most attractive, large, high-power density fast system for closed fuel cycles in countries with fuel service centers.

Researchers will use a consistent plant rating of 2,400 megawatts (MWt) in both designs. The reactor cores will be cooled by forced circulation during normal operation to achieve high power density of at least 100 kilowatts (kW)/liter. Power conversion systems will eliminate the intermediate heat transfer loop, making the system more economically competitive. Safety and core integrity will be achieved through a self-controllable reactor design that ensures safe shutdown for all key transients. Proliferation resistance will be enhanced by eliminating blankets and using transuranics as fuel without separating plutonium.

Research Progress

For the lead-cooled reactor design, researchers confirmed the feasibility of the lead-cooled reactor with a large power rating and flexible conversion ratio that can achieve a conversion ratio of either 1.0 or zero, while having attractive safety features such as the capability of inherent reactor shutdown in key unprotected accidents.

Researchers designed the CR=0 core as a three-batch core with transuranic and zirconium (TRU-Zr) fuel to accommodate a large reactivity swing. The initial fuel composition of 34 weight-percent TRU and 66 percent Zr matrix resulted in a fuel cycle length of about 550 effective full power days (EFPD), corresponding to 1.7 years of operation at a 90 percent capacity factor. Fuel was driven to a discharge burnup of 400 MWd/kgHM. This high burnup was achieved because of a small heavy metal weight fraction in the pins. This is not expected to pose a problem for two reasons: 1) the fission gas release which drives fuel swelling is comparable to that of a CR=1 core because the total number of fissions for the two cores is comparable and 2) more Zr diluent in the pins provides more volume which can accommodate heavy metal swelling. The CR=0 core has higher power peaking than CR=1, but the proposed fuel management strategy makes it possible to maintain radial power peaking below 1.35. The TRU consumption rate is 1,282 kg/yr, or 0.32 kgTRU/yr/MWth. This exceeds the TRU destruction rate of accelerator-driven systems, such as accelerator transmutation of waste (ATW), which reported the value of 0.262 kgTRU/yr/MWt, and is due to the higher capacity factor of a critical reactor.

Reactivity coefficients are all negative except for the coolant temperature reactivity coefficient; however, its value is less positive than the sodium-cooled integral fast reactor (IFR) and is comparable to the CR=1 case. The Doppler coefficient is negative and significantly smaller than for the CR=1 core due to the absence of fertile U238—easily satisfying the first ANL criterion on self-controllability—which makes inherent reactor shutdown possible in accidents without scram. The main challenge for the CR=0 core is related to the inadvertent Control Rod Withdrawal accident, which necessitates the use of control rods in every fuel

assembly to reduce the reactivity worth of any individual rod. Because reactivity excess to be compensated at beginning-of-life (BOL) is large, and even small control rod movements during seismic events could result in unacceptable reactivity insertions, special double-entry control rods that overcome this problem have been devised.

The 1-batch, 3-region, CR=1 core uses metallic U-TRU-Zr fuel, where the composition of transuranics corresponds to that of discharged light water reactor fuel at 50 MWd/kgHM burnup. To maintain low power peaking during core life, researchers took the approach of varying heavy metal loading among different core regions through Zr content adjustment, rather than TRU enrichment grading. Therefore, the core contains three regions, each with different weight fractions of Zr, U, and TRU, as indicated in Table 1 (the TRU-to-heavy-metal ratio remains fixed). This allowed for maintaining the core radial peaking below 1.2 throughout core life and achieving the target core average burnup of 100 MWd/kgHM. The corresponding cycle length is 2,200 EFPD, equivalent to 6.5 years at 90 percent capacity factor, limited by cladding peak fluence.

Region	Zr	U	TRU
1	10	74	16
2	15	69.9	15.1
3	19	66.6	14.4

Table 1. Composition of CR=1 core.

Only one-third of the assemblies of the CR=1 core are equipped with control rod drives (CRDs) due to its smaller reactivity swing. Transition between the CR=0 and the CR=1 core with its much smaller number of CRDs is accomplished through plugging extra vessel head CRD penetrations. Similarly, as for the CR=0 core, all reactivity feedback coefficients are negative except for the coolant temperature coefficient, which is slightly positive. Reactivity coefficient ratios fell within the range, also satisfying the ANL self-controllability criteria.

The key challenges for the 2,400 MWt rating are 1) the feasibility of fitting four intermediate heat exchangers (IHXs), 600 MWt each, into the annular space between the core barrel and the vessel and 2) the assurance of passive decay heat removal. Researchers designed four shell and tube IHXs with enhanced heat transfer surfaces that can fit with four pumps in the 10.2 m guard vessel size. To maximize plant efficiency and to reduce cost, four compact supercritical CO_2 power conversion system trains optimized for lead-cooled reactor parameters (see Figure 1) are employed, each drawing hot CO_2 from one IHX. High plant efficiency of 45 percent can thus be achieved for a core outlet temperature of 574°C. Reactor vessel and internal flow paths have an arrangement of a dual-free-level vessel design to assure the ingress of high pressure CO_2 into the core in case an IHX tube rupture is prevented.

The approach adopted for passive decay heat removal

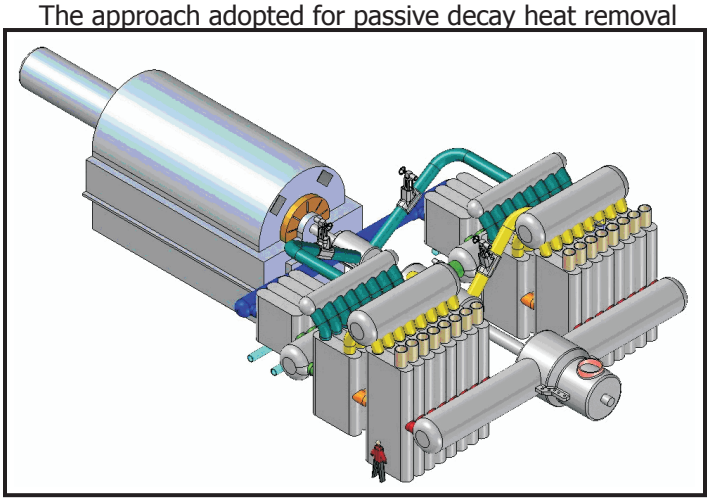

Figure 1. One-out-of-four 265 MWe trains of a SCO_2 power conversion system.

is to use an enhanced reactor vessel auxiliary cooling system (RVACS) in conjunction with a supplementary passive secondary auxiliary cooling system (PSACS). The following RVACS enhancements were adopted as the most promising: a combination of a liquid metal bond in the gap between the reactor vessel and guard vessel, use of a perforated plate in the air gap, and a dimpled guard vessel wall. The PSACS consists of 4x50% safety-grade cooling loops connected to CO_2 IHX inlets that remove decay heat by natural circulation of CO_2 into a passive auxiliary heat exchanger (PAHX) submerged in an in-containment water storage tank. Researchers developed a detailed RELAP5 model of the entire plant and confirmed through simulations that, for a station blackout without scram, the reactor shuts itself down from reactivity feedbacks and the decay heat load based on the ANS-79 standard can be passively removed through the RVACS and PSACS without exceeding structural limits.

Design activities on a liquid salt reactor with CR=1 began with an extensive review of salts to identify the most promising candidate for high power density fast reactor application. Fluoride salts were found to be unable to meet thermal hydraulic and neutronic criteria, primarily due to their high viscosity and thermal expansion coefficient. Researchers identified the ternary chloride salt NaCl-KCl-$MgCl_2$ (30%-20%-50%) as the best performing salt and assembled properties necessary for thermal hydraulic and neutronic analyses.

Researchers designed the liquid salt-cooled 2,400 MWt core, shown in Figure 2, and carried out extensive neutronic and thermal hydraulic analyses to evaluate core performance. The major challenge for the neutronic design is to overcome the large positive coolant temperature reactivity coefficient, which is characteristic of the liquid salts due to their large thermal expansion coefficient. A number of strategies for reduction of this coefficient were explored, including the parfait core shape, axial uranium blankets, axial uranium blankets with $ZrH_{1.6}$ moderator, streaming channels, and reactivity control through moderation using $ZrH_{1.6}$ control rods. Researchers found that although the combination of these approaches can significantly reduce the coolant temperature coefficient, it only marginally achieves the self-controllability criteria at BOL and results in significant performance penalties—most notably reduced cycle length and lower achievable power density. Hence the focus has been redirected to the use of the reactivity control device known as the lithium thermal expansion module (LEM) to meet the core self-controllability criteria.

Thermal hydraulic analysis of the liquid salt-cooled CR=1 core was also carried out using the subchannel approach. An important constraint for the salt-cooled core is pressure drop because of high salt viscosity and the need for a low coolant volume fraction due to neutronic reasons. Researchers found that a pressure drop on the order of 1 MPa is needed to achieve target power density of 100 kW/liter. The three-zone orificing scheme was employed to maximize the core-average outlet temperature and thus plant efficiency. However, the strategies to reduce the coolant temperature reactivity coefficient also reduce the active fuel length. This leads to a larger pin linear power and thus reduces achievable power density by more than 30 percent. Therefore, the complex core configurations with axial blankets and streaming channels were discarded.

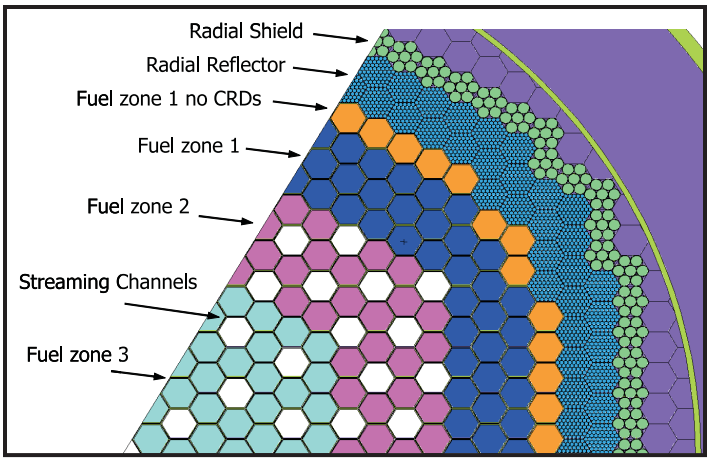

Figure 2. Liquid salt cooled core layout.

Planned Activities

During the final stage of the project, researchers will complete the reactor physics and thermal hydraulic design of a liquid salt-cooled CR=1 reactor using lithium expansion modules. After core feasibility is confirmed, an IHX design will be developed and the plant conceptual design completed. Similarly, as for the lead-cooled core, an enhanced RVACS and PSACS will be used for passive decay heat removal and the supercritical CO_2 cycle as balance-of-plant. RELAP transient analysis will be performed to confirm that the proposed system can withstand key unprotected accidents without exceeding structural limits. Finally, researchers will gather information on ANL's sodium-cooled core designs and MIT's fast gas-cooled design and will compare these four coolant types.

NUCLEAR ENERGY RESEARCH INITIATIVE

Development and Utilization of Mathematical Optimization in Advanced Fuel Cycle Systems Analysis

PI: Paul J. Turinsky, North Carolina State University (NC State)

Collaborators: Argonne National Laboratory, Idaho National Laboratory (INL)

Project Number: 06-047

Project Start Date: March 2006

Project End Date: March 2009

Research Objectives

The objective of this project is to develop mathematical techniques to optimize deployment strategies for advanced nuclear fuel cycle/reactor/fuel facilities. Researchers will employ a stochastic optimization approach, which will determine the tradeoff surface of this multi-objective optimization problem. The optimization will consider economic, energy, environmental, and nonproliferation resistance metrics of the fuel cycle, which will be modeled using the VISION code.

This project will accomplish several goals:

1) The capabilities developed will assure that optimum deployment strategies are determined with reduced scientist/engineering effort, providing higher confidence in utilizing the results in policy decision making
2) The automated capability should make it possible for less technically sophisticated individuals to utilize fuel cycle simulation capability
3) Determination of the tradeoff surface using multi-objective mathematical optimization, resulting in different optimization deployment strategies as one moves across the surface, will provide quantitative data on such items as the relationship of repository capacity to energy costs

Decision makers could use resulting data to establish policies concerning incentives and requirements to encourage the preferred evolution of the commercial nuclear power enterprise.

Research Progress

Work continues on developing the optimization engine coupling capability with the VISION code, partially in response to changes being made to the VISION code. The VISION model has matured and evolved to the point where the number of available simulation settings and adjustments can no longer be easily displayed on the VISION user-interface screen. For this reason, the VISION model has a defined set of "base-case" variables by which a user may completely specify the parameters for a simulation, and for which a predetermined set of values may be automatically chosen. Thus, for example, a user of the VISION model may choose from a set of values that will simulate a once-through fuel cycle or from another set of values that will simulate the use of fast-burner reactors to recycle actinide elements from spent fuel. In order to utilize the full range and flexibility of the VISION model, the optimization wrapper has been expanded to make use of the entire set of these base-case variables.

Expanding the scope of variables controlled by the wrapper yields four advantages. First, as mentioned, a greater degree of range and control over the model parameters becomes available. Secondly, consistency between separate optimization runs may be more readily confirmed, as those variables whose values are most likely to be changed as the VISION model evolves can be compared and corrected against previous simulations. Additionally, an automated means has been implemented to check whether the simulation results of a given base-case are consistent between different VISION releases and between base-case and non-base-case operating modes (i.e., manually inputting base-case values in the model should yield the same results as automatically choosing a base-case). Finally, a base-case represents a valid (if not optimum) set of modeling parameters, thus a base-case makes an ideal starting point for both optimization methods: Simulated Annealing and Genetic Algorithm.

The graphical user interface for the optimization wrapper has been developed and has received several

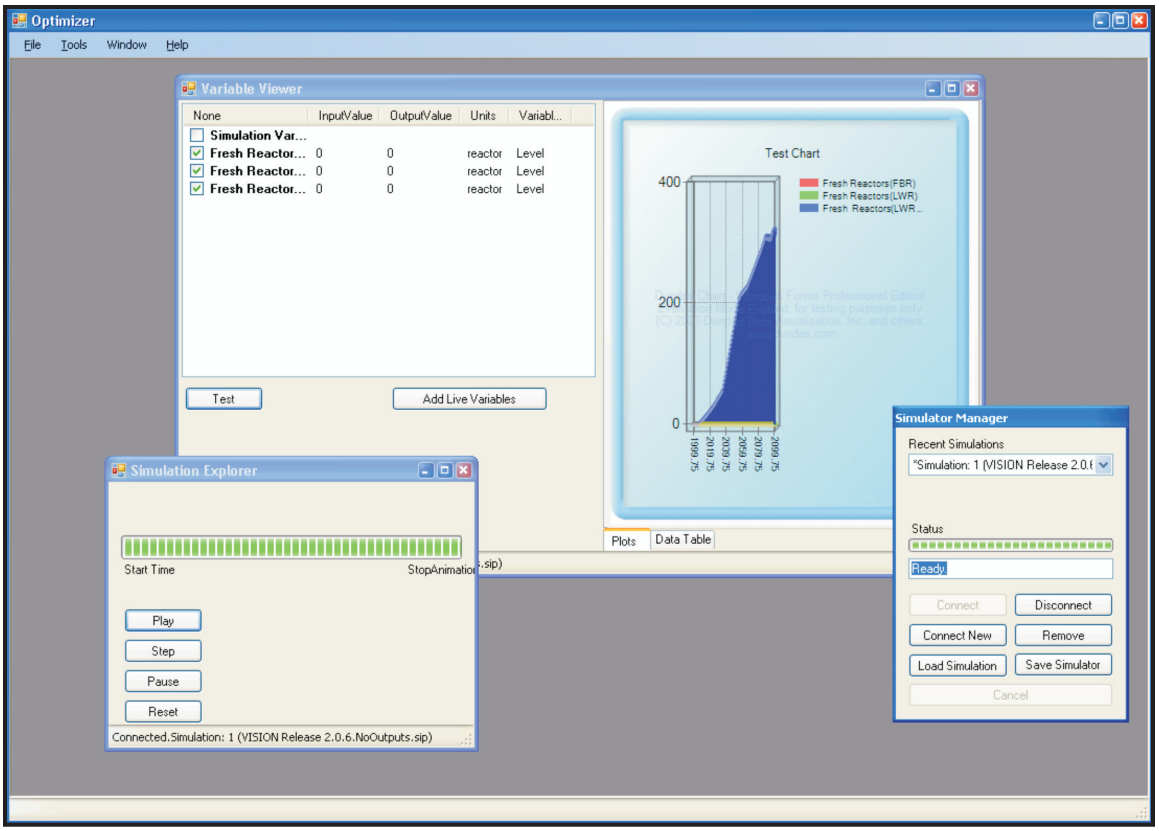

Figure 1. Revised Variable Viewer window featuring data plotting ability.

enhancements based on feedback from potential users. The most notable change is in the Variable Viewer window, where users may now explore the properties and values of saved data-sets and of current simulation variables. In addition, a plotting feature allows users to more easily visualize and compare trends in the data.

Changes have been made to the VISION model in order to more accurately reflect real world simulation. These changes have been made with the assistance of INL's VISION development team. Prior to this summer, fuel fabrication and separation facilities came online in very large increments and with very large facility sizes. This prevented the system from running into any fabricated fuel and separated material shortages. In order to reflect a more realistic scenario and not wreak havoc on the economics, this logic was changed. Fuel fabrication facilities and separation facilities are now ordered based on the demand for fuel and separations. When reactors are ordered, a check is made to see if there is enough fuel fabrication and separations capability to meet the new demand. If there is not enough capability, then the simulation will build new facilities in time to meet this demand. Work is being done, as described below, to predict when fuel fabrication and separation facilities will be needed.

Availability factors and capacity factors were added to VISION to simulate real-time operation. Most facilities in operation can only operate at a certain maximum level below the rated level, which is primarily due to annual maintenance. This maximum level of operation is called the availability of a facility, and in VISION this is reflected by the addition of availability factors for fuel fabrication and separation facilities. The capacity factor for a facility or reactor is an internal calculation that is dependent on the demand for fuel/separated material and energy. The capacity factor for reactors is always at the availability of the reactor (unless there is a fuel shortage). The capacity factors for fuel fabrication and separation facilities are dependent on the amount of fuel or separated material that is being requested and the number of operating facilities. This helps to give the user an indication of how well facilities are being utilized.

A separated materials fuel bank was created in order to help with fuel shortage scenarios. The fuel bank sets aside a certain amount of separated material based on the number of reactors that use separated material. This value can be changed to whatever the user specifies.

A more thorough analysis of fuel cycle costs has also been added. Reactors, fuel fabrication facilities, and separation facilities all have cost components based on

fixed and variable operating and maintenance (O&M) costs and capital costs. Accurate values for fuel fabrication and separation facility O&M costs need to be researched and incorporated into the model before the economics from this section can be deemed accurate.

The changes noted above will not only support the optimization engine activity, but will also support the upset scenario capability that is being added. This is a new task which has been added to assure that facilities' deployment scenarios identified by the optimization engine are robust, i.e., can tolerate uncertainties in facilities operations without major consequences. To accommodate upset scenarios, various recovery strategies are going to be examined as required to accommodate the lack of available services or products due to an upset event, i.e., fuel fabrication facility out of service.

A crude implementation of single-objective simulated annealing (SA) has been completed, with the decision variable being the number of new reactors by type that will startup as a function of time and the key constraints being imposed by the VISION code versus optimization engine. This implementation is intended to demonstrate the capability to develop an external optimization engine that can be successfully linked to the VISION code. The optimization engine wrapper has been designed such that the class of decision variables has been constructed to facilitate implementation of the Genetic Algorithm approach.

Perhaps what may prove the most significant contribution during the past 12 months has been the development of a mathematical representation of an advanced nuclear fuel cycle. The mathematical model captures the decision making logic of when to start construction of new fuel cycle facilities and recovery strategies for an upset event involving a facility for a stage of a fuel cycle. The model also provides a framework for understanding the incorporation of mathematical optimization capabilities.

The mathematical model is based upon a demand-supply model, where facilities for one or more stages of the fuel cycle create demand which is serviced by the supply produced by facilities for another stage. The overall driver triggering the demand is electrical energy produced by nuclear power plants demand, which varies with time. Consider the following example: for a closed fuel cycle, the future electrical energy demand will require an increased supply of electrical energy. If supply is not adequate (always the case since nuclear power plants assumed to operate at Capacity Factor = Availability Factor unless an upset event occurs), new nuclear power plants will need to be built. This will result in an increased demand for fuel fabrication services. If supply and usable inventory is not adequate, new fuel fabrication plants will need to be built, which will result in an increased demand for reprocessing services. Again, if supply and usable inventory is not adequate, new reprocessing plants will need to be built, which will result in an increased demand for spent fuel. If supply and usable inventory is not adequate, new nuclear power plants will need to be built. Note that a circular logic has developed, where we started with building new nuclear power plants due to electrical demand and then returned to this at the end due to spent fuel demand. This implies that some decisions, such as using a mix of advanced light water reactors (LWRs) and fast recycle reactors (FRRs) or a conversion ratio of FRRs, must be made such that the starting and ending states are consistent.

Regarding facilitating the incorporation of mathematical optimization capabilities using the mathematical model representation, by the decision of how supply is going to meet demand, one can create alternative fuel cycle scenarios noting their evolution over time. For example, electrical energy demand can be supplied by several reactor types, which in turn require fuel fabrication capability. In the case of an LWR, this can be met by low enrichment uranium (LEU) fuel or mixed oxide (MOX) fuel, thus creating demand for reprocessed material for MOX fuel that is supplied by reprocessing capability. This creates the demand for spent fuel, which can be supplied by LEU spent fuel (i.e., no MOX recycle in LWRs) or MOX spent fuel (i.e. MOX recycle in LWRs). A similar path for demand-supply decisions can be formulated for the FRR. Which path to pursue is amendable to decision making using mathematical optimization.

Planned Activities

With the assistance of INL, researchers will complete the modifications of the VISION code to support the mathematical model as much as possible within the constraints of the PowerSim software used to develop VISION and the optimization engine. Upset scenarios, in particular recovery strategies, will be assessed. Work on single-objective (SO) optimization capability using the SA approach, denoted SOSA, will be completed. This capability will be extended sequentially to multi-objective Simulated Annealing (MOSA), single-objective Genetic Algorithm (SOGA), and multi-objective Genetic Algorithm (MOGA). The optimization capabilities developed will be exercised for code verification and validation (V&V) purposes and for obtaining useful preliminary results.

Nuclear Energy Research Initiative

Engineered Materials for Cesium and Strontium Storage

PI: Sean McDeavitt, Purdue University

Collaborators: Texas A&M University

Project Number: 06-058

Project Start Date: April 2006

Project End Date: March 2009

Research Objectives

Next generation spent fuel reprocessing methods being developed under the U.S. Department of Energy's Advanced Fuel Cycle Initiative include solvent extraction schemes to isolate cesium (Cs) and strontium (Sr) from spent nuclear fuel. Isolating these isotopes for short-term decay storage eases the design requirements for long-term repository disposal; a significant amount of the radiation and decay heat in fission product waste comes from Cs-137 and Sr-90.

This project is complementary to Idaho National Laboratory's (INL's) efforts to engineer a processing system to immobilize Cs and Sr isotopes using a fluidized bed steam reformer. While INL is focused on the efficacy of process technology, this project is working to develop and characterize a number of candidate host ceramics for the Cs and Sr isotopes. The two major objectives of this project are to synthesize candidate ceramics and to characterize the resulting Cs/Sr-bearing ceramics. A partial list of candidate ceramics includes cesium aluminosilicate and strontium carbonate as well as titanate and zirconate ceramics.

Research Progress

The ceramic synthesis system used in this research has undergone multiple evolutions since the advent of this project. The initial device was constructed at Purdue University and was designed to emulate the steam reforming process at INL. This system operated at nominal temperatures between 600 and 800°C (manual control). The primary components included a steam generator, tube furnace with a sealed alumina process vessel, an atmosphere control system, a manual liquid feed tube, and a post-reaction gas scrubber/steam condenser. The initial experiments used aqueous precursor solutions containing cesium and strontium nitrates ($CsNO_3$ and $Sr[NO_3]_2$) as well as solid powder reactants (kaolin $[Al_2Si_2O_5(OH)_4]$ and carbon).

The products produced from the steam-driven process were never conclusive. It was speculated that most of the reactants were "blown" from the process vessel before the reaction could be completed. The final experiments in the initial apparatus used a manual feed tube to slowly insert the Cs and Sr solutions and an argon cover gas was used (the steam line was removed). This methodology produced cesium aluminosilicate ($CsAlSi_2O_4$) and strontium carbonate ($SrCO_3$) as stable reaction products.

A modified ceramic synthesis system was installed at Texas A&M University. The steam generator was completely eliminated. Further, a new furnace with digital temperature control and an off-gas condensation device for effluent recycling were installed. Instead of a steam environment with high flow rates, the internal energy of the system was reduced by switching to an argon cover gas; vaporized water from the feed solution provides the requisite oxygen and hydrogen to drive the reactions. A low-flow systaltic pump is used to inject the Cs- and Sr-bearing solutions into the reaction chamber, eliminating the manual element of the former design. The first synthesis experiments were repeats of the last experiments from the previous system. The system produced $CsAlSi_2O_4$ and $SrCO_3$, as before, establishing product consistency from system to system.

To date, 14 synthesis experiments have been completed, as summarized in Table 1. Now that the new system has been assembled and functions according to design, the synthesis of new host candidates will proceed. Initial tests with titanium oxide (TiO_2) and other precursor candidates are underway. It is expected that TiO_2 will be too stable to serve as an effective precursor; other Ti-bearing precursors will also be tested.

Experiment Number	Simulated Waste Solution	Cover Gas	Solid Reactants	Results
1 to 5	$CsNO_3 + HNO_3$	Steam	Kaolin + carbon + glass beads	System development experiments (no product)
6	$CsNO_3 + HNO_3$	Steam	Kaolin + carbon + glass beads	Product created; insignificant Cs content
7	$Sr(NO_3)_2 + HNO_3$	Steam	Kaolin + carbon + glass beads	Product created; insignificant Sr content
8	$Sr(NO_3)_2 + CsNO_3 + HNO_3$	Steam	Kaolin + carbon + glass beads	Product created; insignificant Cs and Sr content
9	$CsNO_3 + HNO_3$	Argon	Kaolin + carbon	Powder product identified to be $CsAlSi_2O_4$
10	$Sr(NO_3)_2 + HNO_3$	Argon	Kaolin + carbon	Powder product identified to be $Sr(NO_3)_2$
11	$Sr(NO_3)_2 + CsNO_3 + HNO_3$	Argon	Kaolin + carbon	Powder product identified as $CsAlSi_2O_4$ with negligible $Sr(NO_3)_2$
12	$Sr(NO_3)_2 + HNO_3$	Argon	Kaolin + carbon	Powder product nominally identified as $Sr(NO_3)_2$ (X-ray data weak – repeat)
13	$Sr(NO_3)_2 + HNO_3$	Argon	TiO_2 + carbon	TBD
14	$Sr(NO_3)_2 + HNO_3$	Argon	TiO_2 + carbon + Kaolin	TBD

Table 1. List of ceramic synthesis experiments.

Planned Activities

In the final year of the project, the synthesis experiments will be augmented by smaller scale Differential Thermal Analysis (DTA) to quantify the reaction temperatures and enthalpies for a matrix of candidate reactants. The synthesis experiments will continue and a selected set of the products will be subjected to product consistency testing to examine their relative ability to immobilize Cs and Sr. Finally, waste form fabrication methods will be evaluated to select potential processes that may be able to take the product powders and transform them into monolithic waste forms for storage.

NUCLEAR ENERGY RESEARCH INITIATIVE

Feasibility of Recycling Plutonium and Minor Actinides in Light Water Reactors Using Hydride Fuel

PI: Ehud Greenspan, University of California-Berkeley (UCB)

Collaborators: Massachusetts Institute of Technology (MIT), Argonne National Laboratory

Project Number: 06-065

Project Start Date: March 2006

Project End Date: February 2008

Research Objectives

The objective of this project is to assess the feasibility of improving the plutonium (Pu) and minor actinide (MA) recycling capabilities of pressurized water reactors (PWRs) by using hydride instead of oxide fuels. There are four general parts to this assessment:

1) Identifying promising hydride fuel assembly designs for recycling Pu and MAs in PWRs
2) Performing a comprehensive systems analysis that compares the fuel cycle characteristics of Pu and MA recycling in PWRs using the promising hydride fuel assembly designs identified in Part 1 versus using oxide fuel assembly designs
3) Conducting a safety analysis to assess the likelihood of licensing hydride fuel assembly designs
4) Assessing the compatibility of hydride fuel with cladding materials and water under typical PWR operating conditions

Research Progress

This period focused on assessing the feasibility of multi-recycling in PWRs, utilizing one of the following fuel options:

- Plutonium only
- Plutonium with different amounts of uranium
- Neptunium (Np) along with plutonium
- All the MAs along with Pu loaded in hydride fuel

The hydride fuels considered consist of $ZrH_{1.6}$ mixed with AcH_2, where Ac stands for any of the trans-uranium actinides. The uranium (U), when used, is in its metallic form (as in TRIGA fuel). The hydride fuel is assumed to be loaded uniformly ("homogeneous design") in all of the fuel assemblies in the core. The fuel assembly, fuel rod, and control rod geometry and dimensions are identical to those of the reference enriched uranium-dioxide-fueled PWR. The amount of actinides loaded in the fuel is adjusted in each recycle so that the cycle length will be nearly the same as the reference uranium-dioxide-fueled PWR. The uranium accumulated in the fuel due to the decay of TRU isotopes and due to transmutation reactions is denatured with depleted uranium so that the ^{235}U concentration will never exceed 20 percent of the uranium. The thrust of this study was to find how many recycles are feasible without violating reactivity constraints, as well as to compare the transmutation effectiveness attainable with the different fuel compositions examined. The constraints imposed are that the reactivity coefficient of fuel temperature, coolant temperature, small coolant voiding, and large coolant voiding should all be negative at any time during the cycle. A 3-batch fuel-management scenario was assumed.

Figure 1 summarizes the fraction of TRU that is transmuted per recycle in three of the hydride fuel recycling scenarios evaluated and Table 1 compares selected transmutation characteristics of several hydride and oxide fueled 1st recycled cores. The following was found:

1) ***Using hydride fuel, Pu can be recycled an unlimited number of times.*** This is in contrast with a full mixed oxide (MOX)-fueled core for which the number of permissible recycling is limited by a positive large void coefficient of reactivity. It is the hydrogen in the fuel of the hydride-fueled PWR core that maintains the large void coefficient negative even in cases of complete coolant voiding; the neutron spectrum in the fully voided hydride core is significantly softer than in the fully voided oxide core.

2) ***The fraction of the Pu loaded into a uranium-free hydride-fueled core that is fissioned is approximately 65 percent in the first recycle, 50 percent in the second recycle, and gradually declines to 20 percent in the equilibrium recycle.*** This is a very effective transmutation capability; it is significantly higher than what can be achieved with PuO_2-UO_2 (MOX reference) fuel but comparable to that attainable using PuO_2-ZrO_2 (MOX, no U) fuel (see Table 1). However, the latter cannot be recycled more than a few times.

3) ***The fuel temperature coefficient of reactivity in the first recycle of PuH_2-$ZrH_{1.6}$ fuel becomes positive at approximately 2/3 of the burnup reported in Table 1.*** There are no limitations on the second and following recycles of PuH_2-$ZrH_{1.6}$, as well as on the first recycle of PuD_2-$ZrH_{1.6}$ fuel. The latter fuel (see Table 1) provides comparable transmutation capability.

4) ***It is possible to co-recycle Np with Pu in hydride fuel for at least 6 recycles.*** The combined fractional transmutation is somewhat lower than in Pu-only recycling.

5) ***It is possible to recycle TRU in hydride fuel in PWR, but not more than 2 to 3 times.*** The attainable fractional transmutation is lower than in the case of recycling Pu+Np.

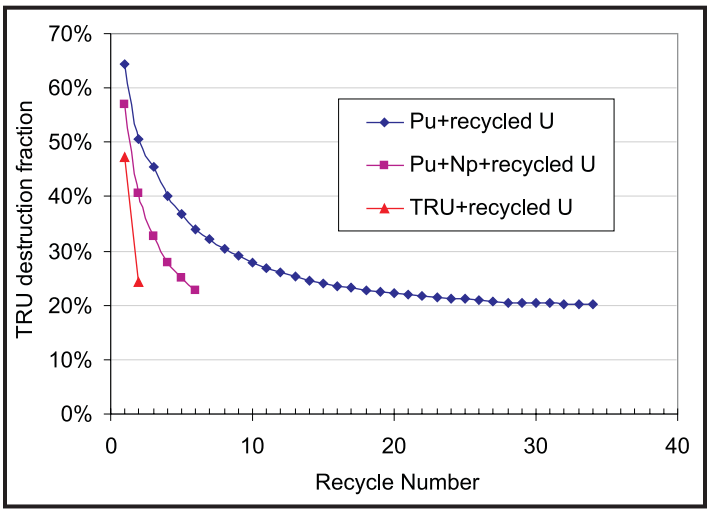

Figure 1. Fraction of the TRU loaded uniformly into the hydride-fueled PWR core that is transmuted per recycle.

Safety analysis of hydride fuel cores performed this period considered a large break loss of coolant accident (LBLOCA) and a main steam line break (MSLB) accident. The consequence of such accidents was evaluated for four core types—an all UO_2—loaded core (reference design), a PWR core loaded with either CORAIL type or CONFU type Pu containing oxide fuel, and a core loaded with Pu-containing inert matrix hydride fuel (PUZH fuel). From the LBLOCA analysis, researchers were able to conclude the following:

1) The 1,478°K cladding temperature limit established by 10 CFR 50.46 is never reached by any of the assemblies investigated.

2) The maximum peak centerline temperature (PCT) for PUZH is much lower than those of the reference oxide fuels. The reference fuels yield maximum PCTs between 1,068 and 1,135°K for the two axial power profiles assumed for the core—a chopped cosine and a top-skewed power profile. On the other hand, the corresponding maximum PCT evaluated for the PUZH fuel is 759°K and 872°K. The lower temperatures for PUZH fuel are due to its higher thermal conductivity that causes its fuel centerline temperature to be about 1,000°K lower than that of the oxide fuels.

From the MSLB accident analysis of the four core types, researchers concluded that the PUZH-fueled core has a better post-MSLB performance relative to the oxide-fueled cores analyzed. For the most limiting scenario typically considered for this accident—a MSLB occurring while the reactor is at the end of cycle in hot zero power condition—the PUZH-fueled core does not reach re-criticality after the break, whereas the oxide cores do. This is because the negative coolant density reactivity coefficient of the PUZH-fueled core is about half of all three oxide cores examined.

Two different uranium-thorium-zirconium hydride fuels were fabricated at Idaho National Laboratory (INL) over the summer: $[UTh_4Zr_{10}]H_{1.9}$ and $[U_4Th_2Zr_9]H_{1.5}$. Fuel microstructure characterization was done at the University of Nevada, Las Vegas, using X-ray diffractometry, scanning electron microscopy, and transmission electron microscopy. These samples will be used to study hydride fuel compatibility with water and with Zircaloy. Researchers also developed coupled heat conduction—hydrogen diffusion model with temperature-dependent material properties—for predicting the behavior of hydride fuel during transients.

Characteristic	MOX reference	MOX No U	Pu hyd no U*	Pu D-hyd No U	Pu hyd 25% Umax	Pu+Np hydride	TRU hydride
Burnup (GWD/MtiHM)	51.4	622.1	627.9	620.1	284.2	555.9	462.4
Residence time (EFPD)	1426	1428	1429	1429	1430	1431	1429
Initial Pu loading (g/cc)	1.0977	0.7617	0.7562	0.7658	0.7511	0.7986	0.8945
Initial Pu loading (w/o)	10.43	16.68	12.70	12.73	11.37	13.30	14.71
Initial U loading (g/cc)	8.1740	0	0	0	0.9301	0	0
Initial Np loading (g/cc)	0	0	0	0	0	0.0614	0.0688
Initial Am loading (g/cc)	0	0	0	0	0	0	0.0637
Initial Cm loading (g/cc)	0	0	0	0	0	0	0.0057
At discharge							
U inventory (g/cc)	7.8894	5.50E-04	5.80E-04	5.60E-04	0.8486	1.14E-03	1.62E-03
^{235}U	1.37E-02	1.12E-04	9.71E-05	1.12E-04	1.02E-03	1.98E-04	2.72E-04
^{236}U	2.60E-03	7.14E-05	7.08E-05	7.167-05	4.13E-04	8.33E-05	9.37E-05
^{238}U	7.8750	6.98E-05	7.79E-05	7.08E-05	0.84678	7.81E-05	7.87E-05
Pu inventory (g/cc)	0.8492	0.2334	0.2292	0.2374	0.3051	0.3068	0.4414
Discharged Pu / initial Pu	0.774	0.307	0.303	0.310	0.406	0.384	0.493
^{238}Pu	0.842	0.577	0.574	0.590	0.665	1.549	2.322
^{239}Pu	0.572	0.029	0.022	0.028	0.093	0.055	0.118
^{240}Pu	0.910	0.404	0.382	0.401	0.547	0.475	0.601
^{241}Pu	1.537	0.787	0.719	0.794	1.084	0.922	1.215
^{242}Pu	1.027	1.484	1.635	1.535	1.508	1.754	1.621
% Pu incinerated/cycle	22.6%	69.4%	69.7%	69.0%	59.4%	61.6%	50.7%
Fissile Pu/ Tot Pu	56.5%	24.5%	21.9%	24.3%	32.8%	27.4%	33.3%
MA inventory (g/cc)	4.86E-02	4.57E-02	4.27E-02	4.47E-02	4.13E-02	6.57E-02	1.04E-01
Th:	3.17E-09	1.51E-09	1.77E-09	1.56E-09	1.87E-09	9.12E-05	9.16E-05
Pa:	6.89E-10	4.17E-10	3.73E-10	4.22E-10	3.86E-10	3.33E-07	2.86E-07
Np:	1.75E-03	2.26E-05	2.22E-05	2.29E-05	1.93E-04	2.47E-02	3.13E-02
Am:	3.30E-02	2.38E-02	2.47E-02	2.35E-02	2.54E-02	2.48E-02	4.11E-02
Cm:	1.39E-02	2.19E-02	1.80E-02	2.12E-02	1.58E-02	1.61E-02	3.17E-02
Bk:	1.02E-09	1.65E-08	4.14E-09	1.40E-08	2.72E-09	2.92E-09	3.17E-08
$^{237}Np+^{241}Am+^{245}Cm$	1.53E-02	4.31E-03	3.72E-03	4.31E-03	5.79E-03	3.02E-02	4.87E-02
Total TRU inventory	0.8977	0.2791	0.2720	0.2821	0.3465	0.3725	0.5457
% TRU incinerated/cycle	18.22%	63.36%	64.04%	63.16%	53.87%	56.69%	47.15%
MA/Pu at discharge (%)	5.72%	19.57%	18.64%	18.84%	13.55%	21.41%	23.63%
Neutron source (n/s/cc)	1.38E+05	2.24E+05	1.89E+05	2.17E+05	1.62E+05	1.70E+05	3.43E+05
Activity (Ci/cc)	40.06	59.33	57.74	58.26	44.71	50.97	60.71
Decay heat (w/cc)	0.27	0.37	0.37	0.37	0.31	0.38	0.82
☐ decay heat (w/cc)	3.07E-03	6.92E-03	6.73E-03	6.73E-03	4.67E-03	5.39E-03	4.73E-03
Neutrons per g Pu (n/s)	6.36E+02	1.25E+03	1.31 E+03	1.26E+03	1.08E+03	1.28E+03	1.19E+03
Neutrons per g HM (n/s)	1.57E+04	8.00E+05	6.95E+05	7.69E+05	1.36E+05	4.55E+05	6.28E+05
Specific heat (w/g Pu)	0.047	0.259	0.256	0.249	0.145	0.209	0.166
Specific heat (w/g HM)	0.031	1.323	1.370	1.321	0.258	1.015	1.504

Table 1. Comparison of selected transmutation characteristics of hydride- (in blue) and oxide-fueled PWR; first recycle.

* In the first recycle, the fuel temperature coefficient of reactivity turns positive at ~2/3 of the reported burnup. There are no limitations on the second and following recycles or on the other first recycles reported in this table.

Planned Activities

Researchers will compare the fuel cycle cost for recycling Pu and MA in PWRs using hydride fuel versus Pu, as well as MA recycling in PWRs using CORAIL—or CONFU—type oxide fuel assemblies. Researchers will also compare the impact of recycling Pu and MA using hydride fuel versus using oxide fuel on the Yucca Mountain Repository (YMR). Following is a list of the performance characteristics that will be compared:

- TRU and fission product quantity and composition that will need to be disposed of
- Radiotoxicity and decay-heat of the high-level waste (HLW)
- Inventory of ^{237}Np and its precursors—a major contributor to the long-term radiation level in the vicinity of the repository due to HLW leakage into the environment
- HLW storage capacity—to be measured by the cumulative amount of energy that could be generated in PWRs as well as the HLW that could be stored at the YMR

As part of the safety analyses, the performance of a PUZH-fueled core during a complete loss of coolant accident (CLOFA) will be investigated and compared to those of all the UO_2–, CONFU–, and CORAIL– fueled cores.

Researchers will also study hydride fuel compatibility with Zircaloy cladding. The possibility and extent of hydrogen attack of the clad will be determined under two different conditions: filling the fuel-clad gap by either helium or liquid metal. Also to be studied is the kinetics of the reaction of hydride fuel with steam at high temperatures. This is necessary to characterize the behavior of the fuel in case of cladding failure.

NUCLEAR ENERGY RESEARCH INITIATIVE

Accelerator-Based Study of Irradiation Creep of Pyrolytic Carbon Used in TRISO Fuel Particles for the VHTR

PI: Lumin Wang and Gary S. Was, University of Michigan

Collaborators: Oak Ridge National Laboratory, Idaho National Laboratory

Project Number: 06-113

Project Start Date: March 2006

Project End Date: March 2009

Research Objectives

Pyrolytic carbon (PyC) is one of the important structural materials in the tri-isotropic (TRISO) fuel particles that will be used in the next generation of gas-cooled VHTRs. When TRISO particles are under irradiation at high temperatures, creep of the PyC layers may cause radial cracking, leading to catastrophic particle failure. Therefore, a fundamental understanding of the creep behavior of PyC during irradiation is required in order to predict overall fuel performance.

The primary objective of this project is to characterize the creep behavior of PyC through a systematic program of accelerator-based proton irradiation and *in-situ* measurements under stress at various temperatures between 400 and 1,200°C. Test data will be analyzed to determine creep coefficients, which will then be correlated to existing coefficients measured under neutron irradiation. In addition, initial experiments on the transport of select fission products (e.g., silver [Ag] and strontium [Sr]) in PyC under irradiation and stress will be conducted by implanting ions into the material. The PyC microstructure will be studied with advanced analytical transmission electron microscopy (TEM).

Research Progress

During the past year, two major tasks for this research project have been completed:

- Construction of an ion accelerator target chamber for an *in-situ* creep test during proton ion beam irradiation and test overall system design and operation
- Production of the PyC material for the *in-situ* creep test under proton irradiation, and electron microscopy microstructural characterization of the material

The following is a brief description of the accomplishments on these two tasks.

Construction and test of the irradiation creep test facility. In order to characterize the creep behavior of PyC under 3.2 MeV proton irradiation in the temperature range of 800 and 1,200°C, a special test assembly has been designed and constructed. The facility design has taken various parameters such as temperature, strain measurement, loading, and thermal insulation into consideration. Figure 1 presents the schematics of the test assembly. As shown in the figure, the test assembly includes a thermal imager for temperature monitoring; a laser speckle extensometer (LSE) for non-contact, high-accurate displacement measurement; a substrate heater and stage assembly for high-temperature application; an aperture system for fine control of the proton beam; and a constant stress loading system. The original thermal imager software installed in the Michigan Ion Beam Laboratory was successful for monitoring irradiation temperatures up to 500°C. The existing system has been extended to measure temperatures up to 1,200°C.

The PyC sample is secured by the ceramic sample holders. Each sample holder is composed of two ceramic holding bars. The samples will be fastened in between holding bars. The top sample holder will hold the samples tightly so they will not slip during the creep test. The bottom sample holder will lightly press against the samples. The application of the second sample holder will hold the samples in good contact with the heating surface, resulting in a more uniform temperature distribution across the irradiated area. The end of the sample is tightly clamped by a custom-made device that connects to a load through a steel wire. The up and down movement of the load tray is controlled by a linear motion feed-through. Two existing

4-inch ports on both sides of the vacuum chamber (not shown in the figure) will provide convenient access of the clamp inside the chamber.

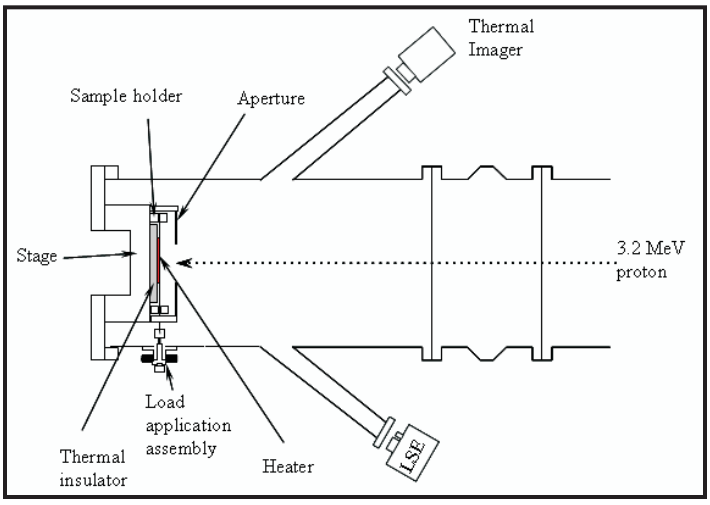

Figure 1. The irradiation creep test system assembly.

The LSE system is composed of a laser source, a high resolution charge-coupled device (CCD) camera, and the LSE evaluating software. Speckle patterns acquired by the CCD camera are processed by the LSE software so that the displacement of each pattern can be tracked. These displacements are then converted into strain. The software can be configured to separately monitor two movements. Researchers have tested the stability of the LSE system, as well as the accompanying software in recording displacement measurements. The capability of the LSE to measure low strain rates (approximately 10^{-8}/s) was evaluated. Beam-on experiments were carried out on both stainless steel foil and PyC samples using 2 MeV protons to test the effects of ion beam current to the temperature of the specimen. A significant amount of heat was contributed from the proton beam for stainless steel. Heated by the proton beam alone, the temperature of the stainless steel sample can easily reach >1,000°C when the beam current density on the sample is >10 μA/cm^2. Heat from the proton beam is less significant for the PyC sample due to its high conductivity and emissivity. At a stage current density of 20 μA/cm^2 (dose rate approximately 4×10^{-6} dpa/s), the temperature increase in the PyC sample due to proton irradiation was around 500°C, which is below the target testing temperature range of 600 to 1,200°C. The beam effect was also evaluated with sample temperatures starting at 200 and 400°C achieved by using a substrate heater.

Production and characterization of the PyC material. Due to various reasons, researchers could not obtain the PyC samples from the national laboratories as originally expected, and the commercially available PyCs are all non-isotropic pyrolytic graphite that is not suitable for the test. Thus, the research team had to synthesize the PyC material in their own laboratory with an existing chemical vapor deposition (CVD) system. A detailed literature search had been conducted before the synthesis work started. PyC coating for TRISO fuel particles has usually been prepared by the thermal decomposition of hydrocarbons such as methane, propane, and propylene in a CVD system. Propylene was first used as the carbon source for the German TRISO particle fuels and has demonstrated high quality and excellent irradiation and safety behavior under reactor relevant conditions. The United States, as well as other countries such as France and China, also uses propylene as the carbon source. Propylene and argon gases were used as the carbon source and carrier gas, respectively, in the process and a quartz tube was heated in the tube furnace from 1,200 to 1,300°C. The gas flow was controlled by mass flow meters. The total gas flow rate, which accounts for the mixture of propylene and argon, was 200 ml/min. The concentration ratio between propylene and argon was 1:1. Quartz plates were used as the substrate for carbon deposition.

The PyC coatings were characterized by scanning electron microscopy (SEM) and TEM. The results demonstrated that isotropic nanocrystalline PyC films with the thickness up to 50 μm have been obtained. Figure 2 shows the high-resolution TEM images and the electron diffraction patterns from the PyC coating. From the plan-view diffraction pattern (Figure 2a), the PyC coating is nano-crystalline instead of amorphous because the diffraction rings are remarkably sharp instead of being diffused. The small crystallites in the coating are randomly orientated, yielding an isotropic microstructure. The high-resolution TEM micrograph demonstrated that the crystalline size is less than 2 nm. The electron diffraction pattern and the high-resolution TEM micrograph from the cross section of the PyC sample (Figure 2b) indicated a small texture in the cross section of the material. The crystallites exhibited a graphite-like layered structure with a small preference for its basal plane to be parallel to the surface of the film. Energy dispersive x-ray spectroscopy (EDS) analysis verified that the synthesized material is pure PyC. Thin films that are as long as 4 cm have been prepared for the radiation creep tests.

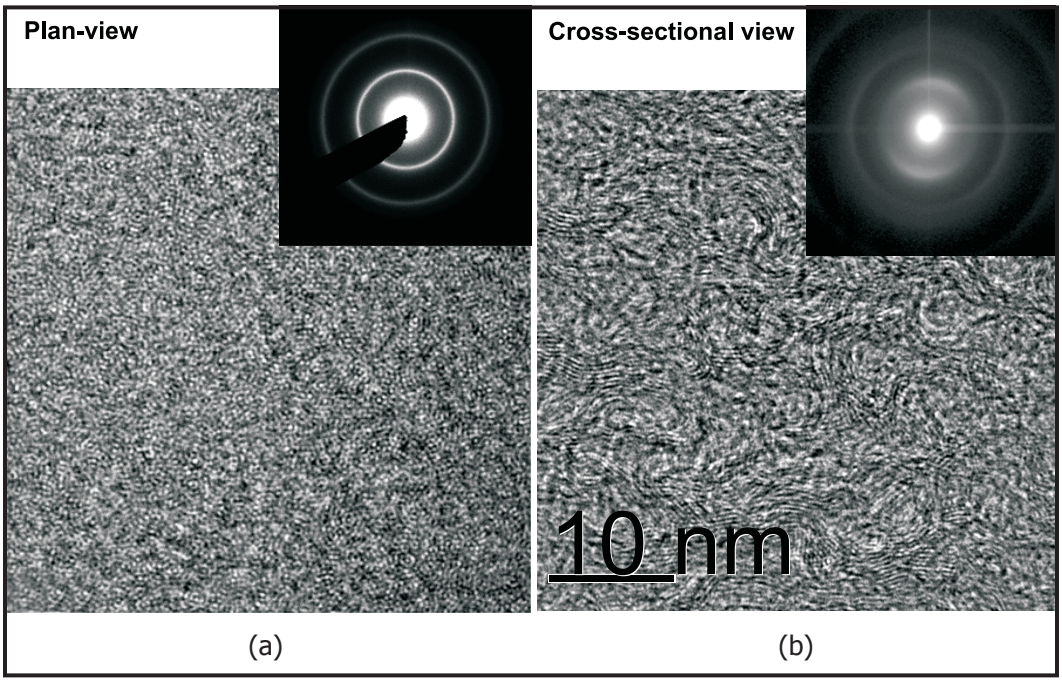

Figure 2. Microstructures of PyC synthesized at 1,300°C observed by TEM. (a) High-resolution TEM micrograph and electron diffraction pattern from plan view (electron beam perpendicular to the surface of the PyC film); (b) Cross-sectional high resolution TEM micrograph and electron diffraction pattern (electron beam parallel to the original surface of the PyC film).

Planned Activities

The following activities are planned for the upcoming year:

- To conduct low-temperature proton irradiation (400 and 600°C) on PyC (unloaded) and to perform data analyses
- To conduct low-temperature irradiation on PyC under stress and to perform data analyses
- To conduct high-temperature irradiation (800, 1,000, and 1,200°C) and to perform data analyses
- To implant selected fission product elements (e.g., Ag and Sr) and to perform irradiation of samples with pre-implanted fission product and cross-sectional TEM analyses
- To conduct final data analyses and empirical modeling

Nuclear Energy Research Initiative

Development of Acetic Acid Removal Technology for the UREX+ Process

PI: R. M. Counce and J. S. Watson, University of Tennessee (UT)

Collaborators: Oak Ridge National Laboratory (ORNL)

Project Number: 06-116

Project Start Date: March 2006

Project End Date: March 2009

Research Objectives

The overall goal of this project is the selection and experimental verification of the most appropriate technology to separate or destroy acetic acid produced from decomposition of acetohydroxamic acid in the UREX+ process. Acetic acid accumulation would hamper reuse of nitric acid and increase waste volume. The goals for the second year are 1) to conduct an in-depth analysis of the leading technologies selected from the literature review performed during the first year and 2) to select the best method to proceed with into the final year. Studies performed this year included an evaluation of the chemistry of selected systems, flow sheet studies of the most promising approach, and selective engineering tests. The objective of this project, then, is to provide reference studies sufficient for incorporating an acetate removal step into the UREX+ process conceptual flow sheet when needed.

Research Progress

The research team conducted a review of appropriate technologies and an evaluation of available thermodynamic information for simulated UREX+ aqueous solutions containing nitric and acetic acids. They determined that the most feasible separation/destruction method is solvent extraction and subsequent analysis will focus on solvent extraction options. The team will consider other options if solvent extraction proves to be less attractive than expected. The alternate options include combined distillation and crystallization and possibly carbon or polymer-based adsorption.

The experimentation stage of the project has begun with determination of distribution coefficients for the acetic-nitric-solvent system. A class of highly polar, highly hydrophobic solvents with large dielectric constants has been determined in initial experiments to give the most promising results for the removal of acetate from the system. It is desirable that this removal/destruction step be selective for acetic acid over nitric acid and that no radioactive materials be removed along with the acetic acid.

The development of a selective process will require further experimental confirmation later in the project, and other aspects of the process are expected to require exploration, such as the stripping option and the behavior of metal ions (radioactivity) in the process step. No literature has been found on this class of solvents as a possible method of acetate removal, so these results are believed to be important new findings. Using an automatic buret and pH meter, several solvents from this class and others are being tested to determine the distribution coefficients and to select the most promising solvents (Figure 1). The titration curve obtained from these apparatuses is shown below in Figure 2. The first inflection point represents the completion of nitric acid neutralization. The second inflection point represents the neutralization of both acids. The amount of base required to neutralize the acetic acid present is observed by the difference between the first and second inflection points. These results are discussed with ORNL staff and other affiliates developing the UREX+ process to determine the best solvent for the extraction of acetate.

Figure 1. Analytical portion of experimental system.

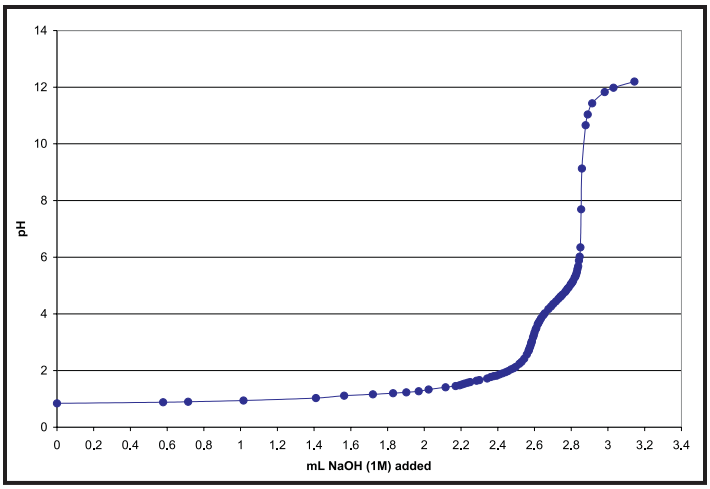

Figure 2. Titration plot of nitric and acetic acids.

Planned Activities

Current efforts are focused on polar hydrophobic solvents that have been found to give higher distributions coefficients than the representative hydrocarbon solvent tested. Evaluation of this class of solvents is continuing to cover a range of solution concentrations of interest in the UREX+ process. The next step after selection of solvents and determination of distribution coefficients will be to determine the behavior of metal ions in the system. Analysis on the behavior of metal ions will focus on those that could contaminate the acetic acid product/waste and increase waste disposal/handling operations. Evaluation of key aspects of the chemistry of acetic and nitric acid extraction will be evaluated further as needed. Flowsheet development and analysis have been initiated and will continue. The physical properties of selected solvents will be evaluated as needed to estimate their performance in engineering equipment. A centrifugal contactor has been purchased and is being set up for verifying the performance of selected solvent(s) in engineering-type equipment. Once flow sheet development and key engineering tests have reached a sufficient state, an approximate cost analysis for adding an acetate removal step to the UREX+ process will be prepared. Both the engineering tests and the economic analyses will involve close association with the ORNL partners.

Nuclear Energy Research Initiative

Separation of Nuclear Fuel Surrogates from Silicon Carbide Inert Matrix

PI: Ronald Baney and James Tulenko, University of Florida

Collaborators: None

Project Number: 06-126

Project Start Date: March 2006

Project End Date: March 2008

Research Objectives

The objective of this project is to identify a process for separating transuranic species from silicon carbide (SiC), a prime candidate for inert matrix fuel (IMF) materials. Viable processes for separating the unspent fuel from the SiC matrix have not been identified by the industry. This project will address the void and establish a protocol for the dissolution and separation of the SiC from ceria, a surrogate for PuO_2. Only technologies compatible with traditional fuel handling processes are being examined. Researchers performed a literature survey to identify and evaluate available methods that could be used for dissolving SiC and recovering the fissile material. After evaluating various candidate methods for ease of separation, degree of safety, and cost, researchers selected a hot corrosion (sodium carbonate molten salt) method as the most promising method to be studied.

SiC is thermodynamically an unstable ceramic towards reaction with oxygen, but oxidation is inhibited by the formation of a passivating silica layer, which prevents oxygen from reaching the underlying SiC. In a molten sodium carbonate environment, sodium ions can flux the silica layer by forming sodium silicate, thus destroying the passivation effect of the silica. The process continues until the SiC is consumed, as occurs in immersion in a melt bath. The dissolution of SiC by alkali and alkali earth compounds has been known since the 1970s and research has continued well into the early 2000s. Previous reported studies have shown that the rate and degree of corrosion varied based on oxygen partial pressure and the type of sodium salt used for the melt bath. The roles of bath temperature and SiC particle size are now being studied by the University of Florida.

In previous reports, experiments were described in which SiC pellets and powders were reacted with sodium carbonate at 1,050°C in an open-ended tube furnace. The powders completely reacted after two hours. Ceria pellets were unchanged under the same reaction conditions. These preliminary studies demonstrated the viability of this process. In this reporting period, the team began identifying parameters affecting the rates of SiC dissolution.

Research Progress

Collection of the Kinetic Data. An open-ended tube furnace was preheated to selected temperatures. Crucibles containing the mixture of SiC powder (1µm) and Na_2CO_3 salt at approximately a one-to-one molar ratio were placed midway in the tube furnace. The samples were held at the selected temperatures for 15 minutes, each hour, for six hours. Samples were then rapidly quenched by immersing them into boiling water to dissolve Na_2SiO_3 and residual Na_2CO_3. The samples were then transferred to centrifuge tubes, centrifuged, dried, and the un-reacted SiC was weighed. The average percent of remaining SiC was determined. Blank experiments were also performed: the weight loss of the commercial SiC powder without the Na_2CO_3, but after boiling, transporting, centrifuging, and drying, was measured in order to obtain the operation error.

Scanning electron microscopy (SEM) images of the SiC powder were obtained to examine particle size distribution. An aerosizer was used to measure the particle size distribution of SiC powder. BET specific surface areas of samples were obtained. The BET method involves determining the amount of an adsorbed monolayer of an inert gas on a solid surface and then calculating the specific surface area from the size of the gas molecule and weight of the solid.

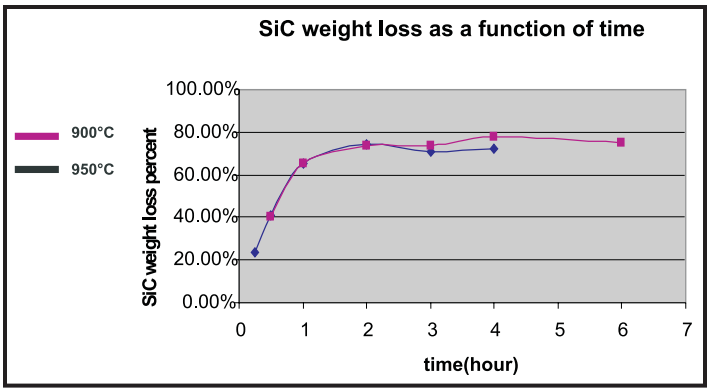

Figure 1. SiC weight loss at 900 and 950°C as a function of time (initial molar ratio of Na_2CO_3 to SiC equals 1.05).

Results and Discussion. The average weight loss of the blank experiments was a negligible 1.24 percent. Figure 1 shows the SiC weight loss when varying the isothermal holding time at 900 and 950°C. In the first two hours, SiC weight loss rate was significant; however, little weight loss occurred after two hours.

The reaction appears to level off and stop at about 75 percent completion. Three factors might explain the "leveling-off" effect:

1) There may not be enough sodium carbonate left to continue the process due to its thermal decomposition into sodium oxide and carbon dioxide. However, addition of more sodium carbonate initially, or after a two-hour temperature hold, had no effect on the leveling-off effect. Therefore, insufficient sodium carbonate concentration is not the cause of the leveling-off effect.
2) A second possible explanation for the leveling-off effect is that the SiC powder consists of a bimodal distribution of particle sizes with approximately 75 percent being very reactive, high-specific surface particles and the remaining being larger particles. BET specific surface area studies and particle size analysis showed that a majority of the particles were larger, not smaller, therefore eliminating this as a cause for the leveling-off effect.
3) A sample of SiC was reacted to the leveling-off point and then separated and re-reacted in a fresh sodium carbonate melt. Again, after two hours, only about 75 percent reacted percent of the remaining SiC reacted. It has been reported in the literature that sodium silicate can phase-separate, coat the SiC pellet, and prevent the fluxing sodium ions from reaching and destroying the passivating silica layer. This explanation now seems most likely to explain the leveling-off effect. A recycling or multi-step process, or a method of removing the sodium silicate coating the SiC, appears practical.

Planned Activities

Researchers plan to perform the following tasks during the remaining period of the contract:

- Test the validity of the sodium silicate leveling-off effect
- Demonstrate a two-step process for complete dissolution of the SiC through particle size reduction or pH control to remove sodium silicate
- Demonstrate hot corrosion dissolution of a SiC containing approximately 5 percent of ceria by the molten sodium carbonate process

Nuclear Energy Research Initiative

Enhancements to High-Temperature In-Pile Thermocouple Performance

PI: John Crepeau, University of Idaho

Collaborators: Idaho National Laboratory (INL)

Project Number: 06-134

Project Start Date: March 2006

Project End Date: March 2008

Research Objectives

There are insufficient data to characterize the performance of new reactor materials in high-temperature, radiation conditions. To evaluate candidate material performance, robust instrumentation is needed that can survive these harsh conditions. Traditional methods for measuring temperature in-pile either degrade at temperatures above 1,100°C or de-calibrate due to transmutation.

Several years ago, INL launched an effort to develop temperature measurement methods suitable for long-duration, high-temperature, in-pile testing. Initial results indicate that specialized alloy thermocouples fabricated from doped molybdenum/niobium-1% zirconium (Mo/Nb1%Zr) have the potential to provide the desired accuracy for long-duration tests. Although the performance of these thermocouples appears promising, there are several options that can potentially enhance their lifetime and reliability.

The major research objective of this project is to quantify the impact of candidate enhancements related to alloy materials, geometry, and fabrication techniques on thermocouple performance. Based on these evaluations, improved thermocouple designs will be fabricated and tested at high temperatures for long durations to quantify thermocouple accuracy, reliability, and lifetime. Ultimately, an optimized thermocouple design will be recommended for high-temperature, in-pile testing.

Research Progress

In Task 1, researchers evaluated alternate alloys for the INL-developed High-Temperature, Irradiation-Resistant Thermocouples (HTIR-TCs). Alloys of molybdenum and niobium were evaluated in this task. Three types of high temperature testing were proposed: 1) ductility evaluations, 2) resolution evaluations, and 3) long duration testing (if results from the prior two subtasks appear promising).

Results from Task 1 evaluations indicate that either ODS-Mo or KW-Mo paired with Nb-1%Zr yielded a thermocouple that best retained its ductility and exhibited the best resolution over the temperatures of interest. Because the ODS-Mo is not commercially available, this material is significantly more expensive to obtain. Hence, initial INL evaluations pairing KW-Mo with Nb-1%Zr yields the best thermocouple combination. Because this thermocouple is being investigated in various long duration, high-temperature tests in other tasks (e.g., Task 2 of this project), no additional long duration testing was performed as part of Task 1.

In Task 2, the performance of thermocouples with alternate geometries was investigated. As part of this task, techniques were developed for fabricating each thermocouple's geometry so that it can withstand high temperatures for a long duration and transient testing. Representative samples of each of these alternate geometry thermocouples were prepared and subject to thermal cycling tests (two cycles up to 1,600°C) and a long duration test (over 2,000 hours) at 1,500°C. Results from these tests show that thermocouples containing larger diameter wire (0.020"/0.508 mm) remained stable for longer time periods.

Planned Activities

For the final task, the team will explore several alternate fabrication techniques for fabricating doped Mo/Nb-1%Zr thermocouples. In particular, efforts are being completed to explore the impact of heat treatment temperatures and durations on thermocouple performance as well as to compare a "loose assembly" thermocouple configuration with the "swaged" type of HTIR-TCs, which was the subject of prior INL evaluations.

Heat treatment evaluations are focusing on thermocouples that are designed to operate at 1,200 and 1,500°C. The table below lists the heat treatment temperatures and durations initially explored for thermocouples to be operated at each of these temperatures. For each operating temperature, fabricated thermocouples were calibrated and then subjected to 100-hour heating tests at higher temperatures.

Operating Temperature (°C)	Heat Treatment Temperature (°C)	Duration (Hours)	Designator
1,200	NA	0	12-0
	1,300	5	12-1300-5
		10	12-1300-10
		20	12-1300-20
	1,400	10	12-1400-10
		20	12-1400-20
	1,500	10	12-1500-10
		20	12-1500-20
1,500	NA	0	15-0
	1,600	4	15-1600-4
		8	15-1600-8
		16	15-1600-16
	1,700	4	15-1700-4

Table 1. Heat treatments investigated.

Nuclear Energy Research Initiative

Design and Development of Selective Extractants for An/Ln Separations

PI: Robert T. Paine, University of New Mexico (UNM)

Collaborators: Washington State University (WSU), Idaho National Laboratory (INL)

Project Number: 06-137

Project Start Date: April 2006

Project End Date: March 2009

Research Objectives

This project is designed to remove transuranic elements from spent nuclear fuel for storage or for reuse in transmutation processes. The proposed method will develop an efficient aqueous separation scheme for recovering americium (Am) and curium (Cm) from the acidic liquid remaining after UREX+2 processing to remove uranium (U), plutonium (Pu), neptunium (Np), cesium (Cs), and strontium (Sr). The method will also separate trivalent actinides from fission product lanthanide ions. The project focuses on the continued development and optimization of "NOPOPO ligands," which the researchers previously demonstrated are effective extractants under laboratory-scale conditions and show promise as a large-scale process add-on to UREX+2.

The primary objectives of this project include 1) the design, synthesis, and extraction performance characterization of 2,6-bis(phosphinomethyl)pyridine N,P,P′-trioxides (NOPOPO) as potential reagents for separating Am, Cm, and fission product lanthanides from other transuranics and fission products; and 2) the development of a separations "platform" for the mutual separation of Am/Cm from the lanthanides. Preliminary analyses indicate that one member of the family of ligands, $(EtHx)_4$NOPOPO, offers improved separation of Am^{3+} ions from acidic aqueous solutions compared to the CMPO ligand used in the transuranic extraction (TRUEX) process. The research is expected to produce a best-case extractant compound, which will undergo a complete round of synthesis optimization and performance characterization with a realistic raffinate stimulant representative of the uranium extraction (UREX+) process.

Specific project tasks include the following:

- Optimize the NOPOPO synthesis
- Conduct further extraction testing of $(EtHx)_4$NOPOPO
- Study extractant phase compatibility as well as hydrolysis and radiolytic stability
- Design and synthesize new NOPOPO derivatives with improved solubility, phase compatibility, and stability characteristics
- Conduct extractive testing of the new derivatives to determine their relative efficacy
- Conduct focused testing on the best-case extractant compound to optimize synthesis and characterize performance with realistic waste solutions
- Perform a cost analysis for the new process

Research Progress

Prior work performed by the research team has shown that modest quantities (2–10 grams) of the family of NOPOPO ligands, 1, with a wide variety of aryl and alkyl R groups, could be prepared from three different synthesis protocols.

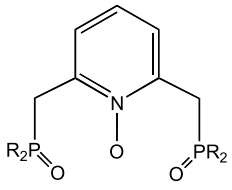

1

Figure 1. New family of NOPOPO ligands.

Subsequent work that focused on developing a hydrocarbon solvent soluble derivative suitable for actinide ion extractions showed that the derivative 3 with R = R′ = 2-ethyl hexyl (EtHx) could be obtained in 10-gram batches with good overall yield. However, as initially described, the synthesis yields varied from batch to batch and the crude

ligand often required extensive efforts to obtain in suitably pure form. Therefore, the initial objective of the new program involved the development of a reliable procedure for synthesis and purification of 3 with R = R´ = 2-EtHx.

During the first 12 months of the project, researchers optimized the procedure summarized in Figure 2.

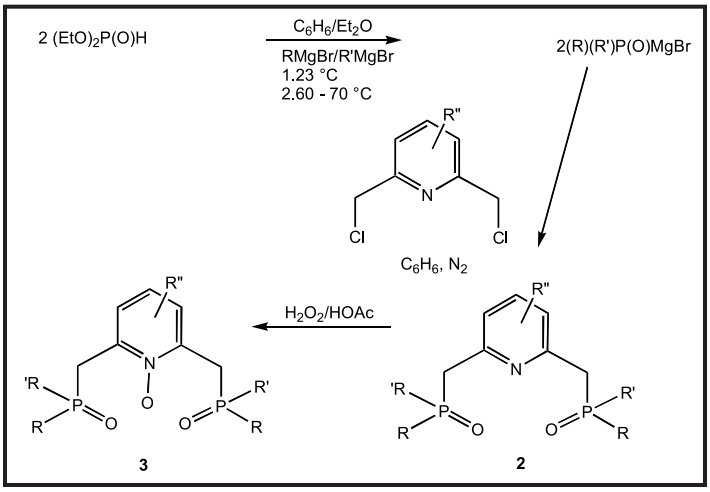

Figure 2. Synthesis and purification of 3 with R = R´ = 2-EtHx.

The synthesis has now been performed on a 20-gram scale with yields of 80 percent or better. The team has identified the source of the troublesome impurities: they appear to originate in the commercial-starting material. Efforts to eliminate the originating species have been partially successful—success on small-scale batches (approximately 2 grams) have been achieved so that only a single chromatographic column separation is required for purification. Work is in progress to extend the batch scale to 20 grams.

The synthesis effort has been expanded to include derivatives that might be soluble in the process solvent FS-13. In this regard, the analogs of 2 and 3, having R = R′ = 2-$CF_3C_6H_4$ and 3,5-$(CF_3)_2C_6H_3$, have been prepared. These compounds have been fully characterized and coordination chemistry is currently being explored.

The studies of aqueous acid stability of 3 (R = R′ = 2-EtHx) continued during the second year of research. The compound appears to remain stable when stored at 20–25°C and while exposed to 0.5–4M HNO_3 as determined by ^{31}P NMR analysis. During the first year of research, an initial radiolysis test was undertaken at INL. The results suggested that some degradation occurs as indicated by reduced extraction performance for Am and Cm. A second round of studies was planned but facility interruptions prevented completion of the study. New tests are expected to take place in the current year.

Single element extraction analyses (Ce, Eu, and Yb) continued during the first research year. No additional unexpected behavior was uncovered in these studies and plans for stimulant testing are being developed.

Planned Activities

The scale-up and purification optimization studies for 3 (R = R′ = 2-EtHx) will continue with specific attention given to purification of the starting material. If a dependable purity level cannot be realized by the commercial supplier, it may become necessary to make this material during this program. In addition, researchers plan to continue the synthesis development and purification of trifluoromethyl derivatives of 3, which may have useful performance in FS-13 process solvent.

The radiolysis behavior and subsequent extraction performance testing at INL will continue, as will the extraction testing at WSU.

Nuclear Energy Research Initiative

Microwave Processing of Simulated Advanced Nuclear Fuel Pellets

PI: D. Clark and D. Folz, Virginia Polytechnic Institute and State University (VT)

Collaborators: University of Tennessee (UT)

Project Number: 06-141

Project Start Date: March 2006

Project End Date: March 2009

Research Objectives

The objective of this project is to sinter simulated (non-radioactive) oxide and nitride inert matrix fuel (IMF) pellets using microwave energy. Researchers will characterize the sintered pellets with respect to density and grain morphology. Researchers on the VT team will use microwave hybrid heating (multi-mode and single mode) to sinter the pellets, while the UT researcher will use direct microwave sintering (no microwave susceptor).

Following are the primary tasks of this work:

- Prepare green pellets
- Demonstrate direct microwave heating (DMH) to achieve sintering
- Demonstrate microwave hybrid heating (MHH) to achieve sintering
- Characterize pellets before and after microwave processing
- Evaluate microwave processes

Research Progress

Cubic zirconium oxide (8 mol% yttria). The processing regime for the sintering of 8YZ is outlined in Figure 1. A similar methodology is being applied to the Dy_2O_3-8YZ pellets.

The forming technique for green pellets was performed using both uniaxial and isostatic pressing. Approximately 4g of as-received powder was poured into a uniaxial mold of 12.5 mm diameter and 70 mm height and subjected to a pressure of 37 MPa. The pellet formed uniaxially was transferred to isostatic bags and further pressed to 175 MPa. The initial green density was 46 percent theoretical density (%TD) (theoretical density calculated using X-ray Diffraction Data [5.96 g/cc]).

The temperature monitoring system and susceptor design developed during the last quarter were used to finish the sintering experiments at different temperatures in both a multi-mode hybrid furnace and a single-mode microwave furnace. For comparing the results as a baseline for microwave-processed samples, researchers have also performed sintering in a conventional furnace.

It was observed that at 1,300°C, the microwave-processed samples showed a higher density; in particular, the single-mode-sintered sample showed a 96 %TD. To obtain a similar density in the conventional furnace, researchers increased the temperature to 1,400°C. As confirmation of these higher densities at 1,300°C, researchers observed the fracture surface of these samples under a scanning electron microscope (SEM). The results can be seen in Figure 2.

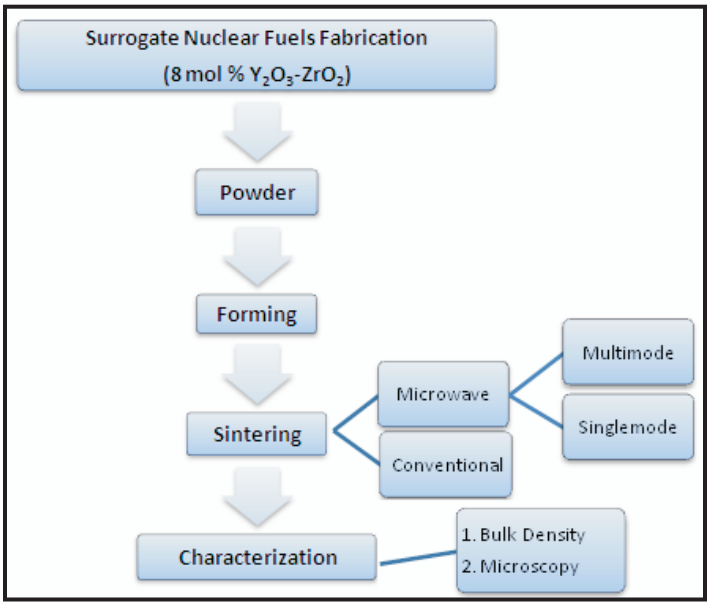

Figure 1. Experimental outline for sintering cycle of 8YZ.

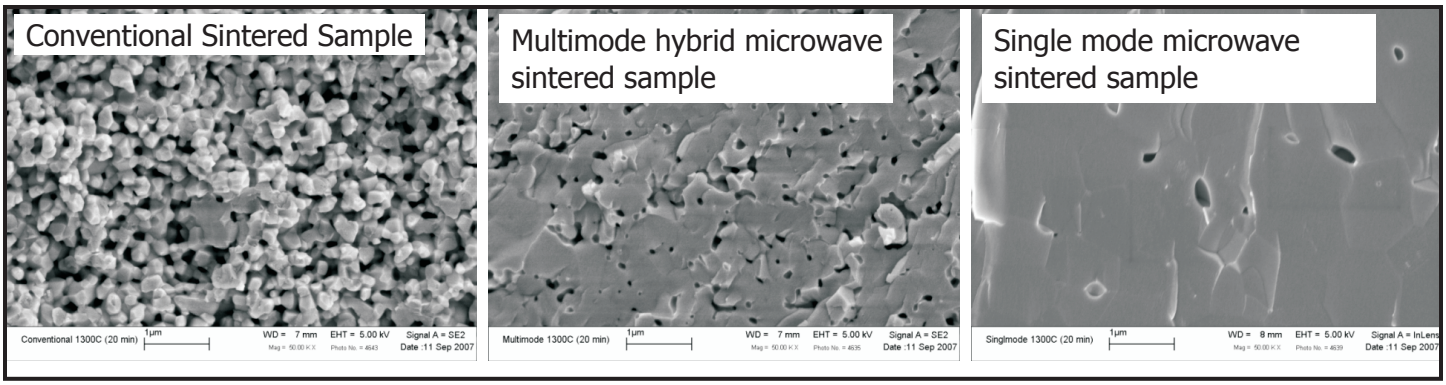

Figure 2. Fracture surface imaging of 8YZ sintered pellets at 1,300°C for conventional, multi-mode hybrid, and single-mode samples.

As is evident in Figure 2, the conventionally processed sample is still in the green state while the microwave-processed sample has shown a significant decrease in porosity. These results obtained for the 8YZ inert matrix material system indicate that higher densities (greater than 95 %TD) can be obtained using microwave energy than with radiant heating when the sample experiences the same soak temperatures for the same amount of time.

Cubic zirconia—dysprosia composite pellets. Researchers have begun incorporating the actinide stimulants into the inert matrix (8YZ) using two different techniques: encapsulation and dispersion. The research team will use these sample configurations to study the stability of the actinide surrogates within the inert matrix materials.

Dysprosia (Dy_2O_3) was selected as the surrogate fuel for americia (Am_2O_3) based on the fact that 1) the atomic size of the outer most "s" shell orbital is similar (approximately 200 pm) for dysprosium and americium, and 2) dysprosia is economical and is commercially available.

For the initial proof of concept experiments, dispersed pellets of 20 wt % Dy_2O_3 were formed into the shape of a tablet using isostatic pressure of approximately 175 MPa. This tablet was covered with 8YZ powder in the uniaxial mold and the composite was pressed at 37 MPa to obtain a cylindrical shape, which was further pressed isostatically to 175 MPa. In a similar fashion, encapsulated pellets of 20 wt % Dy_2O_3 were made by mixing with 8YZ powder and the mixture was allowed to roll on the ball mill for a period of 12 hours. The final powders were pressed at 37 MPa uniaxially to obtain a cylindrical shape and were further pressed isostatically at 175 MPa.

Preliminary results obtained by firing the composite at 1,300°C in a conventional furnace showed that the encapsulated pellet achieved a higher density (79 %TD) when compared to the dispersed pellet (74 %TD). However, the encapsulated pellet showed significant cracking when compared to the dispersed pellet. This behavior could be due to the difference in thermal expansion between pure dysprosia and 8YZ. These tests will continue in the third year.

Samples with 15 mol% Dy_2O_3 were also prepared. They were heated in a 2.45 GHz microwave field to 1,400 and 1,450°C and held at that temperature for 10 minutes. Starting green density of the samples was approximately 48 percent of theoretical while the density after microwave heating at 1,400–1,450°C was approximately 70–71 percent of theoretical. X-ray diffraction (XRD) of these samples show a complete solid solution between ZrO_2 and Dy_2O_3 with only zirconia lines showing on the XRD pattern for 85 mol % ZrO_2 – 15 mol% Dy_2O_3 sample microwave heated to 1,450°C and held at that temperature for 10 minutes.

Zirconium nitride. Work began on fabricating zirconium nitride (ZrN) samples using a chemical precipitation approach. Powder size ranged from approximately 70 to 150 nm. Conventionally produced coarse ZrN powder was obtained from H.C. Starck. Both powders were uniaxially pressed to a density of 46 percent of theoretical. Samples of the chemically precipitated powder and the Starck powder were placed on an Al_2O_3 setter plate that had a covering of ZrN powder. The samples were completely covered with the ZrN powder and argon gas flowed over the samples. The samples were then microwave-sintered at 2.45 GHz for approximately 10 minutes at approximately 1,300°C.

Observation of the sintered pellets showed some slight oxidation on the edge of the samples (a white color). This area was polished off and the samples were then examined using a SEM. The sample made from the chemical precipitation route (S1) appeared to have regions that were very dense with a few large voids while the Starck

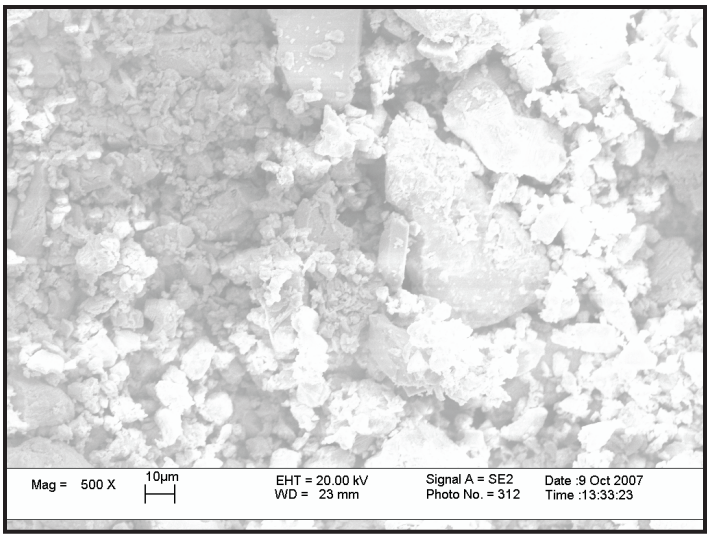

Figure 3a. SEM photomicrograph of S2 (500X).

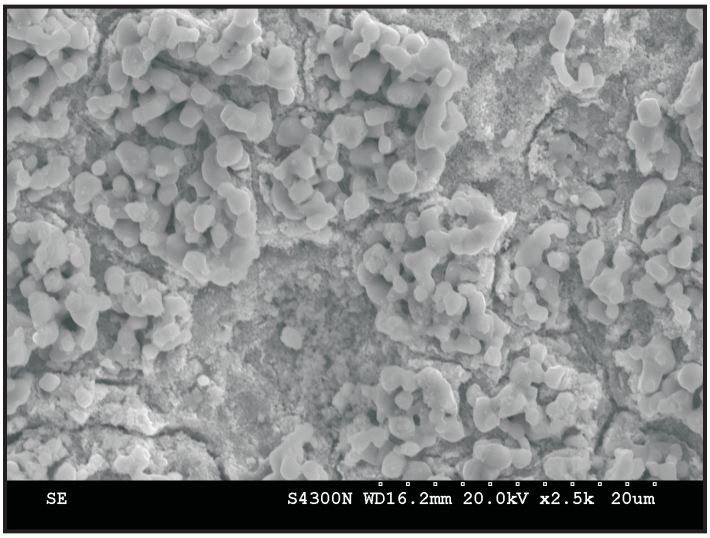

Figure 3b. SEM photomicograph of S1 showing partially sintered starting powder. The matrix pulled away from the powder during sintering (2.5kx).

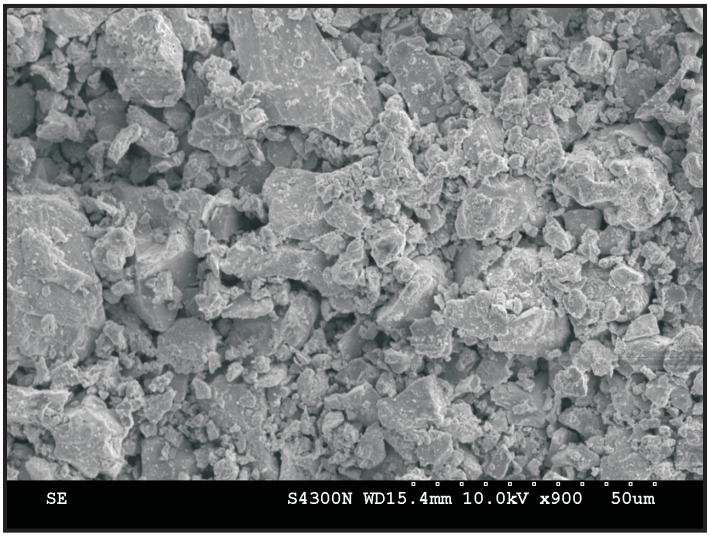

Figure 3c. SEM photomicrograph of Starck powder S2. Note the lack of evidence of much sintering (900X).

material (S2) was generally only partially sintered. At 500X, S1 again appears to have regions that are well sintered while S2 appears to not be sintered to a very high density. Figure 3a shows an area of S1 that pulled away during the sintering process, leaving some partially sintered particles behind. Figures 3b and Figure 3c picture high magnification images of S2, which again showed little sintering.

The density of S1 was determined by the pycnometry technique to be 47 percent of theoretical. This low density may result from extremely small size porosity, which is often observed when sintering sol-gel powders of this average (70–150 nm) particle size. The lack of sinterability could be due also to a thin oxide formation on the ZrN particles.

Lastly, work has been completed on the setup of a microwave facility at Los Alamos National Laboratory (LANL). UT will perform initial trial experiments to prove this system.

Planned Activities

The team will continue to focus on sintering experiments with 8 mol% yttria-stabilized zirconia and on stabilized zirconia with added dysprosia. Using the new microwave system ordered under this project, researchers are moving toward processing under controlled atmospheres to manipulate the oxygen content in the pellets. During the next fiscal year, researchers plan to conduct a thorough characterization of structural and compositional uniformity, percent theoretical density (using pycnometry and Archimedes methods), and hope to begin to measure and evaluate the mechanical properties of these materials as a function of position within the samples (stabilized zirconia, dysprosia-zirconia, and dysprosia-zirconium nitride).

The research team will continue the sintering of ZrN and a solid solution of ZrN/DyN. Powder blends of chemically precipitated ZrN and DyN (with small particle sizes from 70–150 nm) will be pressed and sintered using 2.45 GHz microwave energy. Samples will also be made by blending the chemically precipitated powders with the much larger particle size Starck ZrN powder. These samples will be cold pressed and sintered in a 2.45 GHz field with a cover gas of argon, nitrogen, or a blend of the two.

Work will be continued on fabricating ZrN, DyN, and solid solutions of ZrN and DyN by the chemical precipitation route. Nitride samples will be sintered using a variety of microwave sources. Equipment at UT and LANL will be used to sinter these samples with the possibility of using the new microwave system at VT.

Nuclear Energy Research Initiative

Radiation-Induced Segregation and Phase Stability in Candidate Alloys for the Advanced Burner Reactor

PI: Gary S. Was, University of Michigan and Brian Wirth, University of California-Berkeley

Collaborators: Los Alamos National Laboratory, Oak Ridge National Laboratory (ORNL)

Project Number: 07-015

Project Start Date: September 2007

Project End Date: August 2010

Research Objectives

The objective of this project is to determine the effect of irradiation on the segregation and phase stability in candidate alloys that may be used as structural materials for transmutation in the advanced burner reactor. This project will focus on ferritic-martensitic (F-M) alloys T91 and HT-9; an experimental oxide dispersion-strengthened (ODS) alloy; and an advanced austenitic alloy, D9, to investigate the electronic–magnetic–elastic interactions between chromium and radiation-induced defects. The project seeks to provide an understanding of radiation-induced segregation (RIS) and phase stability that can be used to develop predictive irradiation performance models.

Researchers will conduct experiments by proton and heavy ion irradiation over the dose range of 3–100 dpa and the temperature range of 350–550°C. Analysis of RIS, phase microstructure, dislocation microstructure, and hardening will be conducted on all conditions. Investigators will also use *ab-initio* electronic structure calculations to investigate the configuration-dependent binding and migration energies of chromium (Cr) with vacancy and interstitial defects. This will enable the development of atomistic-based kinetic Monte Carlo models to investigate the Cr diffusivity and segregation behavior by interstitial and vacancy mechanisms.

Research Progress

Alloys HT-9, T91, and D9 have been procured and pre-characterization analysis of the alloys has been completed. Alloy D9 was used in the as-received condition; cold-worked to 18 percent and with an average grain size of 17 mm. The microstructures of T91 and HT-9 are similar, containing martensite laths, precipitates and dislocation cells, and a sparse dislocation network. Dislocation density varied dramatically, ranging from dislocation-free areas to dense tangles in dislocation cell walls that contain a dislocation density of approximately 5.6×10^{13} m^{-2}. Carbide precipitates are located preferentially on grain boundaries as well as on lath boundaries and in the matrix. It is expected that the ODS alloy that will be used in this program will be 14YWT from ORNL, but it has not yet been procured.

Samples of dimensions 2 mm x 2 mm x 30 mm from alloys HT-9, T91, and D9 have been fabricated, ground and polished, and readied for irradiation. The first irradiation will be conducted at 400°C to doses of 3, 7, and 10 dpa. Following irradiation, hardness measurements will be made to determine the extent of hardening at this temperature as a function of dose. Then, TEM discs will be made from the irradiated bars to allow for an analysis of the irradiated microstructure and in particular, the radiation-induced segregation.

Initial *ab-initio* calculations have been performed using the Vienna *ab-initio* simulation package (VASP). The pseudo-potentials for Fe and Cr were chosen from the VASP library and are generated within the projector augmented wave (PAW) approach. The plane wave cutoff energy is 334.9 eV for Fe, 283.9 for Cr, and 334.9 eV for the FeCr alloys. The generalized gradient approximation (GGA) is used to describe the exchange correlation functional, and the Monkhorst and Pack scheme is used for Brillouin-zone (BZ) sampling.

All calculations have simultaneously relaxed the atomic position and the supercell volume (and shape) using the standard conjugate gradient algorithm provided in the VASP. The reference state of pure Fe is a BCC ferromagnetic ground state with a lattice parameter of 0.283 nm and a magnetic moment of 2.19 μ_B, while Cr has a BCC anti-ferromagnetic ground state with a lattice parameter of 0.285 nm and a magnetic moment

of ±1.09 μ_B. The initial calculations have examined the thermodynamics and size of substitutional Cr atoms in the BCC Fe matrix, and subsequent calculations will first evaluate the vacancy migration energies for exchanges with Cr and Fe, as a function of the relative position of Fe and Cr, and later the self- and mixed-interstitial atom migration energies. The nudged elastic band method is used to determine the migration energies of the vacancy exchanges with Cr and Fe, as a function of the relative position of the vacancy and Cr atom.

Planned Activities

The experimental research plans call for the irradiation of T91, HT-9, D9, and an ODS alloy to doses of 3, 7, and 10 dpa at temperatures of 400, 500, and 600°C during the first year of research. Post-irradiation analysis will be focused on radiation-induced segregation, but will also include a characterization of the irradiated microstructure and irradiation hardening. Also, during the first year, the modeling research plans call for the configuration-dependent binding and migration energies of Cr with vacancy defects, including small clusters, as well as for CR with interstitial defects. These values will enable the development of atomistic-based kinetic Monte Carlo models specifically designed to investigate the Cr diffusivity by interstitial and vacancy mechanisms in the later half of the second year. The RIS tendencies of Cr in F-M alloys will be predicted as a function of temperature and dose, based on migration mechanisms and energies obtained from *ab-initio* calculations.

In addition, a second modeling task focusing on the dislocation loop evolution in F-M alloys as a function of irradiation temperature and dose will also begin during the first year. In particular, the modeling will use atomistic molecular dynamics simulations, atomic-scale kinetic Monte Carlo, and rate theory methods as a means to evaluate the formation mechanism of interstitial loops with Burger's vector of a<100>, and to predict the size and density of evolution of both a/2<111> and a<100> loop populations. The predictions will be benchmarked against the experimental database generated by the proton and heavy ion irradiations, in addition to available neutron irradiation data.

Nuclear Energy Research Initiative

Chemistry of Transuranic Elements in Solvent Extraction Processes: Factors Controlling Redox Speciation of Plutonium and Neptunium in Extraction Separation Processes

PI: Alena Paulenova, Oregon State University

Collaborators: Argonne National Laboratory

Project Number: 07-023

Project Start Date: April 2007

Project End Date: March 2010

Research Objectives

The objective of this project is to examine the factors controlling redox speciation of plutonium (Pu) and neptunium (Np) in UREX+ extraction in terms of redox potentials, redox mechanism, kinetics, and thermodynamics. The suite of advanced spent-fuel reprocessing options (UREX+) enables the realization of several goals of the Advanced Fuel Cycle Initiative (AFCI) program. Separation of the transuranics (TRUs) allows the production and fabrication of U-TRU fuel for burnup in fast-spectrum reactors. In addition, removing TRU elements greatly relieves the long-term heat load on geological repositories. The UREX+ process has the added benefit over the PUREX process of providing greater proliferation resistance by recovering only uranium and technetium product, while Pu and Np will be recovered in later processing in a bulk recovery of all TRU elements. The PUREX extractant, tributyl phosphate (TBP), is technologically the most important extractant for nuclear fuels. TBP selectively (and nearly quantitatively) removes tetra- and hexavalent actinides from most fission products and activation products, and rejects trivalent (Am and Cm) and pentavalent (Np) actinides, leaving them with the fission product effluent.

Besides PUREX, employed for over half of the century, there was significant progress achieved in research oriented on developing new, promising extractant systems for actinide separations using solvent extraction or extraction chromatography. These new systems, for example, TRUEX (TRansUranium EXtraction) and TALSPEAK (Trivalent Actinide/Lanthanide Separation by Phosphorus Reagent Extraction from Aqueous Komplexes), are designed either to complement TBP ("Advanced Purex") or to replace it in some applications, thus becoming a part of the UREX+ separation suite. New separation flowsheets for fission products (Cs, Sr, lanthanides) utilize recently developed calixarenes (Cs), crowns (Sr), malonamides (REE), and others.

Researchers will employ radiochemical redox-speciation extractions schemes in parallel to the redox experiment. The distribution of redox species will be studied using methods of visual and near-infrared spectroscopy, electrochemistry, and spectro-electrochemistry. This work will result in the creation of a database on redox stability and the distribution of redox couples in the nitric acid/nitrate electrolyte and the development of redox-buffering systems to stabilize the desired oxidation state of separated radionuclides.

Researchers will evaluate the effects of temperature and concentrations of acid and salt on the redox potential of actinide nitrate, considering a range of chemical matrix conditions. The database generated from the experimental work will be integrated into an existing actinide speciation code (AMUSE).

This project consists of the following three primary tasks:

- Estimate the distribution of oxidation states of TRUs (Np, Pu, U) as a function of acid, nitrate, and temperature
- Determine redox reactivity of Np, Pu, and U (as well as Tc) with studied oxidation/reduction agents and different conditions
- Model distribution ratios and develop a database on redox buffering/separation factors

Research Progress

The research team has accomplished the following tasks during the reported period:

- The team is in the process of reviewing technical literature on redox chemistry of actinides (data are organized according to the experimental conditions) and has measured the reported data.
- Researchers collected data on hydroxyurea and DEHAN for different nitric acid conditions.
- The team collected UV-Vis-nIR spectra of Pu(VI) in the nitric acid solutions at 25°C and has estimated the rate constant for the reduction of Pu(VI) with acetohydroxamic acid (AHA).
- GlobalWorks modeling program has been employed to model redox kinetics of Pu(VI) using measured spectroscopic data.

The chemistry of the light actinides is purely based on their rich redox chemistry and selectivity of ligands; however, the keys to successful separation of actinides (and other metals, too) from multicomponent systems are in the art of many factors, such as maintaining the required oxidation state of metal, pH (acid concentration), solubility, and hydrolytic and radiolytic resistance, also including physicochemical factors (for example, dynamic viscosity).

The relationship between redox activity and complexation in Pu and Np chemistry presents a challenge to scientists attempting to model the speciation of these metals in multicomponent matrices. Ultimately, this can be accomplished by a predictive modeling approach based on a new level of understanding of redox behavior of Np, Pu, HNO_3, HNO_2, and other redox active species (for example, AHA or sulfamic acid) present in separation matrices. It is necessary to predict the specific effect of concentrations of nitric acid, nitrite, and other additives in the chemistry of both target species and separation molecules.

The redox mechanisms of actinide ions in solutions are complex processes complicated by the radiolysis and hydrolysis of solution components. This is due to the rich redox chemistry of Pu and Np. Because some oxidation states can be disproportionate or are unstable, some reactions (e.g., with H_2O_2 and HO_2 formed in irradiated solutions) are reversible, and the reaction direction depends on the reaction conditions. For example, plutonium (VI) in aerated solutions can be reduced to Pu(V) and then oxidized back to Pu(VI); disproportionation [Eq. 1] of Pu(V) gives Pu(IV) and Pu(VI), and, at high radiation doses, Pu(III) is also formed [Eq. 2]:

$$Pu(IV) + Pu(V) \leftrightarrow Pu(III) + Pu(VI) \quad (1)$$

$$Pu(IV) + H_2O_2 \leftrightarrow Pu(III) + HO_2 + H^+ \quad (2)$$

Researchers performed experiments on gamma irradiation of AHA in a HNO_3 solution which is a salt-free additive to the aqueous phase in the UREX extraction. The goal was to reduce Np(VI) and bind Pu(IV) to non-extractable complexes. The result showed that the degradation of AHA is two-fold faster in irradiated solutions than in non-irradiated (Co-60, 33kGy/s). Upon acidic hydrolysis, AHA decomposes to acetic acid and hydroxylamine; however, the Vis and Fourier transform infrared (FTIR) spectroscopic data suggest that the bidentate chelate complexes with metals stabilize the AHA against rapid degradation.

According to the reviewed literature and preliminary measured results, Np in nitric acid solutions behaves as follows:

$$Np^{+4} \rightarrow NpO_2^+ = e^- \quad (2)$$

$$2NpO_2^+ + 3H^+ + NO_3^- \leftrightarrow 2NpO_2^{+2} + NHO_2 + H_2O \quad (3)$$

$$2NpO_2^+ + 4H^+ \leftrightarrow NpO_2^{+2} + Np^{+4} + 2H_2O \quad (4)$$

$$2NpO_2^+ + 3H^+ + NO_3^- \leftrightarrow 2NpO_2^{+2} + NHO_2 + H_2O \quad (5)$$

Hydroxyurea (HU) is one of the proposed stripping reductants for Pu and Np.

Pu(IV)

- Various concentrations of HNO_3 were analyzed to determine synergetic effects with HU
- Pu(IV) is reduced to Pu(III) and stripped at lower concentrations of nitric acid
- Absorbance spectra show strong intensities at approximately 475 nm and approximately 600, indicating the presence of Pu(IV) and Pu(III) before and after the addition of HU, respectively

Np(VI)

- Similar results to that of Pu(IV); Np(VI) is reduced to Np(V)
- Absorption spectra monitored at 723, 960 nm for Np(IV); 618, 980 nm for Np(V), and 1,223 nm for Np(VI)

Hydroxyurea is an effective reducer of both Np and Pu. The rate constant for the reduction of Pu(IV) increases with increasing temperature. Np and Pu are easily reduced at lower nitric acid concentrations (< 2M), but the nitrous acid, produced by reduction or radiolysis of nitric acid, is always present in these chemical matrices. At a small concentration (below 10^{-5}M), nitrous acid becomes a catalyst and oxidizes Np(V) to Np(VI).

The redox reaction for hydroxyurea and Pu can be written as the following:

$$4Pu(IV) + 2H_2NCONHOH + 3H_2O \leftrightarrow 4Pu(III) + 2NH_4^+ + N_2O + 2CO_2 + 2H_3O^+$$

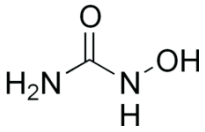

Hydroxyurea

Planned Activities:

During the next period, researchers will aim to accomplish the following task:

- Examine the redox kinetics of actinides (Pu and Np) with various concentrations of nitric and nitrous acid, nitrates, and selected redox agents, utilizing modeling programs for both the ionic equilibrium (Fiteql 4.0) and kinetics (GlobalWorks)

Nuclear Energy Research Initiative

New Fission Product Waste Forms: Development and Characterization

PI: Alexandra Navrotsky, University of California-Davis (UC Davis)

Collaborators: Sandia National Laboratories (SNL); Eltron Research, Inc.; Brigham Young University

Project Number: 07-027

Project Start Date: June 2007

Project End Date: May 2010

Research Objectives

This project will identify advanced methods for the chemical partitioning of spent nuclear fuel into cesium (Cs), strontium (Sr), and minor actinide (MA) constituents that can be stored for future disposition. Researchers will study new waste forms and disposal strategies for the steam reforming process to produce a Cs/Sr storage form that incorporates Sr and Cs, their decay products, and rare earth fission products. A broad characterization study of inorganic ceramic waste form phases and the thermochemistry of these phases will provide a comprehensive data set from which to select the appropriate waste form. Emphasis will be on perovskite phases as a major constituent of the final waste form. The goals of this project are to reduce the costs of the guanidinium carbonate steam reforming waste process; to minimize the risk of contamination to the environment during waste processing; and to provide the Department of Energy (DOE) with technical solutions to a variety of issues related to Cs, Sr, and MA disposal.

The objectives for this project include the following:

- To establish ceramic waste forms for disposing Cs, Sr, and MAs, which consist of transition metal oxides loaded *in-situ* with minimal additional processing steps so that the waste volume is minimized and the process produces durable waste forms for all cations and their decay products
- To fully characterize the phase relationships, structures, and thermodynamic and kinetic stabilities of promising waste forms
- To establish a sound technical basis for understanding key waste form properties, such as melting temperatures and aqueous durability, based on an in-depth understanding of waste form structures and thermochemistry
- To establish synthesis, testing, scaleup, and commercialization routes for waste form implementation throughout in-kind collaborations with Eltron Research
- To co-locate a post-doctoral fellow at UC Davis and SNL who will develop expertise in both the synthesis and characterization of the waste forms and in the calorimetry needed to study those waste forms (see Figure 1) as well as a graduate student who will intern at Sandia and Eltron—these people will experience the university, SNL, and industrial work environments to help stimulate interest in the nuclear field and enhance the pipeline of young people pursuing careers in this field

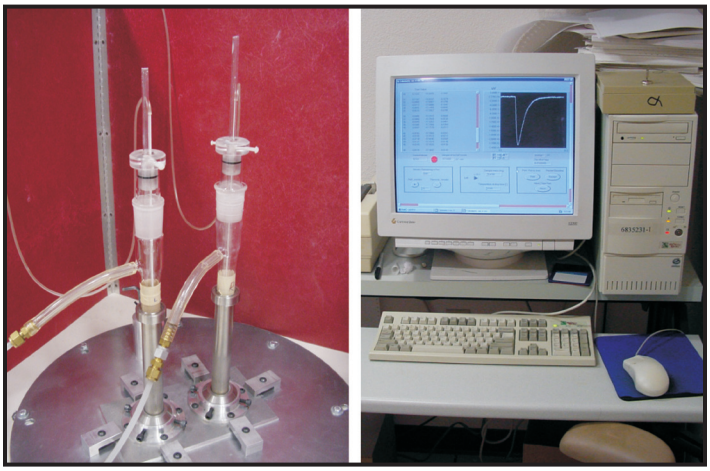

Figure 1. A unique high-temperature calorimeter used for measurements of heats of formation of ceramics.

The proposed work will provide information on the durability and stability of these waste forms so that their potential for viable storage or disposal scenarios can be evaluated. Since Cs and Sr form new elements by radioactive decay over several hundred years, researchers will study the behavior and thermodynamics of these waste forms using non-radioactive analogues.

Research Progress

Funding was received in June 2007; thus, the current three-month period was spent, according to the goals and objectives, in making task assignments and starting the work. However, various activities have been delayed due to the absence of funding, especially at SNL. Once funding is received, work on the delayed activities will begin.

Synthesis of Cs_2O-TiO_2-SiO_2 materials has begun, as well as studies to determine the heat of formation and vitrication of fresnoite, based on some samples provided by other collaborators. Concurrently, a major literature search is being conducted and a list of references made available to all participants.

In addition, work on perovskites has begun, namely the study of perovskite joins that are representative of the radioactive decay of strontium.

Planned Activities

Following is a list of tasks for the coming year:

- Investigate phase relationships and solid solubilities in a $BaTiO_3$-$SrTiO_3$-$CaTiO_3$-$YTiO_{2.5}$ system; measure heats of formation of any solid solutions formed
- Determine enthalpy of formation and vitrification of fresnoite
- Investigate synthesis and phase relations in Cs-bearing systems
- Perform phase identification and phase diagram determination
- Determine structure
- Determine thermochemical stability
- Investigate structure-property relationships

Nuclear Energy Research Initiative

Computations for Advanced Nuclear Reactor Fuels

PI: Sudarshan K. Loyalka, University of Missouri-Columbia

Collaborators: None

Project Number: 07-035

Project Start Date: July 2007

Project End Date: June 2010

Research Objectives

To successfully implement an efficient and effective nuclear power strategy, it is essential to develop new fuels that can provide optimal performance over long periods of time. This research will develop advanced computational techniques to improve the understanding of fission gas distribution and heat transfer in solid fuel under normal and accident conditions.

Research Progress

The literature on molecular, particulate, and phonon transport was extensively reviewed. A Direct Simulation Monte Carlo (DSMC) Program for free-molecular fission product transport in arbitrarily shaped nano-pathways in TRISO coatings was constructed and tested. Good visualization and animation of the transport were successfully realized. A number of parametric studies relating to pathway shapes, sizes, lengths, and boundary conditions have been conducted. Additionally, two DSMC programs for nano-particle flows in cracks were constructed and tested, and a number of results were obtained. The needed algorithms for collisions as described by simple inter-molecular potentials were tested successfully. An algorithm for the computation of collision cross sections for the L-J potential was constructed, and algorithms for improving efficiency of collisional sampling were explored. Construction of a DSMC program for phonon transport was initiated, and several sampling algorithms have been tested. Figure 1 shows a typical binary molecular flow realization in a straight pathway.

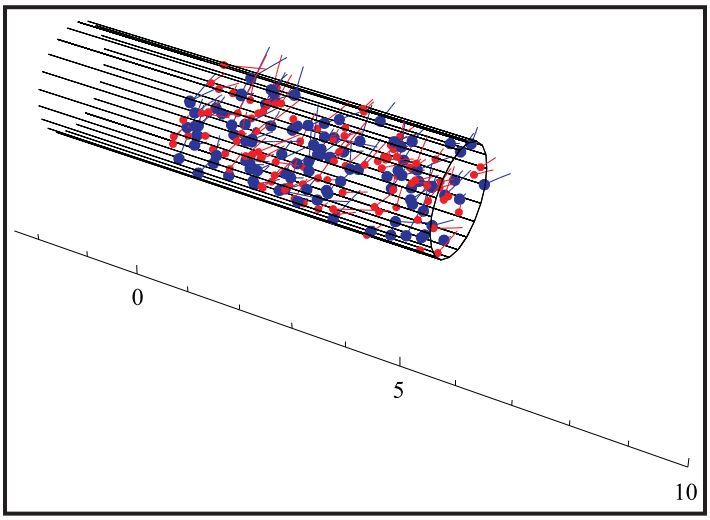

Figure 1. A simulation of fission product transport.

Planned Activities

Over the next year, researchers will continue to construct and improve the computer programs with respect to their fidelity to actual physico-chemical phenomena, geometries, and length and time scales. Continual testing of the programs against available data (as well as other computational techniques and the results obtained through them) will be conducted as the research team incorporates additional rate processes and models. Researchers will be exploring parallel algorithms and improvements in convergence of computations. In addition, the team plans to explore more interfaces that the programs could have with the existing fuel behavior codes, such as FRAPCON and PARFUME.

Nuclear Energy Research Initiative

Experimental Development and Demonstration of Ultrasonic Measurement Diagnostics for Sodium Fast Reactor Thermohydraulics

PI: Akira Tokuhiro, Kansas State University

Collaborators: None

Project Number: 07-037

Project Start Date: June 2007

Project End Date: May 2010

Research Objectives

This research project will address some of the principal technology issues related to sodium-cooled fast reactors (SFRs), primarily the development and demonstration of ultrasonic measurement diagnostics linked to effective thermal convective sensing under normal and off-normal conditions. Sodium (Na) is well-suited as a heat transfer medium for the SFR. However, because it is chemically reactive and optically opaque, it presents engineering accessibility constraints relative to operations and maintenance (O&M) and in-service inspection (ISI) technologies that are currently used for light water reactors. Thus, there are limited sensing options for conducting thermohydraulic measurements under normal conditions and off-normal events (maintenance, unanticipated events). Acoustic methods, primarily ultrasonics, are a key measurement technology with applications in non-destructive testing, component imaging, thermometry, and velocimetry.

This project will yield a better quantitative and qualitative understanding of the thermohydraulic condition of Na under varied flow conditions. The scope of work will evaluate and demonstrate ultrasonic technologies and define instrumentation options for the SFR.

The researchers will demonstrate ultrasonic technology through the following activities:

- Design, construct, and operate a small, simple, university-based Na flow loop with inventory of approximately 5–6 liters
- Develop and demonstrate ultrasonic velocimetry and thermometry, with a focus toward improved SFR O&M (i.e., using velocimetry and thermometry as diagnostic tools during normal and off-normal operations)
- Test a compact sodium-to-supercritical CO_2 heat exchanger and generate convective heat transfer data, correlations, and operational experience under normal and off-normal operations

Research Progress

Previous year's activity. Researchers established a collaboration with Argonne National Laboratory (ANL) so they can participate in ANL's Sodium Plugging Experimental Facility test program below. The present NERI project will contribute to the ANL facility in order to coordinate overall research and development (R&D) in SFR technologies.

With respect to ANL's Sodium Plugging Experimental Facility, the advanced burner reactor (ABR) concept employs a supercritical CO_2 Brayton cycle power conversion technology. A key component for efficient power conversion is a compact heat exchanger known as the printed circuit heat exchanger (PCHE). In the ABR (or similar SFR), this would be a sodium-to-CO_2 heat exchanger. Each PCHE is essentially a monolithic block of stainless steel, containing embedded narrow flow channels. These narrow flow channels may become plugged due to an impurity (e.g., oxides) present in Na, if the sodium becomes supersaturated with impurities. Experimental data is needed to assess the plugging characteristics so that optimum design of the PCHE Na-CO_2 heat exchanger can be realized.

Following are the two specific objectives of the Sodium Plugging Experimental Facility tests:

1) To demonstrate that no plugging occurs in the PCHE flow channel sizes being considered for the sodium-to-CO_2 heat exchanger if the Na temperature is well above the impurity saturation temperature

2) To collect experimental data that can be used to model the plugging behavior as a function of the channel size, as well as the amount of impurity supersaturation

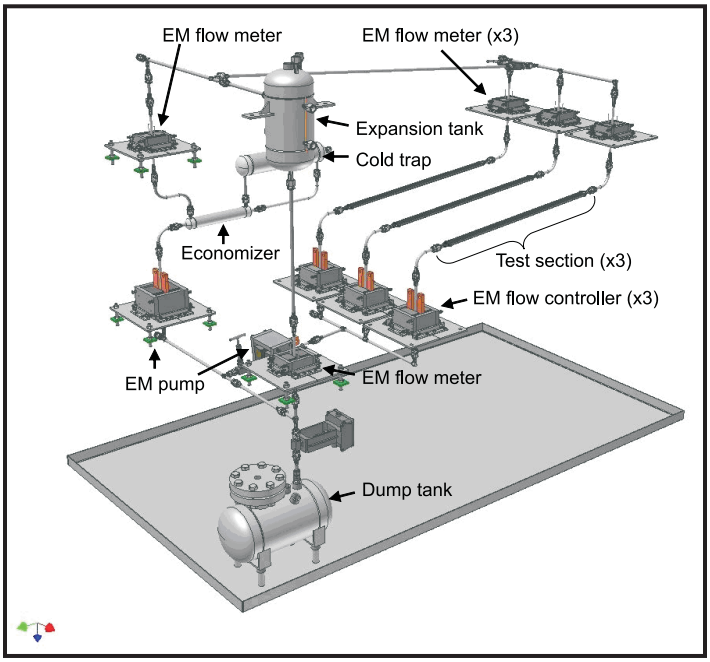

Figure 1. Small sodium loop facility at ANL.

As shown in Figure 1 above, the apparatus consists of a main Na loop including three test sections, a bypass Na loop including a cold trap/economizer assembly, and an auxiliary system comprising Argon and vacuum lines. The main loop, as well as the bypass loop, is constructed from stainless steel tubing. Other major components include electromagnetic (EM) flow controllers, EM pumps, EM flow meters, and expansion and dump tanks. The Na loop system is about 1.8 m tall and is heated by a number of ceramic band heaters. The maximum operating temperature and pressure of the loop are 510°C and 207 kPa (= 30 psig), respectively. The nominal flow rate and pressure head are $4x10^{-5}$ m^3/s (= 2.4 liters/min) and 40 kPa at approximately 800 A, respectively; however, the EM pumps can be operated at up to 1,000 A for higher flow rate and pressure head operations.

Procurement of Ultrasonic Doppler Velocimeter (UDV). Although UDV can be used with gases, as the acoustic velocity in gas is roughly 300m/s versus >1,500m/s in liquids, UDV can be used as a quasi-live velocimetric "tool" in liquids. That is, it provides spatial velocity information (distribution) along its acoustic beamline that can be derived by measuring and sufficiently sampling the Doppler shift (per channel) at the time of echo detection (thus requiring "seeding" of some sort); temporal velocity information as the ultrasonic burst and echo reception (Doppler shift measurement) is rapidly (electronically) cycled. Thus, spatio-temporal velocimetric information is acquired much like laser-based velocimetry methods (laser Doppler, particle image, etc.).

A Met-Flow Ultrasonic Velocity Profile (UVP) model DUO has been purchased for use in this project and has initially been tested. One medium temperature ultrasonic transducer (up to 250°C) manufactured by Imasonic is ready for initial testing with liquids (Na or other) at this temperature.

Planned Activities

Based on the objective to develop and demonstrate ultrasonic technologies for the SFR (above), the following planned scope of work was defined in terms of project tasks and associated metrics:

- Recruit students and arrange summer internships at ANL. The students should support the Sodium Plugging Experimental Facility test planned for summer 2008
- Design pipe flow test section, active "economizer" (cold trap), and sodium-to-CO_2 heat exchanger transition with ports for ultrasonic transducers
- Procure materials and secure machining and manufacturing time as needed for the above components that will be custom manufactured
- Procure additional ultrasonic signal processing instrumentation for velocimeter and configure electronics for ultrasonic thermometry
- Begin computational fluid dynamics (CFD) modeling of the sodium-to-CO_2 heat exchanger
- Start developing operations, safety, and experimental plans when modifications to the Sodium Plugging Experimental Facility are made

Nuclear Energy Research Initiative

Fundamental Processes of Coupled Radiation Damage and Mechanical Behavior in Nuclear Fuel Materials for High-Temperature Reactors

PI: Simon Phillpot, University of Florida

Collaborators: Idaho National Laboratory (INL), Los Alamos National Laboratory

Project Number: 07-046

Project Start Date: June 2007

Project End Date: May 2010

Research Objectives

A long-standing issue for the nuclear industry is the degradation of the mechanical properties of nuclear fuels under irradiation, including both the fissionable material and cladding. Developing fuel systems with improved resistance to radiation damage will allow longer burnups, improved usage efficiency, increased time between refueling, and decreased waste. The objective of this project is to elucidate the relationship among the microstructure, radiation damage, and mechanical properties of nuclear fuel materials. This research will focus on developing an understanding of 1) the fundamental mechanisms of radiation damage in polycrystalline materials, 2) the effect this damage has on plastic deformation, and 3) the effect of mechanical deformation on radiation tolerance.

Researchers will use hexagonal close-packed (HCP) titanium (Ti), which is representative of HCP Ti alloys for fast reactors and zircaloy cladding in thermal reactors, and UO_2. To simulate radiation damage, they will apply state-of-the-art, large-scale, atomic-level simulation through a judicious combination of conventional molecular-dynamics (MD) and accelerated MD methods. The research team will elucidate mechanical behavior by applying large-scale MD simulations. This systematic program for simulating the effects of irradiation on the structural and mechanical properties of polycrystalline Ti and UO_2 will identify radiation damage mechanisms and provide insights into the expected behavior of nanocrystalline microstructures and nanocomposites. This work will ultimately help researchers design microstructures that are less susceptible to radiation damage and thermo-mechanical degradation.

Research Progress

The first four months of this project have focused on developing the computational infrastructure required for the proposed research. This has included the 1) verification of the parallel implementation of the modified embedded atom method (MEAM) to be used for the simulation of HCP Ti, 2) development of polycrystalline UO_2 microstructures suitable for radiation damage simulations, 3) proof-of-principle simulations of radiation damage in UO_2 (see Figure 1), and 4) the validation of the methods to be used for the radiation damage simulations of both nanocrystalline Ti and nanocrystalline UO_2. This work is being performed in collaboration with INL.

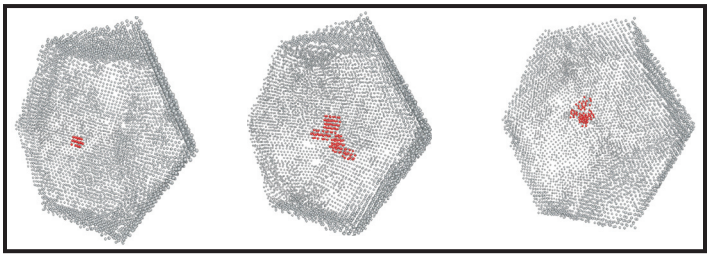

Figure 1. Simulation of radiation damage inside a single dodecahedral grain of UO_2 within a polycrystal. A small cluster of point defects (red) is formed within 20 fs (left) of the impact of the 1keV PKA (left); the defect cluster grows to a maximum size after approximately 400 ps (center); by 1,600 fs (right), defect recombination results in partial healing of the radiation damage.

Planned Activities

As part of the program to elucidate the coupling between radiation damage and mechanical behavior of Ti, researchers will focus on two activities in the upcoming year. First, they will use large-scale molecular dynamics simulations to elucidate the atomic-level processes associated with radiation damage in single-crystal Ti. Because HCP Ti has a strongly anisotropic structure, particular attention will be paid to the dependence of the structure and evolution of the damage cascade on the incident direction of the primary knock on atom (PKA). The effects of energy will also be elucidated. Second, the research team will perform simulations of the deformation of nanocrystalline Ti. Both textured and fully random microstructures will be characterized. Work on UO_2 will focus on elucidating the coupling of radiation damage and microstructure in polycrystalline UO_2.

Nuclear Energy Research Initiative

Economic, Depository, and Proliferation Impacts of Advanced Nuclear Fuel Cycles

PI: K.B. Cady, Cornell University

Collaborators: University of Texas at Austin

Project Number: 07-051

Project Start Date: June 2007

Project End Date: May 2010

Research Objectives

The objective of this project is to compare the use of fast reactor (FR) advanced nuclear fuel cycles with that of inert matrix fuel (IMF) in light water reactors (LWRs) as a means of reducing actinide inventory—focusing on their economics and proliferation resistance. In addition to making use of the current LWR fleet, IMF can offer a four-fold increase in repository capacity when compared to direct disposal of an energy-equivalent quantity of spent LWR fuel, with over 98 percent destruction of plutonium (Pu)-239. Research also suggests that leaving IMF pins in the reactor after their reactivity has been depleted (effectively making them actinide targets) could offer a significant increase in actinide destruction. FRs can potentially increase repository capacity by more than an order of magnitude per kilowatt of electricity generated. However, FR spent fuel must be recycled many times in order to achieve this result, whereas the increase in repository capacity offered by IMF does not require reprocessing of the IMF itself. Unlike previous studies that assumed that spent FR fuel be recycled continuously, this project will analyze the impact of IMF and FR transmutation strategies over a finite period.

Research Progress

During this reporting period, burnup simulations have been run for IMF fuel with compositions as laid out in the proposal and for burnups extending to 650 MWd/kgIHM (for IMF with 12 elements without Pu+Np and 15 without Pu+MA) and 550 MWd/kgIHM (for IMF with 8 elements without Pu+Np and 8 without Pu+MA). The 15 IMF elements without Pu+MA have also been run to 850 MWd/kgIHM.

ORIGEN 2.2 was used in conjunction with the output data from these simulations to calculate the heat and radiological output from the spent IMF. A probabilistic model for the life-cycle cost of IMF and FR fuel cycles is under development. Unit costs are being assembled through the Organisation for Economic Co-operation and Development/Nuclear Energy Agency (OECD/NEA) publications, published data from THORP, and the Advanced Fuel Cycle Cost Basis, which is being assembled by Idaho National Laboratory.

An assessment of ”best case” reprocessing costs was undertaken assuming a system of government-owned reprocessing plants, each with a 40-year service life, that would reprocess spent nuclear fuel generated between 2010 and 2100. A literature survey has been undertaken to review previous work on high burnup IMF and FR fuel cycles applicable to the burn down of transuranics (TRUs) from LWR-based fuel cycles and disposition Pu from dismantled weapons.

Planned Activities

The following are anticipated tasks for the coming year:

1) Determine the material balances (including proliferation-sensitive materials) for IMF and FR fuel cycles that operate over a finite time period
   - Use the burnup/criticality code, MCNPX/MONTEBURNS and REBUS-3, to determine the isotopic balances for representative TRU vectors, typical LWR parameters, and FRs with different conversion ratios
2) Determine the radiological and heat load to a repository for each fuel cycle
   - Use ORIGIN 2.2 and the spent fuel composition for the respective IMF and FR cycles

3) Determine fuel cycle cost in $/kWhr for each of the respective fuel cycles
    - Apply probabilistic discount model unit cost data published by the OECD/NEA and investigate the effect of uncertainties in cost, discount rates, and time

NUCLEAR ENERGY RESEARCH INITIATIVE

Analysis of Advanced Fuel Assemblies and Core Designs for the Current and Next Generations of LWRs

PI: Jean C. Ragusa, Texas A&M University

Collaborators: None

Project Number: 07-059

Project Start Date: September 2007

Project End Date: August 2010

Research Objectives

Existing light water reactor (LWR) advanced fuel assembly designs could reduce the plutonium inventory of reprocessed fuel. Nevertheless, these designs are not effective in stabilizing or reducing the inventory of minor actinides (MAs). The objective of the project is to focus on developing LWR fuel assemblies that can efficiently transmute plutonium and minimize the MA inventories. This project will investigate and analyze advanced LWR assembly designs with improved thermal transmutation capability regarding transuranic elements and especially MAs. Researchers will study various fuel types, namely high burnup advanced mixed oxides (MOX) and inert matrix fuels, in various geometrical designs that are compliant with the core internals of current and future LWRs. Several fuel pin designs and fuel assembly designs will be analyzed and neutronics/thermal hydraulics effects will be considered.

The best performing designs will be used in 3-D core depletion methodology to determine overall transmutation performance in various fuel cycle scenarios. Transmutation efficiency and safety parameters will be used to rank the various designs.

Research Progress

State-of-the-art neutronics lattice codes, thermal-hydraulics sub-channel analysis codes, isotopic depletion codes, and fuel cycle scenario modeling codes have been researched for the purpose of this project.

For fuel assembly neutronic designs, the TransLAT code (developed by Transware under Electric Power Research Institute [EPRI] sponsorship) and the DRAGON code (developed at the École Polytechnique de Montreal, Canada) have been selected based on their outstanding geometric modeling capabilities and robust neutron transport solver features (such as self-shielding formalism and ray-tracing in general 2D/3D geometries with solution procedures based on the method of characteristics and/or collision probabilities). Their flexible geometric modeling capability allows for various pin configurations (cylindrical, annular, and cross-shaped).

The next step was to define two isotopic distributions: one that is representative of past spent fuel and one that is representative of more recent and/or future burnup values. Both isotopic distributions, with adequate cooling and reprocessing times, will be used as input in the assembly designs. Current fuel forms available for design include advanced MOX fuels (with enriched uranium to allow multiple recycles and MA in target locations) and ceramic-metal (CERMET) fuels (zirconium [Zr] metal base with dispersed transuranic oxide [TRUOX]).

Of principal concern is the energy equivalence between standard uranium oxide (UOX) fuel assemblies and innovative fuel assemblies. A metric, based on the K-inf multiplication factor at the time of the expected discharge from the core (hot fuel power conditions, no boron in moderator), has been developed to quantify the notion of energy equivalence between fuel assemblies and has been verified based on public domain data regarding the French experience with UOX/MOX loaded cores. Figure 1 shows the K-inf values for energy-equivalent UOX and MOX fuel assemblies.

Thermal hydraulics analyses will be performed for the most promising fuel configurations. The primary safety requirement for the fuel assembly design from a thermal hydraulic perspective is to ensure adequate heat removal to prevent fuel damage during all normal operating, transient, and accident conditions. In order to provide a comprehensive design evaluation, relevant safety parameters will be investigated, including fuel rod surface

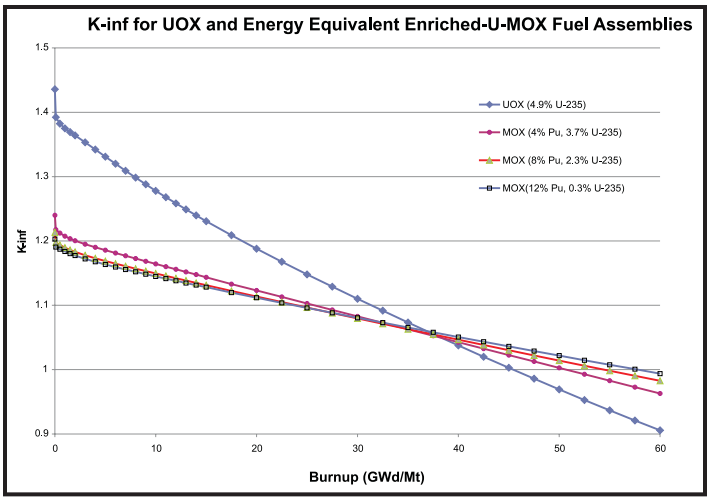

Figure 1. K-inf value for a standard UOX fuel assembly and three energy-equivalent MOX fuel assemblies with various plutonium (Pu) content.

and internal temperatures, coolant flow velocities and thermodynamic states, critical heat flux and departure from nucleate boiling ratio (DNBR) for each rod at predetermined axial locations, and the minimum departure from nucleate boiling ratio (MDNBR) for the limiting fuel rod in the core.

A literature survey was performed on subchannel codes to assess code applicability. Of principal importance in the code selection process was to identify a code with the following characteristics:

- Features robust thermal hydraulics models
- Is capable of simulating complex fuel pin geometries (dual-region, annular, and cruciform)
- Allows the user to define material properties and heat conduction models for evaluating advanced fuel types such as advanced mixed oxide fuels (AMOX) and inert matrix fuels (IMF)
- Is able to calculate the thermal hydraulic parameters mentioned above
- Is well maintained, documented, and widely accepted in the nuclear industry
- Is available for academic research

EPRI's VIPRE code appears to be a suitable code for the current project. A contractual agreement was completed and discussions are starting on code transmission. VIPRE has an additional feature that has been approved for licensing purposes to evaluate the MDNBR of certain reactor designs.

In the future, it is envisioned that a message-passing paradigm will be utilized to perform coupled neutronics/thermal-hydraulics analysis (fine tuning of the designs and safety assessment).

Researchers have received the ORIGEN code from the Radiation Safety Information Computational Center (RSICC) for isotopic depletion and long-term radio-toxicity assessment. The DANESS code has been requested for fuel cycle scenario modeling.

Planned Activities

Following is a list of planned activities to be accomplished over the next year:

- Develop advanced MOX fuel concepts
- Develop advanced ceramic fuel concepts
- Obtain subchannel code (i.e., VIPRE)
- Become familiar with subchannel code mechanics and capabilities
- Identify any VIPRE modeling limitations and possible alternatives for design analysis
- Conduct small-scale modeling of fuel pins and assembly concepts
- Develop linking methodology for passing information to and from neutronics and thermal hydraulic codes
- Conduct full-scale modeling and analysis of potentially viable fuel assembly designs
- Enable iterative exchange of information between neutronics and subchannel codes
- Develop LWR-based fuel cycle scenario (multiple recycles vs. once recycle)
- Develop quantifiable metric for fuel assembly designs (e.g., long-term radio-toxicity per TWe.h/yr, MA inventories per TWe.h/yr, safety parameters, etc.)
- Optimize assembly design
- Perform thermal hydraulic analysis of entire core
- Evaluate core design safety margins

Nuclear Energy Research Initiative

Powder Metallurgy of Uranium Alloy Fuels for TRU-Burning Fast Reactors

PI: Sean M. McDeavitt, Texas Engineering Experiment Station

Collaborators: None

Project Number: 07-060

Project Start Date: April 2007

Project End Date: March 2010

Research Objectives

Fast reactors are being evaluated to enable the transmutation of transuranic (TRU) isotopes generated by nuclear energy systems. TRU isotopes have high radiotoxicity and relatively long half-lives, making them unattractive for disposal in a long-term geologic repository. Fast reactors are able to utilize transuranic elements as fuel, thereby destroying them while releasing their valuable residual energy content. An enabling technology is the fabrication metallic fuel containing TRU isotopes using powder metallurgy methods.

The performance of U-10 wt. zirconium (Zr) and other uranium (U) alloy fuels was demonstrated at the Experimental Breeder Reactor-II between 1964 and 1994. This fuel was fabricated by injection casting rods from a molten pool of U-Zr alloy. Even though this method is proven and effective, it was accompanied by high material losses due to chemical interactions with quartz casting molds. For the newer TRU-bearing fuel designs, direct melt casting is impractical since americium and, to a lesser extent, neptunium, have especially high vapor pressures and cannot be contained in a molten alloy pool at 1,200 to 1,500°C. Recent advances in arc-melting at Idaho National Laboratory have successfully produced research-scale alloys containing metallic TRU isotopes. This process also has material loss issues and is not considered scaleable for the production of reactor fuel assemblies.

Research Progress

This project is striving to develop a powder metallurgical fabrication method to produce U-Zr-TRU alloys at relatively low processing temperatures (500 to 600°C) using either hot extrusion or "alpha-phase" sintering. The fundamental aspects of both processing methods will be quantified. Surrogate low-melting metals (e.g., Mg and Mn) will be used to simulate the TRU elements. If successful, this process will produce novel solutions to some of the nagging issues related to metallic fuels: fuel-cladding chemical interactions, fuel swelling, volatility losses during casting, and casting mold material losses.

To accomplish this objective, two candidate processing pathways are being initiated:

1) Hot working fabrication using mechanical alloying and extrusion. This method will build on the historical database for U powder metallurgy along with modern mechanical alloying developments.
2) Fabrication by sintering of alpha U with liquid phase enhancements at 550 to 650°C. This method will build on the historical database for U powder metallurgy along with the laboratory experience of the principal investigator.

The first priorities of this program are to 1) establish students on research pathways to carry out the program objectives and 2) complete the installation of the equipment required to carry out these objectives, including a large volume inert atmosphere glovebox, a vertical dilatometry apparatus inside of the glovebox, and a hot extrusion press. Progress has been made on all three of these major pieces of equipment and all systems are projected to be in operation by the summer of 2008. Figure 1 shows the glovebox being installed at Texas A&M University (TAMU). The vertical dilatometer should begin operation shortly after the glovebox is closed, leak tested, and put into service. The hot extrusion press was installed under another NERI program (2005-066) and is already fully functional.

Figure 1. Glovebox installed at TAMU for powder metallurgy of U alloys.

Planned Activities

The following activities are planned for next year:

- Complete installation and startup of the controlled atmosphere glovebox
- Install the vertical dilatometer experiment and perform alpha-phase sintering tests
- Initiate hot extrusion tests to demonstrate fuel pin fabrication at 600°C

Nuclear Energy Research Initiative

Neutronic and Thermal-Hydraulic Coupling Techniques for Sodium-Cooled Fast Reactor Simulations

PI: Jean C. Ragusa, Texas A&M University

Collaborators: University of Chicago, Commissariat à l'énergie atomique (CEA), Argonne National Laboratory (ANL)

Project Number: 07-063

Project Start Date: September 2007

Project End Date: August 2010

Research Objectives

The objective of this project is to develop and implement efficient neutronic-thermal-hydraulic coupling algorithms for sodium-cooled fast reactors. This project involves prototyping the following two methodologies: 1) coupling paradigms using an operator-split technique that can preserve the accuracy order of each physics component and 2) coupling paradigms using Jacobian-free formulations, with physics-based preconditioners. The researchers will address the different spatial and time scales found in sodium-cooled fast reactor applications and will apply their methodology to demonstrate inherent safety features of sodium fast reactors with metallic fuel. In addition, typical anticipated transients without scram will be modeled.

Research Progress

In order to assess the inconsistencies of traditional coupling strategies, researchers developed a test-bed code based on reduced physical models that includes the following physics components: multigroup neutron diffusion, monophasic conservation laws (mass, momentum, energy) for the coolant, and nonlinear heat conduction. This code will be used for the following purposes:

1) To demonstrate the loss of accuracy order due to traditional operator-split techniques used in conventional coupling schemes
2) To implement Jacobian-free full resolution coupling schemes
3) To develop adaptive preconditioning techniques
4) To investigate high-order time discretizations and adaptive time stepping strategies

The best performing techniques will be proposed for implementation in the new neutronics/thermal-hydraulics code package Simulation-based High-efficiency Advanced Reactor Prototyping (SHARP) for advanced fast reactor analyses. SHARP is based on the UNIC code (neutronics) and the Nek-5000 code (computational fluid dynamics) developed at ANL. Figure 1 presents the temperature mapping from Nek to UNIC for a coupled calculation of a single fuel element.

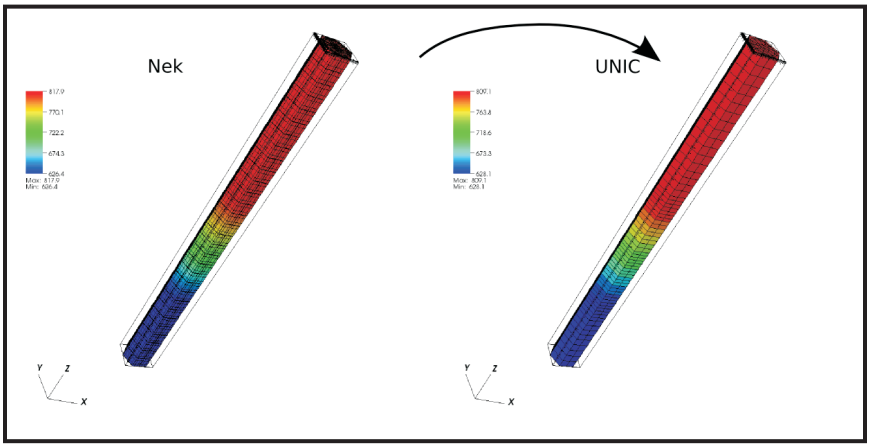

Figure 1. Temperature mapped from Nek to UNIC blocks, single pin. The range of values differs because of block averaging. The vertical axis has been scaled by a factor of 0.05.

Planned Activities

Following is a list of the anticipated tasks for the upcoming year:

- To complete the development of the test-bed code for technique testing, which will include a flexible implementation in order to model both operator-split coupling and full-resolution coupling techniques; the development of Jacobian-free techniques with adaptive preconditioners (i.e., a mechanism to switch between various degrees of representation for off-diagonal terms by recognizing that not all instants in a transient simulation need highly accurate preconditioners for the nonlinear terms); and adaptive time stepping algorithms
- To develop a few transient scenarios representative of a sodium-cooled fast reactor (excluding, at first, the effect of moving meshes)
- To analyze the effect of multi-mesh coupled simulations on the overall accuracy; such situations are typical of coupled simulations, where each physic component is solved on a specific mesh and can introduce inaccuracy, and to address the effect of moving meshes
- To perform a critical analysis of various techniques: a) operator-split vs. Jacobian-free, b) preconditioners, and c) time-stepping strategies based on several transients runs
- To down-select and recommend methods to be implemented in the interface code of SHARP which will drive the coupled neutronic/thermal-hydraulic simulations using UNIC/Nek

Nuclear Energy Research Initiative

Fundamental Studies of Irradiation-Induced Defect Formation and Fission Product Dynamics in Oxide Fuels

PI: James Stubbins, University of Illinois

Collaborators: Argonne National Laboratory, Los Alamos National Laboratory (LANL), Oak Ridge National Laboratory (ORNL)

Project Number: 07-064

Project Start Date: May 2007

Project End Date: April 2010

Research Objectives

This project will address performance issues of oxide-type nuclear fuels in the proposed fast-spectrum advanced burner test reactor (ABTR). Studying radiation effects and fission product transport processes in oxide-type nuclear fuels will establish a fundamental understanding of fuel performance. Researchers will model irradiation effects in cerium and uranium oxide (CeO_{2+x}, UO_{2+x}, and $[CeU]O_{2+x}$) surrogate fuels, comparing their performance with mixed oxide (MOX) fuels. The irradiation effects will be induced by ion implantation over a range of energies and doses to simulate the effects of fission product damage. Transport and trapping of simulated fission products will also be examined. Researchers will use inert gas ions such as krypton (Kr) and xenon (Xe) for ion implantation experiments to cause irradiation damage and for dynamic transport studies to understand trapping and defect mobility processes in these fuel forms. They will also examine ions that simulate fission products and can substitute for uranium (U) or Ce atoms in the oxide structure.

The experimental studies will be complemented by modeling using molecular dynamics (MD) simulations of damage cascades in the oxide lattice and kinetic Monte Carlo (KMC) to study defect dynamics. The MD approach is useful in understanding the early stages of damage during energetic displacement cascades under irradiation. KMC is useful for using the defect configuration energies from MD to examine defect and fission product transport mechanisms.

Research Progress

The research effort during the first half of this year focused on establishing modeling capabilities for molecular statics (MS)/dynamics determination of defect energy states and KMC modeling to determine defect transport and agglomeration characteristics. Both of these efforts are currently being used to benchmark the efforts against other data available in recent literature.

The GULP MD code was utilized for the molecular static and dynamics simulation for defects energies calculations (single charged defect formation energies, neutral Frenkel defect energies, and Schottky defect energies) in UO_2 lattice as well as solution and migration energies of fission products in UO_2 lattice with well-established pair potentials from earlier studies. Molecular static calculations were performed employing the energy minimizations with the Mott–Littleton approach. The preferred defect migration pathways and lattice configurations were also modeled by the GULP code. The calculated energetics data were compared to models with two different potentials as well as available experimental results; the modeling results were found to be higher in general than the experimental data, but consistent with other computational results.

The KMC approach will be used to model migration of fission products in UO_2, utilizing energies modeled using a molecular dynamics code. This code, developed at LANL, has recently been modified to run on a different system and is being used to confirm earlier calculations of oxygen migration as a function of stoichiometry in UO_2. Following this, the migration multiple fission products will be examined. The code, which can only handle the migration of oxygen vacancies and interstitials, is being reconstructed to handle other defect types and structures.

With support from ORNL, this project is working to obtain various UO_2 single crystals for experimental activities. These single crystals will be ion implanted to experimentally determine defect transport and agglomeration processes during the next program period.

Planned Activities

During the next year, the MS/MD and KMC modeling work will be extended to deal with various new atom and defect properties, including defect transport issues. The experimental program will start in full to examine ion implanted UO_2 single crystals. There is also an effort underway to develop a molecular beam epitaxy system to produce individual, thin-film, single crystals.

Nuclear Energy Research Initiative

Identification and Analysis of Critical Gaps in Nuclear Fuel Cycle Codes Required by the SINEMA Program

PI: Adrian Miron, University of Cincinnati

Collaborators: Idaho State University, Idaho National Laboratory

Project Number: 07-071

Project Start Date: July 2007

Project End Date: January 2009

Research Objectives

The research objectives of the project are to 1) carry out a detailed review of the existing codes describing aspects of the nuclear fuel cycle and 2) identify the research and development (R&D) needs required to develop a comprehensive model of a global nuclear energy infrastructure and associated nuclear fuel cycles. Researchers will also recommend appropriate computer codes for integrating into the Simulation Institute for Nuclear Enterprise Modeling and Analysis (SINEMA), the simulation network that will model the global nuclear energy infrastructure, associated fuel cycles, and components. SINEMA will provide an integrated toolbox to support the global and domestic assessment, development, and deployment of nuclear energy systems at various levels of detail. The plan is to implement SINEMA using interconnected and interactive pyramid architecture.

The following three primary tasks will be accomplished:

1) Develop a detailed review of nuclear fuel cycle codes
   - Develop appropriate questionnaires and typical letters to be submitted to code developers and their organizations
   - Conduct a systematic and detailed review of domestic and international nuclear fuel cycle codes
   - Develop a relational database
2) Identify R&D needs and gaps in nuclear fuel cycle computer codes
3) Identify best code packages to be linked within the SINEMA framework

Research Progress

The project's initial effort is to evaluate existing models that describe various aspects of the nuclear fuel cycle. The review includes domestic and international, top-level nuclear enterprise model codes down to micro-scale model codes dealing with all aspects of the nuclear fuel cycle. The codes are assessed through a systematic approach that will focus on input/output (I/O) data, functional and design requirements, method of solution, strengths and weaknesses, computer language and platform, as well as capability to link with other codes. However, the two most important categories for this research are the key I/O parameter description of the codes to be reviewed. These parameters would allow identification of critical gaps in the nuclear fuel cycle codes and particular codes that are going to be linked in the SINEMA's top-level code.

During this reporting period, the team developed questionnaires and typical letters to be submitted to code developers and their organizations. Two main avenues were established for performing the nuclear fuel cycle code review: 1) internet research and 2) literature research. Both avenues have a domestic as well as a foreign component.

Internet research is currently underway at the UC. Three internet resources were reviewed: the Radiation Safety Information Computational Center (RSICC); the Energy, Science, and Technology Software Center (ESTSC); and the Nuclear Energy Agency (NEA) Data Bank. All three databases contain information on codes in line with this research. However, all databases lack code I/O parameter description or do not list them. Since the codes' I/O parameter description is essential for this research,

attempts to establish contact with the managers of these databases was made in order to obtain the missing information. So far, successful communication with RSICC has been established.

Arrangements between the Organisation for Economic Co-operation and Development (OECD)/NEA and the Department of Energy (DOE) require that the information relative to computer codes and nuclear cross section data in the NEA Data Bank is distributed within the United States by U.S. Centers: RSICC and ESTSC for computer codes and NNDC-BNL for nuclear cross sections. Nevertheless, most codes in the NEA database are also contained in the RSICC and ESTSC databases. Efforts have also been made to establish contacts with the Department of Atomic Energy in India, the Chinese Atomic Energy Authority, and the NEA in France.

With ISU's help, Westinghouse agreed to provide information on the codes they are using to model the nuclear fuel cycle.

A list of mining companies from all over the world was also compiled, and almost 1,000 uranium mining companies were found. Efforts will be directed to reduce the list to companies that own or use a code that models the uranium mining and/or fuel fabrication.

Planned Activities

In the next period, efforts will focus on getting the necessary documentation for the code of interest from RSICC. The team will develop a comprehensive list of nuclear fuel cycle codes that are not in RSICC but are in the other two databases. The list will include pertinent codes in the International Atomic Energy Agency database as well.

Supplementary efforts will be dedicated to obtain information for the in-house codes developed by the nuclear industry such as General Electric, AREVA, EXELON, DUKE, American Electric Power, First Energy, etc., and to continue the collaboration with Westinghouse.

Nuclear fuel cycle codes developed by U.S. national laboratories and other institutions such as the Electric Power Research Institute and the Nuclear Energy Institute will also be investigated to complete the comprehensive list of codes of interest.

Literature research is another component of the code review performed in this project. For codes that are not in the comprehensive list of codes of interest developed so far, direct contact with the codes' authors to obtain the necessary information is expected.

Finally, the information gathered will be organized in a database that would allow easy queries on the code's I/O in order to identify critical gaps in the nuclear fuel cycle codes and candidates for linkage in the SINEMA's top-level code.

NUCLEAR ENERGY RESEARCH INITIATIVE

An Innovative Approach to Precision Fission Measurements Using a Time Projection Chamber

PI: Nolan Hertel, Georgia Institute of Technology

Collaborators: Abilene Christian University, California Polytechnic State University, Colorado School of Mines, Los Alamos National Laboratory, Lawrence Livermore National Laboratory, Idaho National Laboratory, Ohio University, Oregon State University

Project Number: 08-014

Project Start Date: October 2007

Project End Date: October 2010

Project Description

The principal objective of this project is to initiate a fission cross section measurement program to provide fission data with unprecedented precision needed for the Global Nuclear Energy Partnership (GNEP) initiative and Generation IV reactor designs. The research consortium will construct, install, and test a prototype of a three-dimensional time projection chamber (TPC) that will carry out fission physics measurements. This will establish the necessary infrastructure for a world-class fission measurement campaign that meets the nuclear data needs required for planning, modeling, designing, and executing the GNEP program.

In addition to providing high-quality fission cross section data, the TPC will generate a rich basic physics dataset of various parameters as a function of neutron energy, including the kinematics and angular distribution of fission products, ternary fission cross sections for light isotopes, and fission product identification. A well-calibrated and tested TPC would reduce fission cross section uncertainty measurements below one percent.

The experimental apparatus will provide precise data on the fission cross sections of key actinides. This will impact the design of actinide-burning targets and reactor designs for GNEP activities as well as the proliferation resistance of potential new fuel cycles. These new data will reduce margins, thus reducing construction and operating costs, and will provide the required precision data during the current engineering/selection phase. In addition, the project will train graduate students and post-doctoral students in experimental nuclear physics and radiation physics, thereby assisting in restoring a much-needed human resource for the anticipated renaissance of nuclear power.

Workscope

In order to produce this high precision, high fidelity instrument, the project has been divided into distinct tasks, each building on the preceding activities:

Year 1

- Begin creating GEANT simulation module and online software
- Develop hardware, including target preparation, gas system, collimation design, the electronics system, and data acquisition system
- Investigate hydrogen scattering standard

Year 2

- Complete simulation efforts on the experimental system and begin creating simulated TPC responses; continue creating database, data fitting, and model for minor actinides
- Process experimental calibration data using online software
- Install gas system; design and fabricate the TPC and electronics; and produce FPGA module
- Measurement tests of the hydrogen cross section

Year 3

- Incorporate calibration function/laser calibration system into online software
- Install TPC with secondary neutron detection system for absolute neutron measurements
- Complete data acquisition for ^{235}U, ^{238}U, and ^{239}Pu; collect minor actinide data and experimental data for the major actinides

Nuclear Energy Research Initiative

Risk-Informed Balancing of Safety, Non-Proliferation, and Economics for the Sodium-Cooled Fast Reactor (SFR)

PI: George Apostolakis, Massachusetts Institute of Technology

Collaborators: Idaho State University, Ohio State University

Project Number: 08-020

Project Start Date: October 2007

Project End Date: October 2010

Project Description

The objective of this project is to develop risk-informed design and evaluation tools for the sodium-cooled fast reactor (SFR) that take into account safety, economics, licensability, and proliferation resistance. These tools will be applied to a number of design alternatives to identify opportunities to reduce the cost of the SFR while maintaining its high level of safety and proliferation resistance.

The proposed design variations, many of which incorporate passive safety features, include loop versus pool-type designs, differing fuel types, and sizes ranging from very large monolithic reactors to small modular ones. The resulting risk-informed methodology will help develop technical requirements for the industrial design organization, identify research needs, assess the technology risk of alternatives, and assist with planning. Industrial groups can use this methodology to perform design tradeoffs that would make the SFR economically competitive and licensable, while still maintaining the reactor's safety and proliferation resistance.

Workscope

The objectives will be achieved through the following activities:

- Establish two reference configurations: 1) a pool design and 2) a loop-type or hybrid design (variations in plant configuration, fuel, and power output will be made relative to these two reference configurations)
- Define appropriate metrics for safety, economics, and proliferation resistance that will serve as the basis for evaluating SFR design alternatives
- Perform probabilistic risk assessments and accident evaluations
- Evaluate costs and identify reduction opportunities
- Evaluate proliferation risks
- Develop a risk-informed, decision-making methodology that would integrate and balance the results of the preceding analyses

NUCLEAR ENERGY RESEARCH INITIATIVE

Deployment of a Suite of High-Performance Computational Tools for Multi-scale Multi-physics Simulation of Generation IV Reactors

PI: Michael Z. Podowski, Rensselaer Polytechnic Institute

Collaborators: Columbia University, SUNY at Stony Brook, Brookhaven National Laboratory

Project Number: 08-033

Project Start Date: September 2007

Project End Date: September 2010

Project Description

The objective of this project is to deploy advanced simulation capabilities for next generation reactor systems utilizing newly available, high-performance computing facilities. The main goals include the following:

1) To develop and deploy high-performance computing tools for coupled thermal-hydraulic, neutronic, and materials multi-scale simulations of the sodium fast reactor (SFR)
2) To apply the new computational methodology to study reactor fuel and core transient response under beyond-design and accident conditions

The work will encompass a broad spectrum of issues that are critical for developing next generation reactors. Deliverables will include multi-physics, multi-scale computational modeling capabilities to investigate the impact of long-term thermal, mechanical loads, and high-burnup fuel on reactor safety and accident mitigation strategies. The consortium will address three major groups of problems:

1) The development of new simulation capabilities for state-of-the-art computer codes (FronTier, PHASTA, and NPHASE) coupled with molecular dynamics (MD)-type analysis
2) The development of advanced numerical solvers for massive parallel computing
3) The deployment of a multiple-code computational platform for the Blue Gene supercomputer simulations of SFR fuel performance during accidents

Workscope

The workscope of the project can be divided into the following major tasks:

- Selection and implementation of MD solver to analyze molecular and micro-scale properties of irradiated fuel for the advanced recycling reactor
- Development of new simulation capabilities of the FronTier code for the simulations of fission product and fuel transport during SFR accident conditions
- Development and implementation of a mechanistic model of pressure-gradient-driven injection of jets of volatile fission products mixed with shattered fuel particles from failed fuel elements into coolant channels
- Development, numerical implementation, and testing of a coupled thermal-hydraulic/neutronic NPHASE-based model of transient multiphase/multicomponent flow and heat transfer in SFR coolant channels
- Development of advanced numerical solvers for massive parallel computing
- Deployment of multiple-code computational platform for the Blue Gene-based simulations of fuel performance, fuel element failure, and core degradation propagation in the SFR system

Nuclear Energy Research Initiative

Real-Time Detection Methods to Monitor TRU Compositions in UREX+ Process Streams

PI: Sean M. McDeavitt, Texas Engineering Experiment Station (TEES)

Collaborators: Purdue University, University of Illinois-Chicago (UIC), Argonne National Laboratory (ANL)

Project Number: 08-039

Project Start Date: October 2008

Project End Date: September 2011

Project Description

The U.S. Department of Energy (DOE) has developed advanced methods for reprocessing spent nuclear fuel. The majority of this development was accomplished under the Advanced Fuel Cycle Initiative (AFCI), building on the strong legacy of process development R&D over the past 50 years. The emergence of the Global Nuclear Energy Partnership (GNEP) has elevated U.S. commitment to advanced fuel cycles. These advanced processing methods must be scaled up and engineered for real-scale implementation.

The most prominent processing method under development is UREX+. UREX+ refers to a family of processing methods that begin with the uranium extraction (UREX) process and, along with a variety of other methods, separate uranium, selected fission products, and transuranic (TRU) isotopes from dissolved spent nuclear fuel. As GNEP moves toward the implantation of UREX+ on a real scale over the next 20 years (e.g., more than 1,000 tons of fuel per day), issues such as safeguards strategies and materials control and accountability methods must be considered. Monitoring higher actinides during aqueous separations is a critical research area for the U.S. GNEP/AFCI program. A key deficiency in such monitoring is the lack of real-time assessments to detect the diversion of TRU elements such as plutonium. By providing on-line materials accountability for the processes, covert diversion of the materials streams becomes much more difficult.

The objective of this consortium is to develop real-time detection methods to monitor the efficacy of the UREX+ process and to safeguard the separated TRUs against unlawful diversion from within a processing facility. To achieve this objective, a comprehensive development strategy is being implemented to enable the incorporation of an array of traditional detectors and advanced metastable fluid detectors into a novel detector assembly designed specifically for application in a UREX+ centrifugal contactor array. The development experiments will range from laboratory benchmarks to hot-cell demonstrations with real UREX+ spent fuel experiments. Consortium team members will also perform supporting research to develop safeguards strategies for the UREX+ process and to evaluate the corrosion behavior of critical component materials in the UREX+ system.

Workscope

Texas A&M University (TAMU) is the lead institution, under the administration of TEES, and will develop the overall detector assembly and safeguards strategy. Purdue University will lead the development of the detector arrays to be inserted into the assembly designed at TAMU. UIC will perform critical corrosion research as well as provide the university-laboratory interface with ANL.

At the end of three years, the proposed detector assembly and detector arrays will be completed, benchmarked, and ready for full-scale application. This will include bench-scale testing with simulated and real UREX+ process fluids. In addition, a complete safeguards strategy will be in place to take advantage of the information stream enabled by this new detector system and a corrosion database will be available to enable material selection for superior detector performance.

Nuclear Energy Research Initiative

Performance of Actinide-Containing Fuel Matrices Under Extreme Radiation and Temperature Environments

PI: Brent J. Heuser, University of Illinois, Urbana-Champaign

Collaborators: University of Michigan, Georgia Institute of Technology, South Carolina State University

Project Number: 08-041

Project Start Date: September 2007

Project End Date: September 2010

Project Description

This consortium will study fundamental details about the response of actinide-containing fuel matrices to the radiation and temperature environments found within an advanced burner reactor. The research is comprised of two parts:

1) An experimental component to study atomic-level details related to the influence of radiation damage
2) A modeling component employing molecular dynamics (MD) and kinetic Monte Carlo (kMC) techniques to study the radiation damage processes

The researchers will use thin films of uranium oxide (UO_2) and zirconium (U-10Zr) matrices, both in well-controlled single-effect experiments and experiments designed to study the combined effects of several factors. The work will focus on the behavior of actinide surrogates cerium (Ce) and neodymium (Nd), implanted non-volatile fission product surrogates such as molybdenum (Mo), and xenon (Xe) fission gas. Researchers will study these materials under the influence of high temperatures (to about 1,400°C), displacement cascade damage, and microstructure defects (grain boundaries and other extended defects). They will experimentally characterize the transport, segregation, and precipitation (or bubble formation in the case of Xe) and will study the processes with atomic-level detail using MD and kMC. The combination of the two components is anticipated to yield a knowledge database for performance of the UO_2 and U-10Zr fuel matrices that does not currently exist.

Workscope

Following are the major tasks associated with this project:

1) Fabrication of polycrystalline and single crystal thin films with controlled concentrations of actinide surrogates (Ce, Nd) and controlled microstructures
2) Implantation of Mo, Xe, and krypton (Kr) at desired concentration and depth profile
3) Heavy ion bombardment induced displacement damage of thin film specimens to induce mixing and segregation
4) Quantification of diffusion, precipitation, and bubble formation versus ion beam treatments
5) Validation of potentials for the UO_2 system by comparison with experiments
6) Application of MD and kMC to study diffusion and precipitation processes in order to ensure adequate agreement with experiments

Nuclear Energy Research Initiative

Radiation Damage in Nuclear Fuel for Advanced Burner Reactors: Modeling and Experimental Validation

PI: Niels Jensen, University of California-Davis

Collaborators: California Institute of Technology, Northwestern University, University of California-Los Angeles

Project Number: 08-051

Project Start Date: October 2007

Project End Date: October 2010

Project Description

In this joint project, researchers will study radiation damage of nuclear fuels through modeling, simulation, and experimental characterization. The project will focus on the behavior, structure, and properties of fuel materials under conditions relevant to Advanced Burner Reactor (ABR) service.

Efficient predictive modeling requires the integration of a range of materials models and numerical methods, spanning multiple length and time scales. This project will result in new simulation tools for predicting active ion transport and damage evolution in nuclear materials, new insights into interatomic force fields relevant for modeling the physical properties of nuclear fuel, an evaluation of bubble formation in crystalline materials, and novel experimental characterization of damage and defect distributions in active materials through (Scanning) transmission electron microscopy. The tools developed through this research will provide specific predictions of relevant materials behavior in nuclear fuel for a closed fuel cycle in a fast burner reactor, as well as new and validated computational techniques that can be applied for further research.

Workscope

Following are the major tasks of this research project:

1) Model fission product and ion range distributions through simplified Molecular Dynamics methods
2) Understand interatomic force fields through first-principles calculations
3) Study crystal defect and noble gas diffusion and aggregation through Kinetic Monte Carlo simulations
4) Assess crystal damage evolution through molecular modeling and empirical relationships between energy deposition and defects
5) Perform experimental characterization to validate multi-scale models

Nuclear Energy Research Initiative

Advanced Instrumentation and Control Methods for Small and Medium Export Reactors with IRIS Demonstration

PI: J. Wesley Hines, University of Tennessee

Collaborators: North Carolina State University, Pennsylvania State University, South Carolina State University, Westinghouse

Project Number: 08-058

Project Start Date: October 2007

Project End Date: October 2010

Project Description

This research project will investigate, develop, and validate advanced methods for sensing, controlling, monitoring, and diagnosing small- and medium-sized export reactors (SMR) and will then apply these techniques to the International Reactor Innovative & Secure (IRIS). The research focuses on three topical areas with the following objectives:

1) To develop and apply simulation capabilities and sensitivity/uncertainty analysis methodologies to address sensor deployment analysis
2) To develop and test an autonomous/hierarchical control architecture for application to the IRIS design
3) To develop and test an integrated monitoring, diagnostic, and prognostic system for SMRs using the IRIS design as a test platform

This research project meets the unique needs of reactors that may be deployed in developing countries with limited support infrastructure. These applications will require smaller, robust reactor designs with advanced technologies for sensors, instrumentation, and control. The project addresses two of the eight needs outlined in the recently published "Technology Roadmap on Instrumentation, Control, and Human-Machine Interface (ICHMI) to Support the Department of Energy (DOE) Advanced Nuclear Energy Programs." Although intended for the SMR designs, the methodologies developed can also be used for sensor deployment analysis, autonomous control, and monitoring/diagnosis/prognosis in other types of nuclear plant or hydrogen facilities.

Workscope

The following key project objectives will be accomplished by integrating the skills of the collaborating researchers:

- NC State will lead the modeling tasks by developing an IRIS simulator
- The University of Tennessee and Penn State will use the simulator to develop autonomous and multivariate control strategies
- The University of Tennessee will develop condition monitoring and prognostic methodologies
- The control strategies for Automated Contingency Management (ACM) will be developed based on the output of these methodologies through control system modification, redistribution, reconfiguration, and re-planning
- The team will develop I&C requirements, including optimal sensor identification and placement

Nuclear Energy Research Initiative

Advanced Aqueous Separation Systems for Actinide Partitioning

PI: Ken Nash, Washington State University

Collaborators: Hunter College (CUNY), Idaho National Laboratory, Lawrence Berkeley National Laboratory, Pacific Northwest National Laboratory, Tennessee Technological University, University of New Mexico, University of North Carolina-Wilmington

Project Number: 08-067

Program Start Date: October 2007

Project End Date: September 2010

Project Description

One of the most challenging aspects of advanced processing of spent nuclear fuel is the need to isolate trans-plutonium actinides from fission product lanthanides. This project expands the scope of two ongoing investigations of americium (Am) partitioning from the lanthanides with the synthesis of new separations materials and a centralized focus on radiochemical characterization of the separation systems that could be developed based on these new materials.

In the predominant trivalent oxidation state, the chemistry of lanthanides overlaps substantially with that of the trivalent actinides and their mutual separation is quite challenging. The two aqueous processing strategies recognized to have the greatest probability of success are 1) the application of complexing agents containing ligand donor atoms that are softer than oxygen (e.g., N, S, Cl-) and 2) changing the oxidation state of americium to IV, V, or VI to increase the inherent differences in the chemistries of the groups. Unfortunately, the softer donor atoms interact less strongly than does oxygen with the hard acid lanthanide and actinide cations (though slightly more so with actinides than lanthanides), and the upper oxidation states of Am are all moderately strong oxidants, hence unstable in typical media. Neither of these factors represents an insurmountable obstacle to developing a successful separation, but creative and perhaps unconventional approaches will be needed to overcome these limitations.

University-based efforts will be to provide new separations materials. The separation potential of these materials will be assessed in radiochemistry laboratories at WSU and Tennessee Tech University. National laboratory scientists will contribute specialized facilities and unique expertise.

Workscope

- Create new separations materials whose potential will be assessed in radiochemistry laboratories
- Advance the scientific basis for nuclear fuels processing and secure the workforce for continued operation of that sector

Nuclear Energy Research Initiative

6.3 Nuclear Hydrogen Initiative

Twelve NERI research projects are currently being performed that closely relate to the goals of NHI, 3 of which were awarded in FY 2005, 6 in FY 2006, 2 in FY 2007, and 1 new NERI-C project in FY 2007.

As discussed in Section 3, the Nuclear Hydrogen Initiative supports the President's vision for a future hydrogen economy by demonstrating economic, commercial-scale hydrogen production using nuclear energy. This initiative will develop technologies to produce hydrogen with heat and/or electricity from next generation nuclear energy systems at costs that are competitive with other transportation fuels.

NERI efforts related to this initiative involve the construction of integrated laboratory-scale experiments in support of the three primary NHI research areas:

- Hydrogen production with thermochemical cycles
- Hydrogen production with high-temperature electrolysis (HTE)
- Support systems for the hydrogen production process

In FY 2007, NHI research projects focused on developing an efficient flowsheet for the Sulfur-Iodine (S-I) cycle, developing simulation tools, and conducting design/analysis of the S-I cycle. Research in high-temperature electrolysis is enhancing electrolyzer performance, developing improved cell materials, and creating new seal designs. Reactor/hydrogen support system research is creating new alloys and ceramics for heat exchangers, and optimizing heat exchanger design/performance.

Planned NERI research efforts under the single newly-awarded FY 2007 consortia project related to NHI will develop and model alternative thermochemical cycles for nuclear hydrogen production.

This section provides an index of the research being performed under NHI and a summary of the ongoing projects.

Nuclear Energy Research Initiative

Project Summaries and Abstracts

Nuclear Energy Research Initiative

The Sulfur-Iodine Cycle: Process Analysis and Design Using Comprehensive Phase Equilibrium Measurements and Modeling

PI: Mark C. Thies, Clemson University

Collaborators: University of Virginia (UVa), Savannah River National Laboratory (SRNL)

Project Number: 05-006

Project Start Date: April 2005

Project End Date: March 2009

Research Objectives

Of the numerous thermochemical hydrogen (H) cycles proposed for the centralized production of H from nuclear power, the Sulfur-Iodine (S-I) cycle has been identified as one of the most promising. However, because the S-I cycle involves complex, highly non-ideal phase behavior and reactions, many of the performance projections associated with this technology are based on uncertain and incomplete data. In order to successfully develop this technology for a future hydrogen economy, basic research on thermodynamic measurements and physical property models of this cycle is needed.

This project will focus on three areas: 1) thermodynamic measurements, 2) physical properties modeling, and 3) process modeling. Researchers will use initial properties and process modeling to select conditions for experimental measurement. Then, as measurements become available, they will refine property models for process modeling and use the results to identify additional experiments for minimizing remaining process uncertainties.

The results of this project will be transferred to the nuclear hydrogen community by process simulation of the S-I cycle, using reactive distillation to affect the decomposition of hydrogen iodide (HI).

Research Progress

For this NERI project, researchers selected the HI decomposition section of the S-I cycle as a priority for experimental measurement and process modeling. A continuous-flow apparatus (CFA) technique was chosen for measuring the complex phase behavior that exists for mixtures of I_2, water, and HI at elevated temperatures and pressures in order to minimize residence times and thus the possibility of reactions.

To confirm the ability of the CFA setup to generate quality phase-equilibrium data at elevated temperatures and pressures, liquid-liquid equilibrium (LLE) measurements were carried out for the benzene-water binary system at temperatures from 200 to 250°C. This test system was chosen because it has several features in common with the I_2-water system, such as LLE and an upper critical solution temperature at elevated temperatures and pressures. In addition, adequate data in the literature were available for comparison. In working with this test system, the research team determined that several changes to the CFA were required to obtain quality data. In particular, the impingement mixing section, whereby the two feed streams are mixed after preheating in order to achieve equilibrium, had to be increased from the original one "impingement" to two. In addition, researchers found that sample sizes needed to be increased to approximately 30 grams each in order to eliminate the effects of two-phase flow and to ensure that representative samples were obtained.

LLE results for the benzene–water system are shown as temperature vs. composition diagrams in Figure 1. Tsonopoulos's prediction is shown only to guide the eye; as stated by him, his predictions above 200°C are not accurate, being based on limited data. The measurements taken ("Experimental Data") are believed to be accurate to within 3 percent deviation for the water-rich phase (e.g., 3.69 ±0.11 wt % benzene at 224.9°C) and 2 percent deviation for the benzene-rich phase (e.g., 5.09 ±0.09 wt % water at 200.2°C). Reported temperatures of 200.2, 224.9, and 249.8°C are believed to be accurate to better than ±0.2°C. In all cases, operating pressures were maintained about 5 bar above the three-phase line and were maintained constant to within ±3 psi for a given run. As seen in the figure, most of the "Literature Data" were found to be in good agreement with the performed work—but some deviated significantly. Results are believed to

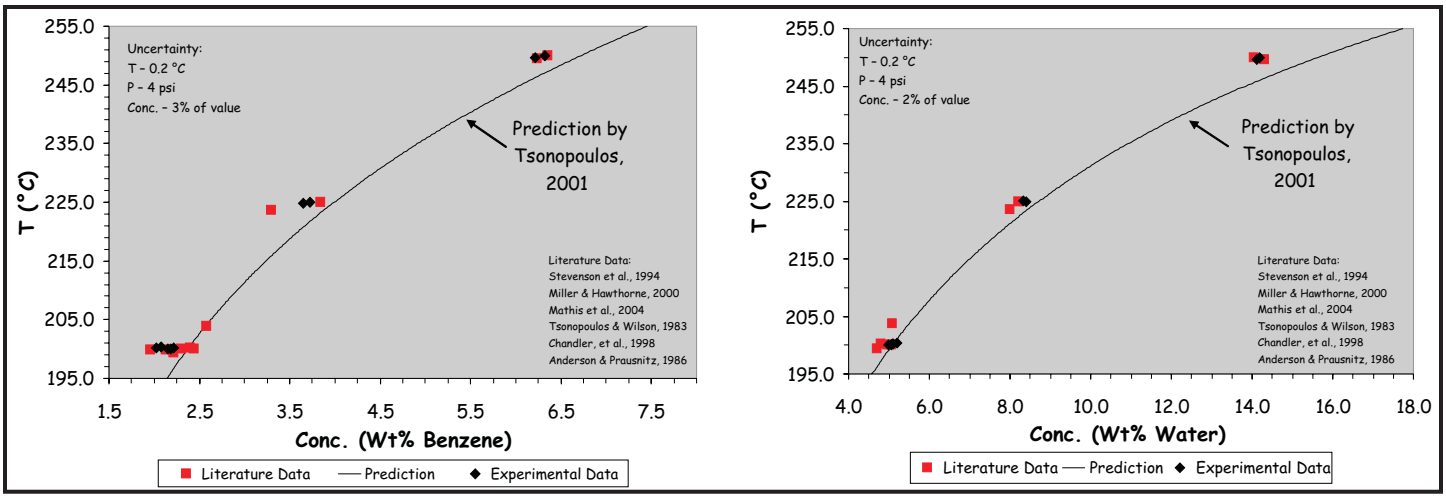

Figure 1. LLE phase compositions for the benzene–water system at temperatures from 200 to 250°C: left, the water-rich phase; right, the benzene-rich phase.

be of high quality, as they were accurately reproduced on different days (and even during different months) and with component feed flow rates to the CFA varying by as much as a factor of three.

In modifying the existing CFA so that the phase behavior of mixtures of I_2, water, and HI could be measured, the premise had been that all apparatus components in the high-temperature zone (that is, in the isothermal bath) should be made of tantalum (Ta), but that components in the lower temperature (150°C max) feed and sample collection sections, where corrosion would be less severe, could be made of less expensive materials and/or Teflon-coated. To further reduce corrosion concerns, researchers focused their initial experimental efforts on the binary I_2-water system. This decision was also driven by the fact that Ta micrometering and on/off valves were not available, as well as by concerns that making these valves and the feed reservoir of Ta would not only be prohibitively expensive but also problematic because of the difficulty in machining Ta. Thus, an inordinate amount of time and effort was spent in FY 2007 on constructing a CFA for the binary I_2-water system using Teflon-coated feed reservoirs, along with Hastelloy C feed lines, on/off valves, and micrometering valves. By June 2007, it became clear through repeated experimentation that mixtures of I_2 and water at even moderate temperatures are not only highly corrosive to Hastelloy C but also readily diffuse through Teflon coatings to attack the base metal underneath.

With this setback, the most logical next step was to alter the CFA so that all wetted parts would be made of Ta, eliminating the possibility of future corrosion problems. To this end, researchers met with personnel at Clemson's Machining and Technical Services (MTS) and developed a plan for machining all wetted parts for the feed and sample collection sections from Ta. Fortunately, MTS has developed considerable expertise in working with Ta and its alloys during the past year, and personnel were now confident that they could, in fact, manufacture all needed fittings and valves from Ta. The proposed apparatus is shown in Figure 2—note that all components in the isothermal bath had already been previously manufactured by MTS from Ta/Ta-W. The I_2 feed reservoir located after the syringe pump in Figure 2 is the Ta-10W reservoir recently constructed by General Atomics (GA).

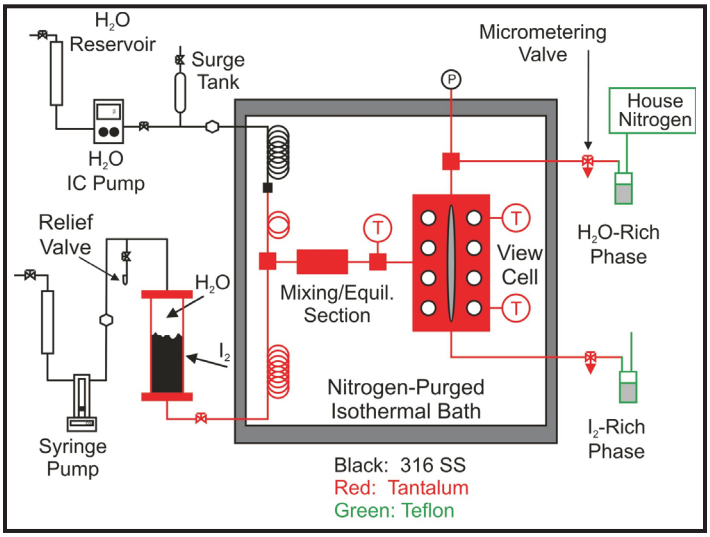

Figure 2. Proposed, all-Ta/Ta-W continuous-flow apparatus. Feed section is to the left and sample collection section is to the right of the isothermal bath, which contains the mixing/equilibrium section and view cell.

Construction of Ta/Ta-W fittings and the on/off valve for the feed section between the I_2 feed reservoir and the mixing/equilibrium section was initiated; work is on schedule and will soon be completed. Ta-2.5W tubing was purchased for this section and will also be installed,

replacing the existing Hastelloy C tubing. Construction of an all Ta/Ta-W sample collection system (i.e., the lines from the view cell to the Teflon sample collection vessels, micrometering valves, on/off valves, and fittings) will be initiated if funds can be obtained for this purpose.

Properties and process modeling of the S-I process also continued during FY 2007. Aspen Plus™ simulations of the three sections of the S-I process were completed, with essentially full consistency being achieved among the sections. The conclusion of this work was that unless significant energy efficiency improvements can be made, the overall S-I process efficiency will not be much above 40 percent. However, none of the properties models used in the simulations can describe the dramatic changes in HI vapor concentration that occur over a small range of liquid concentrations above the ternary "pseudoazeotrope." Thus, the efficiency of the reactive distillation column is likely to be significantly higher than is currently estimated, once experimental data from the project team become available and can be used to revise existing property models.

Another significant project milestone, the model-free analysis of the thermodynamics of water-splitting for the overall process and individual sections, has been completed. There are significant inconsistencies in the results, suggesting that uncertainties in process configurations and efficiencies may be larger than anticipated.

Researchers have been assigned to investigate innovative designs of the reactive distillation (RD) column for Section III of the S-I process, with the goal of improving the overall S-I process efficiency to the target range of 50-60 percent. Discussions are planned related to process and properties modeling, along with opportunities for efficiency improvement in the RD section.

Members of the project team organized the session entitled "Benchmarking of Thermochemical Cycles for Advanced Hydrogen Manufacturing Processes" for the AIChE annual meeting in Salt Lake City in November 2007. Talks from four international organizations (ProSim, CEA, MIT, and UVa/SRNL) highlighted common property modeling issues in S-I research programs from around the world. In addition, an international panel (with representatives from JAEA, CEA, OLI, and GA) discussed the impact of uncertainties and explored the possibility of establishing international standards for reporting results so that valid comparisons can be readily made.

Planned Activities

Upon completing the all-Ta feed section, delivery of molten iodine from the I_2 feed reservoir and into the view cell will be tested. Construction of the all-Ta sample collection system (i.e., the lines from the view cell to the Teflon sample collection vessels, micrometering valves, on/off valves, and fittings) will be initiated by MTS if sufficient funds are available for this purpose. Once the all-Ta sample collection system is complete, experiments to locate the phase boundaries for the binary I2-water and/or ternary I2-water-HI systems can proceed.

Work on the S-I thermodynamic model-free analysis will soon be completed. In addition, thorough testing of property modeling ideas, especially for complexation with HIx data, will be undertaken. Finally, as the phase-boundary measurements described above become available, the use of these new data to improve the existing property models will begin.

Because of the difficulties experienced in the design and construction of the experimental apparatus, a one-year no-cost extension for this NERI project is being requested. The extension will enable researchers to complete apparatus construction and testing, to initiate the measurement of the desired experimental data, and to begin the development of more accurate properties and process models for the S-I process.

Nuclear Energy Research Initiative

Silicon Carbide Ceramics for Compact Heat Exchangers

PIs: Dennis C. Nagle and Dajie Zhang, Johns Hopkins University

Collaborators: None

Project Number: 05-032

Project Start Date: April 2005

Project End Date: April 2008

Research Objectives

The objective of this research is to develop a process for producing silicon carbide (SiC) ceramic materials for high-temperature heat exchangers in the next generation nuclear reactors. The SiC processing technique must produce net-shape and fully dense materials.

The refractory nature and high thermal conductivity of SiC make it an ideal material for high-temperature heat exchange materials. In particular, the melting temperature of SiC is in excess of 2,800°C and it retains its high strength even at elevated temperatures; in fact, the flexural strength of SiC increases until 1,200°C, reaching a maximum near 500 MPa. Additionally, SiC is chemically stable in many caustic high-temperature environments.

The same properties that make SiC a desirable candidate for high-temperature heat exchange applications—that is, its refractoriness—also make it notoriously difficult to process. The research team has created a method by which to produce net-shape, fully dense SiC ceramics by liquid silicon infiltration of porous carbon substrates derived from cellulosic precursors. These porous carbon substrates are reacted with liquid silicon at a temperature of 1,800°C and a pressure of 0.5 Torr over a period of 30 minutes to a few hours.

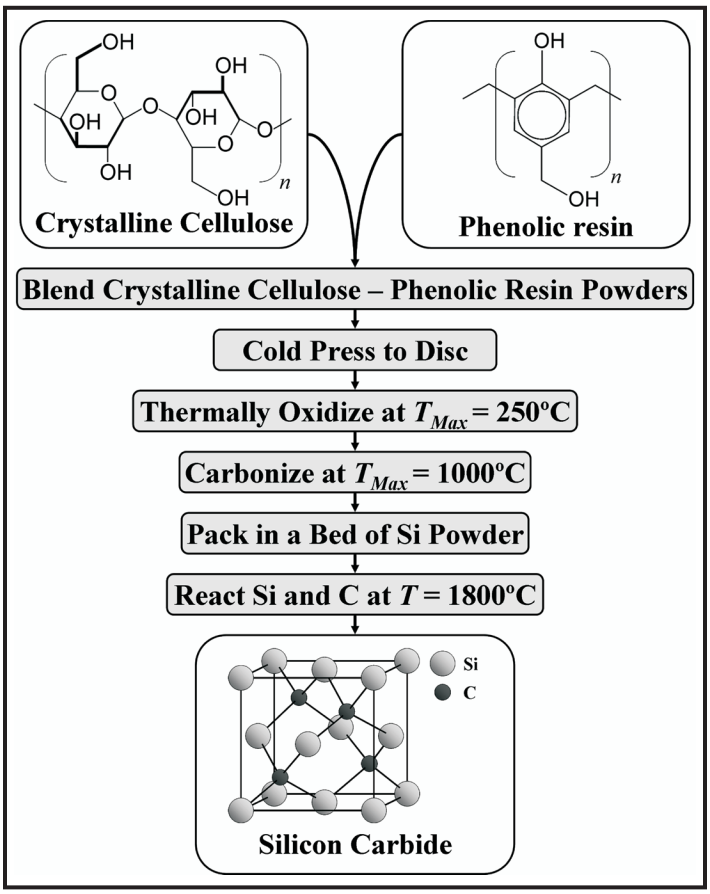

Figure 1. Flowchart of SiC production technique.

Research Progress

Optimization of processing technique. The method developed for the production of net-shape and fully dense SiC ceramics is illustrated as a flow chart in Figure 1. The research team adopted a two-component carbon precursor consisting of particulate crystalline cellulose and particulate phenolic resin. By varying the precursor composition, researchers were able to fine-tune the bulk density, micron-scale porosity, and chemical reactivity of the carbon preform. It was determined that the precursor blended in a 6:4 mass ratio of crystalline cellulose and phenolic resin would give the optimum carbon preform properties. The cellulose and phenolic resin were blended by ball milling without the aid of any solvent, then cold-pressed into disks under 35 MPa, followed by carbonization to a maximum temperature of 1,000°C. The resulting micron-porous carbon preforms were packed in a bed of silicon powder within a covered graphite crucible and liquid silicon infiltration was performed at 1,800°C under an argon pressure of 0.5 Torr for periods of 0, 10, 15, 30, 60, 120, and 300 minutes.

During liquid silicon infiltration, the reduction in surface energies of both the liquid Si and solid carbon leads to reactive wetting and infiltration of porous carbon by liquid Si. The free energy reduction associated with the highly exothermic reaction,

$$Si(l) + C(s) \xrightarrow{T \geq T_M = 1414^\circ C} SiC(s)$$

$$\Delta G_f^\circ = \left(-27100 - 2.73T \log T + 18.1T\right) \text{cal mol}^{-1},$$

leads to the formation of SiC.

Actual density of the reaction products have a maximum value of 2.96 g cm^{-3} at 300 minutes of reaction time, which is over 91.8 percent of the theoretical value of pure SiC. The volume fraction of SiC in the reaction product has a maximum value of 82.47 percent at 120 minutes of reaction time. A photograph of this material is shown in Figure 2 and an optical micrograph of a polished cross section of this material is shown in Figure 3.

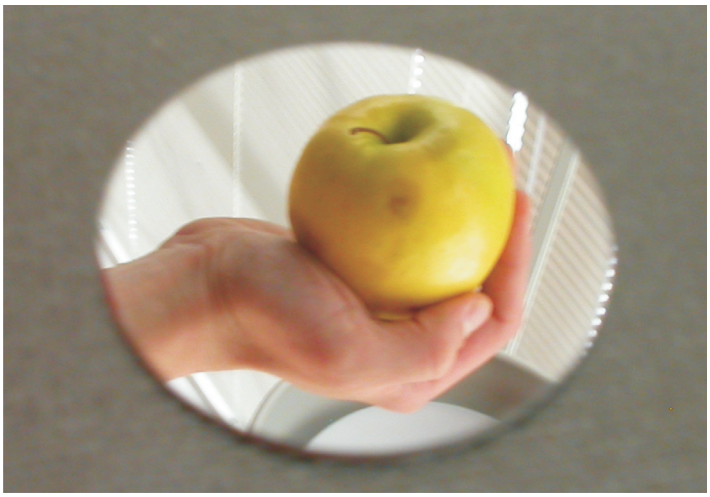

Figure 2. Photograph of polished SiC disk with reflection.

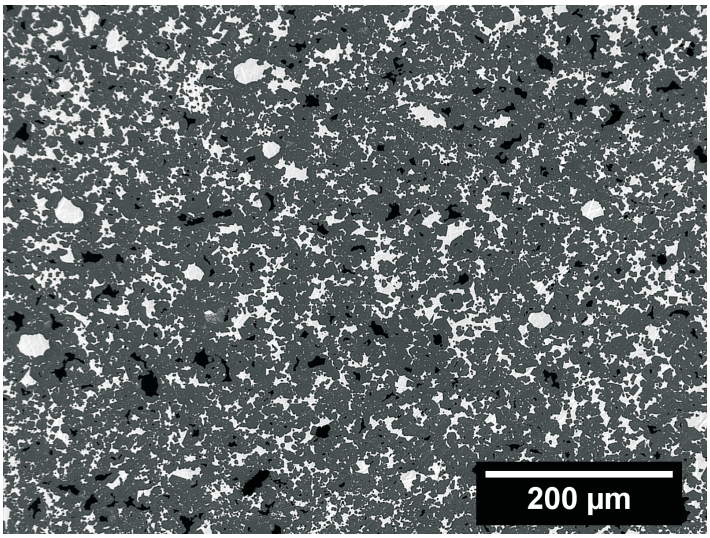

Figure 3. Polished cross section of reaction product.

Chemical analyses of reaction products. The chemical composition of the SiC phase in the reaction products of different reaction times was obtained by electron probe microanalysis (EPMA) in a scanning electron microscope (SEM) using energy dispersive spectroscopy (EDS). An image of the polished microstructure obtained by a backscattered electron detector is shown in Figure 4a. Isolated SiC, silicon, and carbon phases are labeled and a sample electron beam target is indicated by the crosshair within the isolated SiC phase. The beam interaction volume is represented aerially by the dot at the center of the crosshair. The data obtained during these experiments are displayed in Figure 4b. For reaction times of 30 minutes and longer, the average carbon concentration in the SiC phase in the reaction products was found to be 56.75

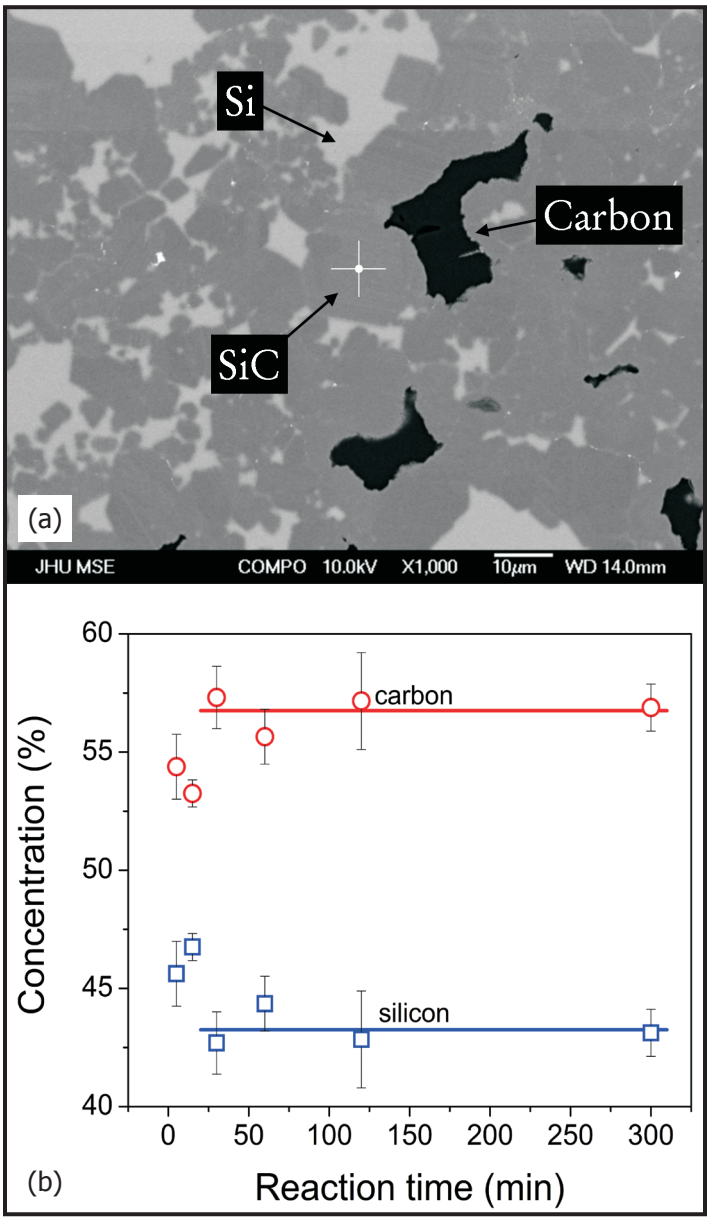

Figure 4. (a) Scanning electron micrograph of polished reaction product cross section and (b) chemical composition in SiC phase.

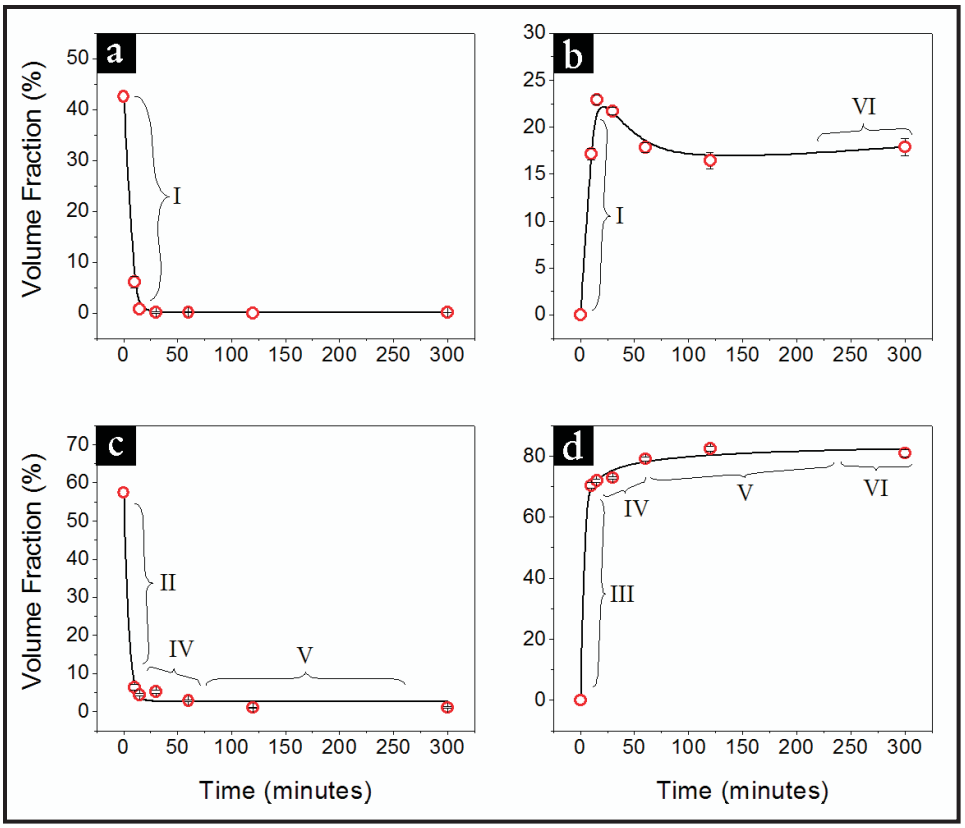

Figure 5. The volume fractions of (a) porosity, (b) silicon, (c) carbon and (d) SiC in the products of time-controlled liquid silicon infiltration reactions.

at%, which is higher than the stoichiometric value of 50 at%. The formation of carbon-rich non-stoichiometric SiC is due to two possible reasons. First, the liquid silicon was observed to be supersaturated with carbon (approximately 10 at%). As a result, the formation of carbon-rich SiC out of this solution may be thermodynamically favorable. Second, the diffusion rate of carbon in SiC at 1,800°C is much higher than that of silicon and it is reasonable to assume that the carbon vacancy concentrations in SiC at this temperature is relatively high. Consequently, high carbon vacancy diffusion through SiC led to the formation of carbon rich non-stoichiometric SiC.

Evolution of the volume fractions of SiC, carbon, silicon, and porosity in the reaction products. The evolution of the volume fractions of SiC, carbon, silicon, and porosity in the reaction products along the reaction time was determined by optical microscopy and digital image processing, segmentation, and analysis. The results of these experiments are plotted in Figure 5. Analysis of these plots has allowed the researchers to identify six events that occurred during the overall liquid silicon infiltration and SiC formation process:

I. Rapid liquid silicon infiltration

II. Rapid carbon dissolution in liquid silicon

III. Rapid SiC formation

IV. Complete formation of a continuous SiC layer at all silicon-carbon interfaces

V. Carbon diffusion through continuous SiC layer to react with liquid silicon

VI. Liquid silicon filling of cracked SiC structure

Rapid liquid silicon infiltration, carbon dissolution in liquid silicon, and SiC formation occur simultaneously during the reaction time interval of 0 to 15 minutes. This early stage culminates with the formation of a continuous SiC layer at all silicon-carbon interfaces. Once the continuous SiC layer is formed, all further reactions occur by carbon diffusion through this layer to react with liquid silicon. After a reaction time of 300 minutes, silicon-filled SiC cracks are observed.

Planned Activities

The following tasks are planned for the upcoming year:

- Production of grooved and channeled reaction products
- Further chemical analyses of reaction products
- Crystallographic analyses of SiC

Nuclear Energy Research Initiative

Molten Salt Heat Transport Loop: Materials Corrosion and Heat Transfer Phenomena

PI: Kumar Sridharan, University of Wisconsin

Collaborators: None

Project Number: 05-154

Project Start Date: April 2005

Projected End Date: April 2008

Project Description

The Next Generation Nuclear Power Plant (NGNP) is likely to be a high-temperature reactor utilizing graphite moderation with TRISO (tri-isotropic coated) fuel particles in either a matrix or pebble bed configuration. The NGNP will be designed to produce electricity and process heat for hydrogen production.

Because the interface between the reactor and the hydrogen production system will involve long heat transfer paths at elevated temperatures, it will require a working fluid with superior heat transfer characteristics. The heat transport fluid should 1) be chemically compatible with the surrounding structural materials, 2) have superior fluid-mechanical and heat transfer properties, and 3) have acceptable safety characteristics under normal and abnormal conditions. Heat transport fluids such as high-pressure inert gas (helium or carbon dioxide) or molten salt are expected to satisfy these requirements. This project investigates the potential of molten salt as a possible transport fluid and also investigates the corrosion resistance of structural materials that would come into contact with the molten salt.

The objective of this project is to demonstrate that molten fluoride salts, specifically 46.5%LiF-11.5%NaF-42%KF (FLiNaK), can be successfully implemented in a low-pressure intermediate heat exchange loop. The project focuses on utilizing molten salt as a process-heat transport fluid and on the corrosion compatibility of this medium with surrounding materials. The research objectives are to 1) plan, design, and execute a series of corrosion compatibility experiments in order to develop a database on the structural materials' behavior for a range of candidate materials that are being considered for the NGNP design; 2) design, fabricate, and operate molten fluoride salt in a flow loop under prototypic NGNP conditions using appropriate geometric scaling; and 3) document the observed corrosion effects and heat transport performance as integral and separate-effects databases.

Research Progress

Researchers have developed an in-depth understanding of various issues pertaining to corrosion testing in a molten fluoride salt environment, focusing particularly on safety and salt purity issues. Specifically, researchers have performed the following tasks:

- Completed corrosion testing and evaluation of a number of candidate alloys in high-purity hydrofluorinated 46.5%LiF-11.5%NaF-42%KF (FLiNaK) eutectic salt obtained from Electrochemical Systems, Inc. (ECS)
- Completed corrosion testing and evaluation of Incoloy 800H in non-hydrofluorinated FLiNaK procured from Idaho National Laboratory (INL) in order to examine the effect of salt purity on corrosion
- Installed glove box facilities to produce FLiNaK salt in-house and tested the corrosion resistance of Incoloy 800H in this salt
- Performed corrosion testing of Incoloy 800H in Incoloy 800H crucible to study the effects of graphite crucible (used in earlier experiments in this project) on corrosion
- Established a method for on-line diagnostics for high-temperature corrosion in FLiNaK salt using principles of high-temperature electrochemistry
- Established the efficacy of neutron activation analysis (using the University of Wisconsin nuclear reactor) to evaluate the composition of the salts before and after corrosion and high-temperature electrochemical tests

- Completed the study on the feasibility of using high-temperature epoxy for joining graphite components due to the importance of graphite as a candidate structural material in molten fluoride salt systems (e.g., advanced high-temperature reactor [AHTR], intermediate heat exchangers)
- Initiated heat transfer modeling in molten salts that will aid in the construction of the molten salt corrosion loop for heat and mass transfer experiments
- Initiated the design and construction of a molten salt flow loop

Corrosion Testing. The research team performed corrosion testing of candidate materials in FLiNaK salt at 850°C for an exposure duration of 500 hours. Testing was performed in POCO graphite crucibles (Grade AXZ-5Q1), purified to a total ash content of 5 ppm or less, a particle size of 5μm, and a pore size of 0.7μm. Salts investigated were high purity hydrofluorinated FLiNaK salt (ECS), non-hydrofluorinated FLiNaK salt (INL), and FLiNaK salt prepared at the University of Wisconsin in a glove box by the addition of carefully measured amounts of individual salt constituents. Figure 1 presents the results of weight loss measurements (measured as weight loss per unit area) after the corrosion tests. In addition, samples of Incoloy 800H were also tested in ECS FLiNaK salt in an Incoloy 800H crucible to evaluate the role of graphite in the corrosion process.

For the iron-nickel (Fe-Ni)-based alloys, it was generally noted that the weight loss due to corrosion increased with chromium (Cr) content in the alloy due to the strong propensity of Cr to dissolve in molten FLiNaK salt. The Nb-1Zr alloy exhibited severe corrosion, and although it is a refractory alloy and has been proposed for the molten salt application, studies have clearly demonstrated the unsuitability of this alloy for use in molten fluoride salts. Results also show that FLiNaK salt purity levels have a minor effect on corrosion. Both Incoloy 800H and 617 (alloys that are code-certified for high-temperature applications) seem to exhibit relatively low corrosion weight loss.

Ni-electroplating appears to be a viable option for protecting materials against corrosion in molten fluoride salts. Results show Ni electroplated 800H alloy to be remarkably resistant to corrosion in molten fluoride salts. Because electroplating is a relatively inexpensive and non-line-of-sight commercial process, this approach may hold considerable promise for structural materials for molten fluoride salt systems. Figure 2a shows the grain boundary attack in Incoloy 800H alloy after exposure to molten FLiNaK; however, Figure 2b shows that corrosion of this alloy can be considerably mitigated by Ni-electroplating. Figure 2b also shows that some diffusion of Fe and Cr does occur through the Ni-electroplating and researchers plan to investigate modifications of the microstructure of the Ni-electroplating to suppress this cationic transport.

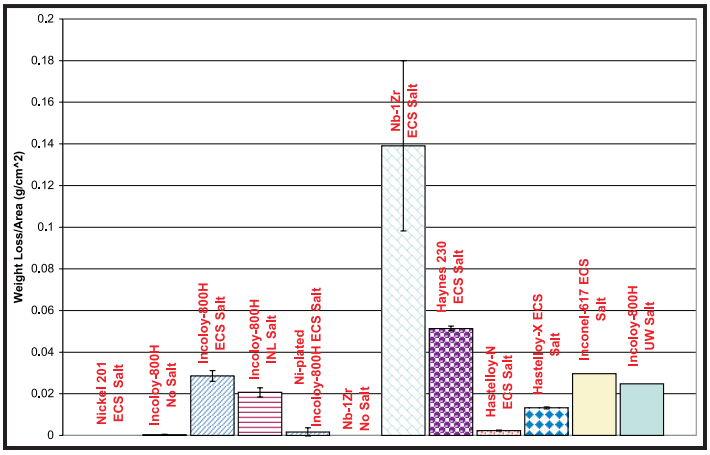

Figure 1. Weight loss due to corrosion for various materials in molten FLiNaK of various purities at 850°C after 500 hours of exposure.

Examination of Hastelloy-X and Haynes 230 showed the presence of molybdenum (Mo) and tungsten (W) at the grain boundaries, respectively, despite the severe grain boundary attack in these alloys. These elements appear to be resistant to dissolution in molten FLiNaK and may be considered as surface treatment species for protection against corrosion in molten fluoride salts. Inductively coupled plasma-mass spectroscopy (ICP-MS) studies are being performed on the FLiNaK salts before and after corrosion tests to establish salt purity and to detect the extent of elemental dissolution in the salts. The results of these tests show a reasonably good correlation between the Cr content in the original alloys and in the salt after corrosion tests are observed.

Neutron Activation Analysis. Neutron activation analysis (NAA) is being performed for both tested and untested salts to accurately determine impurity levels and is being used as a check against the ICP-MS tests. The salts are being irradiated for short and long time periods in the University of Wisconsin Nuclear Reactor (UWNR), and resulting gamma radiation [from (n, γ) reactions] is either counted immediately or after a predetermined amount of time for the determination of specific elements.

High-Temperature Molten Salt Corrosion Diagnostic. In order to gain an understanding of corrosion mechanisms in real time and to develop a practical high-temperature diagnostic to monitor corrosion, researchers

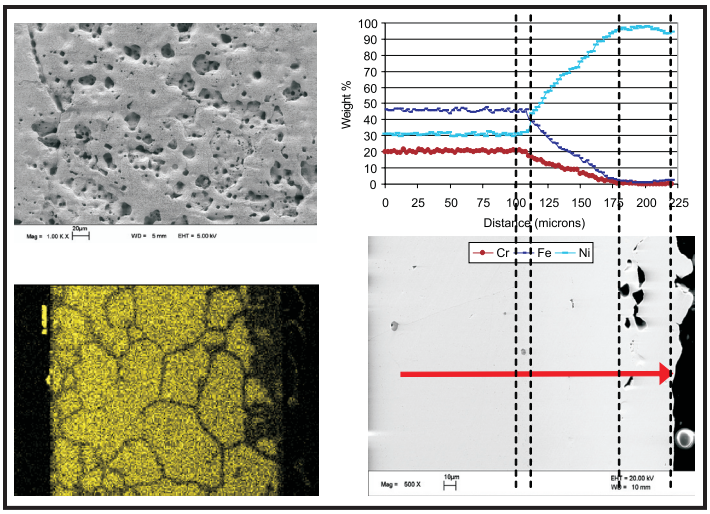

Figure 2. (a) Scanning electron microscopy (SEM) images showing corrosion attack in Incoloy 800H in molten FLiNaK at 850°C and (b) SEM image and energy dispersive spectroscopy (EDS) analysis showing the protective nature of Ni-electroplating on Incoloy 800H in this environment.

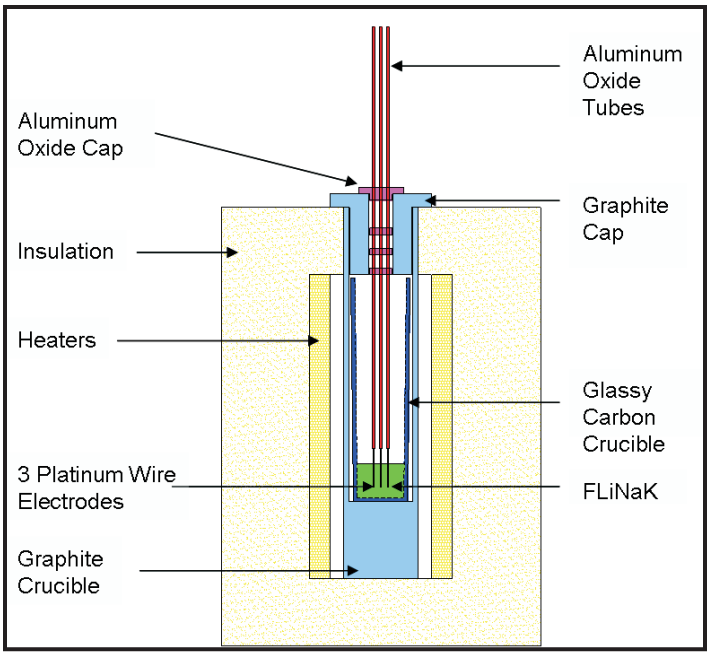

Figure 3. Schematic illustration of three-platinum-electrode high-temperature electrochemistry apparatus. The molten FLiNaK salt electrochemistry experiments are being performed in an argon atmosphere.

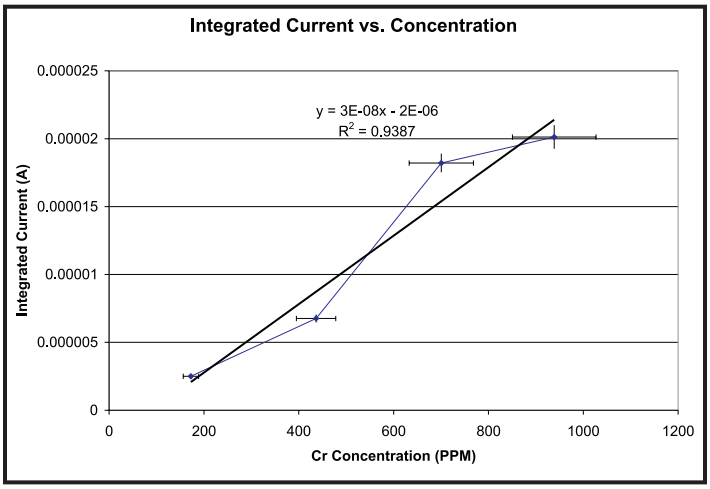

Figure 4. Chromium concentration in the molten FLiNaK salt as determined *in-situ* by high-temperature electrochemistry.

are applying a high-temperature electrochemical technique known as anodic stripping voltammetry (ASV). The technique will allow the research team to quantitatively trace amounts of impurities and dissolved elemental species in the molten FLiNaK salt at specific time intervals during the corrosion test. In ASV, the working electrode is held at a potential negative long enough to reduce the metal cation of interest, so as to deposit it on the electrode. After a sufficient amount of time (long enough to deposit a sufficient amount of metal to achieve a high signal-to-noise ratio), the potential is swept to a more positive value. The anodic potential sweep is termed the "stripping step" since the metal that was previously deposited is now oxidized and, in doing so, gives off an electron current that is read by an ammeter. There are various methods of sweeping the potential, and research focuses on the most simplistic stripping method: linear stripping.

For high-temperature molten salt electrochemistry using the ASV technique, an experimental apparatus, shown in Figure 3, has been developed and is presently in use. Platinum wire has been shown to be a suitable quasi-reference electrode in FLiNaK and has been used as the working and counter electrodes in the experiments and by other researchers working in the area of molten fluoride salts. Results have shown that intensity of the peaks for various elements increases linearly with increasing concentration of the chemical species, as shown in Figure 4.

Testing of High-Temperature Adhesive Strength of Epoxy. Graphite will be an important structural material in molten fluoride salt systems because of its relatively high chemical stability in molten fluoride salts as well as its outstanding high-temperature strength. An engineering issue in the use of graphite will be joining the graphite components by a technique that can provide adequate high-temperature adhesion strength and withstand chemical attack from molten salts. To address this issue, research is underway to evaluate the strength of a graphite epoxy, Resbond 931-1, in a high-temperature molten fluoride salt environment. This epoxy forms a 99.9 percent pure graphite bond and is being evaluated as a possible method for joining graphite components. Small capsule tests are being conducted to evaluate the shear strength

and chemical compatibility of this epoxy in FLiNaK environments up to 1,000°C. Table 1 lists the results of the tests on shear strength of the epoxy. The quoted tensile strength of the epoxy is 2,500 psi and the tests showed that the environment and temperature did not have a significant effect on the strength of the epoxy.

Capsule environment	σmax < 2,500 psi	σmax > 2,500 psi
25°C Argon	1	3
1,000°C Argon	1	4
1,000°C FLiNaK	1	2

Table 1. Summary of the results of shear strength showing the number of ResBond epoxy samples that failed in the three environments tested.

Design and Construction of the Molten Salt Flow Loop. The conceptual design for the molten salt loop at the University of Wisconsin-Madison has been completed. The design was chosen to minimize the amount of material needed for the construction of the loop. The design uses a 24-inch long test section for the heating and cooling sides of the loop. The loop will be constructed out of a high Ni superalloy, most likely Inconel 600 or 316 austenitic stainless steel. Work has been ongoing for obtaining a pump from commercial sources, or building a pump in-house for the liquid salt loop. A bypass section will be incorporated in the loop to obtain the low Re flow. The design will also allow for flow and pressure measurement of the fluid at operating temperatures. Flow measurements will be made using pressure transducers. Pressure transducers are usually limited to 100°C. The melting point of the salts is above 400°C; therefore, the pressure transducer would contain an intermediate fluid that would be stable to 500°C and still be liquid under 100°C. Two fluids are being considered for this application: NaK and gallium (Ga).

Planned Activities

Listed below are the projected activities for this project:

- Study the effects of additions of a reducing agent, zirconium, to FLiNaK on corrosion of Incoloy 800H
- Establish the high-temperature electrochemistry approach (AVS) as a method for understanding the fundamentals of corrosion in real-time and as a diagnostic to evaluate the extent of corrosion on-line
- Complete the design and construction of the molten salt flow loop

Nuclear Energy Research Initiative

Ni-Si Alloys for the S-I Reactor-Hydrogen Production Process Interface

PI: Joseph W. Newkirk, University of Missouri-Rolla

Collaborators: Idaho National Laboratory (INL)

Project Number: 06-024

Project Start Date: March 2006

Project End Date: March 2009

Research Objectives

The goal of this project is to develop materials suitable for use in the sulfuric acid decomposition loop of the sulfur-iodine thermo-chemical cycle for nuclear hydrogen production. Materials must have both acceptable corrosion resistance and sufficient ductility for component fabrication and avoidance of catastrophic failure. Nickel-silicon (Ni-Si) intermetallics show promise for such critical applications as the sulfuric acid vaporizer, vapor superheater, and the decomposer. Past work indicates that adding minor alloying elements to nickel silicide (Ni_3Si) provides significant ductility at room temperature (7-10 percent elongation at failure), a unique property for normally brittle high-silicon materials. Ni_3Si can also be easily joined by traditional methods such as welding, and preliminary studies show that it has excellent corrosion resistance.

In this work, the team will further develop Ni_3Si to maximize its ductility and corrosion resistance, while reducing cost. Researchers will analyze the effects of adding elements such as niobium (Nb), boron (B), and iron (Fe). Microalloying may be used to improve resistance to corrosive impurities in the sulfuric acid processing stream, such as iodine (I). Finally, the team will study the extent to which Fe can be substituted for Ni in Ni_3Si without adversely affecting ductility or corrosion resistance.

Researchers will document the mechanical properties of these new materials over a range of temperatures and strain rates. The results will improve material properties and microstructure. As a final test, corrosion-resistant materials will be subjected to flowing sulfuric acid (H_2SO_4) at temperatures and pressures comparable to the actual sulfuric acid processing loop (120-400°C at <10,000 psi) in order to measure corrosion rates. Various fabrication techniques will also be exercised by forming prototype plates, pipes, and forgings.

Research Progress

In order to produce components for use in the decomposition loop, processing to produce plate is needed. Rolling trials have been carried out on the baseline alloy and some small variations in baseline composition. The three compositions are shown in Table 1. The first is low in Si and high in Nb compared to the baseline. The second is slightly high in Si and low in Nb, while the final one is slightly low in Nb only. Initially, there was an issue with center cracking, but this was solved with higher rolling pressures and now all three alloys can be rolled multiple times without cracking. As shown in Table 1, large total reductions can be achieved at room temperature. The high hardness of the material limits the amount of reduction for each pass. Lower Nb content is actually beneficial to cold rolling as Nb concentrations higher than 3 percent result in a reduced ductility and increased hardness.

Alloy (at.%)	Total reduction	Passes	Rolled R_c	Annealed R_c
$NiSi_{18}Nb_{5.2}$	60%	13	51	40
$NiSi_{20.8}Nb_{2.2}$	53%	10	49	38
$NiSi_{19.7}Nb_{2.2}$	75%	13	48	36

Table 1. Baseline Compositions.

Examination of the microstructures of each alloy during the rolling process indicates that for this size of plate, about five passes are necessary to achieve a high degree of homogenization. Essentially, a wrought structure is obtained from this amount of rolling, which shows that cold rolling could be used to form plate into pipe for use in the process. However, this would be somewhat tedious and better methods would be useful in reducing costs. For this reason, hot rolling will be investigated in the future.

The baseline alloy and several modified alloys containing titanium (Ti) have been analyzed by XPS. The figure shows three spectra from the baseline alloy at different degrees of sputtering. While the major component of the oxide surface is silicon dioxide, Ni and Nb are also components of the oxide. The exact nature of these elements in the oxide is still being investigated but appears to be complicated. Alloys treated with sulfuric acid also have indications of sulfur in the oxide that forms.

Testing of Ti-containing alloys has shown the lack of protection at all levels of Ti additions. XPS of alloys containing 1 percent and 3 percent Ti show significant levels of Ti in the oxide formed on the 3 percent alloy, but not the 1 percent. Work is continuing to understand the deleterious effect of Ti on corrosion properties.

INL has tested this material in pressurized sulfuric acid, which more closely resembles the conditions that will exist in service. Nearly five hundred hours of testing are complete and the baseline alloy, in the homogenized condition (950°C for 4 days), already shows acceptable corrosion rates (<5 mpy), as shown in Table 2.

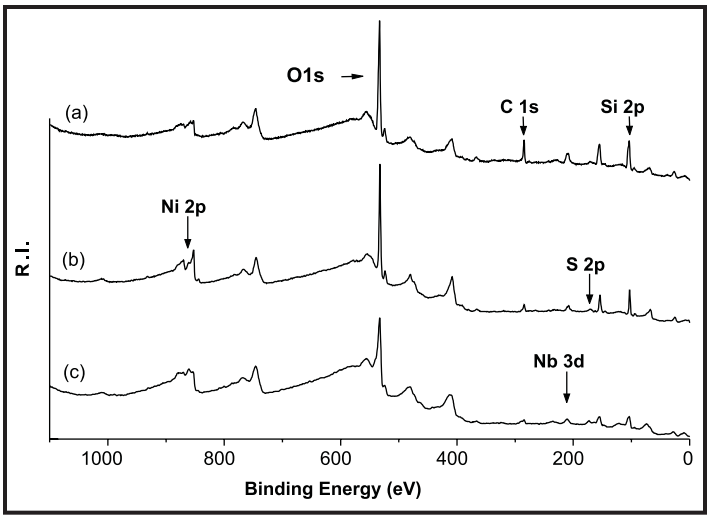

Figure 1. Three spectra from the baseline alloy at different degrees of sputtering.

Two ten-pound heats were ordered from Haynes International, a possible future industrial partner. The nominal compositions of the two heats are given in Table 3. The first alloy is a modification of the baseline composition which is lower in Nb. Observations have proven that the Nb concentration is too high and hence creates an additional phase which does not appear to be beneficial. This heat will allow more of the baseline to be studied as well as to establish a better Nb composition level. The second heat is the first in a series examining additions of Fe. The Fe would make for a dramatic reduction in the cost of the alloy if it does not deleteriously affect the properties. Previous work has shown that adding Fe beyond approximately 3 percent forms a brittle phase with a different crystal structure than the $L1_2$ Ni_3Si. It has been suggested from current alloying theories that copper (Cu) added in the appropriate ratio could prevent this from occurring and allow for the Fe to be retained in solution. This heat has replaced 22 atomic percent of the Ni with the Fe and Cu additions.

Alloy Condition	Sulfuric %	Temp (C)	Pressure (psi)	Corrosion (mpy)
NiSi20Nb3B0.5 As-cast	96	375	500	46.4
NiSi20Nb3B0.5 950°C, 4d	96	375	500	4.0

Table 2. Results of material corrosion rate testing in pressurized sulfuric acid.

Design	Ni	Fe	Cu	Si	Nb	B
2B0-M1	76.48	0	0	21.37	1.61	0.53
2B-10Fe	59.93	7.57	8.97	21.06	1.97	0.5

Table 3. Nominal compositions of ten-pound heats.

Planned Activities

Continued testing and alloy refinement are planned for the following year. This testing will be conducted under conditions that more closely resemble those expected in service. This will consist of elevated temperature studies and analysis of films formed during pressurized testing. In addition, commercialization of the alloy will be studied.

Evaluation of the mechanical properties of the various alloy compositions at elevated temperatures are being planned for testing in the Gleeble at INL. Sample geometries are being decided upon in consultation with INL. The expected temperature range for the decomposition loop is between 300 and 500°C. This range of temperature will be evaluated.

Haynes International is amenable to future collaboration on the development of this alloy. Their capabilities to perform hot rolling and pipe fabrication trials may be needed during the third and final year of the project.

A proposal has been submitted to Oak Ridge National Laboratory (ORNL) to use their analytical equipment to further analyze the films produced.

Nuclear Energy Research Initiative

Microstructure Sensitive Design and Processing in Solid Oxide Electrolyzer Cells

PI: Hamid Garmestani, Georgia Institute of Technology

Collaborators: Pacific Northwest National Laboratory

Project Number: 06-027

Project Start Date: March 2006

Project End Date: March 2009

Research Objectives

This project focuses on improving the properties of electrodes in solid oxide electrolyzer cells (SOEC) by optimizing the microstructure. Inverse materials design is applied in this project to achieve the 1) goals based on a multi-scale model for the treatment of transport properties of electrolyzer materials and 2) methodologies based on spray pyrolysis techniques to synthesize large surface area gradient porous fuel cell electrodes.

Spray pyrolysis is applied to fabricate SOEC cathode materials, lanthanum-strontium-manganite (LSM). After optimizing the process parameters and precursor materials for the newly developed spray pyrolysis technique under the guidance of inverse materials design, the microstructure and properties are examined. The team has developed a statistical mechanics-based model to calculate conductivity and transport properties of fuel cell materials. This model incorporates conductivity, elastic properties, and transport properties of porous microstructures. Within the next year, fluid flow through porous media and other properties will be incorporated into the model. The resulting multi-scale model will be applied to optimize the electrode microstructure. An electrostatic spray pyrolysis system will be set up to provide better control over the resulting microstructure.

Research Progress

During this fiscal year, the team continued theoretical prediction on SOEC electrodes properties and controlling the microstructure of the fabricated electrodes by adjusting spray pyrolysis experimental parameters.

Fabrication of Gradient Porous SOEC Electrodes by Precise Process Design. The goals proposed last year were achieved by selecting the suitable precursors and the experimental parameters to fabricate ideal cathode layers. First, researchers investigated the influence of different solvents on microstructure. Metal-organic precursors with organic solvents have been compared with aqueous solution. Aqueous system achieved coarse microstructure with large cracks. On the other hand, using organic systems gives the SOEC cathode a fine and homogenous deposition layer.

In addition, the influence of temperature and spray speed on the microstructure of LSM was investigated. Results verified that the substrate temperature is the most important parameter to control the morphology of the deposited film. Dense layers appeared when the temperature of the deposited substrate was below 560°C. Porous microstructure gradually appeared after the temperature increased to 560°C. Higher deposition temperatures help to decompose the precursors and result in the formation of highly porous film. Spray speed also has an important role in the microstructure fabricated, mainly on the deposition thickness and degree of agglomeration. Increasing spray speed leads to thinner layers, especially at lower temperatures. On the other hand, increasing the spray speed rate at higher temperatures will cause rapid deposition of a larger number of aerosol droplets, leading to produce a more agglomerated porous structure. Therefore, if the speed rate and temperature are in the optimal range with respect to each other, ideal microstructures with desired porosity and morphology can be obtained.

A gradient porous cathode material was then fabricated using a four-step deposition process. The cross-section scanning electron microscopy (SEM) micrograph of this cathode material, in Figure 1, shows a nanostructured porous film close to the YSZ substrate and gradually coarser layers on the surface. This strongly indicated that the spray pyrolysis is a promising technique to control

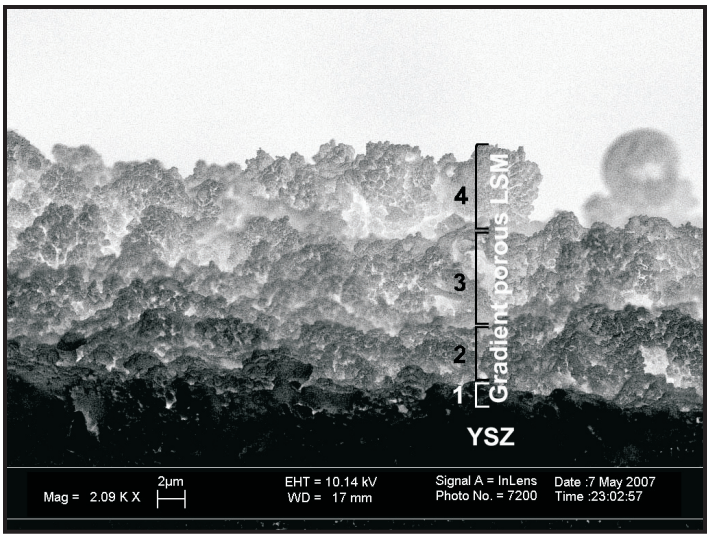

Figure 1. SEM cross-section image of the gradient porous LSM made by precise process design, multiple, carefully controlled spray pyrolysis depositions.

the microstructure, and particularly to process a porous cathode with improved microstructural features and more favorable electrocatalytic characteristics for better performance in SOEC.

Theoretical Modeling and Microstructure Design. The statistical mechanics models used for this investigation use two-point probability density function of vector $\vec{r}$. An improvement in the characterization of the microstructure has been introduced by decoupling $\vec{r}$ into the product of vector length r and direction $\hat{r}$.

From the decomposition above, the probability $P_{ij}(\vec{r})$ can be de-convoluted into two functions:

$$P(\vec{r}) = R(r)\Theta(\hat{r}) \tag{1}$$

Here the function *R(r)* describes the probability of occurrence of a vector with scalar *r*. The function $\Theta(\hat{r})$ describes the probability of the occurrence of a unit vector with direction $\hat{r}$. The dependence of *R(r)* upon the scalar *r* will be carried out by an orthogonal basis function $m_t(r)$, which may take the complex exponential form:

$$R(r) = \sum_t R_t m_t(r) \qquad m_t(r) = \exp\left(2\pi \frac{r}{a} ti\right) \tag{2}$$

To consider the Fourier representation, the dependence of function $\Theta(\hat{r})$ on direction $\hat{r}$ may be carried out by classical surface spherical harmonic functions, $k_u^v(\hat{r})$:

$$\Theta(\hat{r}) = \sum_{u,v} \Theta_u^v k_u^v(\hat{r}) \tag{3}$$

In this way, the probability function can now be expressed by the following product:

$$P(\vec{r}) = R(r)\Theta(\hat{r}) = \sum_t R_t m_t(r) \sum_{u,v} \Theta_u^v k_u^v(\hat{r})$$
$$= \sum_{t,u,v} R_t \Theta_u^v m_t(r) k_u^v(\hat{r}) = \sum_t \sum_u \sum_v {}^t C_u^v m_t(r) k_u^v(\hat{r}) \tag{4}$$

Figure 2 demonstrates how to use the decoupling method to characterize the microstructure. Figure 2a is a SEM micrograph of a cross section of a SOEC electrode. Black points in Figure 2b are experimental probability of P_{11} with vector length r in coarse layer of a SOEC electrode. The red line is the simulated probability function. With the term increased to 10, this Fourier expansion matches the fluctuation of experimental probability function.

To predict the transport property and life expectancy of SOEC electrodes, a statistical continuum mechanics approach is used to predict thermal expansion tensor, thermal conductivity, and transport properties in a heterogeneous media composed of *n* constituents with different thermal expansion tensor, a^i, *(i=1...n)* and partitions v^i. Local deformation ε at any point *x* is

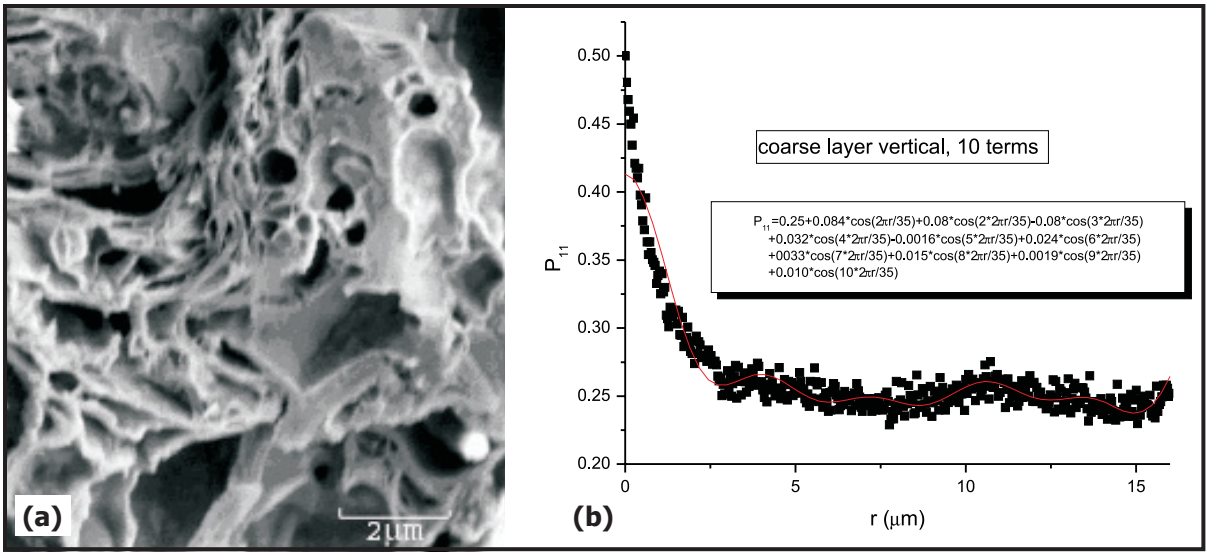

Figure 2. (a) Cross-section SEM micrograph of the coarse layer in a gradient porous SOEC electrode; (b) experimental and simulated probability function of P_{11} in SOEC electrodes.

composed of two parts: elasticity part strain ε_e and strain from the thermal expansion ε_t.

$$\varepsilon(x) = \varepsilon_t(x) + \varepsilon_e(x) = \alpha(x)\nabla T(x) + S(x)\tau(x) \quad (5)$$

Where *S(x)* is the compliance tensor and *τ(x)* is the stress distribution. To obtain the temperature gradient field *∇T*, researchers used Green's function solution *G(x-x')*:

$$\nabla T(x) = \nabla T_0 + \int dx' G(x - x') * \tilde{\alpha}(x')\nabla T(x') \quad (6)$$

In the study of thermal conductivity, the local heat current *q* and local temperature gradient $-\nabla T$ at any arbitrary point *x* satisfy the linear relationship such that:

$$q_i(x) = -k_{ij}(x)\nabla T(x) \quad (7)$$

Effective conductivity σ_{eff} in the heterogeneous media is defined by the following equation:

$$\langle q(x) \rangle = -k_{eff} \langle \nabla T(x) \rangle \quad (8)$$

The ensemble temperature gradient is an average of the temperature field $<\nabla T(x)>_h$ for state *h*, which can be calculated from the following:

$$\langle \nabla T(x) \rangle_h = \nabla T_0 + \int dx' G(x - x') * \langle \tilde{k}(\nabla T_0, h(x')) \rangle_h \nabla T_0 \quad (9)$$

Planned Activities

Previous results showed that spray pyrolysis is a promising method to fabricate SOEC cathode materials with large surface areas, while other traditional methodologies will have difficulty eliminating cracks. The advantage of spray pyrolysis is that the porosity, heterogeneity (and gradient), and morphology may be controlled by adjusting the spray parameters. A gradient porous microstructure, which is ideal in SOEC electrodes, has been achieved in an optimized and precisely controlled set-up.

To empower the researchers with more freedom and capacity to control the microstructure, electrostatic spray pyrolysis will be set up during the third year of this activity. Adjusting the electronic field by changing voltage should have a strong influence on the microstructure. In the next step, other spray parameters, including nozzle-to-substrate distance and oxygen concentration in carrying gas, will also be studied.

In the theoretical part of this work, the team will apply the Strong Contrast methodology to improve the prediction in porous materials, which is treated as a composite of phases with strongly different properties. The researchers will investigate the application of the decoupling method in microstructure characterization. After predicting the thermal, electrical, and mechanical properties of SOEC porous electrodes, the researchers will also apply the statistical mechanics to predict the transport and permeability properties.

Once this is achieved, the team plans to build a more sophisticated computer-controlled spray pyrolysis system. They have already developed a multi-scale model to link the porous microstructure of the cathode material to its transport properties and published the results in several papers.

Nuclear Energy Research Initiative

Dynamic Simulation and Optimization of Nuclear Hydrogen Production Systems

PI: Paul Barton and Mujid Kazimi, Massachusetts Institute of Technology (MIT)

Collaborators: None

Project Number: 06-041

Project Start Date: March 2006

Project End Date: February 2009

Research Objectives

This project is part of a research effort to design a hydrogen plant interfaced with a nuclear reactor—a promising alternative to fossil-fuel-generated hydrogen. The objective is to build models for dynamic simulation and optimization of hydrogen production options using nuclear energy. There is a natural interdependence between design and operational decisions for integrated nuclear hydrogen production systems. This interdependence requires a modeling and simulation environment that can capture the physical design descriptions and map these to steady state and dynamic predictions of the hypothesized system's behavior. Simulating these systems can provide invaluable information for the next step, whether this step is an experiment or design decision. The simulation environment must be adaptable, flexible, and expandable.

This project will develop a dynamic modeling, simulation, and optimization environment for nuclear hydrogen production systems. A hybrid discrete/continuous model will capture both the continuous dynamics of the nuclear plant, the hydrogen plant, and their interface, along with discrete events such as major upsets. This hybrid model will make use of accurate thermodynamic sub-models for the description of phase and reaction equilibrium in the thermochemical reactors. Use of the detailed thermodynamic models will allow researchers to examine the process in detail and have confidence in the accuracy of the property package they use. The hybrid model will also allow researchers to study plant operations and accident scenarios. Researchers will be able to use it to conduct parameter estimation studies to identify possible improvements in materials, mechanical design, and safety issues. The seamless connection between modeling, simulation, and optimization can help establish optimal control schemes. These schemes can then be tested in the model.

Research Progress

This research project includes an analysis of the system interface operation and an overall process safety study. Four tasks were performed this year:

1) A prototype dynamic model was created for the heat transfer loop and for representing the interaction of two heat loops
2) A novel simplification of the gas dynamics equations was developed, taking into account only the relevant time scales for the simulated phenomena
3) The electrolyte non-random two-liquid (NRTL) thermodynamic model was extended for application to multi-electrolyte, mixed-solvent solutions
4) Detailed models for the thermodynamic representation of the aqueous acidic solutions in the sulfur iodine (SI) cycle (sulfuric acid and hydrogen iodide) were developed

Following is a description of the work performed under each task.

Prototype dynamic model for the heat transfer loop. Researchers developed a model of an idealized heat transfer loop. This loop consists of a compressor and a pipe with sections at different exterior temperatures. The compressor closes the loop and provides the pressure differential to make the gas flow inside the pipe. Dimensions and temperatures of this interface are in accordance with the Idaho National Laboratory (INL) design. The model equations constitute a system of quasi-linear hyperbolic partial differential algebraic equations (PDAEs) in time and one spatial dimension on multiple coupled domains (each domain corresponding to an element of the overall heat transfer interface). Previous attempts to simulate similar systems involving a nuclear reactor have used numerical methods that introduce

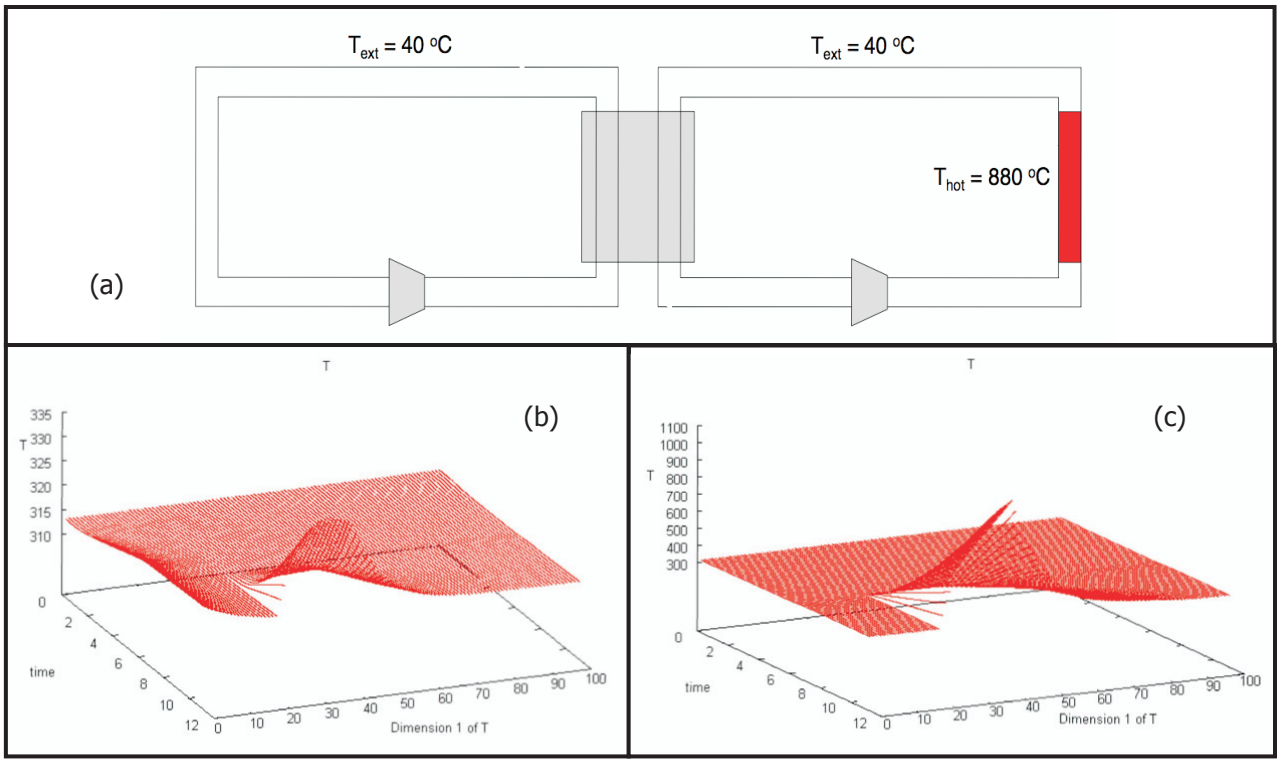

Figure 1. Simulation of the heat transfer interface (a) and corresponding transients for loop 1 (b) and loop 2 (c) using JACOBIAN®.

errors and produce unphysical numerical artifacts, such as oscillations. A particular challenge was to couple the model of the compressor with the explicit numerical method used to solve the gas dynamics equations.

Modeling the interaction of the two heat loops. The prototype dynamic model for the heat transfer loop was the starting point to represent the gas loop removing heat from the nuclear reactor and the second gas loop taking that heat and transferring it to the hydrogen plant. The two heat transfer loops were considered as being coupled through a heat exchanger. Each loop consisted of a compressor and a pipe with sections at different temperatures (Figure 1). The compressor closes the loop and provides the pressure differential to make the gas flow inside the pipe. The gas dynamics in the loops were represented by a novel approximation to the one-dimensional, compressible, inviscid, Navier-Stokes equations. Information is propagated through the gas at different time scales.

The time scales depend on the characteristics of the hyperbolic equations; two of these characteristics are related to the speed of sound and the speed of the gas, and one is related only to the speed of the gas. The characteristics related to the speed of sound are very fast and an accurate simulation of them requires the use of an explicit integrator with high-resolution methods. This kind of integrator has been implemented during the course of this project, with their main drawback being their high CPU requirement. The time steps taken by the explicit integration are very small and the simulations demand a high number of CPU cycles.

Researchers were able to simplify the equations by taking into account only the relevant time scales for the simulated phenomena. In this case, simulation of the fast time scales is often not necessary because discrete disruptions in the flow of the gas are rare. As changes in pressure propagate with the speed of sound, researchers can make a quasi-steady-state approximation (singular perturbation) for the equations related to the fast dynamics. To validate the predictions from the new simplified system of equations, the research team compared its results with simulation results for the compressible, inviscid, Navier-Stokes equations. The simulated experiment consisted of an open pipe where the inlet temperature, inlet pressure, and outlet pressure are set as inputs. The profiles in the simplified case were similar to the profiles of the full system; hence, researchers are now able to use the simplified equations to represent the gas dynamics. This simplification allows the use of implicit integrators; therefore, bigger models can be implemented and faster simulation speeds can be achieved.

A model of a heat transfer system was created using the simplified system of equations for gas dynamics. This system has two loops with a heat exchanger coupling them. Each system has a compressor and one of the loops has a hot section representing the nuclear reactor.

Figure 1 presents the simulation results for the temperature of the gas flowing inside each loop in the coupled system during a start-up scenario.

Refinement of the electrolyte-NRTL model for application to multi-electrolyte, mixed-solvent systems. The major difficulty in simulating the thermochemical SI process for hydrogen generation is modeling the chemical equilibrium in the major unit operations. In particular, special attention has to be paid to predicting the equilibrium of the electrolytes' partial dissociation and the stable phase split. Furthermore, the prediction of speciation in the process sections, which is not among the traditional virtues of electrolyte thermodynamic models, is important for the simulation of thermochemical cycles.

Researchers proceeded to a critical examination of the influence of simplifying assumptions of the electrolyte-NRTL thermodynamic model on the derivation of activity coefficient expressions, as applied to multi-electrolyte systems. A more rigorous and thermodynamically consistent formulation for the activity coefficients was developed, in which the simplifying assumption of holding ionic charge fraction quantities constant in the derivation of activity coefficient expressions is removed. The refined activity coefficient formulations, although much more complex than the original electrolyte-NRTL model, possess stronger theoretical properties and practical superiority that was demonstrated through a case study representing the thermodynamic properties and speciation of dilute to concentrated aqueous sulfuric acid solutions. Moreover, phenomena such as hydration, ion pairing, and partial dissociation were all taken into account and were shown to improve the capability of the model to predict the activity of the species and the speciation of the system (a virtue very important for the simulation of thermochemical cycles).

Modeling of the thermodynamics of the SI thermochemical cycle. The majority of the thermodynamic models developed were validated against a very large database of experimentally measured electrolyte systems. This was done because it was necessary to examine the new model in systems that are widely known and measured. After that, the new models were applied for the simulation of the thermodynamics of the SI cycle.

It was considered imperative to re-examine the accuracy of the available models since they have a significant effect on the prediction of the overall process efficiency. The description of the sulfuric acid system using the refined formulation of the electrolyte-NRTL model appears superior compared to the modeling efforts presented until now. More experimental data and a consistent database are needed for accurate representation of all the sections of the SI cycle.

Planned Activities

During the next year, researchers will finish building the different models for each unit operation and the overall system model. They will develop detailed models for the thermochemical reactors of the SI process and the high-temperature electrolysis unit. The research team will then integrate these models with the heat transfer interface model and perform several case studies, including accident scenarios for analysis, involving the integrated systems.

In addition, researchers will identify relevant process parameters and perform parameter estimation studies through dynamic optimization. They will examine the impact of the parameters on the estimated process efficiency, including factors such as safety and system dynamics. The developed thermodynamic property models will be 1) released to researchers studying thermochemical cycles, 2) validated, and 3) updated with new experimental data, if needed. The resulting dynamic problem will be large-scale and will incorporate the thermodynamic property models, as well as the dynamic models of the reactors and of the heat transfer loops in a large system of PDAEs.

The information gathered during these studies can be used for material selection and other design decisions. Moreover, it will help with the design of more profitable and efficient process flowsheets for the utilization of nuclear heat for hydrogen production. Performance, efficiency, and other determined factors for hydrogen process alternatives will be compared. The performance of process alternatives will be predicted utilizing dynamic models. The different hydrogen production process alternatives for contrasting objectives will also be compared.

Nuclear Energy Research Initiative

High-Performance Electrolyzers for Hybrid Thermochemical Cycles

PI: John W. Weidner, University of South Carolina (USC)

Collaborators: Sandia National Laboratory (SNL), Savannah River National Laboratory, Argonne National Laboratory

Project Number: 06-054

Program Start Date: March 2006

Program End Date: March 2009

Research Objectives

The objective of this project is to provide the scientific basis for developing high-performance electrolyzers for use in two candidate thermochemical cycles for producing hydrogen from nuclear power: 1) the hybrid sulfur process and 2) the modified calcium-bromine cycle. There is still a number of challenges in making these thermochemical cycles commercially viable, including 1) reducing the high cost of platinum and ruthenium catalysts, 2) minimizing sulfur dioxide (SO_2) crossover (a serious lifetime-limiting phenomenon), and 3) finding suitable operating conditions for optimal electrolyzer performance and cycle efficiency. This work will build on the successful application of the proton exchange membrane (PEM) electrolyzer for producing hydrogen through the conversion of water and SO_2 ($H_2O + SO_2 \rightarrow H_2SO_4 + H_2$) as well as the dissociation of hydrogen bromide ($HBr \rightarrow Br_2 + H_2$).

In this project, researchers will explore methods for improving the utilization of platinum and ruthenium in the cathodes and anodes, along with replacing them with other materials (metal alloys, silicides, mixed metal oxides, or a combination). New membranes are being developed with low gas crossover and high conductivity, mechanical stability, and temperature resistance that enable operation at higher temperatures and pressures. The researchers will evaluate the most promising catalysts and membranes in the PEM electrolyzer over a range of conditions (i.e., 30–120°C, 1–10 atm, and 50–80 percent conversions) and will apply mathematical models to optimize cell and process performance.

Research Progress

During the initial phase of this work, the viability of the gas-phase electrolysis was established for both the Hybrid Sulfur Process and the Modified Ca-Br-Cycle. It was also shown that catalyst loading did not play a significant role in electrolyzer performance.

Over the past year, the effects of membrane thickness and type, temperature, and reactant conversion (i.e., flow rate at a given current) on SO_2 electrolyzer performance were investigated. Also, a mathematical model was developed to predict water and SO_2 transport for the Hybrid Sulfur Process. Current-voltage curves, along with the measured and simulated sulfuric acid concentrations and production rates, are given below.

The team investigated the effects of membrane thickness. In this study, membranes of 2, 5, and 7 mil thickness (Nafion® 212, 115, and 117, respectively) have been used as the electrolyte in the hybrid sulfur electrolyzer. In addition, researchers at SNL have developed a sulfonated Diels-Alder polypropylene membrane to resist SO_2 crossover. The polarization curves for these membranes are given in Figure 1.

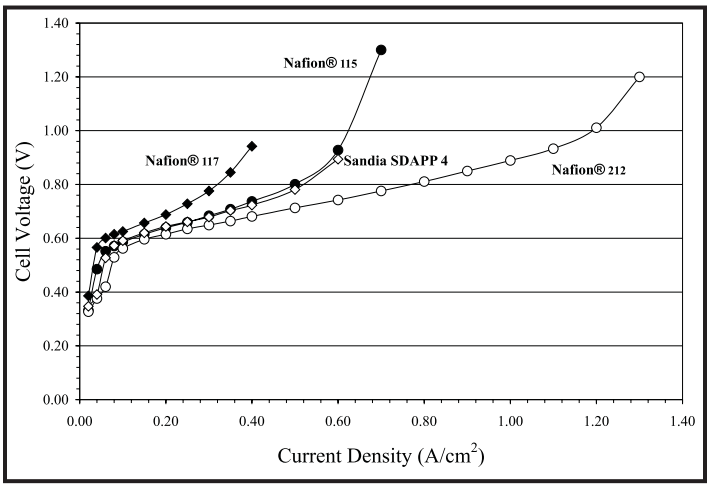

Figure 1. Polarization curves of the membranes tested in the hybrid sulfur electrolyzer. The thinner membranes exhibit better performance due to lower ohmic resistance. The electrolyzers were run at 80°C and 1 atm.

In addition, the effect of operating temperature was quantified for a N212 membrane. The membrane was operated from 50–90°C. As expected, the performance improved as the temperature increased due to lower ohmic resistance in the membrane. The results are presented in Figure 2.

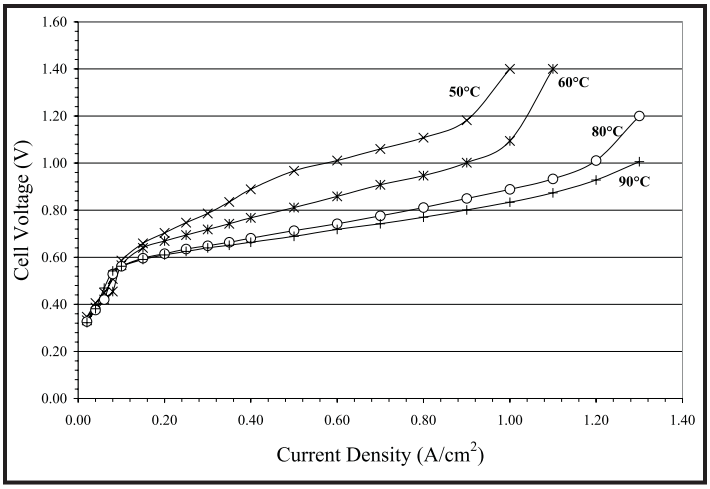

Figure 2. Effect of operating temperature; the electrolyzer was maintained at 1 atm.

The anode product stream was collected to determine the rate at which it exited the electrolyzer (sulfuric acid production rate) as well as the concentration (H_2SO_4 production rate and water transport through the membrane). The sulfuric acid molar flux for the three membranes tested is given in Figure 3. Also shown in Figure 3 are the model predictions (lines) for the sulfuric acid concentration as a function of current and membrane thickness.

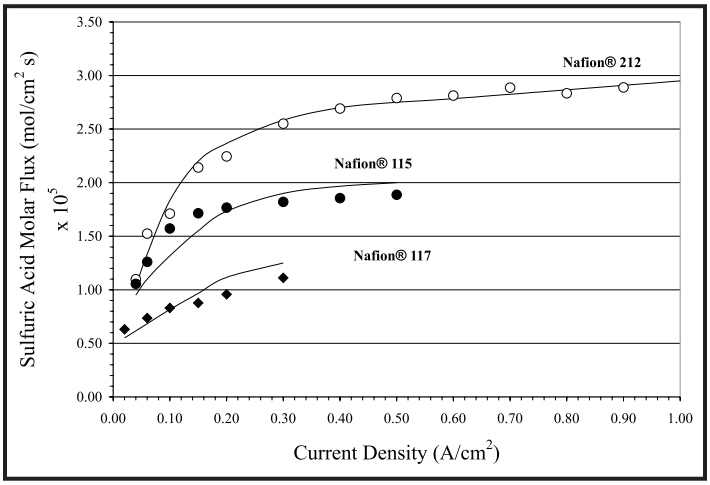

Figure 3. Model predictions (lines) and experimental data (points) for the sulfuric acid flux; the electrolyzers were run at 80°C and 1 atm.

The model was also used to determine the contributions of water and H_2SO_4 to the total flux. The results for Nafion® 212, i.e., the simulations (lines) compared to the data (points), are given in Figure 4. Similar agreement between the model and experiments is seen for Nafion 115 and 117.

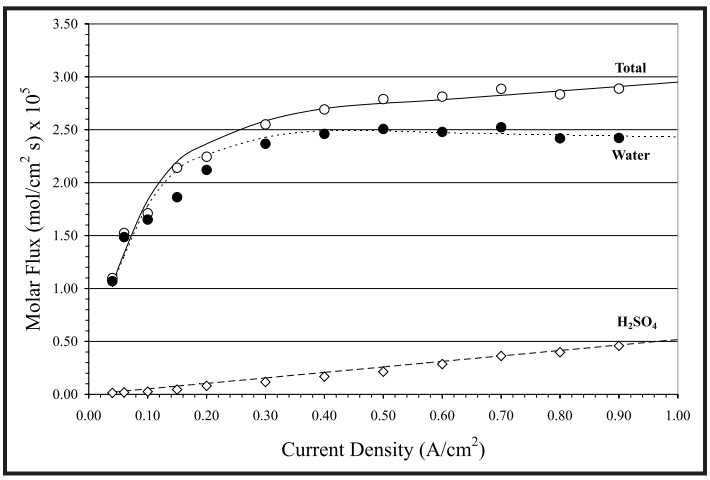

Figure 4. Model predictions (lines) and experimental data (points) for the contributions of water and H_2SO_4 to the total flux; the electrolyzer was run at 80°C and 1 atm.

As shown in Figure 4, as the current density increases, the mole fraction of water at the anode decreases due to consumption of the water in the oxidation step. This leads to increased diffusion of the water from the cathode to the anode, as illustrated in Figure 3. As the current density increases, however, the electro-osmotic drag becomes important, and water is dragged with the protons from the anode to the cathode. This results in a decrease in the net water flux at higher current densities.

Finally, the sulfuric acid concentration has been measured as a function of the current density. The results are given in Figure 5. Again, the model predictions closely represent the data, especially at high current densities where the electrolyzer will be run.

Finally, an attempt has been made to quantify the extent to which SO_2 crosses the membrane and reduces to sulfur at the cathode. This is a parasitic reaction that consumes current that would otherwise be used for the hydrogen evolution reaction.

Because of the solubility of SO_2 in water, the fact that water is diffusing from the cathode to the anode, and because the flux of water increases with current density, it has been proposed that at sufficiently high current densities, SO_2 does not reach the cathode. It is instead solvated in the water diffusing to the anode.

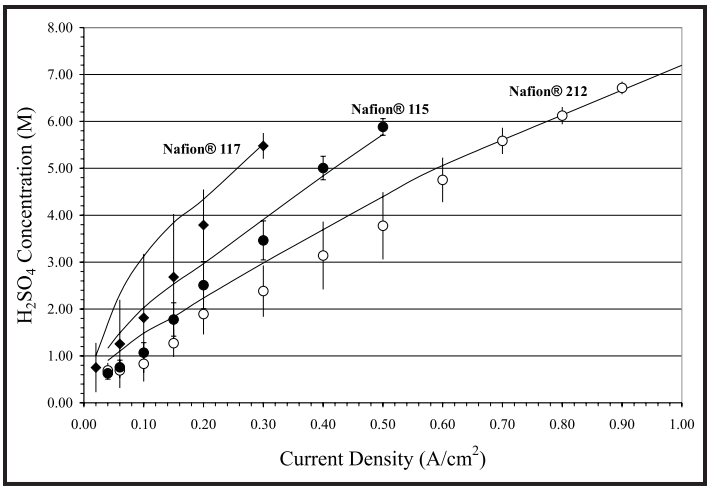

Figure 5. Model predictions (lines) and experimental data (points) for the H_2SO_4 concentration leaving the electrolyzer; the electrolyzers were run at 80°C and 1 atm.

Two experiments have been conducted, one in which the electrolyzer was held at 0.02 A/cm^2, and one in which the electrolyzer was held at 0.25 A/cm^2 for 10 hours. Scanning electron microscopy (SEM) images were taken of the membrane cross sections (shown in Figure 6).

Elemental analysis showed that in the cathode of the high current membrane electrode assembly (MEA), the sulfur atomic percent was approximately 0.10 at%, while the Pt percent was approximately 10.0 at%. In comparison, the cathode of the low current MEA had a composition of approximately 1.7 at% sulfur and 2.3 at% Pt. This would suggest that at the lower current densities, SO_2 diffuses through the membrane and reduces as sulfur inside the porous catalyst.

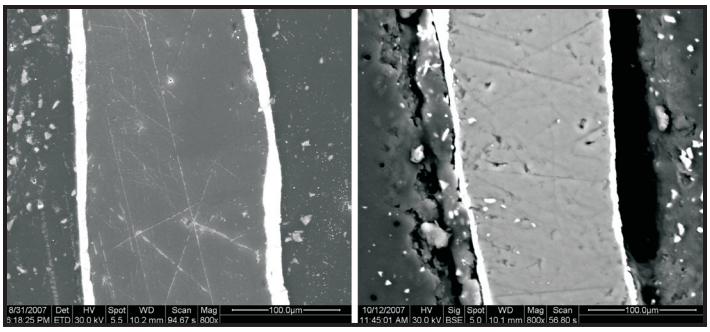

Figure 6. The high current (left) and low current (right) membranes. In each image, the cathode is at the left (white vertical line) and the anode is at the right.

Planned Activities

These results show that the electrolyzer's performance is strongly dependent on current, membrane thickness, and temperature. This provides design and operating parameters that can be adjusted to achieve the desired performance.

Researchers on this project have developed a mathematical model that predicts electrolyzer performance. This model will be incorporated into process flow sheets to determine the overall efficiency of the Hybrid Sulfur Process as a function of operating conditions. They have also shown that the detrimental effect of SO_2 crossover is not as serious as originally feared. However, more work is needed to determine its effect on long-term electrolyzer operation.

The four key activities for next year include the following:

1) To operate the electrolyzer above 1 atm
2) To quantify SO_2 crossover during long-term electrolyzer operation
3) To develop and test non-precious metal catalysts to minimize or replace Pt in the electrolyzer
4) To test membranes developed by SNL that can operate at temperatures above 100°C

Nuclear Energy Research Initiative

Development of Efficient Flowsheet and Transient Modeling for Nuclear Heat Coupled Sulfur Iodine Cycle for Hydrogen Production

PI: Shripad T. Revankar, Purdue University

Collaborators: None

Project Number: 06-060

Project Start Date: April 2006

Project End Date: March 2009

Research Objectives

The main goal of this project is to develop a flowsheet for the closed-loop sulfur iodine (SI) cycle for nuclear hydrogen production. This flowsheet will use current advances in acid decomposition and product gas separation to achieve high thermal efficiency. It will result in the development of transient analysis methods for the SI cycle. Although the closed-loop SI cycle has recently been demonstrated on a bench-scale, several challenges remain, such as maintaining stable operation, enhancing efficiency, obtaining thermodynamic data for the reactions, coupling to a high-temperature nuclear reactor, and determining transient behavior of the coupled system. This project will develop models to study transient performance of the closed-loop SI cycle. In addition, this research will explore several alternatives to SI cycles that have been proposed.

Specific objectives of the project include the following:

- Perform benchmark flowsheet analysis of the baseline SI cycle
- Investigate membrane techniques for hydrogen-iodide (HI) and sulfuric acid (H_2SO_4) decomposition and separation processes
- Perform comparative flowsheet analyses of the modified cycles
- Develop component-wise SI cycle models for application to the transient analysis
- Perform preliminary analysis of transient behavior of the closed-loop SI cycle

Research Progress

The SI cycle consists of three chemical reactions expressed as the following equations:

Section I - Bunsen reaction:

$$I_2 + SO_2 + 2H_2O \rightarrow 2HI + H_2SO_4$$

Section II - Sulfuric acid decomposition:

$$H_2SO_4 \rightarrow H_2O + SO_2 + 1/2O_2$$

Section III - HI decomposition:

$$2HI \rightarrow H_2 + I_2$$

For the current work, the flowsheet that General Atomics (GA) previously developed for the SI cycle was considered as a baseline. During the first year, efforts focused on developing and benchmarking a simulation model for the GA SI cycle flowsheet. This analysis was carried out to establish the simulation capability and to check the GA flowsheet model's repeatability. The Section II convergence was achieved.

During the second year, the SI thermochemical cycle was simulated using the chemical process simulation code ASPEN PLUS version 12. The team studied the GA flowsheet and developed ASPEN models for Sections I and III. A step-by-step simulation was performed starting from the single component simulation to the whole Section simulation. For the single component simulation, converged solutions were obtained comparable to GA's results. For the whole Section simulation, results of the converged solution for Section III were also comparable to GA's. Figure 1 shows that the present ASPEN results compare very well with GA's reported results for the HI stream for Section III.

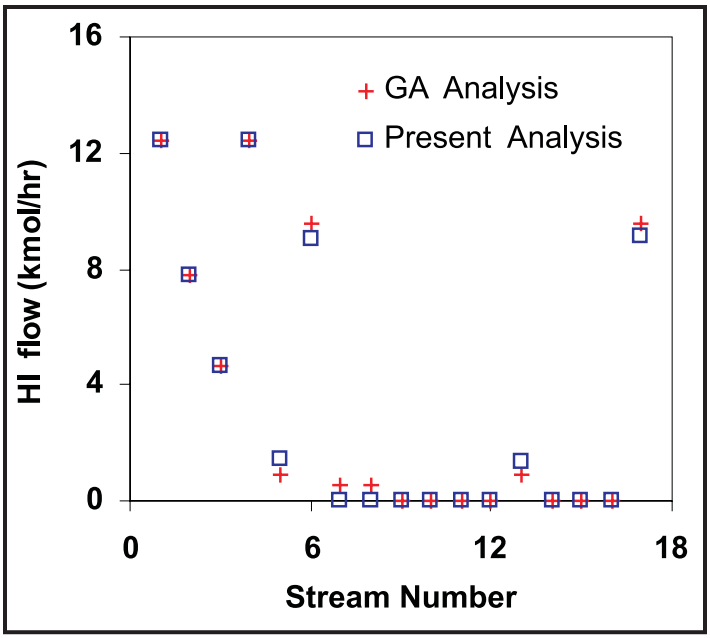

Figure 1. Comparison between GA and current ASPEN analysis.

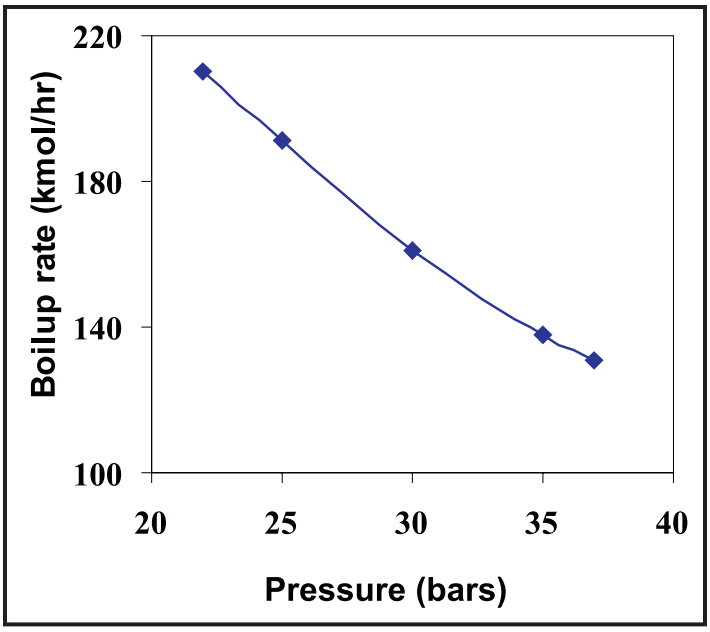

Figure 2. The effect of the pressure on the boil-up rate in the reactive distillation column.

The pressure dependence to the boil-up rate was also studied and the results are presented in Figure 2. When the pressure is increased, the boil-up rate must be decreased to maintain the same hydrogen production rate of 1 kmol/hr.

Researchers have obtained converged solutions for GA's flowsheet Section I for almost the entire flowsheet. The convergence is achieved for the reactor R101, the 3-phase separator, the boost reactor C103, the absorber C105, the stripper C102, and the scrubber C101—the results compare very well with GA's results. The whole flowsheet simulation is being completed.

Table 1 presents the analysis results and Figure 3 provides the comparison with GA's results for H_2SO_4 flow.

#	Stream	H_2O	I_2	HI	SO_2	H_2SO_4	O_2	Total (kmol/hr)	Temp (K)	Press (bar)	Phase
1	115	72.7279	48.7791	10.9846	2.266	0.2173	0.5	135.47	393	7	L
2	116	71.2535	48.0419	12.4590	1.5288	0.9545	0.5	134.74	393	7	L
3	117A	0.0338	0.0075	0	0.1424	0	0.5	0.68	393	7	V
5	118A	5.152	0	0	0.0154	0.9544	0	6.12	393	7	L
6	119A	66.0677	48.0344	12.4590	1.3710	0.0001	0	127.93	393	7	L
7	131	4.1377	0.0187	0	0.0478	1.0150	0.0155	5.23	384.5	1.85	L
8	138	66.07	47.92	12.459011	0.0000	0.000106	0	126.45	390.5	1.85	L

Table 1. Present analysis results for the Section I.

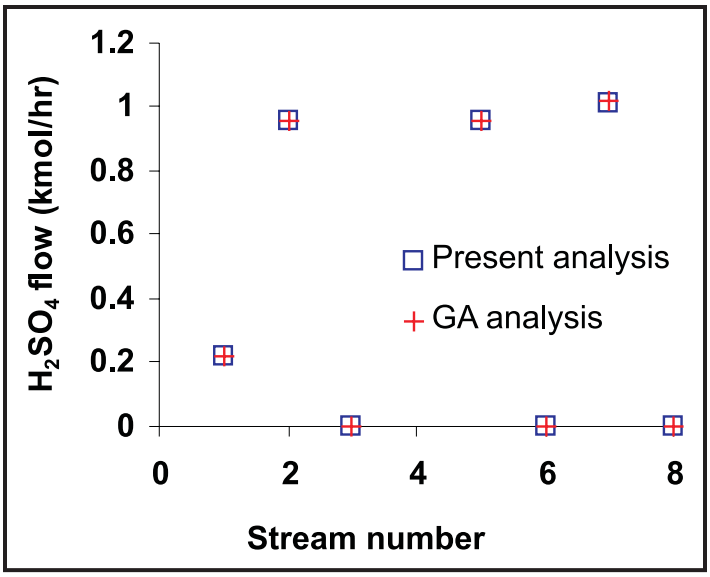

Figure 3. Comparison between GA and current ASPEN analysis.

Planned Activities

The remaining tasks for the third year are to 1) develop a modified SI Model based on the GA flowsheet and comparative study with the modified and baseline SI Cycle and 2) develop a membrane technique flowsheet for Section III and a simulation model for the membrane. The planned activities include modifying the three-phase separator in Section I and the reactive distillation column in Section III so that converged solutions can be obtained from the ASPEN simulation. A comparative study will then be made with the baseline SI cycle flowsheet. Researchers will conduct a literature search on the membrane separation techniques for implementing into Section III for HI decomposition. The flowsheet for Section III will be modified using membrane techniques and the simulation will be carried out.

Nuclear Energy Research Initiative

Gradient Meshed and Toughened SOEC Composite Seal with Self-Healing Capabilities

PI: Kathy Lu, Virginia Polytechnic Institute and State University

Collaborators: Idaho National Laboratory

Project Number: 06-140

Project Start Date: June 2006

Project End Date: May 2009

Research Objectives

Hydrogen generation through high-temperature electrolysis, using nuclear heat from advanced gas-cooled or liquid-metal-cooled reactors, will play a significant role in the Nuclear Hydrogen Initiative (NHI). High-temperature steam electrolysis enhances the efficiency of hydrogen production by adding substantial external heat, which reduces electricity consumption. Very high-temperature advanced reactors can provide the necessary heat to enable high-efficiency hydrogen production without the use of carbon fuels. However, the seals currently used in solid-oxide electrolyzer cells (SOECs) hinder this promising technology due to a mismatch in thermal expansion coefficients that causes seal cracking and gas leakage. The objective of this project is to match the SOEC seal thermal expansion coefficient with other cell components by using a glass-filled, titanium-nickel-hafnium (TiNiHf) high-temperature shape memory alloy (SMA) mesh to create a transition gradient. This novel seal design will enable long-term SOEC operation by providing mechanisms for glass matrix toughening and crack self-healing.

Researchers will conduct experiments to prove the proposed thermal stress release mechanisms and predict long-term cell performance. They will assess overall stability, performance, and interaction of the seal with other cell components.

Research Progress

Researchers have synthesized TiNiHf and have successfully achieved the proposed shape memory effect. Differential scanning calorimetry and microscopy have shown that the alloy has shape memory phase changes between 180 and 250°C. After the alloy solidifies, a homogenization heat treatment is necessary in order to visualize the shape memory effect. New composition TiNiHf alloy powder with a slightly higher Ni concentration has been successfully synthesized by gas atomization.

Extensive work has been carried out for the three-dimensional printing (3DP) parameter optimization. Two major 3DP variables, printing layer thickness and binder saturation level, were evaluated in order to print the 3D mesh structure of TiNiHf powder with high green strength and dimensional accuracy. SMA powder was printed into 3D mesh structures of 200 μm wire width (Figure 1). Thirty-five μm printing layer thickness and 170 percent binder saturation level offer the best mesh structure integrity and the smallest dimensional deviation, thus are the most preferred printing condition for the designed 3D mesh structure. At the same printing layer thickness, breaking force increases with the binder saturation level, up to 170 percent. At the same binder saturation level, 35 μm printing layer thickness yields 3D mesh structures with the highest integrity and lowest dimensional deviation.

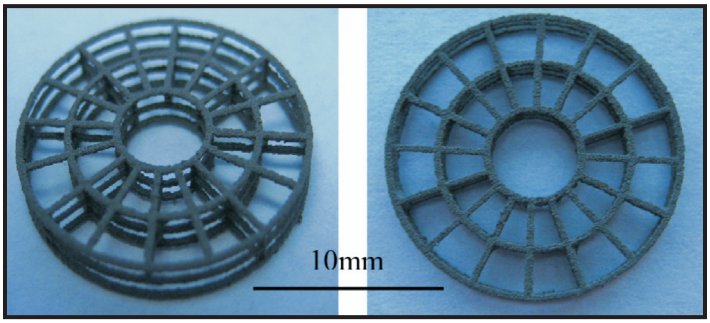

Figure 1. 3D mesh structures printed with 35 μm printing layer thickness and 170 percent binder saturation level.

3D wire mesh sintering was conducted using a two-step sintering method: pre-sintering the wire mesh under vacuum atmosphere and then sintering at higher temperatures in Ar. The wire mesh densification can be drastically improved. In addition, the wire mesh dimension showed substantial shrinkage. It has been observed that the sintering temperature might be higher than needed. At some wire mesh locations, partial wire melting was observed. There was some distortion but the mesh structure has been well maintained. Also, the mesh

structure is fairly strong and can be handled easily. This demonstrates that the intricate mesh structure can be preserved during sintering.

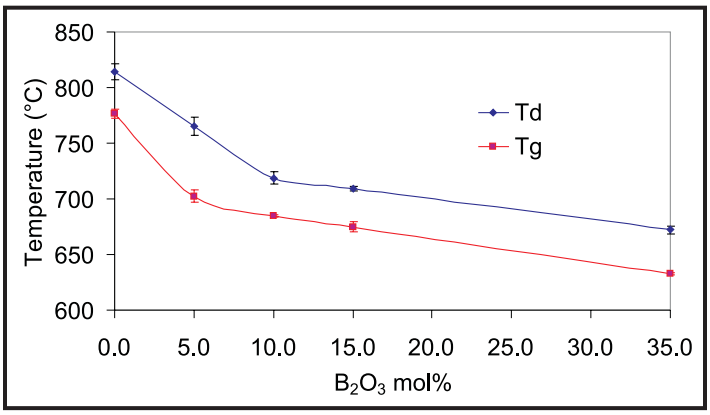

Figure 2. Plot of glass transition temperature (T_g) and dilatometric softening point (T_d) with boron oxide (mol%) content in the SLABS glasses.

Neutron diffraction provides 0.001 Å measurement resolution for the TiNiHf alloy lattice parameter change. The thermal stress generated from the glass matrix shifts the SMA austenite to martensite phase transformation temperature to a higher temperature during cooling. The thermal expansion coefficient at the lattice level from the neutron diffraction matches well with the coefficient of thermal expansion (CTE) measurement from the dilatometry.

Glasses are synthesized by quenching (25-X)SrO-20La_2O_3-(7+X)Al_2O_3-40B_2O_3-8SiO_2 oxides, where X varies from 0–10 mol% at 2.5 mol% interval. Devitrification behavior and thermal properties have been characterized by dilatometry and differential scanning calorimetry. The team performed microstructural studies using scanning electron microscopy, energy dispersive spectroscopy, and X-ray diffraction. Significant improvement in devitrification resistance was observed as X increased from 0 to 10 mol% without deteriorating the thermal properties required for this sealant material. All of the (25-X)SrO-20La_2O_3-(7+X)Al_2O_3-40B_2O_3-8SiO_2 compositions show >620°C T_g and >826°C T_c, and 9.0-14.5x10^{-6}/°C CTE after the first thermal cycle. La_2O_3 and B_2O_3 contribute to devitrification by forming $LaBO_3$. Al_2O_3 stabilizes the glass by suppressing the devitrification. The role of other oxides on the stability of this system is not significant.

New glass designs following the above series show progressive stability at high-temperature thermal holding. Devitrification behavior and thermal properties of these novel glasses are also characterized by dilatometry. Microstructural studies are performed by X-ray diffraction. The properties studied include glass transition temperature,

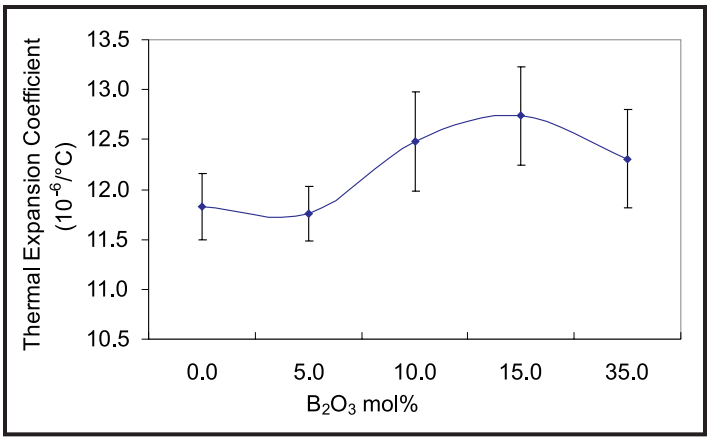

Figure 3. CTE variation with B_2O_3 content.

T_g; softening temperature, T_d; thermal expansion coefficient, CTE; and thermal stability. These new glasses desirably have T_g from 635–775°C, T_d from 670–815°C (Figure 2), and CTE from 11.5 -13.0 x 10^{-6}/°C (Figure 3). The glasses of less than 5 mol% B_2O_3 content are thermally stable after being kept at 850°C for 100 hours. To the research team's best knowledge, this is the only BaO-free glass system so far that exhibits such a desirable combination of CTE and high-temperature stability.

Adding Ni to the newly studied SLABS glass can effectively lower the glass transition temperature T_g and softening temperature T_d without substantially affecting the glass thermal expansion coefficient CTE and thermal stability.

Planned Activities

Researchers plan to perform the following tasks over the next fiscal year:

- Continue to study TiNiHf high-temperature SMA and SrO-La_2O_3-Al_2O_3-B_2O_3-SiO_2 (SLABS) glass seal systems and tailor their compositions to produce complementary thermal behaviors during SOEC operation
- Fill SLABS glass into the meshed TiNiHf structure, transitioning into pure glass on the electrolyte side, to make seals with transformation toughening and crack self-healing capabilities
- Conduct comprehensive seal testing to demonstrate smooth thermal expansion coefficient transition, cracking resistance, and crack self-healing capabilities of the new composite seal
- Make seals using actual SOEC seal configurations and model the process to optimize cost and performances

NUCLEAR ENERGY RESEARCH INITIATIVE

Liquid Salts as Media for Process Heat Transfer from VHTRs: Forced Convective Channel Flow Thermal Hydraulics, Materials, and Coatings

PI: Kumar Sridharan, University of Wisconsin-Madison

Collaborators: None

Project Number: 07-030

Project Start Date: June 2007

Project End Date: May 2010

Research Objectives

This project investigates the use of liquid salts as heat transfer fluids to utilize process heat from very high-temperature reactors (VHTRs) and other Generation IV reactors for hydrogen production. Favorable thermal properties of liquid salts (such as their lower melting point, high boiling point, high heat capacity, chemical stability, and low pumping power requirements) allow for efficient transport of high-temperature thermal energy. Successful implementation of a liquid salt reactor/hydrogen production process interface will require an accurate assessment of the thermal hydraulics in small-diameter channel, high-efficiency, compact heat exchangers. In these small channels, under high flow velocity and high-temperature conditions, both thermal hydraulics and materials will be key operational issues. In particular, information on corrosion/erosion resistance of materials and coatings for the construction of intermediate heat exchanger systems will be needed, along with operational experience to determine the minimum channel sizes to avoid clogging and to optimize heat transfer.

The specific objectives of the project are to 1) investigate materials and coatings corrosion performance in liquid salts by performing static corrosion tests in liquid FLiNaK and liquid 32%$MgCl_2$-68%KCl salts at 850°C for 500 hours, 2) fabricate a forced convection loop to study thermal hydraulics in small channels (including clogging effects) and particle transport and deposition issues, and 3) evaluate materials and coatings under prototypic velocity liquid salt flow conditions. Materials to be investigated include 1) Inconel alloys 800H, 600, and 617; and 2) carbon-carbon and silicon-carbide (SiC) composites. Coatings to be studied include optimized electroplated Ni as well as hard carbon and pyrolytic carbon coatings.

Research Progress

Fluoride and Chloride Salt Preparation. In order to cost-effectively prepare fluoride and chloride salts in quantities large enough for static and flow loop studies, a new glove box has been installed and is now operational. The new salt preparation glove box, shown in Figure 1, is designed to be used as a hypobaric chamber and to operate at slightly positive pressures. Oxygen and water are removed from the system by vacuuming the system to a lower pressure, then purging with argon for several hours to remove oxygen. The individual constituents of the salts are weighed and introduced into the crucible inside the glove box. Poco-Graphite and alumina crucibles are being used to prepare FLiNaK fluoride salt and $MgCl_2$-KCl salt, respectively. The crucibles are then encapsulated in a 304 stainless steel container.

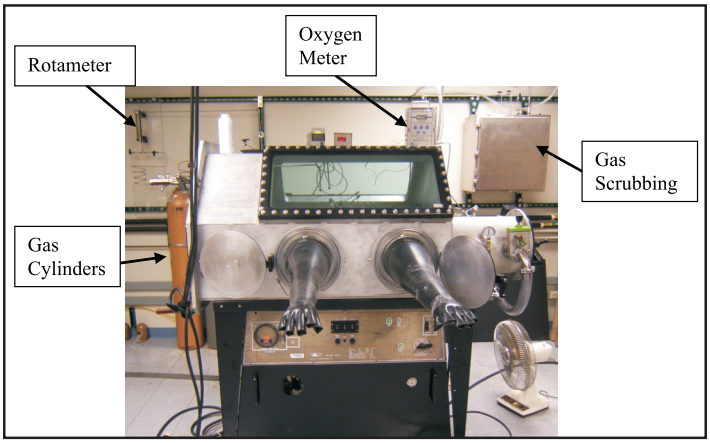

Figure 1. The new glove box (with gas addition facilities and treatment systems) for in-house preparation of fluoride and chloride salts.

All tubing into and out of the glovebox is constructed out of 304 stainless steel, except for the tube that is in contact with the salt, which is constructed with Inconel

600. The purifying gas is introduced into the glovebox from an ultra high purity tank of argon gas. This argon gas contains less than 0.2 ppm O_2 and less than 0.05 ppm H_2O. The volumetric flow rate of the gas is controlled by a Cole-Parmer SS Rotameter. The built-in range for this particular rotameter is 0 to 212 cm^3/min. The gas flows through 0.25" stainless steel tubing until it reaches the gas inlet for the 304 stainless steel containment vessel. The gas inlet goes to approximately 3/8" above the bottom of the graphite crucible where the gas is bubbled through the salt. The exiting gas stream is directed to the gas scrubber where it is bubbled through a 1N NaOH solution to remove any contaminants from the gas stream before it is vented to the outside. Researchers used a K-type thermocouple, calibrated using platinum resistance temperature detectors (RTD), to accurately determine the liquidus temperature of the prepared salt, as an indicator of salt purity. A LabView script is used to control the temperature as well as heating and cooling rates.

After initial studies, experimental batches of salts (approximately 0.75kg), FLiNaK and 32%$MgCl_2$-68%KCl, have been successfully prepared. Both of these salts represent eutectic compositions. Figures 2 and 3 show the heating and cooling curves for the FLiNaK and 32%$MgCl_2$-68%KCl salts, respectively, which indicate a plateau at temperatures near the expected melting points of these salts. This plateau suggests that salts with acceptable levels of purity were produced.

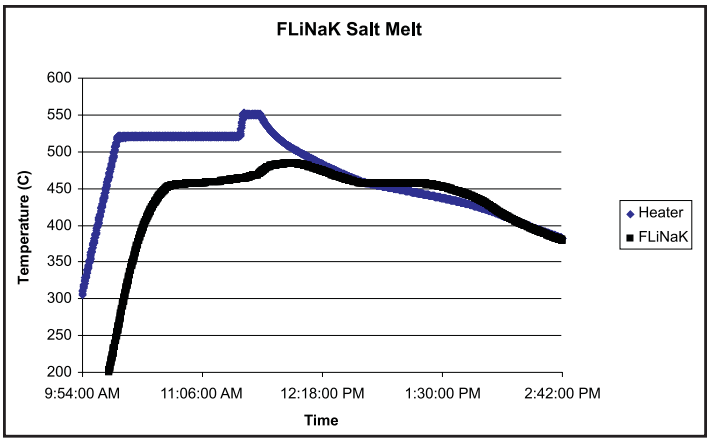

Figure 2. Heating and cooling curves from FLiNaK fluoride salt showing a plateau in temperature very close to the theoretical melting point of FLiNaK (454°C). This close match is indicative of the salt purity.

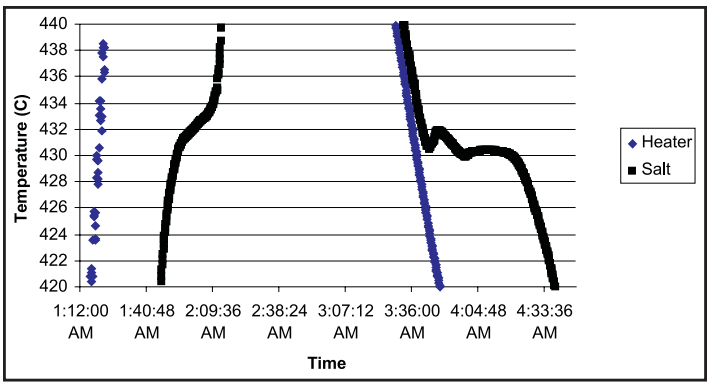

Figure 3. Heating and cooling curves for 32%$MgCl_2$-68%KCl chloride show the plateau in temperature at the melting point. The small perturbations indicate a two-phase region that is confirmed by the $MgCl_2$-KCl phase diagram.

SiC-Composite and Pyrolitic Carbon-Coated SiC-Composite for Corrosion Tests in Molten Salts. SiC composite and pyrolitic carbon-coated SiC composite are being considered for process heat exchanger material for the intermediate salt loop. SiC composite and pyrolitic carbon-coated SiC composite samples were obtained from the University of California-Berkeley and the initial pre-corrosion characterization of these samples has been completed. The SiC composites were produced by the German aerospace company DLR, and the pyrolytic carbon coating was deposited by chemical vapor deposition (CVD) process by Hyper-Therm High Temperature Composites, Inc. Figure 4 shows scanning electron microscopy (SEM) plan-view images of the surfaces of both the uncoated and coated samples. The untreated SiC shows fibers or strands of SiC, whereas the coated sample shows the coating to be uniform with occasional features with a globular morphology. There were no cracks or discontinuities in the coating. Figure 5 shows a cross-sectional view of the pyrolytic carbon-coated SiC composite sample. The coating is about 80 µm thick and defect-free. There is no visible evidence of delamination at the interface.

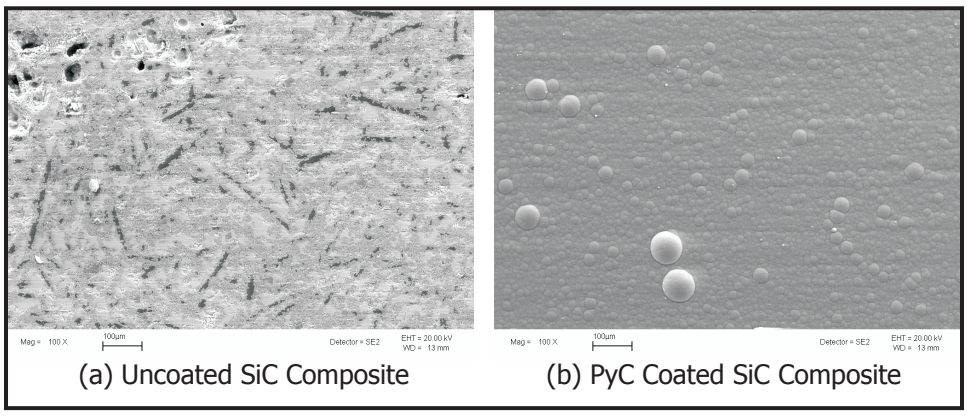

Figure 4. SEM plan view images of the surface of (a) uncoated and (b) pyrolytic carbon-coated SiC composite samples.

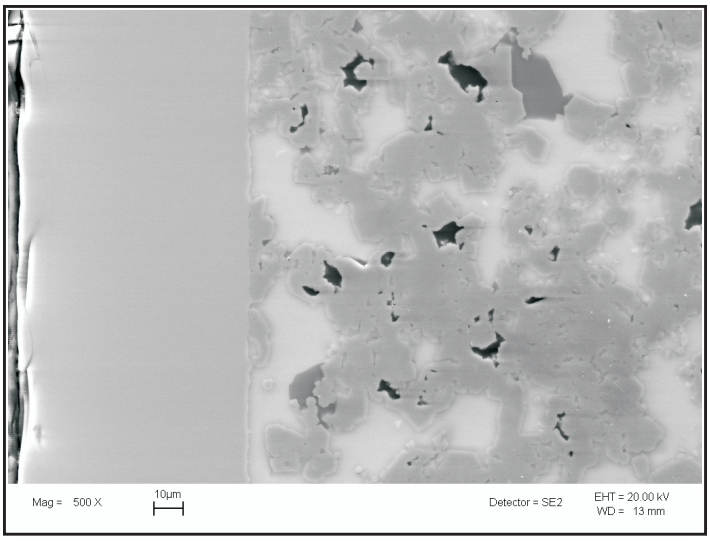

Figure 5. SEM cross-sectional view of pyrolytic carbon SiC composite. The PyC coating (left) is about 80 µm thick.

Planned Activities

Plans for the upcoming year include performing static corrosion tests of Incoloy 800H, SiC composite, and pyrolytic carbon-coated SiC in FLiNaK salt (prepared at a University of Wisconsin laboratory) at 850°C for 500 hours. The corrosion performance of Incoloy 800H, when bench-marked against earlier results on its performance in commercially procured high-purity FLiNaK, will shed light on the effect of salt purity on corrosion. Four purification approaches will be investigated for the molten chloride salts: 1) purging with dry inert gas, 2) purging with HCl and H_2, 3) CCl_4 method, and 4) magnesium contact method. Static corrosion tests will be performed with Inconel 800H in salts produced by each of these purification approaches in order to understand and evaluate the role of salt purity on corrosion in chloride salts. Researchers are currently performing activities toward using the University of Wisconsin's nuclear reactor for neutron activation analysis (NAA) of the salts to accurately monitor impurities and metal dissolution. Initial results are encouraging; however, the technique needs to be optimized for this application. Other immediate planned activities include the optimization of Ni-electroplating, deposition of hard carbon coating using plasma-based technologies, and procurement and characterization of carbon-carbon composites from Oak Ridge National Laboratory (ORNL).

Design analysis has commenced for the forced convective liquid salt loop at the University of Wisconsin. The objective will be to examine the effects of liquid salt flow through small channels, similar to channels for the intermediate heat exchanger (IHX). Diameters for these IHX channels in the test section will range from 1 to 10 mm. These tests are intended to produce experimental pressure drop and heat transfer data for small channel flow of liquid salts in heating and cooling conditions. In addition, these tests would also serve as corrosion tests with exposure time of up to 1,000 hours.

Nuclear Energy Research Initiative

Optimization of Heat Exchangers

PI: Ivan Catton, University of California-Los Angeles (UCLA)

Collaborators: None

Project Number: 07-057

Project Start Date: June 2007

Project End Date: June 2010

Research Objectives

The objective of this research is to develop tools to design and optimize heat exchangers (HEs) and compact heat exchangers (CHEs) for intermediate loop heat transport systems found in the very high-temperature reactor (VHTR) and other Generation IV designs by addressing heat transfer surface augmentation and conjugate modeling.

This research will be performed in two parts. In the first part, researchers will search for augmented heat transfer surface morphologies using a combination of experiment and modeling. For a particular type of surface augmentation, they will conduct experiments to obtain closure of the model and then apply it to optimize the surface. A final experiment will confirm the findings of the model. These surfaces will become candidates for the next part of the research, where they will be integrated into a HE design. The objective is to develop and demonstrate a model that can be used to optimize HEs. The model equations are available but have not been used for a two-fluid-stream HE, nor has closure been fully developed. Researchers will also design and optimize a printed circuit heat exchanger (PCHE) for either a high-temperature Brayton cycle in support of the VHTR or for the reactor-hydrogen production process interface. The results of this research will be a validated computer program for the design of HEs that maximizes heat transfer and minimizes pumping power.

The major technical objectives of this research include the following:

1) Develop a surface that increases surface heat removal effectiveness by a factor of four without a marked increase in pumping power
2) Develop a new type of mathematical model capable of predicting flow and heat transfer in two-dimensional (2-D) and three-dimensional (3-D) spatial structures at different scales
3) Design and carry out experiments to measure heat transfer augmentation and validate the HE and CHE models used for optimization
4) Design and test a PCHE for a high-temperature inert gas cycle

Research Progress

During the first quarter of this work, researchers focused on developing a computer code capable of predicting friction and heat transfer over surfaces augmented with 2-D and 3-D roughness elements. The code is based on a rigorous spatial averaging technique used for heterogeneous media transport phenomena called Volume Average Theory (VAT). For this research, VAT is applied to the conjugate heat transfer problem of turbulent transport through HEs modeled as porous media.

Researchers have developed a code for solving the VAT transport equations for the case of fully developed turbulent flow in a channel with surfaces augmented with regular morphology consisting of 2- and 3-D roughness elements. The 2-D rib augmented surfaces consist of periodic rectangular, triangular, and semi-circular ribs. The 3-D augmented surfaces consist of cones, cylinders, spheres, and hemispheres.

The VAT code has been validated against experimental results for the smooth channel and channels with 2-D ribbed augmentation. The smooth channel results are in excellent agreement with theoretical and experimental values. Experimental data for channels augmented with ribs varying in geometry, size, and pitch were compared

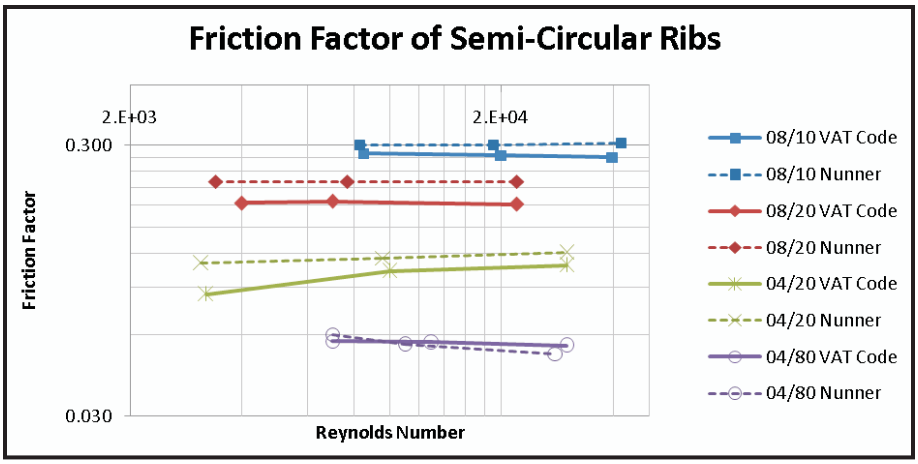

Figure 1. Comparison of computed friction factors with experimental data from Nunner for channels with four semi-circular rib configurations.

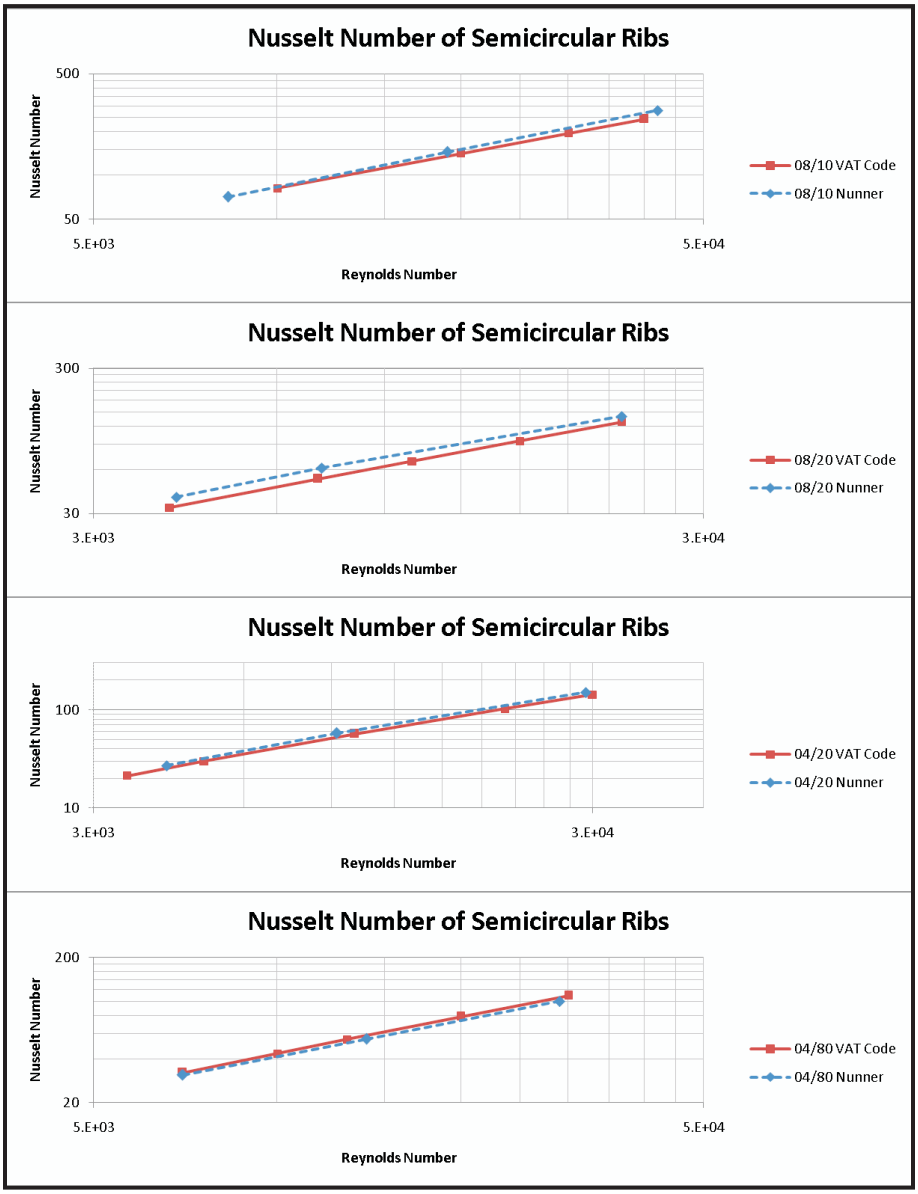

Figure 2. Comparison of computed Nusselt numbers with experimental data from Nunner for channels with four semi-circular rib configurations.

with results from the VAT code to show very good agreement in the friction factor and excellent agreement in Nusselt number. Figure 1 shows the results of friction factor for four configurations of semi-circular ribbed channels compared to experimental data from Nunner. Figure 2 illustrates the heat transfer prediction agreement in the Nusselt numbers for the same four configurations. The other ribbed geometries agreed with experimental data in similar fashion.

The VAT code was also used to calculate the effectiveness of rib augmented surfaces. Researchers found that the increased pumping power required to overcome the added friction caused by the rib augmented surface did not produce a great enough increase in the heat removal for the augmentation to be worthwhile. Figure 3 plots the effectiveness of semi-circular and square rib augmented channels normalized by the effectiveness of a smooth channel. The figure clearly shows that no performance increase is gained from ribbed augmentation compared to a smooth surface. This finding directs the search for augmented surfaces away from 2-D ribbed surfaces and towards 3-D augmentation.

The computational fluid dynamics (CFD) software package, SC/TETRA, is being used to simulate flow and heat transfer over specific types of surface augmentation geometries. Researchers are developing ways to extract the local drag and heat transfer coefficients from the CFD results to use in closure of the VAT equations. For complex geometries, this requires that certain SC/TETRA internal results be processed in a predetermined way to obtain the closure needed.

During the second quarter, researchers are focusing on further developing the VAT code. More sophisticated and efficient numerical techniques are being implemented to produce the type of

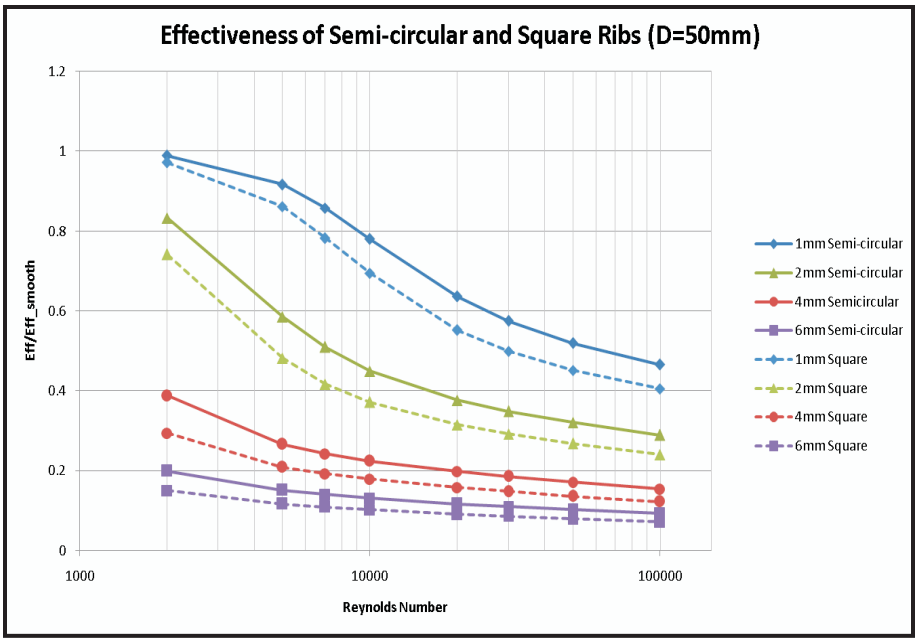

Figure 3. Augmented surface effectiveness for semi-circular and square ribs normalized by smooth surface effectiveness.

fast running code necessary for optimization purposes. Researchers are also adding the capability to handle irregular surface morphologies, such as roughness elements, that change in height in the flow direction. Furthermore, the capability to handle two fluid streams is being incorporated into the code.

Researchers have set up a wind tunnel, heating system, and data acquisition system for use in the experimental side of this project. The wind tunnel will be used to measure heat transfer augmentation, to obtain the necessary closure for particular types of surface augmentation, and to validate the HE models used for optimization. A new heater and fan are being purchased for the wind tunnel.

Planned Activities

The following are planned activities for the upcoming year:

- Perform a theoretical study to investigate ways of obtaining the necessary local drag and heat transfer coefficients required for the closure of the VAT equations (this will allow separation of convection effects from conduction in the conjugate problem to allow true geometric optimization)
- Complete the development and validation of an augmented surface model
- Complete data sets needed for a surface augmented model by conducting experiments using laboratory wind tunnel and CFD
- Conduct an optimization study of selected surfaces
- Develop a VAT-based HE model, implementing a 3-D alternating direction implicit (ADI) method to evaluate the full HE
- Validate the HE model
- Develop an initial design using VAT-based optimization code
- Select high-temperature conditions and materials for further study
- Propose some PCHE candidates for study

Nuclear Energy Research Initiative

Advanced Electrochemical Technologies for Hydrogen Production by Alternative Thermochemical Cycles

PI: Serguei N. Lvov, Pennsylvania State University

Collaborators: University of South Carolina (USC), Tulane University, Argonne National Laboratory

Project Number: 08-047

Project Start Date: October 2007

Project End Date: September 2010

Project Description

The main objective of this consortium is to establish the most efficient technologies for hydrogen production that are compatible with nuclear-generated heat sources. The heat produced by nuclear power plants can be utilized by moderate-temperature thermochemical cycles to convert water into hydrogen and oxygen. Researchers will investigate a number of prospective thermochemical cycles and key reactions via experimental work and process simulation to evaluate their efficiency and viability for future sustainable energy infrastructure.

Several promising alternative thermochemical cycles merit further research: 1) three copper-chloride (Cu-Cl) reactions, 2) three calcium-bromide (Ca-Br) reactions, and 3) two active metal alloy reactions. Potential benefits of these cycles include medium temperature (≤ 700°C) operation, high efficiency, simple unit operations, and relatively simple separations. This project focuses on the development of advanced electro-chemical technologies, which will lead to overall improvement in cycle performance.

The work for this project will include the following tasks: 1) development of membranes, electrocatalysts, electrode materials, and membrane electrode assemblies (MEAs) for all of the cycles; 2) separation of reaction products; 3) identification and modeling of species involved in the electrochemical processes; and 4) flowsheet analyses to guide the experimental program towards higher efficiency and lower cost processes. The modeling and experimental work will be iterative. As the technology evolves, the flowsheets will be updated and optimized to find other opportunities for increasing efficiency and reducing costs.

Material demands for these alternative cycles are expected to be less severe than the temperature required for the baseline sulfur cycle (i.e., 825°C). While this project is primarily concerned with alternative thermochemical cycles, the technologies developed will be applicable to proton exchange membrane (PEM) electrolyzers and other hydrogen production processes.

Workscope

The objectives will be achieved through the following activities:

Cu-Cl Cycle

- Synthesis of new materials (membranes and catalysts) for CuCl(aq)/HCl(aq) electrolytic cell
- Characterization of new membranes and catalysts
- Development of MEAs using new membranes and catalysts
- Experimental tests with an advanced CuCl(aq)/HCl(aq) electrolytic system
- Potentiometric studies of thermodynamic properties and speciation in $CuCl_2$(aq) solutions
- Development of an analytical method for online analysis of Cu compounds in highly concentrated aqueous solutions
- Fabrication of an electrodialysis system for concentrating $CuCl_2$ and determination of the system capabilities and limitations
- Experimental tests with the electrodialysis system: determination of the extent to which $CuCl_2$ can be concentrated, identification of the possible limits, and determination of the extent to which electrodialysis can separate Cu(I) from Cu(II)

- Development of a complete process model and flowsheet for the Cu-Cl cycle with available electrolysis information
- Updating the model and providing efficiency and cost estimate of the cycle
- Coordination of activities related to the thermochemical cycle

Ca-Br Cycle

- Synthesis and characterization of low-cost nanostructured electrocatalysts and supports for use in the anode and cathode
- Optimization and operation of the electrolyzer via performance studies, mathematical models, and process simulators
- Development of advanced proton-conducting membranes for high temperature/vapor-phase electrolysis systems
- Cycle modeling and simulation
- Coordination of activities related to the thermochemical cycle

Active Metal Alloy Cycles

- Development of K-Bi thermochemical cycles: experimentation and modeling
- Thermodynamic analysis of Na-Sn thermochemical cycle
- K-Bi cycle modeling
- Coordination of activities related to the thermochemical cycle

Index of NERI Projects

FY 2005 Projects

FY 2006 Projects

FY 2007 Projects

FY 2007 NERI-C Projects